micropaleontology

volume 53, numbers 1-2, 2007

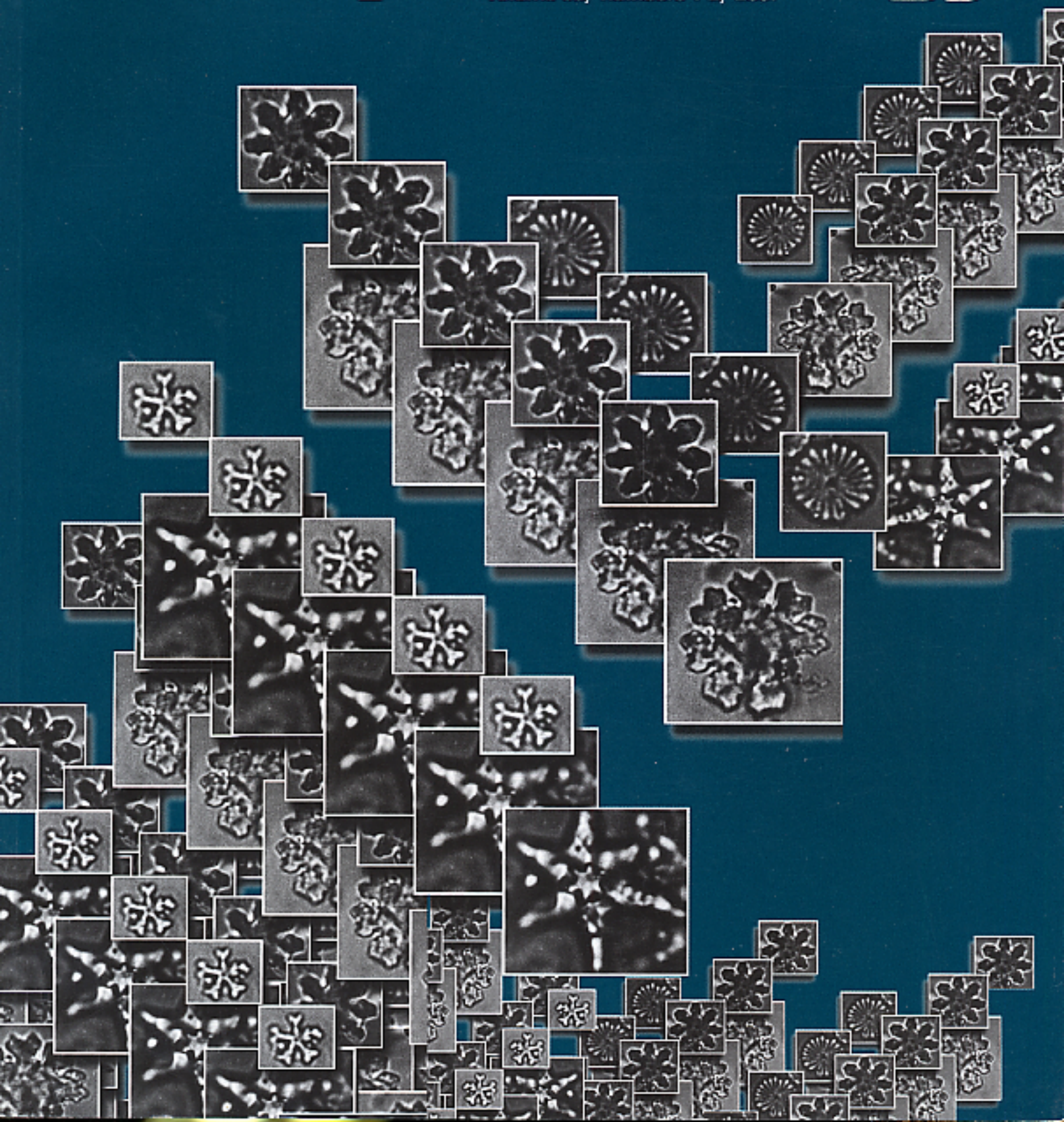

CONTENTS **Volume 53** **Numbers 1 & 2** **2007**

Halimeda (green siphonous algae) from the Paleogene of (Morocco) – Taxonomy, phylogeny and paleoenvironment

Ovidiu N. Dragastan[1] and Hans-Georg Herbig[2]

[1]*University of Bucharest, Department of Geology and Paleontology, Bd. N. Balcescu No.1, 010041, Bucharest, Romania*
email: ovidiud@geo.edu.ro

[2]*Universität zu Köln, Institut für Geologie und Mineralogie, Arbeitsgruppe für Paläontologie und Historische Geologie, Zülpicher Strasse 49a, 50674 Köln, Germany*
email: herbig.paleont@uni-koeln.de

ABSTRACT: Calcareous algae of order Bryopsidales, family *Halimedaceae* abound in shallow marine ramp facies of the Jbel Guersif Formation (late Thanetian), Ait Ouarhitane Formation (middle – late Ypresian) and Jbel Tagount Formation (latest Ypresian to late Lutetian or latest Bartonian), southern rim of central High Atlas, Morocco. The genus *Halimeda* includes nine new species, *Halimeda erikfluegeli, H. lacunosa, H. barbata, H. marcconradi, H. praetaenicola, H. unica, H. praemacroloba, H. praegoreaui, H. praecuneata.* Additionally, 14 modern and fossil taxa occur: *H. cylindracea, H. incrassata, H. monile, H. opuntia, H. opuntia f. triloba, H. simulans, H. tuna, H. tuna* f. *platydisca, H. gracilis, H. copiosa, H. scabra, H. fragilis, H. nana, H. praeopuntia.* For the first time, gametangia were observed in fossil species.

All new species were of short range. Most appeared during adaptive radiation in the late Thanetian, associated with some already known fossil species and an ancient stock of modern *Halimeda* taxa (*H. cylindracea, H. incrassata, H. monile, H. opuntia*). The adaptive radiation was connected with the marine transgression at the southern rim of the central High Atlas and is interpreted as part of the recovery phase after the end-Cretaceous decline of green algal diversity. Mid Ypresian to late Lutetian or latest Bartonian assemblages show minor origination rates but the onset of long-ranging extant species. These assemblages are interpreted to represent the stabilization phase of Paleogene green algal evolution, dominated by well-adapted species. At the beginning of the Lutetian, already twelve modern taxa of *Halimeda* were present. This proves geological longevity extending over more than 50 million years and characterizes the corresponding species, respectively the genus *Halimeda*, as living fossils. The results also prove the early origin of the basal clades of the genus *Halimeda*, defined from morphological and molecular data of extant species. Origin of the extant Sections Rhipsalis, Micronesicae, Halimeda and of an opuntoid basal clade is assumed to be prior to the Late Thanetian, either in the late Cretaceous or in the earliest Paleocene, following the end-Cretaceous extinctions. Separation of the opuntoid basal clade into the lineages of the present-day sections Pseudoopuntia and Opuntia was achieved before Mid Ypresian and further differentiation of the clades during the Ypresian and Lutetian, much earlier than hitherto postulated. Presumed timing of the origin of the basal clades of *Halimeda* and delayed first occurrences in southern Morocco invoke speciations of the recognized extant taxa outside of the peculiar Atlantic-bound Moroccan epeiric sea somewhere on the wide shelfs of the southern Tethys. Neogene vicariance events influencing the evolution of *Halimeda* are shortly discussed. Concerning the fossil record, they seem to be of minor importance except for the Holocene outburst of Recent taxa, which might be a sampling or preservational artifact.

Halimeda-rich facies at the southern rim of the central High Atlas is comparable to modern *Halimeda* meadows and banks of the Great Barrier Reef. This concerns the almost total absence of other algae, minor lateral changes in the composition of the *Halimeda* flora, high diversity with analogous percentage of composition patterns, which show few dominant and common taxa, and quite a lot rare to very rare taxa. In both cases, psammophytic and lithophytic species co-occur, demonstrating sufficiently coarse-grained, immobile substrates. Both *Halimeda* floras flourish due to upwelling of cold, nutrient-rich waters.

INTRODUCTION

Halimeda is one of the most common green alga in modern tropical marine environments. Thirty-four species, arranged in five morphological groups (Sections) are recognized in traditional taxonomy. Gene sequencing (Hillis et al. 1998; Kooistra et al. 1999, revisions in Kooistra et al. 2002 and Verbruggen and Kooistra 2004) proved good correlation with several morphological characters in spite of some phenotypical similar but para- or polyphyletic entities. The ecological and sedimentological constraints of the genus are well studied (e. g. Hillis-Colinvaux 1980) and were already highlighted in the classical textbooks of Milliman (1974) and Wray (1977). Although *Halimeda* is essentially a dweller of tropical environments, *Halimeda cuneata* Hering (in Krauss 1846) is mostly subtropical (Hillis-Colinvaux 1980, see also Hillis 2001), and *Halimeda tuna* (Ellis and Solander 1786) Lamouroux 1812 extends to the temperate zone of the Mediterranean (compare Fornos et al. 1972). The alga has considerable extension into the deep sublittoral (e. g. Goreau and Goreau 1973; Blair and Norris 1988; Littler and Littler 2000a). Recently, Bandeira-Pedrosa et al. (2004) recorded *Halimeda* from depth of more than 160m off Brazil. It is famous for its extensive contribution to carbonate production through decay into algal gravel and micritic aragonite needles (first noted by Chapman and Mawson 1906, and, among many others Ginsburg 1956; Neumann and Land 1975; Enos 1977; Drew and Abel 1985, 1988a; Macintyre and Reid 1995). Discovery of extensive *Halimeda* bioherms (Davies and Marshall 1985; Roberts et al. 1987, 1988; Hine et al. 1988; Mar-

shall and Davies 1988) prove its important potential to form hydrocarbon reservoirs. However, fossil *Halimeda* bioherms have been described only from the Messinian (Late Miocene) of southeastern Spain (Braga et al. 1996) and southern Italy (Bosellini et al. 2002).

Halimeda soltanensis Poncet 1989 from the Late Permian has been considered to be the oldest true *Halimeda* (Poncet 1989), but Bucur (1994) did not exclude homeomorphism of another taxon. Subsequent taxa from the late Triassic (Flügel 1975, 1988; Kemper et al. 1976; Dragastan et al. 2000) are now assigned to *H. cylindracea* Decaisne 1842 (Dragastan et al. 2002). Having originated from Paleozoic ancestors grouped in the family Protohalimedaceae, "*Boueina*" (late Triassic to early Cretaceous), "*Arabicodium*" (mid Jurassic to Paleogene) and "*Halimeda*" (early Cretaceous to Recent) all belong to the modern genus *Halimeda* (Dragastan et al. 2002). *Halimeda*, resp. its synonyms are commonly recorded in Cretaceous shallow-water carbonates of the Tethyan realm and abound throughout the Cenozoic (Flügel 1988 cum lit.; Dragastan et al. 2002, 2003). Although *Halimeda* has been extensively used as an indicator of tropical climate and mostly lagoonal and reefal to peri-reefal shallow-water environments, the taxonomy of fossil material on species, genus, and even suprageneric level is strongly hampered by the great variabilitiy of modern and fossil taxa (Bassoullet et al. 1983; Flügel 1988; Dragastan et al. 2002), by the differences in the degree of calcification and corresponding preservation potential (Flajs 1977; Dragastan et al. 2002), by the decay of the plants into segments of different shape and diameter (Dragastan et al. 2002) and randomly orientated sections in thin-sections from carbonate rocks. Consequently, in many taxonomic studies, *Halimeda* has been described in open nomenclature, i.e. without assignment to discrete species.

Suprageneric taxonomic controversies on fossil halimediform algae are well elucidated by Dragastan et al. (1997). They were the first to place fossil *Halimeda* into the order Bryopsidales Schaffner 1922, suborder Halimedineae Hillis-Colinvaux 1984, family Halimedaceae Link 1832 following the assignment of modern *Halimeda* by Hillis-Colinvaux (1984). At the generic level, Steinmann (1899), Pia (1927) and Le Maitre (1937) long ago emphasized the close relationship between *Boueina* and *Halimeda*. Later, Elliott (1965) regarded *Boueina* and *Arabicodium* as subgenera of *Halimeda* and Johnson (1968) postulated the synonymy of these taxa with *Halimeda*, which has priority. Flügel (1988) also commented on the widely discussed taxonomic assignment of *Boueina*, *Arabicodium*, *Leckhamptonella* and *Halimeda*. In an extensive study based on material from the western Pacific, Dragastan et al. (2002) compared Miocene to Pleistocene species with modern species and discussed taphonomic problems. They postulated the existence of numerous synonymous fossil taxa on genus and species level due to different calcification, description of randomly oriented thin-sections, reference to single algal segments, not to plants, and insufficient amounts of studied material. As a result, the synonymy of *Boueina*, *Arabicodium*, *Leckhamptonella* and *Halimeda* suggested by previous authors was strongly supported. Based on segment morphology and, to a lesser degree, on the utricles of the cortex, Dragastan et al. (2002; see also Dragastan and Soliman 2002) postulated the presence of three phylogenetic lines starting first in the late Triassic (*H. cylindracea* lineage – taxa with undifferentiated cylindrical to spheroidal thallus segements and cylindrical utricles), respectively in the late Cretaceous (?) (*H. incrassata* lineage – taxa with undifferentiated cylindrical to reniform and subcuneate thallus segments and conical utricles), and around the Cretaceous-Paleogene transition (*H. opuntia* lineage – taxa with extremely variable, laterally compressed thallus segments and differentiated utricle morphology).

Morphological and molecular cladistic analyses of Recent *Halimeda* identified three major basal clades (Hillis et al. 1998; Kooistra et al. 1999) Opuntia + Micronesica, Rhipsalis, and Halimeda, i. e. the major modern sections of the genus. The clades were modified by subsequent studies (Kooistra et al. 2002; Verbruggen and Kooistra 2004), but the major clades Rhipsalis, Halimeda, and an opuntoid clade (Opuntia + Pseudoopuntia clades) are still recognized; the small clade Micronesicae was newly assembled from its earlier representatives *H. micronesica*, *H. fragilis* and the hitherto morphologically isolated deeper-water species *H. cryptica*. Two basal clades apparently match the phylogenetic lineages postulated by Dragastan et al. (2002) from the paleontological record. The *H. cylindracea* lineage, the most ancient lineage, and the next ancient *H. incrassata* lineage both plot into basal clade/extant section Rhipsalis. The somewhat younger *H. opuntia* lineage seems to correspond to the opuntoid basal clade (i. e. extant sections Pseudopuntia and Opuntia, Verbruggen and Kooistra 2004). The third basal clade, section Halimeda, was not recognized as a primary paleontological stem line. Hillis (2001) postulated three vicariance events within the genus, i. e. speciation events due to the emergence of geographic barriers. The oldest one, associated with the Cretaceous-Tertiary boundary, should introduce the three basal clades. The second event was associated with the late Miocene closure of the circumtropical Tethys seaway and the Messinian salinity crisis. It should cause subdivision of the section Rhipsalis. The third vicariance event could be related to the closure of the Panama seaway during the Pliocene. However, due to the sparseness of modern taxonomic studies of fossil *Halimeda*, timing of the phylogenetic tree remained hypothetical and Hillis (2001) emphasized that the apparent Holocene spike in *Halimeda* speciation seemed to be a sampling artifact.

In the meantime, Dragastan and coworkers contributed appreciably to the knowledge of fossil *Halimeda*. In a contribution on Upper Pleistocene (Sangamon) *Halimeda* from southern Florida, Dragastan et al. (2003) compared Pleistocene and modern diversities and discussed evolution of diversity in Mesozoic and Cenozoic times. Only three modern taxa had been identified by Dragastan and Soliman (2002) from the Ypresian (early Eocene) of Egypt. However, *H. cylindracea* Decaisne 1842 and *H. incrassata* (Ellis) Lamouroux 1816 have to be present in that time slice due to the antiquity of their lineages. From the late Miocene onwards, eight modern species are well represented (see Dragastan et al. 2002, fig. 5). Another outburst of species was recorded in the late Pleistocene, but the true stratigraphical range of modern *Halimeda* species remains unknown, as well as the general diversity of the genus in the Paleogene (Dragastan et al. 2003). Because all three phylogenetic lineages were present at the onset of the Cenozoic, a considerable diversity and diversification should have occurred in the Paleogene. A paucity of studies has precluded verification of this hypothesis.

Abundant and excellently preserved *Halimeda* from well-dated late Paleocene to middle Eocene strata at the southern rim of the central High Atlas, Morocco (Pfender in Moret 1938; Herbig 1986, 1991; Kuss and Herbig 1993) provide an important regional case study to assess this problem and considerably modify our conception on evolution of *Halimeda* (Herbig and

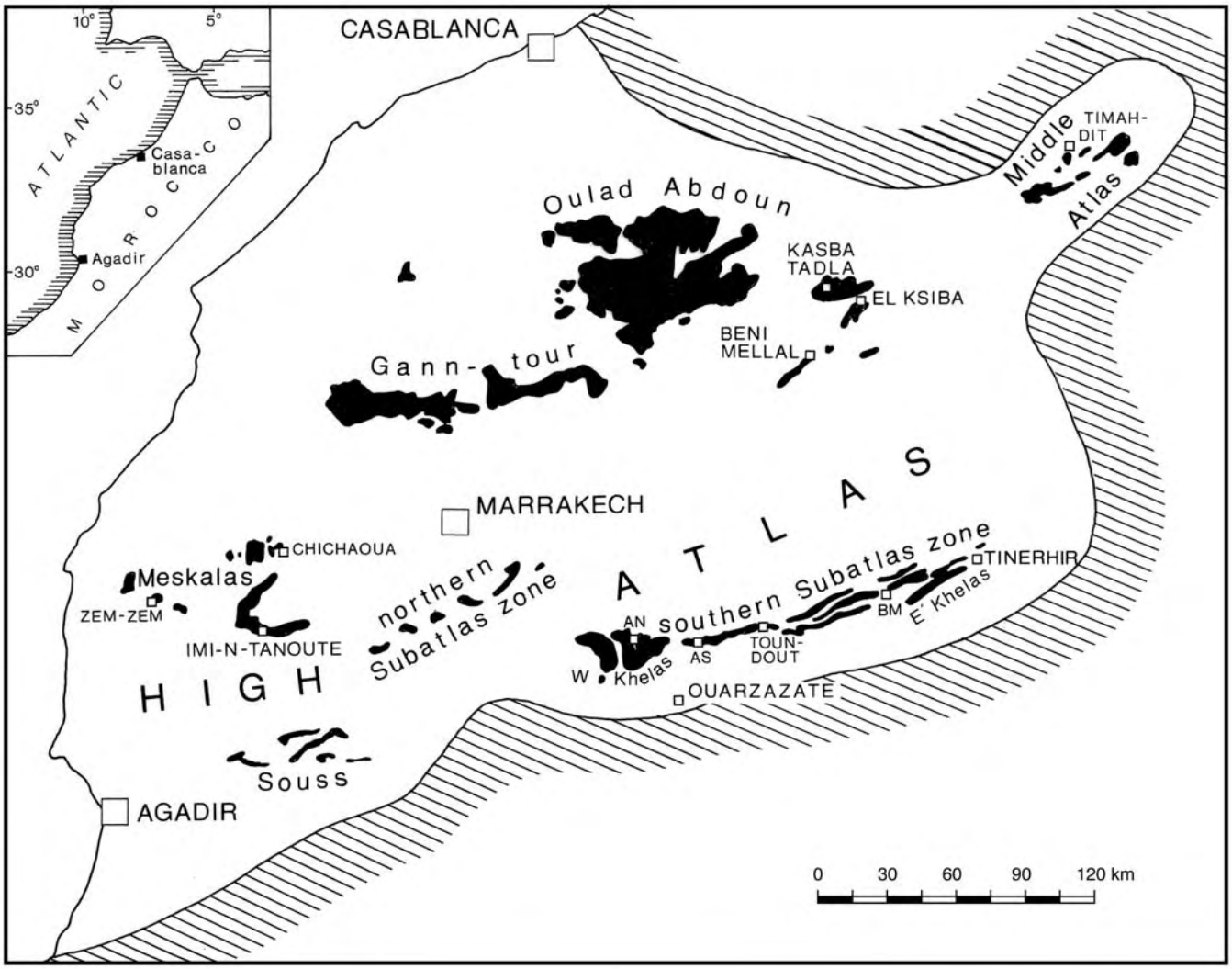

TEXT-FIGURE 1
Inferred maximum extension of the Paleogene sea in central Morocco during late Thanetian to late Lutetian or latest Bartonian. Outcrop areas of these strata are shown in black. They outline the central Moroccan phosphate basin (Ganntour, Oulad Abdoun including the Beni Mellal – El Ksiba region, and the increasingly marginal depositional realms of the Meskalas, Souss, northern and southern Subatlas zone, and the Middle Atlas realm. AN – Anmiter, AS – Asseghmou, BM – Boumalne. From Herbig and Trappe 1994.

Dragastan 2005). Time-equivalent strata from the same marine basin in the Middle Atlas also yield abundant *Halimeda* (Pia in Pia et al. 1932; Segonzac et al. 1986; Herbig 1991; Kuss and Herbig 1993), but the stratigraphy is imprecise. This microflora will be dealt with in a separate paper.

GEOLOGICAL SETTING AND STRATIGRAPHY

General paleogeography and facies of the central Moroccan Paleogene sea

Marine Paleogene successions at the southern rim of the Moroccan central High Atlas were part of an extensive bowl-shaped epicontinental sea, which invaded central Morocco in the Maastrichtian and retreated in the late Lutetian or latest Bartonian. During its maximum extension, from late Thanetian to late Lutetian–?Bartonian, the sea advanced to the northern margin of the Anti-Atlas Mountains between Ouarzazate and Tinerhir, and extended into a northeastern Middle Atlas gulf (text-fig. 1). Deposits include (1) the phosphate deposits of central Moroccan phosphate basin in the mining districts of Ganntour and Oulad Abdoun, (2) a variegated series of phosphatic sands, dolomites, porcellanites, marls and limestones in the Meskalas and western Souss, and (3) marl-limestone successions in the northern and southern Subatlas realms, and the Middle Atlas realm. The lithostratigraphic units outside the phosphate basin, collectively termed Subatlas Group, were formally described by Trappe (1989, 1991) and Herbig (1991). A synoptic overview is from Herbig and Trappe (1994).

Paleogeographic reconstruction (text-fig. 1) is based on detailed lithostratigraphic and facies studies of Herbig (1986, 1991) and Trappe (1989, 1991, 1992), who independently developed a ramp model for the Paleogene epeiric sea of central Morocco. Silty and sandy redbeds grading into greenish and greyish mudflat deposits are locally preserved at the basin margins in the eastern Souss, the southernmost and easternmost Southern

Subatlas Zone, and the northeasternmost Middle Atlas. The mudflat deposits grade into diverse bioclastic carbonate rocks of the shallow ramp, followed by phosphatic limestones, and finally by deeper ramp phosphorite-porcellanite-marl successions in the central Moroccan phosphate basin. The western margin of the basin faced an upwelling zone at the northwest African continental margin.

This paleogeographic model deviates strongly from earlier reconstructions based on the spatial distribution of preserved Paleogene strata, which postulated three independent gulfs intruding from the Atlantic (Choubert and Marçais 1952, 1956; Choubert and Faure-Muret 1960-1962; Boujo 1976), respectively from another model postulating a complex array of islands, continental peninsulas, gulfs and bays (Salvan 1960; Azmany-Farkhani et al. 1986 – compare sketches in Michard 1976; Herbig 1991; Trappe 1991). However, all authors agree that the Paleogene sea was an Atlantic-bound basin, separated from Tethys, respectively the northern Moroccan Rif basin by the "Land of the Idrissides" (Choubert and Faure-Muret 1960-1962), situated north of the central Moroccan phosphate basin in the region of the present-day Moroccan Meseta. Marine connections with the Paleogene seas of Tunisia or the epicontinental Libyan basins along the southern rim of the High Atlas can be ruled out because of differences between Moroccan and typical Tethyan faunal assemblages of Tunisia and Libya, and by the replacement of marine strata by lacustrine and palustrine deposits east of the basin margin, east of Tinerhir (Herbig 1986, 1988). In fact, Moroccan Maastrichtian to Lutetian–?Bartonian biota are quite different from time-equivalent deposits of the southern Tethys. Foraminifers are generally rare and extremely low diversified, except for abundant miliolids and almost monospecific mass occurrences of the rotaliid *Rotalia skourensis* Pfender (in Moret 1928) in strata south of the central High Atlas. Larger foraminifers apparently are completely absent. Except for Acetabulariaceae, dasycladalean green algae are strongly impoverished compared with Egypt, which is typical southern Tethys (Kuss and Herbig 1993). Coralline algae and corals are also remarkably rare (Herbig 1991).

Reasons for the biotic differences were discussed by Kuss and Herbig (1993). They postulated extrabasinal barriers preventing immigration and intrabasinal ecological barriers. Extrabasinal barriers were missing migration routes along the narrow westernmost Mediterranean (mostly southern) Tethys shelf, depicted e.g. in Dercourt et al. (1986, pls. 6, 7), and upwelling of cold waters at the northwestern African continental margin.Intrabasinal ecological barriers were the surplus of phosphorous in wide areas of the Moroccan epeiric sea.

Marine Paleogene at the southern rim of the central High Atlas

Marine Paleogene strata (Subatlas Group) at the southern rim of the central High Atlas extend along strike for 185km from the Marrakech–Ourazazate road in the west to Tinerhir in the east. However, outcrop width normal to strike is generally less than 10km except for the extended plateaus of the Khelas northwest of Ouarzazate. The Subatlas Group is mostly part of the Southern Subatlas Zone (Moret 1931, Roch 1939; Gauthier 1957; Zylka and Jacobshagen 1986), a tightly folded, south vergent and in part imbricated structural unit consisting of Cretaceous to Neogene rocks south of the Triassic to predominant Jurassic rocks of the central High Atlas. Towards the south, that unit passes rapidly into the Khelas, a typical cuesta of almost flat-lying strata, which overlie the Proterozoic to Paleozoic basement of the Anti-Atlas (text-figs. 1, 2).

Following the early monographs of the French authors, important contributions are from Herbig (1986, 1991, cum. lit.), Trappe (1989, 1991, 1992), and Gheerbrant et al. (1993, 1998). Herbig and Trappe (1994) defined two facies realms with separate lithostratigraphic units. In the west, the "High Atlas realm" includes all outcrops in the Southern Subatlas Zone west of Toundout and, additionally, the outcrops of the Northern Subatlas Zone south and southwest of Marrakech. The facies realm is characterized by (1) a lower carbonate unit (supratidal siltstones, dolomites and limestones of the Asseghmou Formation, overlain by commonly phosphate-bearing bioclastic limestones and a few intercalated fossiliferous phosphatic marls of the Anmiter Formation), (2) a middle marl unit (fossiliferous grey marls of the Ounila Formation), and (3) an upper carbonate unit (mostly bioclastic limestones of the Thersitea Formation).

The facies of the Eastern Ouarzazate basin develops gradually from the High Atlas facies realm east of Toundout. That facies assembles a well-differentiated carbonate-siliciclastic succession, almost without phosphatic rocks. The Eastern Ouarzazate basin yielded the rich flora of green siphonous algae described herein, though green algae are also known from the High Atlas facies realm (Pfender in Moret 1938; Trappe 1989, 1991, 1992).

Formal lithostratigraphy of the eastern Ouarzazate basin (text-fig. 3) is from Herbig (1991). He discussed and revised earlier biostratigraphic assignments based mostly on molluscans (Moret 1938; Gauthier 1957) and included new biostratigraphic data from vertebrates (Cappetta et al. 1987 – see also Gheerbrant et al. 1993), palynoflora (Mohr and Fechner 1986), and calcareous algae and oysters (Geyer and Herbig 1988). His results indicate an almost perfect correlation between sea-level history and sedimentary facies of the succession, a fact which is related to deposition on the margin of the stable Pan-African West African craton (Herbig 1986, 1987). The biostratigraphic assignments are well compatible with those of Gheerbrant et al. (1993), included already in Herbig and Trappe (1994). Additional biostratigraphic and few magnetostratigraphic data from Gheerbrant et al. (1998) modify the previous results only slightly, but should be discussed below.

As in the High Atlas realm, the marine Subatlas Group of the eastern Ouarzazate basin realm overlies an extensive redbed series, the "Série rouge supérieur" (Senonian–Danian). Initial deposits are greenish supratidal siltstones, dolomites, and micritic lacustrine-palustrine limestones (Asseghmou Formation). The overlying Jbel Guersif Formation consists of one to several shallowing-upward cycles of shallow marine, white to pale-rose colored bioclastic limestones. At its top, a sedimentary break is indicated by borings, slight erosional relief and sharp-cut facies boundaries. Herbig (1991) attributed a basal Thanetian age to the Asseghmou Formation, and a late early to mid Thanetian age to the Jbel Guersif Formation. Gheerbrant et al. (1998) confirmed a general Thanetian age for both formations by the presence of strongly recrystallized, probable *Discoaster* rosettes, which were also recorded from the transition to the following Ait Ouarhitane Formation. *Discoaster* rosettes first occur in zone NP 7, i.e. somewhat above the base of the Thanetian. Discussing additional paleomagnetic data, Gheerbrant et al. (1998) attributed a mid Thanetian age to the Asseghmou Formation, spanning chron C26n and parts of the underlying and overlying

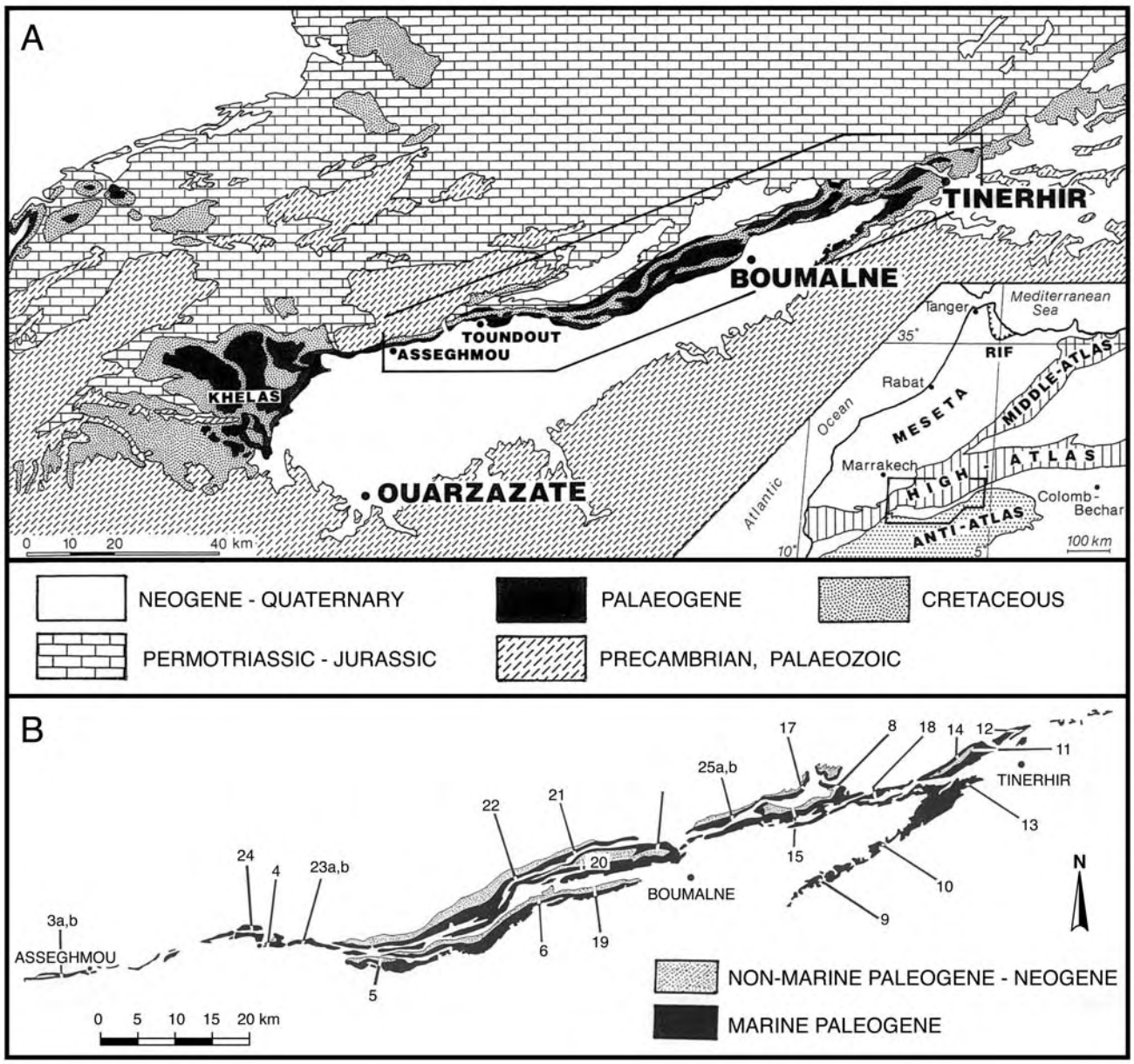

TEXT-FIGURE 2
Marine Paleogene strata (Subatlas Group) at the southern rim of the central High Atlas, Morocco. A – Geological map showing structural setting of Paleogene strata between Permo-Triassic and predominant Jurassic of the High Atlas and Precambrian–Paleozoic of the Anti-Atlas. Studied area of Southern Subatlas Zone is outlined (from Herbig 1986). B – Detailed outcrop pattern of marine Paleogene strata and position of sections studied. See also appendix 1 (from Herbig 1991).

reversed chrons. A late Thanetian age was attributed to the Jbel Guersif Formation, ending somewhat above chron C25n.

The overlying Jbel Ta'louit is subdivided into three unnamed members. Lower and upper members consist of greyish to greenish-grey siltstones with some intercalated sandstone horizons. Red sediment colors and sandstones become predominant east of the Dades valley. The middle member is composed of marginal-marine, often sandy, oolitic and oyster-bearing limestones. The Jbel Ta'louit Formation is latest Thanetian to basal Ypresian according to Herbig (1991), who correlated the calcareous middle member with the significant global sea-level rise in the latest Thanetian (text-fig. 3). Vertebrates from transitional strata to the overlying Ait Ouarhitane Formation are of early Ypresian age. These strata were assigned to the Jbel Ta'louit in Herbig (1991), Herbig and Gregor (1992) and Herbig and Trappe (1994), but to the Ait Ouarhitane by Gheerbrant et al. (1993). Paleomagnetic data by Gheerbrant et al. (1998) cannot rule out that the base of the Jbel Tal'louit straddles the Thanetian-Ypresian boundary, but the top of the formation is assumed to be within or on top of chron C24n. This would indicate a mostly early Ypresian age for the formation.

The overlying Ait Ouarhitane Formation is a composite shallowing-upward megacycle of variegated yellow bioclastic limestones. According to Herbig (1991), it is correlated with the

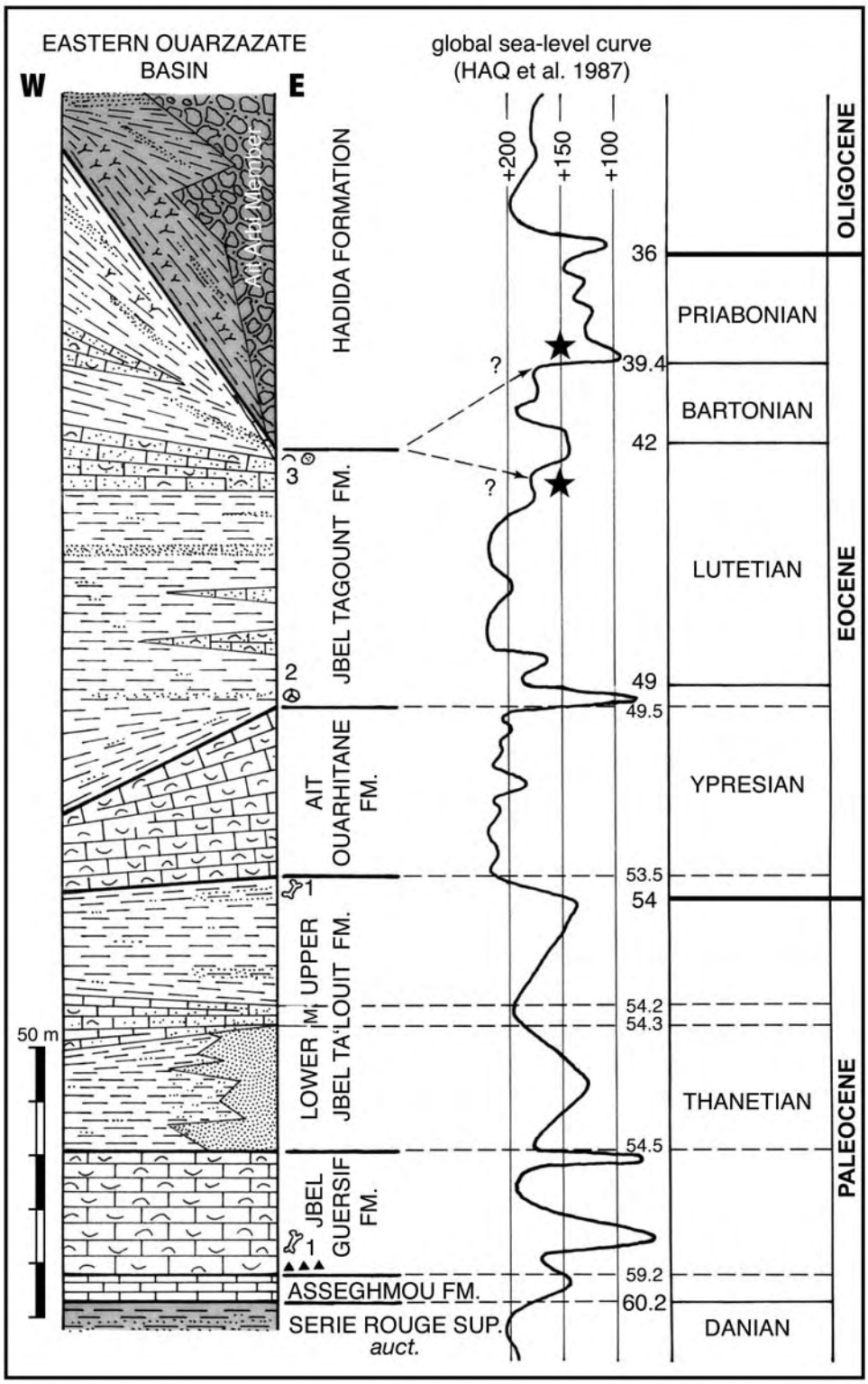

TEXT-FIGURE 3
Lithostratigraphy, biostratigraphic assignments and correlation with eustatic sea-level variatons of the marine Paleogene strata (Subatlas Group), eastern Ouarzazate basin, modifed from Herbig and Trappe (1994). Vertical axis is thickness, showing variations for the different formations from west to east. Correspondingly, time-scale and sea-level curve are distorted, especially obvious for the latest Thanetian. Note that paleomagnetic data of Gheerbrant et al. (1998) indicate a mid Thanetian age for the Asseghmou-Formation, and a mid Ypresian base for the Ait Ouarhitane Formation. Triangles indicate onset of marine transgression on top of lacustrine-palustrine Asseghmou Formation. Asterisks indicate the ambiguous position of the final regression of the Subatlas sea, which could not be resolved biostratigraphically, but apparently is related to sea-level fall in the late Lutetian or latest Bartonian. Lithofacies indicated by conventional signs. Y – gypsum; ∩∪ – lumachelles; dotted – sand content or sandy horizons; shaded - continental rocks. Important biostratigraphic markers: 1 – vertebrate faunas of Capetta et al. (1987) and Gheerbrant et al. (1993); 2 – palynoflora of Mohr and Fechner (1986); 3 – oyster fauna and calcareous alga *Ovulites margaritula* (Lamarck) Lamarck of Geyer and Herbig (1988).

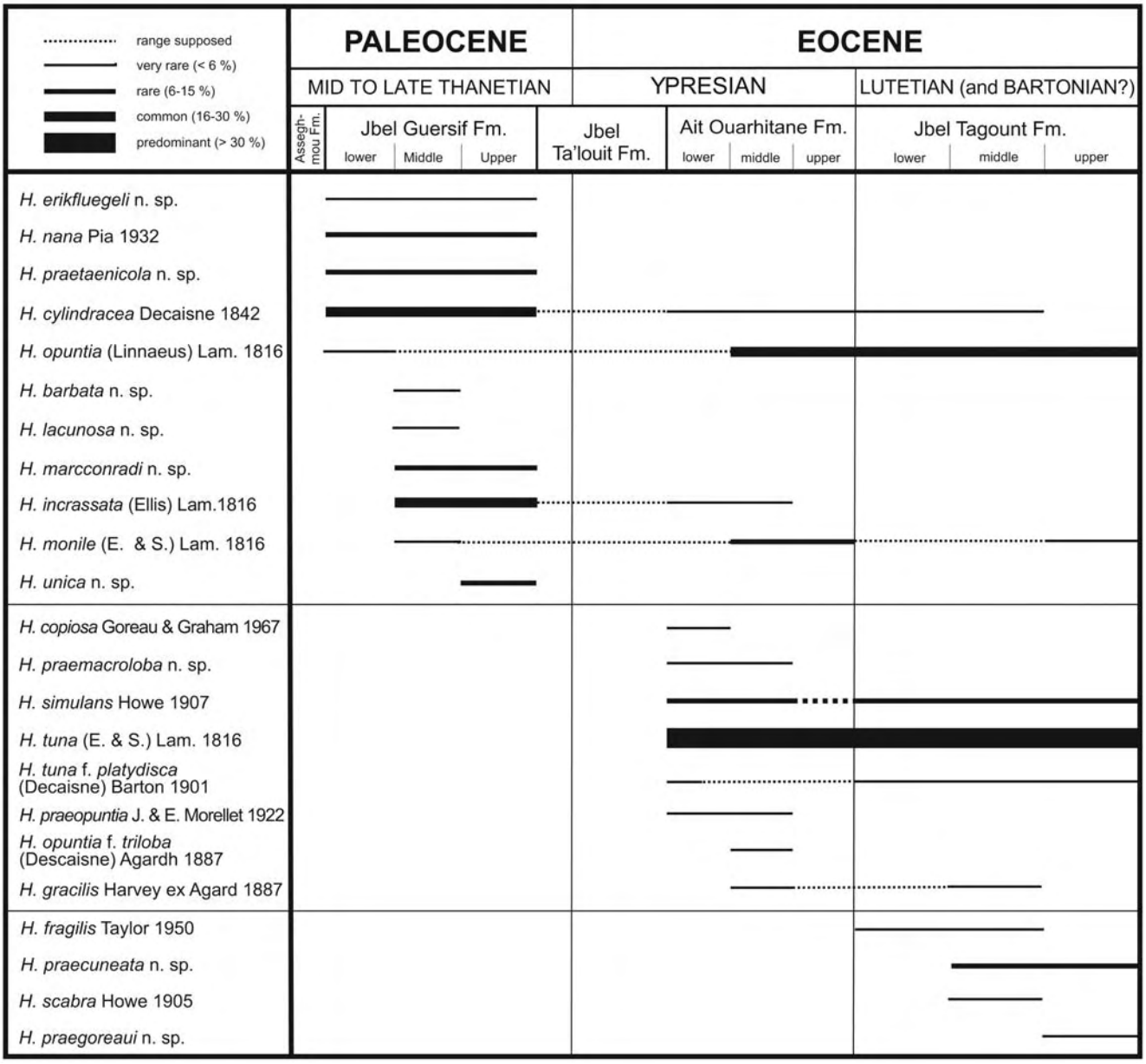

TEXT-FIGURE 4
Range chart of *Halimeda* taxa, Subatlas Group, eastern Ouarzazate basin, southern rim of central High Atlas, Morocco.

high sea-levels throughout the Ypresian, base and top of the stage excepted (cf. Haq et al. 1987). Paleomagnetic data (Gheerbrant et al. 1998) indicate a mid Ypresian base, within or on top of chron 24n.

The overlying Jbel Tagount Formation is a mixed carbonate-siliciclastic succession of shallow-marine to marginal-marine greenish-grey siltstones, subordinate sandstones, and irregularly intercalated bioclastic limestones. The base is latest Ypresian, as shown by palynomorphs (Mohr and Fechner 1986). The top is either late Lutetian or latest Bartonian according to biostratigraphic data from Gauthier (1957) and Geyer and Herbig (1988; see also discussion in Herbig 1991) and correlation with one of the two major sea-level drops towards the end of the middle Eocene.

The transgressive-regressive megacycle of the Subatlas Group along the southern rim of the central High Atlas is conformably overlain by a complex continental succession (Imerhane Group, Herbig 1991), starting with sebkha-type redbeds (Hadida Formation).

CENOZOIC EVOLUTION OF *HALIMEDA*

The stratigraphical range of Recent and fossil species of *Halimeda* remains provisional or unknown due to the lack of sufficient data from the pre-Cenozoic times. Still missing or scarce are data from the Cretaceous-Tertiary boundary interval, from late Eocene and Oligocene, early Miocene, and from some intervals of Pliocene and Pleistocene.

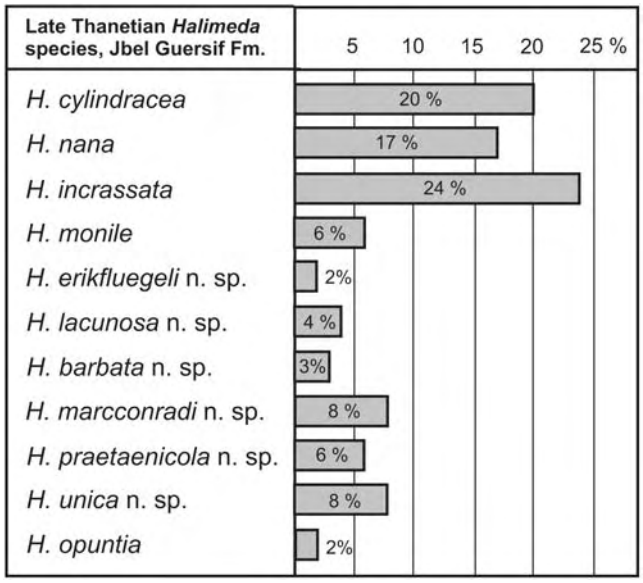

TEXT-FIGURE 5
Percentage distribution of *Halimeda* species in the Jbel Guersif Formation (late Thanetian).

According to present knowledge, *Halimeda* showed little diversification during the Mesozoic, represented only by the phyletic line of *H. cylindracea*. The phyletic line of *H. incrassata* was added, possibly in late Cretaceous, but stratigraphic assignment of the earliest representative is questioned and might be Paleocene or Eocene (Dragastan et al. 2002). Around the Cretaceous-Tertiary boundary the phyletic line of *H. opuntia* originated; the earliest representative is "*H. johnsoni*" = *H. opuntia* from the Maastrichtian to Paleocene. Thus, the genus began to diversify in the Paleocene at latest and during the early to middle Eocene through modifications in internal anatomy and external morphology of the thallus segments. Diversification continued during the Miocene and Quaternary.

From the Paleocene–Eocene interval, three unequivocal fossil species (*Halimeda elliotti, H. nana, H. praeopuntia*) were known for long time. Three still extant species (*H. opuntia, H. fragilis* and *H. tuna*) were reported from the Ypresian of Egypt by Dragastan and Soliman (2002). Also *H. cylindracea* and *H. incrassata* should be present during that period due to the antiquity of their phylogenic lineages and herein *H. cylindracea* is unequivocally identified from the late Thanetian to late Lutetian–(?)latest Bartonian, *H. incrassata* from the late Thanetian–Ypresian (text-fig. 4). All further Paleocene and Eocene species (e. g. those listed in Flügel 1988) were considered to be junior synonyms of these two taxa by Dragastan et al. (2002). The taxonomic position of fossil *H. eocaenica* Morellet and Morellet and *H. johnsoni* Pal remained uncertain to the latter authors, but striking similarity with *H. opuntia* was noted and in our study *H. eocaenica* and *H. johnsoni* are definitely synonymized with *H. opuntia*.

Dragastan et al. (2002) reported eight modern taxa from the late Miocene of Palau: *H. discoidea*, *H. gracilis*, *H. cylindracea*, *H. monile*, *H. bikinensis*, *H. incrassata*, *H. tuna*, *H. tuna* f. *platydisca*. Although not all of these taxa were recorded in overlying Pliocene strata, first occurrences of *H. fragilis*, *H. simulans* and *H. opuntia* raised the number of modern taxa to eleven. Additionally, another taxon, *H.* cf. *bikinensis* was identified.

The Pleistocene revealed another diversification trend. Data from Dragastan et al. (2003) on *Halimeda* species from the Key Largo and Miami Limestone Formations (late Pleistocene, Sangamon interstadial, Florida) demonstrate the presence of nine modern species: *H. incrassata*, *H. monile, H. scabra*, *H. gracilis*, *H. simulans*, *H. opuntia*, *H. tuna*, *H. copiosa*, and *H. discoidea*, acompanied by a new fossil taxon, *H. floridiana* n. sp., and two species in open nomenclature (*Halimeda* sp. 1, *Halimeda* sp. 2). Additionally, *H. opuntia* f. *opuntia*, *H. opuntia* f. *triloba* and *H. micronesica* from probable Upper Pleistocene limestones of Palau are the first appearances in the fossil record (Dragastan et al. 2002). Neglecting the gaps in the record, 15 extant taxa were present during the Pleistocene.

Our results from the Moroccan Thanetian to late Lutetian–(?Bartonian) interval change this picture considerably and demonstrate the still fragmentary knowledge concerning the evolution of *Halimeda*. Altogether, 23 taxa are recorded, nine of them new (text-fig. 4). Twelve are still flourishing today. The fluctuating percentages of species and discontinous records of some modern species await explanation.

Late Thanetian *Halimeda* flora

From the late Thanetian (Jbel Guersif Formation), eleven species of *Halimeda* were identified (text-figs. 4, 5). They represent three categories of taxa: a single well-known fossil species (*Halimeda nana*), four Recent taxa (*H. incrassata*, *H. cylindracea*, *H. opuntia*, *H. monile*), and six new species (*H. erikfluegeli* n. sp., *H. lacunosa* n. sp., *H. barbata* n. sp., *H. marcconradi* n. sp., *H. praetaenicola* n. sp. and *H.unica* n. sp.). Thus, the percentage of orginating species is high in the late Thanetian, showing maximum diversification within the late Thanetian through Lutetian–(?)Bartonian interval. Fossil taxa outnumber taxa surviving into modern time.

Two modern species, *H. cylindracea* and *H. incrassata*, were considered by Dragastan et al. (2002) to have originated in the late Triassic, and in the late Cretaceous or Paleocene, respectively. This is their first unequivocal ocurrence in the Thanetian. This is the earliest record of the Recent species *H. opuntia* and *H. monile.*

Percentage distribution of *Halimeda* species (text-fig. 5) shows two dominant taxa, *H. incrassata* and *H. cylindracea*, contributing 24% and 20%, respectively, of the total *Halimeda* flora. The exclusively Paleocene species, *H.nana*, contributed 17%, but the remaining species only 2–8%.

During the Thanetian, the dominant shape of thallus segments was cylindrical with some compressed variants. Only one common species, *H. nana*, had segments, which were lobate or incipiently branched. *H. opuntia*, a species with flat, disc-like segments, appeared for the first time, but remained very rare. Alhough the morphology of the thallus segments was little diversified during the Thanetian, the cortex system evolved from simple utricle series with two cortical siphons to multiple series containing three to four utricle series. The exception is *H. erikfluegeli* n. sp., unique among all known *Halimeda* species in having a single primary utricle series.

Mid to late Ypresian *Halimeda* flora

In the mid to late Ypresian Ait Ouarhitane Formation, the *Halimeda* flora changed fundamentally regarding further prolif-

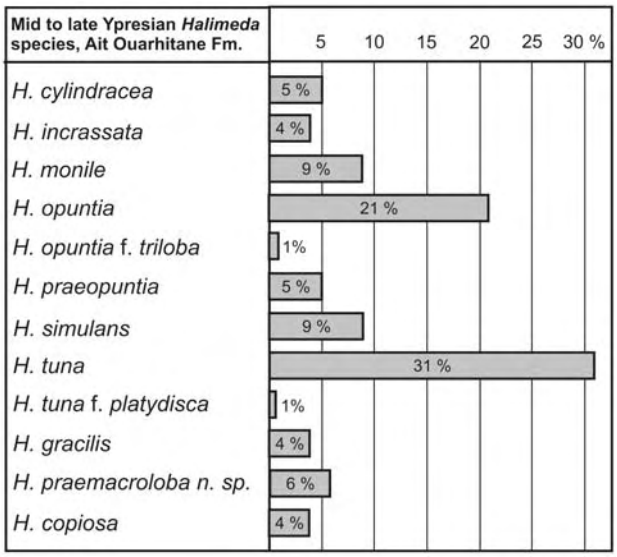

TEXT-FIGURE 6
Percentage distribution of *Halimeda* species in the Ait Ouarhitane Formation (mid to late Ypresian).

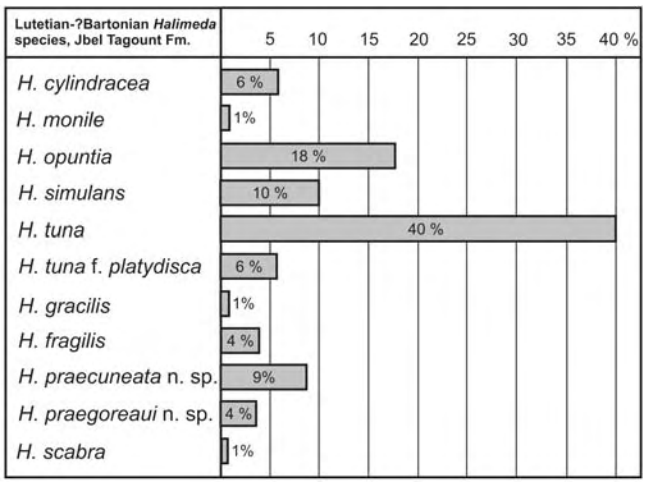

TEXT-FIGURE 7
Percentage distribution of *Halimeda* species in the Jbel Tagount Formation (latest Ypresian to late Lutetian or latest Bartonian).

eration, percentage distribution of taxa, and representation of Recent species (text-figs. 4, 6). Twelve taxa were identified. Among them are a single previously known fossil species (*H. praeopuntia*), one new species (*H. praemacroloba* n. sp.), and ten Recent species. Besides *H. incrassata, H. cylindracea, H. opuntia,* and *H. monile*, already recorded from the late Thanetian, *H. opuntia* f. *triloba*, *H. simulans*, *H.tuna*, *H. tuna* f. *platydisca*, *H. gracilis*, and *H. copiosa* appeared. This is the earliest record of all these taxa, which before had been noted from the Miocene, Pliocene, and late Pleistocene (see above), except for *H. tuna*, which previously was reported from the Ypresian of Egypt.

In contrast to the Thanetian, originating species include only one new taxon, *Halimeda praemacroloba* n. sp.Taxa surviving to the present greatly outnumber fossil ones.

As in the late Thanetian, two *Halimeda* species, but different ones dominate. *Halimeda tuna* and *H. opuntia* contribute 31%, respectively 21% to the total *Halimeda* flora (text-fig. 6). *H. monile* and *H. simulans* remain quite common (9% each). Other species contribute less than 6% each. *H. opuntia* f. *triloba* and *H. tuna* f. *platydisca* are extremely rare.

During the mid to late Ypresian, the dominant morphology of thallus segments was disc-like with many variants, including cuneate, subcuneate, and reniform. Some taxa exhibit modifications in the distribution and arrangement of medullary siphons: loosely, compact, parallel, more or less parallel, intermingled, or separated into round bundles found in *Halimeda tuna*. Concurrently, cortex structures became more complex, as the number of utricle series increased to a maximum of five. Shape and diameter of the utricles became more diverse.

Lutetian–?Bartonian *Halimeda* flora

Although the basal meters of the Jbel Tagount Formation are still latest Ypresian (Mohr and Fechner 1986; Herbig 1991; text-fig. 3), most *Halimeda* should have been derived from Lutetian and questionable Bartonian strata. Therefore, the Jbel Tagount algal flora is generally termed "Lutetian and (?)Bartonian".

The *Halimeda* flora is similar to the mid and late Ypresian (text-figs. 4, 7). Eleven taxa were identified, including nine modern species and two new fossil species. *H. praecuneata* n. sp. and *H. praegoreaui* n. sp. are considered ancestral to the extant species *H. cuneata* and *H. goreaui*. No previously occurring fossil species are present. As in the mid and late Ypresian, the percentage of originating species is low and taxa surviving to the present greatly outnumber exclusively fossil ones.

Of the modern taxa, seven continued from the Ypresian (*H. cylindracea*, *H. monile*, *H. simulans*, *H. tuna*, *H. tuna* f. *platydisca*, *H. gracilis*, *H. opuntia*) and two taxa (*H. fragilis*, *H. scabra*) first occurred in southern Morocco. *H. fragilis* was already known from the Ypresian of Egypt (Dragastan and Soliman 2002), but the range of *H. scabra*, previously known only from the late Pleistocene of Florida (Dragastan et al. 2003), is greatly extended. Three modern taxa identified in the mid to late Ypresian Ait Ouarhitane Formation, were not found in the younger Jbel Tagount Formation, *H. incrassata*, *H. copiosa*, *H. opuntia* f. *triloba*.

Halimeda tuna shows extreme predominance (40%), increasing from the Ypresian (31%). The second most abundant species, *H. opuntia* (18%), continued with almost unchanged dominance (21%). As in the Ypresian, *H. simulans* remained quite common (10% versus 9%), accompanied by the new species *H. praecuneata* n. sp. (9%). Remaining species are rare (<6%), including *H. monile*, which was common in the mid and late Ypresian (9%). *H. gracilis*, and *H. scabra* are extremely rare.

Morphology of thallus segments continued to be predominantly disc-like, as in the mid and late Ypresian, with folded, ribbed, or lobed margins, accompanied by many other types of small ornamentations. Arrangement of medullary siphons did not change significantly; intermingled dispositions and round bundles prevailed. Structure of the cortex system remained similar to that of the mid and late Ypresian.

Mechanisms of evolution

The evolution patterns of the paleoecologically closely related green algal order Dasycladales, described by Barattolo (2002), is useful for comparison with the evolution of *Halimeda* at the southern rim of the central High Atlas. Both probably experienced analogous extinctions at the Cretaceous-Tertiary boundary and adaptive radiation during the Paleogene. According to Barattolo (2002), the recovery phase began in the late Danian and continued into the Thanetian. It was characterized by new occurrences and major increase in diversity. This fits well with the large number of our late Thanetian *Halimeda* species and the appearance of many short-ranging new species, a pattern of adaptive radiation well-known from the fossil record. However, two facts have to be taken into account concerning the *Halimeda* flora at the southern rim of the central High Atlas. First, the sea invaded the area as late as late Thanetian. Thus, immigration and diversification might have been delayed in comparison to the general pattern sketched by Barattolo (2002). Second, the Moroccan epicontinental sea encroached from the Atlantic, without direct connection to Tethys. This could cause the rise of endemic species, but should not invalidate the general model of adaptive radiations.

For Dasycladales, the Ypresian–Bartonian represents the stabilisation phase, indicated by an increasing number of species per genus (Barattolo 2002). In the Moroccan *Halimeda*, the stabilisation interval is indicated by the onset and proliferation of better adapted, i. e. long-ranging taxa. This is a reasonable explanation of the relatively slight floral differences in the interval from the mid Ypresian to the late Lutetian–(?)latest Bartonian. The stable, long-ranging taxa are without exception modern, which proves their exceptional longevity and, indeed, gives the genus *Halimeda* the character of a living fossil (Kooistra et al. 1999). Notwithstanding our results, the time and place of speciation of the modern taxa encountered remains unknown. Considering the paleogeographic setting of the Moroccan epicontinental sea as a relatively small embayment of the Atlantic ocean, bordered by an upwelling zone and characterized by predominantly phosphatic deposits, immigration of taxa originating elsewhere in the course of the Danian-Thanetian recovery phase seems to be more reasonable. We envisage speciation on the wide shallow-water platforms of Tethys and spreading by the circum-equatorial paleo-current to the west. Both, substitution by better adapted taxa and extinction of the new short-ranging late Thanetian species was probably related to a sea-level fall at the top of the Jbel Guersif Formation. The fall is demonstrated by an erosional unconformity and onset of mostly siliciclastic, marginal-marine environments in the overlying Jbel Ta'louit Formation (text-fig. 3), which did not yield *Halimeda* in the study area (Herbig 1991).

The Ypresian–Lutetian transition was less drastic in terms of sea-level history. In the uppermost Ypresian to late Lutetian–(?)latest Bartonian Jbel Tagount Formation distribution of species is extremely uneven, with one species predominating (*H. tuna* 40%) and three others becoming very rare (1%). Some modern taxa, identified in the preceding Ypresian, are absent. This distribution pattern suggests relatively unfavourable ecological conditions, probably triggered by stronger fluctuating sea-levels and concommitant stronger influx of terrigeneous material (text-fig. 3). As an effect, only the best adapted species proliferated in the lack of competition. These unfavourable conditions are clearly demonstrated by the mixed carbonate-siliciclastic succession of the shallow marine to marginal marine Jbel Tagount Formation (Herbig 1991). It is interesting to note that Barattolo (2002) described a gradual decrease of Dasycladales during the Bartonian. It is apparently closely related to global sea-level fall (Haq 1987 and text-fig. 3) and concomitant climate deterioration. Analogously, several species in our *Halimeda* flora decline in the upper Jbel Tagount Formation (text-fig. 4).

Towards the end of the Bartonian and continuing through the Priabonian, a new crisis was indicated for Dasycladales, followed by renewed proliferation starting in the early Oligocene (Barattolo 2002). This evolutionary pathway seems reasonable, accompanying the drastic global sea-level fall and climate deterioration during the late Eocene mentioned before. Although data are lacking, a very similar development may be envisaged for late Eocene–Oligocene *Halimeda*.

Data presented herein show that modern species of *Halimeda* evolved much earlier than hitherto thought (text-fig. 8). From the late Thanetian, four modern taxa have been identified that prove the antiquity of the three phyletic lines postulated by Dragastan et al. (2002), *H. cylindracea*, *H. incrassata* and *H. opuntia*. In the mid and late Ypresian, ten modern taxa were present. In the Lutetian–?Bartonian twelve modern taxa occurred, including those known from the Ypresian, which could not be identified from the younger stage at the southern rim of the central High Atlas. Thus, the postulated first diversification in the late Miocene (Dragastan et al. 2002, see above) has to be revised, since only two additional modern taxa appeared at that time, *H. discoidea* and *H. bikinensis*. This raises the number of known modern taxa to fourteen. In the Pliocene, no new taxa have been encountered. Also a Pleistocene diversification is not supported by fossil data, as only one additional modern species (*H. micronesica*, Palau Limestone, Dragastan et al. 2002) was identified, increasing the number of modern taxa to fifteen.

Hillis (2001) discussed the timing of the diversification of *Halimeda* into phylogenetic lineages by vicariance events using molecular-morphological phylograms presented by Hillis et al. (1998) and Kooistra et al. (1999). Based on the material from the Moroccan Paleogene, Herbig and Dragastan (2005) evaluated her hypotheses. They stated diversification of the basal clades, i. e. the extant Sections, already in early to mid Eocene times, i. e. much earlier than postulated. Accordingly, they stressed the attribution of the genus *Halimeda*, including quite a lot of its extant species, as living fossils, as already done by Kooistra et al. (1999) based on DNA data.

Molecular phylogenetic reconstructions from Kooistra et al. (2002) modified the earlier phylograms and in a subsequent paper by Verbruggen and Kooistra (2004) resulted in a revised subdivision of Halimeda in five basal clades/sections (lineage 1 – Rhipsalis; lineage 2 – Micronesicae; lineage 3 – Halimeda; lineage 4 – Pseudoopuntia; lineage 5 – Opuntia). Of importance for our discussion is a revised content of lineage 2 –Micronesicae, which now is closer to Rhipsalis than to Opuntia. Besides its earlier representatives *H. micronesica* and *H. fragilis* it contains the anatomically and ecologically quite isolated *H. cryptica*, which before formed the monospecific clade/section Cryptica (Hillis-Colinvaux 1980). *H. gracilis* and *H. macroloba*, previously very isolated in clade/section Halimeda (Kooistra et al. 1999), now form the new lineage 4 – Pseudoopuntia, which together with lineage 5 – Opuntia is grouped in a opuntoid basal clade. Further attributions remain unchanged.

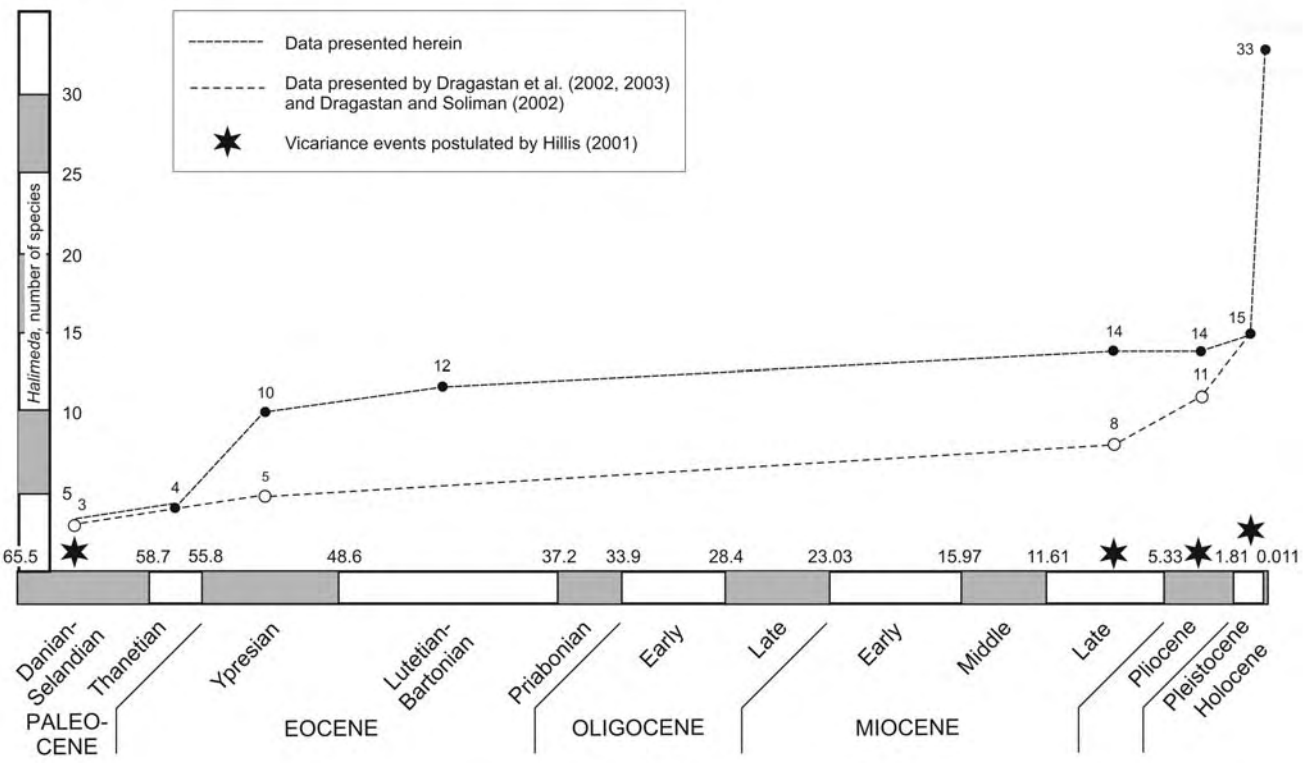

TEXT-FIGURE 8
Evolution of diversity of modern species and subspecies of *Halimeda* according to data presented herein and data from previous authors. The curve suggests that the post-Pleistocene *Halimeda* outburst might be an artefact due to insufficient knowledge of fossil material, or to insufficient preservation/palaeontological differentiation of certain Recent species. Calibration of Cenozoic stages from Gradstein et al. (2005).

These revisions were not taken into account by Herbig and Dragastan (2005) and are discussed below.

According to the data from southern Morocco and compatible with cladistic data from Kooistra et al. (2002) and Verbruggen and Kooistra (2004), lineage 1 – section Rhipsalis, is the oldest clade. It contains the oldest paleontologically defined stem lines of the genus, i. e. *H. cylindracea* lineage, known since the late Triassic, and the next oldest stem line, *H. incrassata* lineage, known since the late Cretaceous (?), latest since Paleocene or Eocene (Dragastan et al. 2002). The antiquity of the lineage Rhipsalis is stressed by *H. monile*, cooccurring with *H. cylindracea* and *H. incrassata* in the oldest marine (late Thanetian) strata from southern Morocco.

The earliest representative of the third paleontologically defined stemline, *H. opuntia* lineage, is latest Cretaceous (Maastrichtian) (Dragastan et al. 2002). In southern Morocco, *H. opuntia* occurs first in the late Thanetian. This means that separation of lineage 1 – Rhipsalis, and lineages 4+5 - the opuntoid basal clade, must be prior, either already in the late Cretaceous, or, if one does not accept the Maastrichtian *H. opuntia*, latest above the Cretaceous-Tertiary boundary in the earliest Paleocene, as postulated by Hillis (2001) for separation of all basal clades. Since in the phylogram of Kooistra et al. (2002) the opuntoid basal clade shares a common ancestor with basal clade Halimeda, and both a common ancestor with basal clade Micronesicae, separation of all basal lineages from clade Rhipsalis has to be sought in the late Cretaceous to early Paleocene interval. As with Dasycladales (Barattolo 2002), separation of the clades might be connected to adaptive radiation in the early Paleocene, following extinction events at the Cretaceous-Paleogene boundary.

In southern Morocco, oldest occurrence of a taxon from lineage 3 – basal clade Halimeda, is mid Ypresian, documented by the outburst of *H. tuna*. Oldest known occurrence of a taxon from lineage 2 – basal clade Micronesicae, is Lutetian with first occurrence of *H. fragilis*. The late occurrence of members of these lineages in Morocco supports our hypothesis that the origin of the species is elsewhere on the wide shelfs of the southern Tethys.

Separation of the opuntoid basal clade into lineage 4 – Pseudoopuntia, and lineage 5 – Opuntia, already occurred before mid Ypresian; at that time *H. gracilis*, a taxon belonging to section Pseudoopuntia occurred first in southern Morocco. Further separation of lineage 5 – Opuntia apparently was rapid and also might have occurred prior to the mid Ypresian. This is indicated by the mid Ypresian first occurrence of *H. copiosa* and the Lutetian first occurrence of *H. praegoreaui*, a precursor of *H. goreaui*, which form a remarkable subclade in the phylogram of Kooistra et al. (2002).

As already outlined by Herbig and Dragastan (2005), species richness in the late Palaeocene–middle Eocene of southern Mo-

rocco indicates rapid diversification within the five basal clades in the early Paleogene. Diversifaction occurred much earlier than the postulated vicariance event in the late Miocene, with closure of the circum-equatorial Tethys currents and the Messinian salinity crisis (Hillis 2001). According to paleontological data, the late Miocene event was of minor importance, with only the *H. discoidea* subclade originating. However, based on phylogram patterns, Kooistra et al. (2002) even postulated an origin of the complete extant *Halimeda* clade at that time, and considered older *Halimeda* to be the result of iterative evolution in different lineages. The wealth of detailed data from the Moroccan Paleogene contradicts that hypothesis. Moreover, it has to be stressed that Paleogene *Halimeda* was restricted to the Tethys realm from eastern Asia and beyond to the westernmost Mediterranean, i. e. Spain and Morocco. Until the late Miocene that latitudinal tropical seaway offered mostly unrestricted genetic exchange across wide shallow carbonate shelfs. Therefore, it apparently accommodated a common genetic pool of *Halimeda* species of the modern Indo-Pacific province. For unknown reasons, there is no undoubted record of *Halimeda* in the Caribbean-Florida province before the Miocene (fide Bassoullett et al. 1983, see also Dragastan et al. 2003, tab. 1). This settlement should be the starting point of (in part still cryptic) allopatric speciations observed in DNA-based phylogenetic trees of extant *Halimeda*.

The Pliocene closure of the Panama seaway seems to have had no effect on speciation according to paleontological data, contrary to the suggestions of Hillis (2001). However, Kooistra et al. (2002) convincingly related so-called pan-tropical species of Indo-Pacific and Atlantic cognate pairs to that vicariance event, which are phenotypically almost identical but genetically different. Also phenotypical convergent but taxonomically differentiated Atlantic and Indo-Pacific taxa, which moreover occupy same habitats, were related to that event.

Latest speciations within *Halimeda* apparently occurred in the Pleistocene.

PALEOENVIRONMENTAL ASPECTS

The marine Paleogene at the southern rim of the central High Atlas was a shallow carbonate ramp sloping towards north and west (Herbig 1991). Due to later uplift of the Jurassic central High Atlas in the north and ensuing complete erosion of all Paleogene strata, the northward directed slope is not well preserved (Herbig 1986, 1991). For the late Thanetian Jbel Guersif Formation, Kuss and Herbig (1993, figs. 5, 6) deduced a tidal flat and restricted lagoon in the easternmost 30 kilometers of the outcrop area around Tinerhir (text-figs. 1, 2). Further west an open lagoon passed into deeper ramp facies some kilometers east of Toundout, west of section SA-5 Oued Imassine. A similar pattern is valid for the mid to late Ypresian Ait Ouarhitane and the uppermost Ypresian to late Lutetian or latest Bartonian Jbel Tagount Formation, but higher energy, oolitic fore-shore deposits replaced tidal flats in the easternmost outcrop areas. Reef and fore-reef deposits are completely missing, so facies models for modern *Halimeda* distribution developed in steep platform-margin environments (e. g. Goreau and Goreau 1973, Johns and Moore 1988) cannot be applied unambiguously to these ramp deposits.

Our *Halimeda* distribution shows little facies-related differentiation. Within the late Thanetian Jbel Guersif Formation, *Halimeda* diversity is highest in shoreward sections (SA-5, SA-8, SA-11, SA-13; text-fig. 2b) in restricted lagoon and tidal flat environments. Fossil assemblages are characterized by predominance of low-diverse miliolids and thick-shelled rotaliids (*Rotalia skourensis* Pfender in Moret 1938), accompanied by echinoids and oysters occurring in lumachelles and (?) biostromes. In the mid to late Ypresian Ait Ouarhitane Formation, maximum *Halimeda* diversity shifted from very nearshore environments to somewhat more open environments, mostly in the transition towards, and within the outer lagoon depicted by Kuss and Herbig (1993) (sections SA-21, SA-7, SA-15, SA-8, SA-18, SA-14, SA-11). Characteristic accompanying biota are molluscs (bivalves, gastropods), commonly as cortoids, and bryozans with a predominance of flexible cellariiform growth types. Oolitic fore-shore facies in the easternmost sections still contain quite common *Halimeda*. Within the latest Ypresian to late Lutetian or latest Bartonian Jbel Tagount Formation, maximum *Halimeda* diversity is concentrated in the transition towards the outer lagoon (section Sa-25a) and in inner lagoon to fore-shore environments (sections SA-18, SA-11) east of Boumalne. Associated biota are predominately echinoids, miliolids, and cellariiform bryozoans in bioclastic facies in section Sa-25a. Oolitic facies becomes important in both eastern sections, and oyster-rich facies is abundant in the easternmost section SA-11. In all formations, grainstones, packstones, and rudstones composed almost exclusively of *Halimeda* segments occur. Many segments are unbroken, suggesting an autochthonous to parautochthonous source.

The best modern analogue may be luxuriant, non-reefal *Halimeda* meadows of the Great Barrier Reef province (Drew and Abel 1985, 1988a, Orme and Salama 1988). They grow in outer shelf environments without mound (biohermal) morphology or association with reefs. Diversity and percentage distribution pattern of species is similar to our fossil examples. Latitudinal position, 10 to 23° S, is comparable with the Paleogene paleolatitude of the southern rim of the central High Atlas, 22 to 23° N (Herbig 1986).

The great diversity of Paleogene *Halimeda* at the southern rim of the central High Atlas and the distribution pattern, with two predominating species, one or two quite common species and many rare to very rare species is remarkable, but not exceptional in modern environments (e. g., Eniwetok atoll/Pacific, Hillis-Colinvaux 1980; Chagos Archipelago/Indian Ocean, Drew 1995; Caribbean region, Littler and Littler 2000; Florida; Dragastan et al. 2003, tab. 1). In the Great Barrier Reef province, Drew and Abel (1985, 1988a) identified fourteen species from *Halimeda* meadows. *Halimeda* assemblages consist of one or two dominant species with maximum abundances of about 18 to 65%, generally one common species with abundance of about 10 to 20%, and several rare species. Species composition and percentages of species varied among traverses, but without showing a certain pattern or gradient. This is perhaps analogous to irregular variations between single sections in each of the studied formations. Possibly, it also reflects the unexplained compositional differences among the different time slices in our study according to Walther's law (text-figs. 5–7). Drew and Abel (1988a) stressed that taxa of section Opuntia, which are lithophytic and normally prefer somewhat sheltered reef crevasses (Hillis-Colinvaux 1980), are the most common contributors. Moreover, the lithophytic taxa of section Halimeda, which favor high-energy reefal environments are present in minor percentages, and the psammophytic taxa of section Rhipsalis are generally quite rare. This means that the *Halimeda*-rich gravels of the Great Barrier Reef province must offer sufficiently stable

substrates for colonisation, and that the high species diversity reflects the preference of the three species groups (sections) for different (micro-)habitats within the *Halimeda* meadows. At the southern rim of the central High Atlas, the dominant late Thanetian species, *H. cylindracea* and *H. incrassata*, belong to the psammophytic taxa of section Rhipsalis and point to existence of wide-spread mobile sands. In contrast, the dominant mid Ypresian to late Lutetian or latest Bartonian species, *H. tuna* and *H. opuntia*, belong to the lithophytic sections Halimeda and Opuntia, in the sense of Hillis-Colinvaux (1980). They point to the existence of coarse, stable gravels. Mobile sands may still have been present during the mid and late Ypresian because the psammophytes, *H. simulans* and *H. monile*, are quite common, but the abundance of mobile sands apparently further decreased during the Lutetian–?Bartonian, where only the psammophyte *H. simulans* remained somewhat common. Another parallel between the Recent *Halimeda* meadows of the Great Barrier Reef province and our Paleogene deposits is the abundance of *Halimeda* to exclusion of other algae, apparently representing dense, monogeneric stands.

The almost imperceptible spatial floral gradient at the southern rim of the central Atlas appears well comparable to that of the extended *Halimeda* meadows of the Great Barrier Reef province. Drew and Abel (1985) extensively sampled the meadows between Cooktown and Lizard Island, an area about 125km long and less than 20km wide. It is comparable to our outcrop belt in size and shape. Like in the fossil counterpart, *Halimeda* distribution does not show any spatial gradient along the length of the area (= along strike), though composition varies irregularly between single traverses. In width (= across strike) no data are available, but considering the open marine outer shelf setting, variations seem unlikely. Differentiation of *Halimeda* species in transects across fore-reef, reef, and lagoon environments appears to be much stronger developed due to highly varied ecological factors (e.g. Goreau and Goreau 1973). In contrast, *Halimeda* meadows developing in open-marine environments, like in the modern Great Barrier Reef province, or on ramp settings, like at the southern rim of the central High Atlas, are characterized by very low paleoenvironmental gradients, resulting in almost unchanged to very slowly changing distribution patterns.

Halimeda can take up nutrients very rapidly. The luxuriant *Halimeda* meadows of the Great Barrier Reef province are connected with upwelling bringing cold, nutrient-rich waters into otherwise nutrient-depleted outer-shelf areas (Drew and Abel 1985, 1988a). *Halimeda* bioherms in the eastern Java Sea (Indonesia) are also tied to upwelling (Roberts et al. 1988). In the case of the Moroccan Paleogene, nutrient-rich waters were delivered via upwelling at the northwest African continental margin, as recorded by the central Moroccan phosphate sea. Riverine input from the hinterland might also have contributed (Herbig and Gregor 1992).

Although no mound-shaped *Halimeda* accumulations, resp. *Halimeda* bioherms could be proved in the Paleogene at the southern rim of the central High Atlas, comparison with lithofacies of modern examples is useful. Hine et al. (1988) described *Halimeda* bioherms from the Caribbean region, which border as a continuous band the margins of a shallow open seaway, the Miskito channel. Dredge samples are coarse, poorly cemented packstones and grainstones, dominated by mostly unbroken, disarticulated *Halimeda* segments set in a poorly sorted sandy matrix. Same lithologies are common in our Paleogene samples. Though we consider the existence of *Halimeda* meadows, not bioherms, the comparison stresses the volumetrically important contribution of *Halimeda* to the shallow Paleogene ramp limestones, probably forming a similar algal belt than in the modern Carribean example.

PALEOALGOLOGY

Green siphonous algae from Morocco

Dasycladalean algae and coralline algae are rare in the central Moroccan epicontinental Paleogene deposits (Herbig 1991, Kuss and Herbig 1993), but green siphonous algae belonging to *Halimeda* and *Ovulites* abound in shallow-marine ramp limestones in certain horizons of the eastern Souss, in the western part of the southern Subatlas-Zone, and the western Khelas (Trappe 1989, 1991, 1992). Both taxa are especially widespread in the eastern Ouarzazate basin (Herbig 1986, 1991), forming extensive *Halimeda* grainstones, packstones and rudstones. In most parts of the Middle Atlas deposits *Halimeda* is ubiquitous, but *Ovulites* is completely absent (Herbig 1991). However, taxonomic studies of the Paleogene algae from Morocco are rare. Pfender (in Pia 1932) noted abundant *Halimeda* from the early Thanetian to late Lutetian or Bartonian Bekrit-Timahdit Formation (Herbig 1991, following Rahhali 1971). She defined *Halimeda nana* from material from a section in the village of Timahdit, Middle Atlas. Material from the type section was restudied by Segonzac et al. (1986), who noted similarities with *H. elliotti* Conard and Rioult 1977 and *H. praemonilis* Morellet 1940. Moreover, she mentioned two bigger-sized species of *Halimeda* in open nomenclature.

Pfender (in Moret 1938, pl. 10, fig. 1-2) noted common *Halimeda* sp. from Skoura, southern rim of the central High Atlas; "*Griphoporella arabica*" Pfender 1938 [= *Ovulites arabica* (Pfender 1938) Massieux 1966] is from the "calcaire à Nautiles de Tamdakht of the western Khelas, about 27km northwest of Ouarzazate. The type stratum is most probably correlated with the nautilid concentrations known from the Middle Anmiter Formation (Kuss and Herbig 1993), a lateral equivalent of the latest Thanetian middle Jbel Ta'louit Formation (Herbig and Trappe 1994, figs. 6, 7). The taxon was reconsidered by Pfender (1940) and Massieux (1966). Herbig (1991) and Kuss and Herbig (1993) did not find typical *Ovulites arabica* in the Middle Anmiter Formation some 55km ENE of the type region, but noted sections corresponding in diameter to *O. maillolensis* Massieux 1966. That taxon was considered by Elliott (1968) to be a junior synonym of *O. arabica*. At the southern rim of the central High Atlas, *O. arabica* is restricted to the latest Thanetian Middle Anmiter Formation (Kuss and Herbig 1993).

Herbig and Geyer (1988) noted abundant *Ovulites margaritula* (Lamarck 1801) Lamarck 1816 from the topmost marine beds (uppermost Jbel Tagount Formation) in sections in the eastern Ouarzazate basin. It commonly occurs at the southern rim of the central High Atlas in the Anmiter and Thersitea Formation (Trappe 1989, 1992) as well as in the Ait Ouarhitane and Jbel Tagount Formation (Herbig 1991). Thus, its local stratigraphic range is restricted from the mid Ypresian to the late Lutetian or Bartonian (Kuss and Herbig 1993).

Herbig (1991) gave short taxonomic descriptions of *Halimeda* sp., *O. arabica*, and *O. margaritula* from these formations, amply illustrated corresponding algal microfacies, and sketched the major spatial distribution of the green siphonous algae at the southern rim of the central High Atlas and in the Middle Atlas.

This material was also used in a taxonomic comparison of green algae between Egypt and Morocco (Kuss and Herbig 1993). In addition data on *Halimeda nana* Pia was reported for the first time from the southern rim of the central High Atlas. It is restricted to the late Thanetian Jbel Guersif and Middle Anmiter Formation (Kuss and Herbig 1993).

Pathways of taxonomy and the evolution of green siphonaceous algae

Conceptions regarding suprageneric taxonomy, anatomy and thallus architecture of Recent green siphonaceous algae have been synthetized amongst others by Feldmann (1946, 1954), Taylor (1950, 1960), Round (1963, 1984), Emberger (1968), Hillis-Colinvaux (1980, 1984), Mattox and Stewart (1984), Lee (1989), Silva (1980, 1982), and Silva et al. (1996). The evolution of these partly strongly deviating taxonomic concepts, including that of fossil siphonaceous algae was portrayed by Dragastan et al. (1997).

Classification of fossil – calcified – green siphonaceous algae is based on skeleton morphology. In general, internal morphology shows siphons, arranged in central medulla and external cortex. Descriptive terms have been used with different meanings, such as tubes or filaments. Littler and Littler (1990, 1992) correctly emphasized that the term filament, used by previous workers, is generally defined as a chain of cells and is incorrectly applied to siphonaceous algae such as *Udotea*, *Halimeda*, and *Penicillus*. They proposed the terms siphon for the medulla and utricle for the cortex.

"Tubular filamentous algae" were assigned to the Codiaceae (*Hedstroemia*, *Garwoodia*) by Rothpletz (1913) and Garwood (1913, 1914), or to different families by Elliott (1956, 1963, 1965, 1975, 1982) including Siphonocladiaceae (*Pycnoporidium*), Codiaceae (*Arabicodium*), or later, Udoteaceae (*Aphroditicodium*, *Boueina*, *Arabicodium*, *Halimeda*).

Tappan (1980) first applied data from Recent algae (morphology, reproductive cycle, and genetic code) to fossil material and related skeletal thallus morphology of fossil algae to modern classification. She jointly assigned modern and fossil siphonaceous genera to the class Bryopsidophyceae, as follows:

(1) Order Codiales Setchell 1929 with families Bryopsidaceae (Bory) De Toni 1888 (*Bryopsis*) and Codiaceae (Trevisan) Zanardini 1843 (*Codium*).

(2) Order Caulerpales Setchell 1929 with four families: Garwoodiaceae (Johnson) Shuysky 1973 (*Garwoodia*, *Hedstroemia, Mitcheldeania, Ortonella*), Udoteaceae (Endlicher) Agardh 1887 (*Anchicodium*, *Arabicodium*, *Avrainvillea*, *Bacinella*, *Boueina*, *Clibeca*, *Halimeda*, *Hikorocodium*, *Litaneia*, *Lithocodium*, *Marinella*, *Orthriosiphon*, *Paleoporella*, *Udotea*, *Uva*, *Zaporella*), Dichotomosiphonaceae Chadefaud ex Feldman 1946, Caulerpaceae Greville 1830. Only Garwoodiaceae and Udoteaceae include modern and fossil taxa.

Concerning fossil siphonaceous genera like *Arabicodium*, *Halimeda*, *Boueina* and *Ovulites*, Bassoullet et al. (1983) used in part earlier classifications, like that from Feldmann (1946, 1954) and Tappan (1980), and placed these taxa in class Chlorophyceae, order Caulerpales, family Udoteaceae. Shuysky (1987), in a work mostly devoted to Paleozoic algae, included them in class Siphonophyceae, order Siphonales, which is characterized by genera with thalli crossed by a polysiphonal medullar zone. However, he dispersed the taxa in different families. Again, Mu (1991) discussed the tortuous pathway and divergent opinions concerning suprageneric taxonomy of siphonous green algae. Though he mentioned "Halimedaceae" with reference to Hillis-Colinvaux (1984), he still placed Halimeda into Udoteaceae.

Hillis-Colinvaux (1984), Dragastan et al. (1997), Littler and Littler (2000, 2003), and Dragastan et al. (2000) referred to the inner structure of Recent and fossil *Halimeda* thalli and indicated that they are correctly assigned to the class Bryopsidophyceae, order Bryopsidales, family Halimedaceae Link 1832.

In a scheme proposed by Dragastan et al. (1997), taxa from the suborder Halimedineae Hillis-Colinvaux 1984 were given higher rank and new suprageneric taxa were introduced. Accordingly, the class Bryopsidophyceae, order Bryopsidales, includes two suborders: Bryopsidineae Hillis-Colinvaux 1984 with three families containing uncalcified extant genera, and Halimedineae Hillis-Colinvaux 1984 with six families. The latter are:

(1) Halimedaceae Link 1832 - they contain Recent and fossil taxa; thalli are calcified, disc-like or more diverse in shape, the segments are crossed by medullar and cortical siphons (utricles), the latter branched (two to seven times). Type genus is *Halimeda* Lamouroux 1812.

(2) Udoteaceae Endlicher 1843 - also known from Recent and fossil material; they are characterized by calcified thalli composed of three parts: uncalcified rhizoidal mass, an upright corticated stalk (= stipe), and a fan-shaped terminal blade or flabellum.The blades are crossed by dichotomically branched siphons and various lateral appendages (Littler and Littler 1990). Type genus is *Udotea* Lamouroux 1812. Fossil taxa include the genera *Ovulites* and *Pseudopenicillus* from the Mesozoic and Cenozoic as well *Penicillus dumetosus* from Pleistocene limestones of the Florida Keys (Dragastan et al. 2003). Kooistra (2002) showed that the brush of genus *Penicillus* is essentially an uncorticated *Udotea* blade, in which the siphons lost their adherence. This demonstrates that *Penicillus* belongs to family Udoteaceae and not to the Caulerpaceae or Halimedaceae.

Further families are the (3) Caulerpaceae Feldmann 1946 and (4)–(6) three families introduced by Dragastan et al. (1997) (for latin diagnoses see also Dragastan and Richter 1999): Pseudoudoteaceae, containing only calcified fossil genera like *Pseudoudotea*, *Hydraea*, *Carpathea*, *Garwoodia*, and *Hedstroemia*; Avrainvilleaceae, containing the non-calcified Recent *Avrainvillea*, and the calcified fossil taxa *Mitcheldeania*, *Pseudomitcheldeania*, *Niteckiella*, and *Bevocastria*; and Rhipiliaceae, containing the non-calcified Recent *Rhipilia,* and the calcified fossil genera *Baratangia* and *Dendronella*(?).

Hillis et al. (1998) and Kooistra et al.(1999) studied morphological features in relation to molecular phylogeny of the 34 known Recent species of *Halimeda* and described three principal lineages corresponding to sections Rhipsalis, Halimeda, and Opuntia + Micronesicae. In a following study, Verbruggen and Kooistra (2004) stated the existence of five sections, resp. monophyletic lineages, Rhipsalis, Micronesicae, Halimeda, Pseudoopuntia, and Opuntia. In spite of punctuated uncertainties, they recognized surprisingly good correlation between molecular data and morphology. Only one morphological character, breadth of segments, does not correlate, a fact already

noted by Barton (1901), who also mentioned that the shape of segments is so different along the thallus of the same specimen that this parameter is not taxonomically useful. However, the results of Hillis et al. (1998) and Kooistra et al. (1999) mean that the morphology of fossil and Recent Halimeda segments are comparable for taxonomic purposes, if suitable parameters are used.

However, Hillis (2000) still doubted the possibility to align fossil and extant species of *Halimeda*. On the contrary, she pointed out that "the apparent explosion of speciation during the Holocene is most likely an artifact of effort." Our study now unequivocally demonstrates the fossil roots of modern species by using primarily the characters of the utricular system, introduced for extant *Halimeda* by Littler and Littler (1997, 2000), and successfully used e.g. by Bandeira-Pedrosa et al. (2004) as a main character for recognition of species.

Dragastan et al. (2000) first used that concept in fossil material and segregated two evolutionary lines of Halimedaceans during the Phanerozoic. The more ancient evolutionary line included fossil and Recent taxa with cylindriform primary cortical siphons (utricles); it evolved in the Ordovician. The second evolutionary line is characterized by vesiculiferous (conical), bulbuous primary siphons; representatives are known from Permian to Recent.

Dragastan et al. (2002) stressed the fact that extant species of *Halimeda* present variable shapes of the segments with a concomitant wide range of internal anatomical differences. *Halimeda* thalli have a large degree of variation regarding the siphon diameters within the inner portion of the medullary zone, as well as a variable number of utricle layers. Therefore, if the thallus segments are disconnected during fossilization, individual segments will present varying numbers and dimensions of utricle layers. Consequently, segments from the base of a plant might be mistaken as separate species from those at the middle or the top. However, due to their relatively narrow-spaced stratigraphical occurrences and identical morphology, *Halimeda* segments from late Miocene to Pleistocene limestones of Palau, western Pacific, were considered to represent the same species than the modern anatomical counterparts. This stresses the concept of punctuated equilibrium (Gould and Eldredge 1977) for *Halimeda* species, which thrived in morphological stasis for long periods after first appearance (see also Kooistra et al. 2002: 133). It contradicts the assumption of homology and paralellism between fossil and Recent taxa, as expressed for *Halimeda opuntia* by Hillis (2000), as well as the model of iterative evolution forwarded by Kooistra et al. (2002).

Nevertheless, the cortical system with variously shaped utricle series remains the primary key for identification of fossil material and corresponding extant species. Currently, only a few fossil *Halimeda* species can be considered true species. Based on the utricular characters, it can be shown that 21 Triassic–Cenozoic taxa were based on the long-ranging *Halimeda cylindracea* (late Triassic to Recent), which has only two segment morphotypes. Only a few taxa remained valid (Dragastan et al. 2002). *H. incrassata* (Cretaceous–Recent) has variously shaped segments. It includes seven apparently synonymous fossil taxa. *H. opuntia*, which originated at the K/T-boundary and still thrives today, has extremely variable thalli segments and includes two synonymous fossil taxa (*H. johnsoni* and *H. eocaenica*).

Taxa now included in the family Halimedaceae originated from the Paleozoic and Mesozoic family Protohalimedaceae, which represents an ancestral group of green siphonaceous algae (Dragastan et al. 2002, 2003). Data gathered in recent years from Pleistocene, Pliocene, and Miocene, and data presented herein from early and mid Eocene, and late Paleocene demonstrate that *H. cylindracea*, *H. incrassata*, and *H. opuntia* have persisted in various shallow-marine calcareous facies. Many gaps still remain in our knowledge concerning the stratigraphical record of *Halimeda* species, particulary in pre-Cenozoic and Oligocene strata, at the Oligocene-Miocene boundary, and in parts of the Pliocene and Pleistocene. However, it is clear that the genus *Halimeda* can be considered as a living fossil (Kooistra et al. 1999), because more than twelve species evolved between the Cretaceous-Tertiary boundary and the Pleistocene.

Identification of fossil and modern *Halimeda* species based on segment morphology

Identification keys for modern *Halimeda* species were given by different authors (e. g. Taylor 1960; Hillis-Colinvaux 1980; Littler and Littler 1997, 2000, 2003;Verbruggen et al. 2005b). Mostly, the general morphology of the thallus (holdfast, shape of segments, branching, ornamentations, nodes, medullary siphons and the shape of utricle series are the most important characters to discriminate species. A special attention was given to the shape and distributional pattern of surface utricles, respectively peripheral utricles by Hillis-Colinvaux (1980, p.38, fig. 17) ,which correspond to tertiary or higher utricle series in the nomenclature of fossil *Halimeda*. We propose to use the same nomenclature regarding the utricle series for fossil and modern *Halimeda* species. Accordingly, primary utricles are disposed closest to the medulla, followed by secondary utricles, tertiary utricles (= equivalent of peripheral utricles), etc., towards the periphery of the cortex. Nodal structure, which is an easily observed, important character for discrimination of modern species, is not preserved in fossil material.

Verbruggen et al (2005a, b) presented a complete key for modern *Halimeda* species from section Rhipsalis. They used different morphometric methods and discriminant analysis for species differentiation, starting from segment morphology and internal anatomy. Not all anatomical characters are equally important for recognition of fossil species, as rarely preserved peripheral utricles, nodal height, or even medullar siphons, which might be completely dissolved.

Attribution of calcified segments of fossil and modern *Halimeda* to discern species is based on hierarchical morphological/dimensional criteria (Tab. 1), as seen in ideal sections crossing thalli segments at least in two planes: vertical-axial, transversal, and, subordinate, in a third vertical tangential cortical section. As stressed above, size, shape and arrangement of cortical utricles are the most important criteria to discriminate species. For the first time in fossil record, cavities were observed in the cortex of some species (*Halimeda monile*, *H. lacunosa* n. sp., *H. praetaenicola* n. sp.), which are interpreted to be gametangia. In modern species, differences in size, shape and position of gametangia are species characters (Hillis-Collinvaux 1980; Drew and Abel 1988b; Bandeira et al. 2004), but were not included by Verbruggen et al. (2005) in their key of modern *Halimeda* species.

TABLE 1
Hierarchical grouped identification characters for extant and fossil species of *Halimeda* based on segment morphology

1	**Inner morphology of the thallus segment**
1.1	**Cortex**
1.1.1	Primary utricles: shape, proximal and distal diameter
1.1.2	Number of dichotomic series, shape of secondary, tertiary, and subsequent utricle series
1.1.3	Length of each utricles series
1.1.4	Thickness of cortex
1.1.5	Disposition of primary utricles in vertical section (dense, loose, regular, etc.)
1.1.6	Presence of cavities (= gametangia) in the cortex, their shape (pedunculate, claviform, pear-shaped) and dimensions (length and width)
1.1.7	Location of cavities: utricular in first, second, third, etc. series; or only in between utricles
1.2	**Medulla**
1.2.1	Shape; contact between medulla and cortex (regular, undulatory, irregulary, etc.), diameter and relation to width of cortex (medulla-cortex ratio)
1.2.2	Disposition and distribution of medullar siphons in the vertical section (linear, intermingled, loose, dense, etc) and in transverse section (compact, loosely, etc.)
1.2.3	Number of the rows of medullary siphons in vertical and transverse section
1.2.4	Diameter of medullary siphons
1.2.5	Shape of medullary siphons (cylindrical, constricted, pear-shaped, etc., dichotomously branched or not)
2	**External morphology of the segment** cylindrical, cuneate, ovoid, disc-like, with lobes (how many?), ribs, protuberances, branched or unbranched. But note: along thallus, the shape of segments might be differentiated

Studied material and repository

The study is based on 410 stratigraphically collected samples from 25 sections. About 100 thin-sections were studied, 7×10cm or 10×15cm in size, from *Halimeda*-rich facies containing thousands of segments. Sample numbers refer to sections in Herbig (1991, figs. 17, 27, 30). Numbering is based on sampling date followed by number of each sample taken during the day (day-month-year/xx). All thin-sections are housed at the Institut für Geologie und Mineralogie, Universität zu Köln, under these numbers. Figured thin-sections received additional numbers GIK 1872 to GIK 1919 (collections "Geologisches Institut Köln"); suffices a–x denote either different figured species or holotype and paratypes within a single thin-section.

SYSTEMATIC PALEONTOLOGY

Division CHLOROPHYTA
Class BRYOPSIDOPHYCEAE Round 1963
Order BRYOPSIDALES Schaffner 1922
Suborder HALIMEDINEAE Hillis-Colinvaux 1984
Family HALIMEDACEAE Link 1832
Genus *Halimeda* Lamouroux 1812
Type species: *Halimeda tuna* (Ellis and Solander) Lamouroux

Halimeda cylindracea Decaisne 1842
Plate 1, figures 1–6; Plate 2, figures 1–7; Plate 16, figures 1–4; Plate 27, figures 1–4

Halimeda cylindracea n. sp. – DECAISNE 1842, p. 103. – HILLIS-COLINVAUX 1980, p. 100; figs. 4-5, 104. – DRAGASTAN, LITTLER and LITTLER 2002, pl. 2, figs. 1- 3. – LITTLER and LITTLER 2003, p. 244-245.
Halimeda sp. – PFENDER in MASSIEUX 1966, pl. 5, figs. 5-6, 8, 10. – DELOFFRE, POIGNANT and TEHERANI 1977, pl. 6, figs. 3-4. – RADOICIC 1990, pl. 12, fig. 3. – SIMMONS and JOHNSTON 1991, pl. 2, figs. 1-2. – RADOICIC 1992, pl. 9, figs. 1-2. – KUSS and HERBIG 1993, pl. 8, fig. 9.
Boueina (?) *pygmaea* Pia. – BECKMANN and BECKMANN 1966, pl. 9, fig. 129.
Halimeda sp. 1 – SEGONZAC, PEYBERNES and RAHHALI 1986, pl. 1, fig. 3.
Halimeda elliotti Conard and Rioult 1977 – RADOICIC 1998, p. 186; pl. 3, only fig. 2.
Halimeda nana Pia. – KUSS and HERBIG 1993, pl. 5, fig. 8.
Arabicodium tibeticum Yu-Ling. – RADOICIC 1998, pl. 6, fig. 7.

Material: lower–upper Jbel Guersif-Formation, late Thanetian (Pls. 1, 2) – 130584/5, section SA-5 (GIK 1874a); 160584/8, section SA-8 (GIK 1879a); 180584/6, section SA-11 (GIK 1886a); 031085/5, section SA-13 (GIK 1897a).

Middle–upper Ait Ouarhitane Formation, mid to late Ypresian (pl. 16, figs.1–4) – 160584/16, section SA-8 (GIK 1882a); 180584/26b, section SA-11 (GIK 1889); 180584/28b, section SA-11 (GIK 1890a); 121085/8, section SA-21 (GIK 1916a).

Lower–middle Jbel Tagount Formation, latest Ypresian to late Lutetian or latest Bartonian (pl. 27) – 091085/15, section SA-18 (GIK 1912a); 161086/6, section SA-25a (GIK 1918); 161086/7, section SA-25a (GIK 1919a)

Description: Thalli segments cylindrical, in some cases slightly compressed, crossed in the central area by tubular, medullar siphons (pl. 1, figs. 1–2, 5–6; pl. 2, figs. 1, 7). The medullar area has plenty of tubular siphons, or in some cases is empty or partially preserved.

In a transverse section, the medullar area appears round in shape, with medullary siphons more or less parallel and regularly disposed (pl. 2, fig. 6). In oblique-longitudinal section the medullary siphons are pearl-shaped, with slightly constricted

TABLE 2
Size parameters of *Halimeda cylindracea* Decaisne 1842 (in millimeters) from Paleogene formations, southern Morocco and late Miocene interval of Palau Limestone (Dragastan et al. 2002).

Halimeda cylindracea **DECAISNE 1842**	**LATE THANETIAN**	**MID TO LATE YPRESIAN**	**LUTETIAN–?BARTONIAN**	**LATE MIOCENE**
Outer diameter (D)	2.50–2.70	2.80–3.o	3.20–3.70	3.80–4.0
Medulla diameter (md)	0.50–0.54	0.62–0.70	1.0–1.20	1.60–1.80
Medulla siphon diameter (msd)	0.040–0.042	0.048–0.050	0.058–0.070	----
Cortex thickness (cth)	0.16–0.17	0.18–0.35	0.23–0.30	0.78
Primary utricle proximal diameter (pudp)	0.028–0.030	0.030–0.032	0.032–0.036	0.030
Primary utricle distal diameter (pudd)	0.065–0.070	0.080–0.086	0.085–0.090	0.090
Primary utricle length (pul)	0.10	0.10–0.12	0.10–0.12	0.10–0.12
Secondary utricle diameter (sud)	0.030	0.040	0.040–0.050	0.020–0.060
Secondary utricle length (sul)	0.060	0.078	0.070–0.085	0.030–0.080
Tertiary utricle diameter (tud)	0.015	0.015	0.015	0.015–0.030
Tertiary utricle length (tul)	0.020	0.020	0.020–0.026	0.015–0.025
Quaternary utricle diameter(qud)	0.010	0.012–0.015	0.012–0.018	0.010–0.015
Quaternary utricle length (qul)	0.010	0.012–0.014	0.010–0.015	0.010–0.015

intervals between. They are dichotomously branched, in some cases at 90 degree and are loosely disposed in parallel to irregular manner. The number of rows of medullar siphons is variable between fourteen to eighteen, exceptionally up to twenty (pl. 1, figs 5–6; pl. 2, figs. 6–7).

The cortex system is moderately thick and has three or four utricle-series (pl. 1, figs. 2–3; pl. 2, figs. 6–7).

The primary utricles are long, cylindrical, faintly conical in shape, increasing slightly in diameter distally. The primary utricles support secondary utricles, which are small and tubular in shape and branch dichotomously. These secondary utricles bear short, tubular, slightly inflated distally tertiary utricles and these support a ultimate, fourth series of utricles, very short, and extremely small in diameter. Dimensions are listed in Table 2.

Remarks: Specimens from the late Thanetian and from the mid Ypresian to late Lutetian or latest Bartonian interval differ somewhat in morphology of medullar siphons, and shape and dimensions of the cortical utricle series. The specimens from the mid to late Ypresian (pl. 16, figs. 1–4) have strongly calcified segments, much longer and larger in diameter, but with thinner cortex.The medullar area is larger and crossed by numerous rows of siphons (maximal 14). In tangential sections, distributional pattern for terminal utricles is the same, being disposed like a "rosette" with 8 up to 10 very small, round siphons (pl. 2, figs. 2–3 – arrows; pl. 16, figs.2–3 – arrows). The Lutetian–?Bartonian specimens of *Halimeda cylindracea*, mostly seen in longitudinal-oblique and transverse sections in entire or broken segments, present slightly larger dimensional parameters of thalli compared with specimens from the late Thanetian and mid to late Ypresian. In the Lutetian–?Bartonian, the specimens have only three utricle series: primary are long, cylindrical (pl. 27, figs. 1–4), secondary are tubular and distally also slightly inflated, dichotomously branched (pl. 27, figs. 1, 3), third series of very short and tubular utricles (pl. 27, figs. 1, 4).

Halimeda cylindracea is considered to be the oldest taxon from the stock of fossil and Recent *Halimeda* species, arising latest in the late Triassic (Dragastan et al. 2002). The morphological and biometrical data of specimens from the late Thanetian, mid to late Ypresian, Lutetian–?Bartonian, and late Miocene (material from Dragastan et al. 2002) conserved the same medullar pattern and cortex structure with three or four utricle series, almost identical with Recent specimens.

H. cylindracea can be compared with Paleocene *H. nana*, which also has cylindrical thallus, small in diameter, but the latter differs because some segments are branched. Segments are crossed by 6-8 rows of medullary siphons. The cortex presents in most cases two, rarely three utricle series. Also Recent *H. incrassata* differs by the morphology of the utricles. Primary utricles are sturdy, well inflated distally, secondary are medium long, subglobose and the tertiary ones are short and conical in shape.

Halimeda nana Pia 1932
Plate 3, figures 1–9; Plate 5, figures 5–6

Halimeda nana n. sp. – PIA 1932 in PIA, PFENDER and TERMIER, pl. 2, fig. 4. – ELLIOTT 1955, p. 126, p. 128; pl. 1, fig. 3. – SEGONZAC, PEYBERNES and RAHHALI 1986, p. 502; pl. 1, figs. 1, 2, 4, 5-8. – BASSOULLET et al. 1983, p. 488; pl. 7, figs. 5-6. – TRAGELEHN 1996, pl. 48, fig. 1. – KUSS and HERBIG 1993, p. 277; pl. 5, figs. 1-5; pl. 8, figs. 4-5.
Halimeda sp. 2 – SEGONZAC, PEYBERNES and RAHHALI 1986, p. 503; pl. 1, fig. 4.

Material: lower–upper Jbel Guersif-Formation, late Thanetian – 130584/3, section SA-5 (GIK 1872a); 160584/12, section SA-8 (GIK 1881); 180584/6, section SA-11 (GIK 1886b); 031085/2, SA-13 (GIK 1895a).

Description: Thallus segments cylindrical, small in diameter, in some cases branched or with a small lobe or protuberance (pl. 3, fig. 8). Segments crossed by narrow medullar area; siphons fine, undulose, disposed more or less parallel in 6–8 rows and dichotomously branched (pl. 3, figs. 1–2, 4, 6–7, 9; pl. 5, fig. 6). Cortex not thick, composed in majority of specimens by two, or,

TABLE 3
Size parameters of *Halimeda incrassata* (Ellis) Lamouroux 1816 (in millimeters) from Paleogene formations, southern Morocco, late Miocene interval of Palau Limestone (Dragastan et al. 2002), and late Pleistocene Key Largo Formation, Florida (Dragastan et al. 2003).

***Halimeda incrassata* (ELLIS) LAMOUROUX 1816**	**LATE THANETIAN**	**MID TO LATE YPRESIAN**	**LATE MIOCENE**	**LATE PLEISTOCENE**
Outer diameter (D)	2.20–2.80	2.70–3.0	1.50–2.50	3.0–5.0
Medulla diameter (md)	0.60–0.80	0.80–1.0	---	1.30–1.60
Medulla siphon diameter (msd)	0.10–0.12	0.10–0.16	0.12–0.15	0.12–0.16
Cortex thickness (cth)	0.30–0.45	0.35–0.50	---	0.050–0.080
Primary utricle proximal diameter (pudp)	0.020	0.026	0.028	---
Primary utricle distal diameter (pudd)	0.040	0.048	0.060	0.030–0.060
Primary utricle length (pul)	0.10	0.12	0.12–0.14	0.12–0.16
Secondary utricle diameter (sud)	0.030–0.045	0.060	0.045–0.060	0.030–0.045
Secondary utricle length (sul)	0.080–0.090	0.10	0.090–0.10	0.080–0.10
Tertiary utricle diameter (tud)	0.010	0.012	0.010–0.015	0.010–0.020
Tertiary utricle length (tul)	0.020	0.020–0.025	0.025–0.032	0.020–0.030

rarely, three utricle series. Primary utricles rather short, tubular, cylindrical inflated to the distal part (pl. 3, figs. 1, 9; pl. 5, fig. 5). Secondary utricles short, cylindrical, dichotomously branched; tiny tertiary utricles very short (pl. 3, fig. 9, arrow).

Dimensions in mm (for abbreviations see table 2): D – 0.30-0.87, md – 0.15–0.38, msd – 0.016–0.035, cth – 0.082–0.10, pudp + pudd – 0.010–0.016, pul – 0.060–0.082, sud – 0.012–0.020, sul – 0.025–0.032, tud – 0.005–0.007 (rarely present), tul – 0.010–0.012?

Remarks: Pia (1932) described *Halimeda nana* quite insufficiently from its type locality Timahdit, Middle Atlas (Morocco). Originally considered to be Danian in age, Herbig (1991) concluded a late early Thanetian–Lutetian–?Bartonian age of the algal-bearing strata (see also Segonzac et al. 1986). According to Kuss and Herbig (1993) and our data, the species is restricted to the Paleocene; at the southern rim of the central High Atlas, it is an index species of the Thanetian. A revision based on specimens from the type locality by Segonzac et al. (1986) provided biometric data, a good description of the medullar area and the structure of the cortex, and very good ilustrations. In spite of that study the taxon needs further consideration, since it is only represented by small, cylindrical thallus segments close to the stock of *H. cylindracea*. Like the Turonian *H. elliotti*, a species with four cortical utricle series, it might fall into synonymy with *H. cylindracea*.

Halimeda incrassata (Ellis) Lamouroux 1816
Plate 4, figures 1–9; Plate 5, figures 1–4; Plate 16, figures 5–6

Corallina incrassata n. sp. – ELLIS 1768, p. 408; figs. 20-27.
Halimeda incrassata (Ellis) – LAMOUROUX 1812, p. 186. – LAMOUROUX 1816, p. 307. – HILLIS-COLINVAUX 1980, p. 93; fig. 22. – LITTLER and LITTLER 2000, p.402-403; figs. 1 -2. – DRAGASTAN, LITTLER and LITTLER 2002, p. 10; pl. 3, fig. 7. – DRAGASTAN, LITTLER and LITTLER 2003, p. 21; pl. 1, figs. 1-11; pl. 2, figs. 6-7; pl. 5, figs 3-4, 7; pl. 6, fig. 3.
Halimeda pipaldehlaenisis n. sp. – BADVE and NAYAK 1983, p. 140; pl. 6, figs. 1-2, 4, 10.
Halimeda robusta n. sp. – BADVE and NAYAK 1983, p. 140; pl. 6, figs 9, 12.
Halimeda corneola n. sp. – BADVE and NAYAK 1983, p. 140; pl. 6, fig. 11.
Halimeda densituba n. sp. – BADVE and NAYAK 1983, p. 142; pl. 6, figs. 6-7.
Halimeda triradiata n. sp. – BADVE and NAYAK 1983, p. 142; pl. 6, figs. 3, 5, 8.
Halimeda chiplonkari n. sp. – BADVE and KUNDAL 1986, p. 155; fig.13.
Halimeda agharkari n. sp. – BADVE and KUNDAL 1986, p. 156; figs. 14-15.
Halimeda nana Pia – KUSS and HERBIG 1993, pl. 5, fig. 7; pl. 8, fig. 10.

Material: lower–upper Jbel Guersif-Formation, late Thanetian (pl. 4; pl. 5, figs. 1–4) – 130584/4, section SA-5 (GIK 1873a); 130584/5, section SA-5 (GIK 1874b); 160584/8, section SA-8 (GIK 1879b); 160584/11, section SA-8 (GIK 1880a); 170584/31, section SA-10 (GIK 1885); 031085/4, section SA-13 (GIK 1896a); 031085/5, section SA-13 (GIK 1897b); 131085/16; section SA-22 (GIK 1917a).

Lower and middle Ait Ouarhitane Formation, mid to late Ypresian (pl. 16, figs. 5–6) – 041085/4, section SA-14 (GIK 1900a); 061085/2; section SA-15 (GIK 1905a).

Description: Thallus segments mostly cylindrical in shape, in some cases flattened. Segments crossed by medullar area with large variability in diameter. The medullar area is pierced by long, cylindrical, parallel siphons disposed in 8–10 rows (pl. 4, fig. 6; pl. 5, fig. 1). The cortex is thick, but thickness depends on position, that is, age of segment within specimen; it consists of three, in some cases up to five utricle series (pl. 4, figs. 8–9).The primary utricles are sturdy, cylindrical–conical, well inflated towards the distal end and have large diameters (pl. 4, figs. 1, 5, 8–9; pl. 5, fig. 4; pl. 16, figs. 5–6). The primary utricles support tubular, medium-long, subglobose, dichotomously branched secondary utricles, which in turn bear short tertiary utricles, small in diameter and conical in shape (pl. 4, figs. 6, 8–9, pl. 5, figs. 1–2, 4, pl. 16, fig. 5). In tangential section, the tertiary utricles are round in shape; they are disposed in regular polygonal pattern. Dimensions are listed in Tab. 3.

Remarks: Fossil *Halimeda incrassata* was found in the late Miocene of Palau limestone, western Pacific (Dragastan et al. 2002). Thalli segments are cylindrical in shape, crossed by large medullar area and cortex with three utricle series. The cortex

TABLE 4
Size parameters of *Halimeda monile* (Ellis and Solander) Lamouroux 1816 (in millimeters) from Paleogene formations, southern Morocco, late Miocene interval of Palau Limestone, (Dragastan et al. 2002), and late Pleistocene Key Largo Formation, Florida (Dragastan et al. 2003).

***Halimeda monile* (ELLIS AND SOLANDER) LAMOUROUX 1816**	**LATE THANETIAN**	**MID TO LATE YPRESIAN**	**LUTETIAN–?BARTONIAN**	**LATE MIOCENE**	**LATE PLEISTOCENE**
Width (W)		5.0	3.0	---	5.20–7.50
Outer diameter (D) resp. thickness (th)	(D)0.67–0.80	(th) 1.60	(th) 0.80	---	(th) 1.50–2.00
Medulla diameter (md)	0.35–0.40	0.40–0.80	0.40–0.60	1.20	1.50–1.80
Medulla siphon diameter (msd)	0.038–0.040	0.032–0.075	0.030–0.080	0.090–0.10	0.080–0.11
Cortex thickness (cth)	0.16–0.20	0.35	0.45	0.30–0.60	---
Primary utricle proximal diameter (pudp)	0.020–0.026	0.020	0.028	0.030	---
Primary utricle distal diameter (pudd)	0.046	0.048–0.050	0.052	0.060–0.075	0.035–0.060
Primary utricle length (pul)	0.080–0.086	0.090	0.10	0.15	0.12–0.15
Secondary utricle diameter (sud)	0.016–0.020	0.030	0.035	0.030–0.035	0.030–0.038
Secondary utricle length (sul)	0.050–0.060	0.058	0.075	0.090	0.072–0.090
Tertiary utricle diameter (tud)	0.006–0.008	0.015–0.020	0.030	0.025–0.030	0.015–0.025
Tertiary utricle length (tul)	0.015–0.018	0.025	0.035	0.060	0.047–0.058
Diameter of gametangial cavities (dsc)	---	0.15–0.25	0.20	---	---
Length of gametangial cavities (lsc)	---	0.25–0.30	0.20	---	---

utricles are of shape and dimensions close to the specimens found in the late Pleistocene limestones from the Florida Keys (Dragastan et al. 2003).

During the late Thanetian and mid to late Ypresian, *Halimeda incrassata* had only cylindrical thalli segments with some tendency to flattening. However, in the Upper Pleistocene deposits the same species has variable shaped segments, depending on their position along the thallus: segments from the basal part of the thallus are predominantly cylindrical, those from the middle part and from the tips of the thallus are subcuneate to flat-subtriangular.

We suppose that the differentiation into variously shaped thallus segments started in the Eocene and became more intense during the Miocene. This observation is a solid argument that fossil representatives of *H. incrassata* belong to the evolutionary line of Recent *H. incrassata* and do not represent morphological nearly identical, that is, homologous species evolving in parallel.

See *H. cylindracea* for discussion of differences.

Halimeda monile (Ellis and Solander) Lamouroux 1816
Plate 6, figures 2–5; Plate 14, figures 1–6

Corallina monile n. sp. – ELLIS and SOLANDER 1786, p. 110; pl. 20, fig. C.
Halimeda monile (Ellis and Solander) – LAMOUROUX 1816, p. 306. – HILLIS-COLINVAUX 1980, p. 98; fig. 24. – DRAGASTAN, LITTLER and LITTLER 2002, p. 10; pl. 2, figs. 4–5. – LITTLER and LITTLER 1989, p. 92. – DRAGASTAN, LITTLER and LITTLER 2003, p. 22; pl. 2, figs. 1-5; pl. 5, fig. 6. – LITTLER and LITTLER 2000, p. 404; figs. 1-2.
Halimeda incrassata f. *monilis* (Ellis and Solander) – BARTON 1901, p. 27.

Material: middle Jbel Guersif-Formation, late Thanetian (pl. 6, figs. 2–5) – 130584/4, section SA-5 (GIK 1873b); 131085/16, section SA-22 (GIK 1917b).

Middle–upper Ait Ouarhitane Formation, mid to late Ypresian (pl. 14, figs. 1–2, 4–6) – 180584/23, section SA-11 (GIK 1888), 180584/28b, section SA-11 (GIK 1890b); 121085/8, section SA-21 (GIK 1916b).

Upper Jbel Tagount Formation, Lutetian–?Bartonian (pl. 14, fig. 3) – 110988/3, section SA-5 (GIK 1875a).

Description: Thallus segments cylindrical, semicylindrical or plane, disc-like in shape, trilobed or ribbed (pl. 6, figs. 3–4). In transverse-oblique sections, the cylindrical or semicylindrical segments (pl. 6, figs 2–3, 5) show a narrow central medullar area, which is crossed by few medullar siphons disposed in 4–6, more or less parallel rows, loosely disposed. In transverse and oblique sections (pl. 6, figs. 3–5), the disc-like segments have some ribs, small lobes or protuberances. In the central area of the medulla, the siphons are loosely disposed and large in diameter. To the margin of the medulla, they become small in diameter, and are dense and regular disposed. In oblique transverse section, we observed in some cases that the small medullary siphons are arranged in round, compact bundles, which radiate to the outside (pl. 6, fig. 2).

The cortex, not so thick, is composed of three utricle series. Primary utricles are subtriangular to conical in shape. They support numerous parallel, medium short, gently conical secondary utricles, which are dichotomously branched. The secondary utricles bear very small and short tertiary utricles, distally less expanded. In the mid Ypresian to late Lutetian or latest Bartonian deposits, many plane, disc-like segments occur, disposing large cavities within the cortex in the place of utricles, where gamentangial cavities first originated, to continue as

gametophore towards the outside (pl. 14, fig. 3). In many cases, they are located on the secondary or tertiary utricles and rarely on the primary utricles. The cavities are of elongate, ellipsoidal to sphaeroidal shape, large in diameter. In some cases they are disposed intracortical instead of utricular. Dimensions are listed in Table 4

Remarks: Recent *Halimeda monile* has a thallus composed by cylindrical, elsewhere disc-like or trilobed segments, 1–5 mm wide, 3–8 mm long and 0.70–1.5 mm thick. The cortex is crossed by three to five utricle series (Hillis-Colinvaux 1980; Littler and Littler 2000). Fossil specimens of *H. monile* also have differently shaped segments, cylindrical in the late Thanetian, disc-like, flattened during the mid Ypresian to late Lutetian or latest Bartonian, and in the late Miocene. During late Pleistocene, many isolated thalli segments deriving from the middle part of branched thalli, and also some deriving from the tips, are disc-like, trilobed, similar to Recent forms.

Recent and fossil specimens differ somewhat in the constitution of the cortex. Only three utricle series are observed in pre-Pliocene specimens, three to five from the Pliocene onward to the Recent. Additionally, to present knowledge, segments of pre-Pliocene specimens show only one, maximally three morphotypes compared with Pliocene–late Pleistocene thalli, which contain multiple morphotypes, similar to the the multiple-shaped segments in the branched thallus of Recent specimens.

From Recent *Halimeda monile*, Hillis-Colinvaux (1980, p. 203) described the shape of gametangia and the gametophores. She mentioned that gametangia arise as extensions from peripheral or secondary utricles in the cortex, a fact which is now proved in fossil specimens. Like in the Recent, their position is intracortical or utricular. Such cavities were also cited and described as gametangial cavities from Dasycladaceae, Halimedaceae or Gymnocodiaceae (see *Permocalculus*? *halimedaformis* described by Bucur 1994).

The Paleocene–Eocene *H. praemonilis* Morellet is very close to *H. monile*, but to present knowledge, it seems not to be identical. However, a revision of the type material, which could not be located, is urgently needed.

Halimeda erikfluegeli Dragastan and Herbig **n. sp.**
Plate 6, figures 6–7

Derivatio nominis: dedicated to Prof. Dr. Erik Flügel from Erlangen University, Germany, for his contributions to carbonate microfacies and a life dedicated to paleontology.

Holotype: Plate 6, figure 6, sample 021085/7 (GIK 1894a).

Paratype: Plate 6, figure 7.

Locus typicus: Section SA-12 of Herbig (1991) (see Appendix 1).

Stratum typicum: upper Jbel Guersif Formation, late Thanetian

Additional material: 031085/2, section SA-13 (GIK 1895b), lowermost Jbel Guersif Formation, late Thanetian.

Description: Thallus segments cylindrical, with large medullar area crossed by long, parallel siphons, and surrounded by a thin cortex. In longitudinal section (pl. 6, fig. 6), the medullar siphons have a small diameter and are disposed in very long, regular rows parallel along the axis. The cortex is crossed only by primary utricles. They are of subconical shape and are distally inflated club-like. The transverse section (pl. 6, fig. 7) presents a circular (round) thallus segment crossed by six to eight medullar siphons.

Dimensions in mm (for abbreviations see table 2): D – 0.58–0.60, md – 0.36–0.42, msd – 0.0320.040, cth – 0.090–0.10, pudp – 0.024–0.026, pudd -0.036–0.042 , pul – 0.076–0.090.

Remarks: *Halimeda erikfluegeli* n.sp. is a unique taxon from the late Thanetian, which has only primary utricles in the cortex. Their shape is characteristic for the new species. The presence of only primary utricles might represent a primitive character.

To our knowledges, all other fossil and Recent *Halimeda* species have a cortex pierced at least by two utricle series; the majority of the taxa have multiple utricle series, from three up to seven.

The genus *Codium*, a non-calcifying modern green siphonaceous alga could be compared with the new taxon because it also has a large medullar area and a cortex pierced only by primary utricles. However, medullar siphons intermingle and are not regularly arranged.

Halimeda lacunosa Dragastan and Herbig **n. sp.**
Plate 7, figures 1–3

Derivatio nominis: "lacunosa" – from the presence of large cavities or excavations in the cortex.

Holotype: Plate 7, figure 1, sample 031085/4 (GIK 1896b).

Paratype: Plate 7, figure 2, an additional section from the same sample (GIK 1896c).

Locus typicus: Section SA-13 of Herbig (1991) (see Appendix 1).

Stratum typicum: middle Jbel Guersif Formation, late Thanetian

Additional material: 160584/11, section SA-8 (GIK 1880b), middle Jbel Guersif Formation, late Thanetian.

Description. Thallus segments cylindrical or subglobose, crossed by medium large medullar area; cortex well calcified.

The medullar area presents fine medullar siphons, small in diameter, disposed in ten to twelve rows. Medullar siphons are not preserved in the two additional specimens known (pl. 7, figs. 2–3). The cortex is pierced by three to four utricle series. Large gamentangial cavities occur intracortical or utricular (pl. 7, figs. 1–3). They are ellipsoidal or sphaeroidal in shape (pl. 7, fig.3). The primary utricles have a cylindrical shape (pl. 7, fig. 1, arrow). They are followed by shorter secondary utricles, also cylindrical and dichotomously branched. They support the tertiary utricles, which are fine, short, tubular and also dichotomously branched. In some cases a fourth utricle series appears, extremely short and very small, observed only in completely preserved areas of the most external part of the cortex (pl. 7, fig. 1).

Dimensions in mm (for abbreviations see table 2): D – 1.20–1.50, md – 0.28–0.35, msd – 0.020–0.024, cth – 0.18–0.22, pudp + pudd – 0.024–0.030, pul – 0.10–0.12, sud – 0.014–0.020, sul – 0.065–0.070, tud – 0.008–0.010, tul – 0.018–0.020, dsc – 0.065–0.072, lsc – 0.22–0.28.

Remarks: *Halimeda lacunosa* n. sp. is comparable with the modern species *H. micronesica*. Both have three utricle series, but differ in shape, diameter, and length of the utricles. The fossil species also shows more loosely disposed medullary siphons. Another modern species, *H. lacunalis*, is comparable by presence of two to four utricle series in the cortex. Moreover, both Recent species have multiform segments (subcylindrical, subcuneate, obovate, discoidal to reniform, occasionally ribbed) opposed to cylindrical to subglobose segments of the new species. The latter can be also compared with *Permocalculus*? *halimedaformis* Bucur 1994 from the Lower Cretaceous. Bucur (1994) considered that taxon was a green alga which has some characteristics of the genus *Halimeda*, like the structure of the cortex and the presence of large gametangial cavities disposed in places of cortical utricles (see Bucur 1994, pl. 6, fig. 4). However, we consider that this taxon belongs to *Halimeda*.

Halimeda barbata Dragastan and Herbig **n. sp.**
Plate 7, figures 4–5

Derivatio nominis: "barbata" – from the Latin, "bearded", referring to the tiny, short "hairs" of the ultimate utricle series disposed in solitary tufts.

Holotype: Plate 7, figure 4, sample 160584/11 (GIK 1880c).

Paratype: Plate 7, figure 5, an additional section from the same sample (GIK 1880d).

Locus typicus: Section SA-8 of Herbig (1991) (see Appendix 1).

Stratum typicum: middle Jbel Guersif Formation, late Thanetian.

Description: Thallus segments entire or broken, cylindrical in shape, crossed by a large, empty medullar area. The cortex is medium thick, pierced by four utricle series. The primary utricles are long, tubular (cylindrical), increasing gently to the distal part (pl. 7, fig. 4, arrows). They support secondary utricles, which are short, also tubular, and dichotomously branched. The secondary utricles bear tiny, very short tertiary utricles. The following fourth utricles are extremely short, hair-like, appearing like a row of very small pores along the cortex margin (pl. 7, figs. 4–5 ,arrow).

Dimensions in mm (for abbreviations see table 2): D – 1.08–1.10, md – 0.50, msd – not observed, cth – 0.28–0.30, pudp – 0.020–0.025, pudd – 0.030, pul – 0.14–0.16, sud – 0.015–0.016, sul – 0.045-0.050, tud – 0.010, tul – 0.015–0.020, qud – 0.006, qul – 0.004.

Remarks: *Halimeda barbata* n. sp. can be compared with the Recent species *H. gracilis*, *H. micronesica*, and *H. lacunalis*. Fossil (late Miocene, Dragastan et al. 2002) and Recent *H. gracilis* show a cortex composed of two or three utricle series. The long primary utricles of *H. gracilis* are conical to bulbuous and, thus, differ from the new taxon. The primary utricles of *H. gracilis* support clavate secondary utricles, which in turn bear short subconical tertiary utricles, which again differ from those of the new species.

H. micronesica presents a cortex mainly of three, rarely of four utricle series with successive dichotomies. The morphology of primary, secondary and tertiary utricle series is nearest to the new species, only the fourth utricles differ.

H. lacunalis also has a cortex pierced by four utricle series. The primary utricles are identical, secondary and tertiary utricles are clavate, and thus different from the new species. The fourth, densely disposed utricles differ by their tiny conical shape

Halimeda marcconradi Dragastan and Herbig **n. sp.**
Plate 8, figures 1–5

Derivatio nominis: dedicated to Dr. Marc Conrad for his contributions in the field of Paleoalgology.

Holotype: Plate 8, figure 1, sample 021085/7 (GIK 1894b).

Paratypes: Plate 8, figures 2-5, additional sections from the same sample (GIK 1894c-f).

Locus typicus: Section SA-12 of Herbig (1991) (see Appendix 1).

Stratum typicum: upper Jbel Guersif Formation, late Thanetian.

Description: Thallus segments of cylindrical shape. The segments show a medium, large medullar area surrounded by a thick cortex. The medullar area is crossed by long siphons distributed in 6–14 parallel rows of siphons, slightly constricted and not branched (pl. 8, fig. 5). Due to abrasion in transport, some segments present empty medullar areas (pl. 8, figs. 3–4). The cortex is composed only of two utricle series. The primary utricles are long, tubular and slightly inflated in their distal part (pl. 8, figs 1–3). They support medium long, tubular, dichotomously branched secondary utricles, also distally inflated (pl. 8, figs 1–2, 4). Broken segments in plate 8, figure 3 show only a part of the medullar area and the cortex.

Dimensions in mm (for abbreviations see table 2): D – 0.58–1.0, md – 0.20–0.25, msd – 0.032–0.040, cth – 0.20–0.30, pudp – 0.020–0.030, pudd – 0.032–0.038, pul – 0.070–0.082, sud – 0.016–0.024, sul – 0.040–0.046.

Remarks: The characteristic feature of the new species is the thick cortex pierced only by two utricle series combined with a medullar area, which is rich in siphons, disposed in up 14 rows. *Halimeda marcconradi* n.sp. is comparable to fossil specimens of *H. gracilis* from late Miocene and late Pliocene (Dragastan et al. 2003), and also to Recent specimens by identically shaped cylindrical, somewhat compressed segments, but it differs by the cortex, pierced only by two utricle series. Moreover, *H. gracilis* has multiform segments, including subcuneate and reniform segments, showing entire,undulose or lobed margins.

Halimeda praetaenicola Dragastan and Herbig **n. sp.**
Plate 9, figures 1–6

Derivatio nominis: "praetaenicola" – comparable with the modern species *H. taenicola*, but occuring earlier in geologic history.

Holotype: Plate 9, figure 1, sample 021085/7 (GIK 1894g).

Paratypes: Plate 9, figure 5, an additional section from the same sample (GIK 1894h).

Locus typicus: Section SA-12 of Herbig (1991) (see Appendix 1).

Stratum typicum: upper Jbel Guersif Formation, late Thanetian.

Additional material: 130584/3, section SA-5 (GIK 1872b), 031085/2, section SA-13 (GIK 1895c), both lower Jbel Guersif Formation, late Thanetian.

Description: Thallus segments cylindrical or subcylindrical, having a large medullar area and pierced by six to eight cylindrical medullary siphons, large in diameter (pl. 9, figs. 2, 4). In some cases, siphons not preserved in the central area of the medulla (pl. 9, figs. 1, 6). Thick, strongly calcified cortex crossed by two or rarely three utricle series. Primary utricles of moderate length, tubular, slightly increasing distally (pl. 9, figs. 1, 3, 5) and becoming club-shaped near the connection to the secondary utricles (pl. 9, figs. 3, 5). Secondary utricles subconical and dichotomously branched (pl. 9, fig. 3). In some cases tertiary utricles appear short and conical (pl. 9, fig. 3). In transverse sections, the morphology of primary and secondary utricles is very clear (pl. 9, figs. 2, 4, 6). In one transverse section (pl. 9, fig. 2), two utricles are very long, club-shaped, and project across the margin of the segment. They correspond to pedunculate gametangia. The club-shaped, long terminal part represents the origination place of the gametangium, which is situated already outside of the proper thallus.

Dimensions in mm (for abbreviations see table 2): D – 0.84–1.80, md – 0.42–0.72, msd – 0.040–0.060, cth – 0.16–0.36, pudp – 0.024–0.036, pudd – 0.042–0.048, pul – 0.084–0.096, sud – 0.016–0.032, sul – 0.032–0.050, length of gametangial penducule – 0.20–0.24, diameter of club-shaped gametangia – 0.070–0.085.

Remarks: *Halimeda praetaenicola* n.sp. is comparable with the Recent *H. taenicola*, which has a thallus composed of cylindrical to subcuneate segments. Subcuneate segments are absent in the new species. The morphology of primary utricles is very similar, but the secondaries are different, being short, club-shaped in the new species. The tertiary utricle series known from the Recent species was not found in the new taxon. The Paleocene species *H. nana* has also cylindrical, rarely branched segments, but differs in its internal structures with two, rarely three utricle series densely disposed in the cortex. Primary utricles are short, tubular to slightly inflated and secondaries are short and tubular. *H. praeopuntia* differs by disc-like, in cases trilobed segments. The cortex of the new species differs from the comparable species discussed above having a cortex with three to four utricle series.

The presence of utricles, modified into gametangia and projecting outside the cortex, is an important discovery with taxonomic relevance and a suggestion of the "power of proliferation" in some fossil species. In modern species, the size, shape, and number of mature gametangia are of significant taxonomic value for species discrimination (Hillis-Colinvaux 1980; Drew and Abel 1988b).

Halimeda unica Dragastan and Herbig **n. sp.**
Plate 10, figures 1–7

Derivatio nominis: "unica" – from unexpected morphology, respectively unique in the spectrum of *Halimeda* species.

Holotype: Plate 10, figure 1, sample 031085/5 (GIK 1897c).

Paratypes: Plate 10, figures 2-7, additional sections from the same sample (GIK 1897d-i).

Locus typicus: Section SA-13 of Herbig (1991) (see Appendix 1).

Stratum typicum: lower Jbel Guersif Formation, late Thanetian.

Description: Thallus segments long, cylindrical in shape, crossed by a medium-large medullar area (pl. 10, figs. 1–2); medullary siphons only in some cases preserved (pl. 10, figs. 4–5, 7). In longitudinal or oblique-longitudinal sections, long, undulose medullar siphons, filiform, small in diameter, distributed in 6–14 parallel rows (pl. 10, figs 1–2). In transverse section, segments of circular outline, empty or with many medullar siphons in the central area (pl. 10, figs. 4–5). Medium-thick cortex, pierced by three utricle series. Primary utricles subcylindrical, medium-long and distally slightly inflated. Short secondary utricles also cylindrical, dichotomously branched, carrying fine, short tertiary utricles (pl. 10, figs 2, 4–6). In tangential section, the tertiary utricles show a regular disposition in polygonal bundles of six to eight siphons (pl. 10, fig.3, arrow).

Dimensions in mm (for abbreviations see table 2): D – 0.60–0.96, md – 0.42–0.48, msd – 0.032–0.038, cth – 0.14-0.16, pudp – 0.020–0.024, pudd – 0.030–0.032, pul – 0.060–0.068, sud – 0.016–0.020, sul – 0.030–0.046, tud – 0.006, tul 0.005–0.006.

Remarks: In overall shape, *Halimeda unica* n. sp. is comparable to Recent and fossil *H. cylindracea* and *H. incrassata*, and to the Paleocene *H. nana*. However, *H. cylindracea* differs from the new taxon by having a cortex with four utricle series, and *H. incrassata* by a different morphology of the utricle series, which are more conically inflated distally. *H. nana* is a small cylindrical, branched or unbranched species having a protuberance or lobe and a cortex with two, rarely three, utricle series (see descriptions).

Halimeda opuntia (Linnaeus) Lamouroux 1812
Plate 6, figure 1; Plate 11, figures 1–11; Plate 12, figures 1–4; Plate 24, figures 1–5

Corallina opuntia n. sp. Linnaeus 1758, p. 805.
Halimeda opuntia (Linnaeus) – LAMOUROUX 1812, p. 3; p. 181-188. – MORELLET and MORELLET 1922, p. 296; pl. 12, figs. 1-5. – HILLIS-COLINVAUX 1980, p. 110; figs. 19, 51, 52. – BASSOULLET et al. 1983, p. 490; pl. 7, fig. 9. – LITTLER et al.1989, p. 94-95. – LITTLER and LITTLER 2000, p. 406-407. – DRAGASTAN, LITTLER and LITTLER 2002, p. 12; pl. 9, figs 1-2. – DRAGASTAN and SOLIMAN 2002, p. 18; pl. 7, figs 5-8, 10. – DRAGASTAN, LITTLER and LITTLER 2003, p. 23; pl. 3, figs 1-3; pl. 5, fig. 2.
Halimeda eocaenica n.sp.– MORELLET and MORELLET 1940, p. 203-205; fig. 2.
Halimeda sp. – PFENDER in MASSIEUX 1966, p. 126; fig. 6.
Halimeda johnsoni n.sp. – PAL 1971, p. 133-134; pl. 1, fig. 1.
Halimedacea gen et sp. indet. 1 – TRAGELEHN 1996, pl. 48, fig. 6.

Material: Lower Jbel Guersif-Formation, late Thanetian – 180584/6, section SA-11 (GIK 1886c).

Middle–upper Ait Ouarhitane Formation, mid to late Ypresian (pl. 11, pl. 12, figs. 1–4) – 160584/22, section SA-8 (GIK 1883a); 061085/2, section SA-15 (GIK 1905b); 091085/9, section SA-18 (GIK 1908); 091085/10, section SA-18 (GIK 1909a).

Lower–upper Jbel Tagount Formation, latest Ypresian to late Lutetian or latest Bartonian (pl. 24) – 110988/3, section SA-5 (GIK 1875b); 180584/36, section SA-11 (GIK 1893a); 041085/18, section SA-14 (GIK 1902a).

TABLE 5
Size parameters of *Halimeda opuntia* (Linnaeus) Lamouroux 1812 (in millimeters) from Paleogene formations, southern Morocco, Pliocene interval of Palau Limestone, (Dragastan et al. 2002), and Late Pleistocene Key Largo Formation, Florida (Dragastan et al. 2003).

***Halimeda opuntia* (LINNAEUS) LAMOUROUX 18112**	**LATE THANETIAN**	**MID TO LATE YPRESIAN**	**LUTETIAN–?BARTONIAN**	**PLIOCENE**	**LATE PLEISTOCENE**
Medulla diameter (md)	0.15	0.15–0.20	0.20–0.40	0.15–0.40	1.20–1.60
Medulla siphon diameter (msd)	0.030–0.040	0.050–0.075	0.045–0.060	0.050–0.065	0.050–0.060
Cortex thickness (cth)	0.90–0.12	0.10–0.15	0.10–0.20	---	---
Primary utricle proximal diameter (pudp)	0.010	0.020–0.025	0.015–0.020	0.030	0.030
Primary utricle distal diameter (pudd)	0.040	0.050–0.060	0.040–0.050	0.045	0.042
Primary utricle length (pul)	0.080	0.10–0.12	0.10–0.14	0.14–0.15	0.12–0.14
Secondary utricle diameter (sud)	0.025	0.020–0.030	0.025–0.040	0.050–0.60	0.045–0.050
Secondary utricle length (sul)	0.046	0.060–0.075	0.050–0.070	0.18–0.20	0.16–0.18
Tertiary utricle diameter (tud)	0.012	0.010–0.012	0.015	0.025–0.30	0.020–0.025
Tertiary utricle length (tul)	0.015	0.015	0.015	0.010–0.14	0.008–0.010

Description: Thallus segments disc-like, flat or somewhat contorted, frequently ribbed. The upper margin entire, undulate, or rarely lobed. Numerous randomly cut sections allowed an idealized reconstruction of the general shape of the segment (pl. 11, fig. 11), since the outlines of the cutting planes (pl. 11, figs 1–9) are a function of their position in the thallus and, thus, can be attributed to base, middle part, or upper part of the segments or to the laterals. Transverse sections of the middle and upper part of the segments show their true flat disc-like shape and prove that the large undulose margins have ribs or small angular protuberances (pl. 11, figs. 3–4, 9). Oblique transverse sections across the lower part of the laterals of the segments are of the same shape, also showing large, undulose margins (pl. 11, figs. 1–2, 5). Oblique longitudinal sections across the laterals in the upper parts of the segments again demonstrate the flat, disc-like, in cases somewhat ribbed, shape (pl. 11, figs. 7–8).

A single late Thanetian specimen (pl. 6, fig. 1) presents a disc-like shape with large, undulose margins, but without ribs. mid to late Ypresian segments (pl. 11, figs. 1–11; pl. 12, figs. 1–4) are somewhat larger. They are also disc-like in shape, but contorted with ribs or folded. Their margins are entire and undulose.Thallus segments from the Lutetian–?Bartonian have a very flat, disc-like shape, some with small lobes (pl. 24, figs. 1, 3); the entire margins are less undulose.

In transverse section, the segments are crossed in the central area by numerous medullary siphons. They are grouped in eight to ten round bundles, each containing six siphons. In some specimens, large cavities filled with microcrystalline calcite conceal the medullar siphons (pl. 11, figs. 3–4). In oblique-transverse section, the segments present only the medullar siphons and traces of a thin cortex destroyed during reworking.

In transverse section, the cortex shows small internal projections, which separate the medullar bundles (Pl 11, fig. 10). The primary utricles are long, tubular, and distally slightly inflated. They support tubular, medium-long, dichotomously branched secondary utricles (pl. 11, figs. 5–6, 8; pl. 12, figs. 1, 4), which, in turn, support short, tiny, subconical tertiary utricles, which are also dichotomously branched (pl. 11, figs. 1–2, 8). Dimensions are listed in Tab. 5.

Remarks: Most mid to late Ypresian specimens of *Halimeda opuntia* are small, flat, disc-like thallus segments with undulose margins and ornamented by ribs, developing into small lobes during Lutetian–?Bartonian. The late Thanetian specimen is of same general shape, but less ornamented. Pliocene and Pleistocene specimens of *H. opuntia* have large, millimetric-sized, disc-like segments, and are ornamented by ribs, contortions and lobes. Recent thallus segments are of identical shape, but still larger and variously ornamented. Thus, in general size and ornamentation of thallus segments has apparently been increasing since the Thanetian. A similar development is seen in the cortex. From Thanetian until late Miocene, it conserves three utricle series, but in Pliocene and Pleistocene has five utricle series.

It seems plausible that some areas of the cortex of fossil specimens, which are very thin or almost disappear, represent the locations of cavities at which gametangia start to develop from the inner part of the cortex (pl. 12, fig. 1, lower right). In Recent *Halimeda opuntia*, gametangia originate at the top and the lateral margins of the segments within the cortex and migrate towards the outside. They are visible as black spots on the marginal part of the segments in text-fig. 9.

Halimeda opuntia* f. *triloba (Decaisne) Agardh 1887
Plate 12, figure 5

Halimeda triloba n. sp. – DECAISNE 1842, p. 102.
Halimeda opuntia f. *triloba* (Decaisne) – AGARDH 1887, p. 84.
Halimeda opuntia f. *triloba* (Decaisne) – LITTLER and LITTLER 2000, p.406-407. – DRAGASTAN, LITTLER and LITTLER 2000, p. 12; pl.10, figs. 6-9; pl. 11, figs. 1, 4; pl. 12, fig. 8.\

Material: middle Ait Ouarhitane Formation, mid to late Ypresian – 150584/12, section SA-7 (GIK 1878a).

Description: A single slightly oblique transverse section shows a well-calcified thallus segment of discoidal, wing-like shape. The segment is slightly contorted, possibly ribbed with three lobes, one in the central part and two lobes towards the extremi-

TEXT-FIGURE 9
Halimeda opuntia (Linnaeus) Lamouroux 1816. Branched calcified thallus composed by disc-like segments showing gametangia at their margins (black in photograph, green in life). Recent, Atlantic Ocean (Coll.Dragastan), ×5.

ties. It is crossed by a large round to elongate medullar area; medullar siphons are grouped in large round bundles, observed well on the left side of the segment figured on plate 12, figure 5. The thick cortex is crossed by three utricle series. The primary utricles are slightly conical and support short, cylindrical, dichotomously branched secondary utricles. Secondary utricles bear small, very short, conical tertiary utricles.

Dimensions in mm (for abbreviations see table 2): dm – 0.90–1.20, dms – 0.070–0.10, cth – 0.030–0.040, pud – 0.060–0.10, pul – 0.20–0.25, sud – 0.030–0.042, sul – 0.10–0.12, tud – 0.020–0.030, tul – 0.030–0.045.

Remarks: The mid to late Ypresian segment of *Halimeda opuntia* f. *triloba* differs from Pleistocene segments of the same species by its small dimensions, and the tendency of medullary siphons to be disposed in round bundles, crossing the segment vertical and radially.

Halimeda simulans Howe 1907
Plate 13, figures 1–7; Plate 26, figures 1–7

Halimeda simulans n. sp. – HOWE 1907, p. 503, pl. 29. – HILLIS-COLINVAUX 1980, p. 103; fig. 26. – LITTLER and LITTLER 1997, p. 112; fig. 163. – LITTLER and LITTLER 2000, p. 408. – DRAGASTAN, LITTLER and LITTLER 2002, p. 11; pl. 7, figs. 6-8; pl. 9, figs. 3-4. – DRAGASTAN, LITTLER and LITTLER 2003, p. 23; pl. 3, figs. 4-6; pl. 5, fig. 5; pl. 7, fig. 5.

Material: lower-middle Ait Ouarhitane Formation, mid to late Ypresian (pl. 13) –150584/11, section SA-7 (GIK 1877a); 031085/12, section SA-13 (GIK 1899); 041085/4, section SA-14 (GIK 1900b); 061085/2, section SA-15 (GIK 1905c).

Lower and uppermost Jbel Tagount Formation, latest Ypresian to late Lutetian or latest Bartonian (pl. 26) – 180584/31, section SA-11 (GIK 1891a); 180584/36, section SA-11 (GIK 1893b).

Description: Thallus segments flat, subcylindrical or subcuneate; segment margins entire, but mostly fragmentarily preserved. In transverse section, the subcuneate shape is clear (pl. 13, figs. 4–5). Segments well calcified, with a medium-large medullar area in the central part (pl. 13, figs.1–6). Long, more or less parallel, cylindrical medullary siphons, loosely disposed. Depending of age and position along thallus, segments show numerous medullary siphons (pl. 13, fig.1), or, distally, fewer siphons (pl. 13, figs. 2, 6). In some specimens siphons are not preserved (pl. 13, fig. 7). Thick cortex crossed by two, rarely by three, utricle series. Primary utricles (pl. 13, figs. 3–4, 6–7) are conical in shape and support small, bulbuous, shorter secondary utricles, which are dichotomously branched. Rarely, segments have a third utricle ; series consisting of very short, conical, distally inflated utricles (pl. 13, fig. 7, pl. 26, fig. 6–7). Dimensions are listed in Table 6.

Remarks: Mid Ypresian to Pleistocene *Halimeda simulans* show in the cortex mostly two utricle series, rarely three series. Recent specimens differ by the presence of three to five utricle series (Littler and Littler 2000).

Halimeda praeopuntia Morellet and Morellet 1922
Plate 15, figures 1–4

Halimeda praeopuntia n. sp. – MORELLET and MORELLET 1922, p. 295-296; pl. 12, figs. 6-10, 12-14.
? *Halimeda eocaenica* n. sp. – MORELLET and MORELLET 1940b, p. 203-205; fig. 2.

Material: lower–middle Ait Ouarhitane Formation, mid to late Ypresian – 091085/10, section SA-18 (GIK 1909b); 111085/18, section SA-20 (GIK 1914); 121085/6, SA-21 (GIK 1915a).

Description: Thallus segments more or less flat, disc-like or fan-shaped, having undulose margins. In longitudinal and oblique longitudinal sections, the segments show a slight expansion in the central part, indicating an incipient small lobe (pl. 15, fig. 1). The large medullar area is crossed by sparse, intermingled medullar siphons, which are cylindrical, slightly constricted and arranged in four to six rows (pl. 15, figs. 1–4). Cortex of variable thickness, with an irregular transitional zone between medulla and cortex. Cortex pierced by two or three utricle series. Primary utricles are conical to subconical, medium-short, and support short, tiny, conical, dichotomously branched secondary utricles. Sometimes they bear ultra-short, fine tertiary utricles.

TABLE 6
Size parameters of *Halimeda simulans* Howe 1907 (in millimeters) from Paleogene formations, southern Morocco, Pliocene interval of Palau Limestone, (Dragastan et al. 2002), and late Pleistocene Key Largo Formation, Florida (Dragastan et al. 2003).

***Halimeda simulans* HOWE 1907**	**MID TO LATE YPRESIAN**	**LUTETIAN–?BARTONIAN**	**PLIOCENE**	**LATE PLEISTOCENE**
Medulla diameter (md)	0.42–0.60	0.45–0.68	0.60	0.80–1.10
Medulla siphon diameter (msd)	0.032–0.050	0.032–0.060	0.065– 0.075	0.065–0.072
Cortex thickness (cth)	0.16–0.45	0.18–0.60	0.60–0.75	---
Primary utricle distal diameter (pudd)	0.040–0.056	0.045–0.060	0.060–0.070	0.060–0.072
Primary utricle length (pul)	0.10–0.14	0.12–0.14	0.15–0.18	0.12–0.15
Secondary utricle diameter (sud)	0.018–0.020	0.020–0.028	0.030–0.040	0.040–0.045
Secondary utricle length (sul)	0.042–0.056	0.046–0.050	0.075–0.090	0.070–0.085
Tertiary utricle diameter (tud)	0.008–0.010	0.010	0.020–0.025	0.025
Tertiary utricle length (tul)	0.004–0.006	0.006	0.030	0.025

Dimensions in mm (for abbreviations see table 2): md – 0.28–0.47, msd – 0.028–0.076, cth – 0.090–1.20, pudd – 0.042–0.048, pul – 0.068–0.075 , sud – 0.014–0.020, sul – 0.018–0.022, tud – 0.004–0.006, tul – 0.04.

Remarks: *Halimeda praeopuntia* was described by Morellet and Morellet (1922), and *H. eocaenica* by Morellet and Morellet (1940b), both based only on the outer morphology of detached segments; internal features are unknown. The present study tried to use entire or broken segments (pl. 15, figs. 1, 3–4) in cutting planes very close to Morellet's illustrations. *H. eocaenica* appears to be very similar to *H. praeopuntia* in segment morphology. It might be a junior synonym.

Halimeda tuna (Ellis and Solander) Lamouroux 1816
Plate 17, figs 1–10; Plate 18, figs. 1–15; Plate 21, figs. 1–8; Plate 22, figures 1–10

Corallina tuna n. sp. – ELLIS and SOLANDER 1786, p. 111; pl. 20, fig. e.
Halimeda tuna (Ellis and Solander) – LAMOUROUX 1816, p. 309. – HILLIS-COLINVAUX 1980, p. 122; fig. 35. – LITTLER and LITTLER 1997, p. 113; fig. 164. – LITTLER and LITTLER 2000, p. 408. – DRAGASTAN, LITTLER and LITTLER 2002, p. 11; pl. 4, figs. 1-3; pl. 11, figs. 7-8; pl. 12, figs 1-6. – DRAGASTAN and SOLIMAN 2002, p. 16; pl. 6, figs 1-4, 6. – LITTLER and LITTLER 2003, p. 252-253. – DRAGASTAN, LITTLER and LITTLER 2003, p. 22; pl. 2, figs. 9-10.
Halimeda sp. – PFENDER in PFENDER and MASSIEUX 1966, p. 124; fig. 5.
Halimeda praemonilis Morellet 1940 – DELOFFRE, POIGNANT and TEHERANI. 1977, p. 43; pl. 6, figs. 1-2.
Halimeda segments – MARTIN, BRAGA and RIDING 1997, p. 447; fig. 7a.

Material: lower–upper Ait Ouarhitane Formation, mid to late Ypresian (Pls. 17, 18) – 150584/11, section SA-7 (GIK 1877b); 150584/12, section SA-7 (GIK 1878b); 160584/16, section SA-8 (GIK 1882b); 160584/22, section SA-8 (GIK 1883b); 031085/10, section SA-13 (GIK 1898); 041085/4, section SA-14 (GIK 1900c); 041085/16, section SA-14 (GIK 1901); 061085/2, section SA-15 (GIK 1905d); 061085/4, section SA-15 (GIK 1906); 091085/10, section SA-18 (GIK 1909c); 121085/6, section SA-21 (GIK 1915b).

Lower–upper Jbel Tagount Formation, latest Ypresian to late Lutetian or latest Bartonian (Pls. 21, 22) – 110988/3, section SA-5 (GIK 1875c); 110988/5, section SA-5 (GIK 1876); 041085/18, section SA-14 (GIK 1902b); 041085/20, section SA-14 (GIK 1903); 041085/21, section SA-14 (GIK 1904); 091085/14, section SA-18 (GIK 1911a); 101085/13, section SA-19 (GIK 1913); 161086/7, section SA-25a (GIK 1919b).

Description: Thallus segments extremely variable in shape, corresponding to orientation of randomly cut sections. The lightly calcified segments are flat, disc-like, linear or recurved in mid to late Ypresian samples (Pls. 17–18), some in Lutetian–?Bartonian specimens are contorted (Pls. 21–22). In general, the segments are not ornamented by lobes or ribs and pointed at the extremities; only rarely the segments have small lobes (pl. 22, fig. 1). The medullar area is moderate in size, pierced by long, medium-large medullar siphons distributed in round to oval, compact bundles, composed by four to six siphons. The bundles are disposed separate from each other, diverging towards the top the segment (pl.17, figs. 1–3, 5, pl. 18, fig.2). In Lutetian–?Bartonian specimens, these siphons bundles are separated by small inner projections of the cortex (pl. 21, figs. 7-8). The cortex system is composed of two or three utricle series similar to Recent *Halimeda tuna*. Primary utricles are short, robust, conical in shape. They support numerous small, subconical, dichotomously branched secondary utricles. The latter bear various very small, conical tertiary utricles. (pl. 18, fig. 5). Dimensions are listed in Table 7.

Remarks: Fossil *Halimeda tuna* were first described from Upper Miocene limestones of Palau, western Pacific (Dragastan et al. 2002). Pfender and Massieux (1966) figured eight vertically and transversely sectioned specimens from the Egyptian Eocene, showing typical discoidal fan-shaped segments. Their figs. 5.5 (vertical section) and 5.6 (transverse section) present disc-like segments crossed by a narrow medullar zone with two parallel, tubular siphons and a cortex system showing three utricle series. Dragastan and Soliman (2002) confirmed the presence of the species in the Ypresian of Egypt. Deloffre et al. (1977) figured two thallus segments from the Paleocene of central Iran, which were referred to *Halimeda praemonilis* Morellet. The disc-like segments and the internal anatomy clearly correspond to *H. tuna*. Finally, three thallus segments figured by Martin et al. (1997) from the late Miocene of south-

TABLE 7
Size parameters of *Halimeda tuna* (Ellis and Solander) Lamouroux 1816 (in millimeters) from Paleogene formations, southern Morocco, late Miocene interval of Palau limestone (Dragastan et al. 2002), and late Pleistocene Key Largo Limestone, Florida (Dragastan et al. 2003).

***Halimeda tuna* (ELLIS AND SOLANDER) LAMOUROUX 1816**	**MID TO LATE YPRESIAN**	**LUTETIAN–?BARTONIAN**	**LATE MIOCENE**	**LATE PLEISTOCENE**
Medulla diameter (md)	0.23–0.40	0.25–0.30	0.30	0.90–1.0
Medulla siphon diameter (msd)	0.050–0.070	0.060–0.075	0.060–0.090	0.060–0.080
Cortex thickness (cth)	0.090–0.10	0.060–0.080	0.10–0.12	---
Primary utricle distal diameter (pudd)	0.050–0.060	0.050	0.060–0.065	0.050–0.060
Primary utricle length (pul)	0.090–0.10	0.060–0.070	0.040–0.075	0.045–0.070
Secondary utricle diameter (sud)	0.030–0.040	0.025–0.030	0.030–0.035	0.030–0.042
Secondary utricle length (sul)	0.050–0.060	0.060	0.080–0.10	0.070–0.10
Tertiary utricle diameter (tud)	0.010	0.008–0.010	0.015–0.018	0.015–0.020
Tertiary utricle length (tul)	0.015	0.012	0.025–0.032	0.025–0.030

eastern Spain also belong to species *H. tuna* based on the shape of the cortical utricles, occuring in three series.

Halimeda gracilis Harvey ex Agardh 1887
Plate 19, figures 1-3; Plate 23, figure 1

Halimeda gracilis n. sp. – HARVEY ex AGARDH 1887, p. 82. – HILLIS-COLINVAUX 1980, p. 144; fig. 44. – LITTLER and LITTLER 2000, p. 402. – DRAGASTAN, LITTLER and LITTLER 2002, p. 9; pl. 1, figs. 6-8; pl. 3, figs. 1-4, 6, 8. – LITTLER and LITTLER 2003, p. 246-247. – DRAGASTAN, LITTLER and LITTLER 2003, p. 24; pl. 3, figs. 7-16; pl. 5, fig. 1; pl. 7, fig. 4.

Material: Middle Ait Ouarhitane Formation, mid to late Ypresian – 061085/2, section SA-15 (GIK 1905e); middle Jbel Tagount Formation, Lutetian–?Bartonian – 091085/13, section SA-18 (GIK 1910a).

Description: The broken, well-calcified thallus segments are flat disc-like, oval to reniform in shape. Due to the fragmented material and availability of only longitudinal and oblique longitudinal sections, the outer shape of the segments is only suggestive, but internal structure is clear (pl. 19, figs. 1–2).The narrow medullar area is crossed by less than six thin, slightly intermingled medullary siphons. The medium-thick cortex is pierced by two utricle series. Primary utricles are approximately cylindrical, distally clavate (pl. 19, fig. 2). They support short tubular, distally conical secondary utricles.

Dimensions in mm (for abbreviations see table 2): md – 0.20–0.36, mds – 0.032–0.040, cth – 0.30–0.45, pudd – 0.035–0.050, pul – 0.020–0.050, sud – 0.020–0.028, sul – 0.020–0.036.

Remarks: *Halimeda gracilis* is rare in the mid Ypresian to late Lutetian or latest Bartonian (text-figs. 6, 7). It is comparable to specimens from the late Miocene (Dragastan et al. 2002) and the late Pleistocene (Dragastan et al. 2003), which differ only slightly in biometric data. It is also similar to Recent specimens of the species.

Halimeda praemacroloba Dragastan and Herbig **n. sp.**
Plate 19, figures 4–8

Derivatio nominis: "praemacroloba" – comparable with the modern species *H. macroloba*, but occuring earlier in geologic history.

Holotype: Plate 19, figure 4, sample 061085/2 (GIK 1905f).

Paratypes: Plate 19, figures 5-6, additional sections from the same sample (GIK 1905g-h).

Locus typicus: Section SA-15 of Herbig (1991) (see Appendix 1).

Stratum typicum: Middle Ait Ouarhitane Formation, mid to late Ypresian.

Additional material: Ait Ouarhitane Formation, mid to late Ypresian – 150584/12, section SA-7 (GIK 1878c); 160584/16, section SA-8 (GIK 1882c).

Description: Most thallus segments are broken debris; shape possibly compressed cylindrical (pl. 19, figs. 5–6), discoidal (pl. 19, fig 4), in some cases subreniform with entire, undulating margins. Medium-large medullar area filled by six cylindral medullar siphons, which are medium-large in diameter, round in transverse sections, tubular in oblique longitudinal sections, slightly intermingled. Well calcified, thick cortex pierced by two (pl. 19, figs. 4, 6) or three (pl. 19, figs 7–8) utricle series. Primary utricles long, conical, claviform (pl. 19, figs. 4, 7). They support short, subconical, distally inflated secondary utricles, which are dichotomously branched (pl. 19, figs. 5–8). The tiny tertiary utricles are also short and subconical (pl. 19, figs. 4, 7–8).

Dimensions in mm (for abbreviations see table 2): md – 0.15–0.50, msd – 0.060–0.12, cth – 0.15–0.25, pudd – 0.058–0.075, pul – 0.10–0.12, sud – 0.028–0.036, sul – 0.050–0.070, tud – 0.020–0.026, tul – 0.030–0.032.

Remarks: *Halimeda praemacroloba* n. sp. is comparable with the Recent species *H. macroloba*, which has identically shaped segments. *H. macroloba* has however short, claviform primary utricles and globose secondary utricles. The new species is also comparable with the Recent *Halimeda stuposa*, which has cylindrical or subcylindrical, compressed or plane segments,

TABLE 8
Size parameters of *Halimeda tuna* f. *platydisca* (Decaisne) Barton 1901 (in millimeters) from Paleogene formations, southern Morocco and late Miocene and Pliocene intervals of Palau Limestone (Dragastan et al. 2002).

***Halimeda tuna* f. *platydisca* (DECAISNE) BARTON 1901**	**MID TO LATEYPRESIAN**	**LUTETIAN–?BARTONIAN**	**LATE MIOCENE**	**PLIOCENE**
Medulla diameter (md)	0.10–0.12	0.12–0,14	0.14–0.15	> 0.15
Medulla siphon diameter (msd)	0.050–0.060	0.065–0.070	0.065–0.075	0.070
Cortex thickness (cth)	0.080–0.090	0.10–0.14	0.010–0.016	0.016
Primary utricle distal diameter (pudd)	0.030–0.035	0.040–0.050	0.040–0.050	0.060
Primary utricle length (pul)	0.050–0.060	0.060	0.050–0.075	0.060–0.070
Secondary utricle diameter (sud)	0.025–0.030	0.030–0.035	0.030–0.040	0.040
Secondary utricle length (sul)	0.050–0.060	0.060–0.065	0.060–0.070	0.050–0.070
Tertiary utricle diameter (tud)	0.030	0.030	0.030–0.050	0.0.60
Tertiary utricle length (tul)	0.040	0.045	0.045–0.050	0.060

which become subcuneate and subsphaerical towards the apex. Differences are obvious, because *H. stuposa* has commonly more utricle series in the cortex (three to five); primary utricles are long, subcylindrical; secondary utricles cylindrical; tertiary utricles short, subglobose and dichotomously branched; fourth utricles tiny, globose; fifth utricles short and filiform.

Halimeda copiosa Goreau and Graham 1967
Plate 20, figures 1–3

Halimeda copiosa n. sp. – GOREAU and GRAHAM 1967, p. 433; figs. 1-10. – HILLIS-COLINVAUX 1980, p. 118; figs. 33, 101. – LITTLER et al., p. 88. – LITTLER and LITTLER 2000, p. 398-399. – DRAGASTAN, LITTLER and LITTLER 2003, p. 23; pl.2, figs. 11-15.

Material: lower Ait Ouarhitane Formation, mid to late Ypresian – 180584/22, section SA-11 (GIK 1887); 091085/8, section SA-18 (GIK 1907).

Description: Thallus segments preserved entire or broken; segments are disc-shaped with smooth, undulating, rarely ribbed margins (pl. 20, figs. 1–3). In transverse section, the segments present a narrow medullar area pierced by numerous, densely arranged medullar siphons, small in diameter and round to oval in transverse sections. They are disposed in four to six, round to oval bundles. The cortex is composed of three utricle series (pl. 20, figs. 1). Primary utricle series are long, cylindrical, slightly inflated distally; secondary utricles are short, conical, dichotomously branched, and tiny tertiary utricles are short, filiform. The utricle series have morphology similar to the Recent species.

Dimensions in mm: md – 0.28–0.32, msd – 0.030–0.045, cth – 0.12–0.15, pudd – 0.032–0.042, pul – 0.060–0.075, sud – 0.016–0.030, sul – 0.038–0.040, tud – 0.022–0.028, tul – 0.022–0.030.

Remarks: *Halimeda copiosa* is for the first time described from the Ypresian. The fragmentarily preserved specimens are smaller than Upper Pleistocene specimens (Dragastan et al. 2003) and Recent ones. Morphology of cortical utricle series is similar to Recent specimens.

Halimeda tuna* f. *platydisca (Decaisne) Barton 1901
Plate 20, figure 4; Plate 25, figures 1–4

Halimeda platydisca n. sp. – DECAISNE 1842, p. 102.
Halimeda tuna f. *platydisca* (Decaisne) – BARTON 1901, p. 14; pl. 1, fig. 2. – LITTLER and LITTLER 2000, p. 408. – DRAGASTAN, LITTLER and LITTLER 2002, p. 11; pl. 4, figs. 4-5.

Material: Ait Ouarhitane Formation, mid to late Ypresian (pl. 20, fig. 4) – 160584/16, section SA-8 (GIK 1882d).

Lower–uppermost Jbel Tagount Formation, latest Ypresian to late Lutetian or latest Bartonian (pl. 25) – 180584/31, section SA-11 (GIK 1891b); 18584/36, section SA-11 (GIK 1893c); 91085/15, section SA-18 (GIK 1912b).

Description: Thallus segments are disc-shaped, in cases show two small lateral wings. Medullar area narrow or large. Medullar siphons are large in diameter and round in transverse section. The cortex of the Ypresian specimen, a broken segment, is pierced by three utricle series (pl. 20, fig. 4, arrow). Primary utricles are medium long, claviform in shape. They support conical, dichotomously branched secondary utricles, which are bulbous at the distal end. Tertiary utricles are very short, also conical. The morphology of the utricle series is similar to Recent specimens described from the Carribean by Littler and Littler (2000). The Lutetian–?Bartonian specimens (pl. 25, figs. 1–4) are disc-like, with a large medullar area. The medullar area contains densely packed medullar siphons in four to six vertical rows and are round in transverse section. The cortex is composed by three utricle series, also similar in morphology to Recent specimens. Dimensions are listed in Tab. 8.

Halimeda praegoreaui Dragastan and Herbig **n. sp.**
Plate 23, figures 2–3

Derivatio nominis: "praegoreaui" – comparable with the modern species *H. goreaui*, but occuring earlier in geological history.

Holotype: Plate 23, figure 3, sample 180584/36 (GIK 1893d).

Paratype: Plate 23, figure 2.

Locus typicus: Section SA-11 of Herbig (1991) (see Appendix 1).

Stratum typicum: uppermost Jbel Tagount Formation, Lutetian–?Bartonian

Additional material: 110988/3, section SA-5 (GIK 1875d), upper Jbel Tagount Formation, Lutetian–?Bartonian.

Description: Thallus segments flat, subcuneate, possibly barrel-shaped, according to the shape of the two known transverse sections, which cross the basal part of the segment (pl. 23, fig. 2) and a lateral in the upper part of a segment (pl. 23, fig. 3). Medullar area large, covering most of the central part of the segments. In transverse section, the medullary siphons, large in diameter, are round or oval to elongated. Loosely disposed siphons, without contact to each other, are arranged in four to six round bundles. Cortex of variable thickness, crossed by two utricle series. Primary siphons are of conical shape, long compared with secondary utricles (pl. 23, fig. 3). The latter are very small, short, cylindrical, distally slightly inflated, and dichotomously branched.

Dimensions in mm (for abbreviations see table 2): md – 0.15–0.25, mds – 0.040–0.042, cth – 0.042–0.10, pudd – 0.038–-0.040, pul – 0.070–0.090, sud – 0.010–0.014, sul – 0.012–0.018.

Remarks: *Halimeda praegoreaui* n. sp. is a species with flat, subcuneate, unornamented thallus segments and a simple cortex system composed only by two utricle series. In contrast, Recent *H. goreaui* has thallus segments of various shapes and a cortex crossed by multiseriate utricles. The long, claviform primary utricles support also long, cylindrical, distally slightly inflated, dichotomously branched secondaries. The secondaries continue with short cylindrical tertiary utricles, and conical fourth urticles, both dichotomously branched. In some cases, *H. goreaui* presents five to six utricle series. It differs from *H. gracilis*, which has short, dichotomously branched medullar siphons and different shape and dimensions of cortical utricles.

Halimeda scabra Howe 1905
Plate 23, figure 4

Halimeda scabra n. sp. – HOWE 1905, p. 241; pls. 11-12. – HILLIS-COLINVAUX 1980, p. 125; fig. 37. – LITTLER and LITTLER 2000, p. 406-407. – DRAGASTAN, LITTLER and LITTLER 2003, p. 24; pl. 3, fig. 17.

Material: middle Jbel Tagount Formation, Lutetian–?Bartonian – 091085/14, section SA-18 (GIK 1911b).

Description: Only one moderately calcified, broken thallus segment was observed. It is disc-like in shape, with rounded undulate margin. The large medullar area contains sparse medullar siphons of medium large diameter. The relatively thin cortex is crossed by three utricle series. Primary utricles are long, tubular, distally slightly inflated and continue into short, conical, dichotomously branched secondary utricles. The latter bear very small, hair-like tertiary utricles. They are disposed regular and linear along the margin of the segment (pl.23, fig. 4, arrows). Dimensional data are not diagnostic for the broken segment available.

Remarks: *Halimeda scabra* is identified for the first time in Lutetian–?Bartonian deposits. Previously, it was known only from a single, completely preserved segment from the late Pleistocene Key Largo Formation, Florida (Dragastan et al. 2003).

Halimeda fragilis Taylor 1950
Plate 23, figures 5–7

Halimeda fragilis n. sp. – TAYLOR 1950, p. 80; pl. 48, fig. 2. – HILLIS-COLINVAUX 1980, p. 151; fig. 47. – DRAGASTAN, LITTLER and LITTLER 2002, p. 11; pl. 5, figs. 1-9. – DRAGASTAN and SOLIMAN 2002, p. 18; pl. 7, figs. 1-3.

Material: middle Jbel Tagount Formation, Lutetian–?Bartonian - 091085/13, section SA-18 (GIK 1910b); 161086/7, section SA-25a (GIK 1919c).

Description: Thalli segments flattened, broken, possibly subcuneate in shape. The actual shape of the segments difficult to reconstruct. The narrow medullar area is crossed by medium-long siphons disposed in four more or less parallel rows (pl. 23, figs. 6–7). Cortex composed of three utricle series. The primary utricles are long, cylindriform (pl. 23, fig. 5). The short secondary utricles are cylindrical, slightly inflated distally, and dichotomously branched. The secondary utricles bear very short, tiny conical tertiary utricles.

Dimensions in mm (for abbreviations see table 2): md – 0.25–0.30, msd – 0.060–0.080, cth – 0.10–0.15, pudd – 0.040–0.050, pul – 0.090–0.10, sud – 0.028–0.036, sul – 0.040–0.060, tud – 0.010, tul – 0.020.

Remarks: *Halimeda fragilis* was previously described from the Ypresian of Egypt (Dragastan and Soliman 2002) and from the Pliocene of Palau, western Pacific (Dragastan et al. 2002).

Halimeda praecuneata Dragastan and Herbig **n. sp.**
Plate 28, figures 1-3

Derivatio nominis: " praecuneata" – comparable with the modern species *H. cuneata*, but occuring earlier in geologic history.

Holotype: Plate 28, figure 1, sample 180584/35 (GIK 1892).

Paratypes: Plate 28, figures 2-3.

Locus typicus: Section SA-11 of Herbig (1991) (see Appendix 1).

Stratum typicum: Uppermost Jbel Tagount Formation, Lutetian–?Bartonian.

Additional material: 041085/18, section SA-14 (GIK 1902c), middle Jbel Tagount Formation.

Description: Thallus segments flat, discoidal, slightly cuneate with entire, undulate margins, which in cases have local small protuberances (pl. 28, fig. 1). The medullar area is narrow in juvenile segments, medium-large in mature segments. It contains numerous, loosely to densely disposed medullary siphons of round shape in transverse section. Cortex is composed by three utricle series. Long primary utricles are conical, globose to claviform in shape (pl. 28, figs. 1–3). They support short, subconical, dichotomously branched secondary utricles. The very short third utricles are cylindrical (pl. 28, fig. 1, arrow lower right).

Dimensions in mm (for abbreviations see table 2): md – 0.10–0.25, msd –.028–0.070, cth – 0.050–0.10, pudd – 0.042–0.052, pul – 0.050–0.070, sud – 0.025–0.050, sul – 0.020–0.052.

Remarks: *Halimeda praecuneata* n. sp. can be compared with Recent *Halimeda cuneata*, which has more or less the same shape of segments and the same shape of primary and secondary utricles. Contrary to *H. praecuneata*, which has only primary and secondary utricles, *H. cuneata* has up to six utricle series.

CONCLUSIONS

The present study of *Halimeda* from the eastern Ouarzazate basin, southern rim of the central High Atlas, Morocco, was the first study of the genus relying on abundant, systematically sampled material from numerous, well-dated Paleocene to middle Eocene strata, which were previously thoroughly described as far as carbonate microfacies, paleoecology, and paleogeography are concerned. Three *Halimeda*-bearing time slices were discerned, i. e. late Thanetian (Jbel Guersif Formation), mid to late Ypresian (Ait Ouarhitane Formation), latest Ypresian to late Lutetian or latest Bartonian (Jbel Tagount Formation).

Nine new species and fourteen modern and fossil taxa are described. Eleven late Thanetian taxa are represented by one fossil species, four modern taxa, and six new species. The new species are short-ranging and restricted to the Thanetian. They developed by adaptive radiation during transgression of the Moroccan epeiric sea to the southern rim of the central High Atlas and represent the recovery phase following extinctions at the Cretaceous-Tertiary boundary, as analogous shown for dasycladalean algae (Barattolo 2002). In the Ypresian, twelve taxa were identified, and in the Lutetian–?Bartonian eleven taxa, most belonging to modern species of *Halimeda*. The onset of long-ranging taxa and the low rate of originating taxa indicate the stabilization phase known from Dasycladales (Barattolo 2002). Disappearance of some taxa in the upper Jbel Tagount Formation seems to indicate a gradual decrease in diversity in the late Lutetian or Bartonian and the onset of a new crisis, known for Dasycladales from the Priabonian. The recovery phase with adaptive radiation, stabilization phase, and onset of a new crisis are most surely related to global eustatic sea-level changes. Moreover, deterioration of climate towards the end of middle Eocene contributed to the late Eocene crisis.

Modern species of *Halimeda* evolved and diversified much earlier than hitherto thought. From the Thanetian, four modern taxa were identified. They prove the antiquity of the phylogenetic lines postulated by Dragastan et al. (2002). The *Halimeda cylindracea* lineage began at latest in late Triassic; *H. incrassata* lineage doubtfully in the late Cretaceous, at latest in the Paleocene or Eocene, and *H. opuntia* lineage at earliest in Maastrichtian, at latest in the Paleocene. The results also match cladistic phylogeny of the genus based on molecular characteristics (Hillis et al. 1998, Kooistra et al. 1999) and discussed for their geological relevance by Hillis (2001) (see Herbig and Dragastan 2005). Revised phylograms (Kooistra et al. 2002) and resulting revision of the subdivision of the genus Halimeda in five phylogenetic lineages/sections (Verbruggen and Kooistra 2004) modified the results but slightly. Accordingly, the lineages of the present-day sections Rhipsalis, Micronesicae, Halimeda, and the opuntoid basal clade originated prior to the late Thanetian, either in the late Cretaceous or in the earliest Paleocene. Incorporating data from Dragastan (2002) and the Barattolo model (2002) for evolution of Dasycladales, a common origin in the earliest Paleocene, subsequent to end-Cretaceous extinctions, seems to be most reasonable. Separation of the opuntoid basal clade into the lineages of the present-day sections Pseudoopuntia and Opuntia was achieved before mid Ypresian. Further differentiation of the basal clades occurred during the Ypresian and Lutetian, since ten and twelve modern taxa were already present. Concomitantly, morphological features of medullar siphons and complexity and variety of cortex structures increased. This suggests that the assumed vicariance event in the late Miocene (Hillis 2001), when only two new taxa appeared, is of minor importance. The origin of the extant clades of the genus *Halimeda* during that time, based on phylogram patterns (Kooistra et al. 2002) is rejected due to the wealth of detailed paleontological data presented herein, and the assumption of genetically homogenous Halimeda species flourishing without barriers on the wide shallow shelfs of the Paleogene Tethys. A Pliocene vicariance event associated with the closure of the isthmus of Panama resulted mostly in genetic differentiation of cognate pairs. Also the proposed major Pleistocene radiation (Hillis 2001) apparently results from sampling and study bias. Still, the diversification between late Pleistocene (15 modern taxa) and Recent (34 taxa) remains unexplained. It might be mostly attributed to the fact that weakly calcified extant species are not preserved in the fossil record.

Strong similarities in ecology are noted between the extensive and luxuriant *Halimeda* meadows of the modern Great Barrier Reef province and the *Halimeda*-rich facies at the southern rim of the central High Atlas. Both are characterized by predominance of *Halimeda* and near absence of other algae, by minor lateral floral changes, by high diversity with comparable percentage distribution patterns, and in showing two dominant species, one or two quite common, and several rare to very rare species. Both environments show psammophytic and lithophytic taxa of the three most important sections of the genus, i. e. Rhipsalis, Opuntia, and Halimeda, suggesting that the high diversity results from habitat differentiation. The important contribution of lithophytyic taxa at the southern rim of the central High Atlas indicates the presence of sufficiently coarse-grained, non-mobile *Halimeda* sands and gravels, as indicated by microfacies analysis (Herbig 1991). Finally, in both the modern and Paleogene case nutrient-rich waters are due to upwelling. *Halimeda* meadows were very important sediment factories stretching as an almost continuous band along the shallow ramp of the southern Moroccan Paleogene sea.

Our results prove the extreme geological longevity of at least twelve of the thirdy-four Recent *Halimeda* taxa, which originated between 57 million years (late Thanetian) and 45 million years (early Lutetian) ago. This gives *Halimeda* truly the character of a living fossil (Kooistra et al. 1999, Herbig and Dragastan 2005). The place and exact time of speciation is still uncertain, because the Atlantic-bound Moroccan epeiric sea most probably saw the immigration of taxa that originating earlier elsewhere in Tethys. Therefore, investigation of other Paleocene–Eocene strata is needed to solve this question. Also needed are studies of hitherto non-analysed Cenozoic time slices in the long interval between late Eocene and late Miocene.

ACKNOWLEDGMENTS

Field work of the present study was part of a research program “Mobility of active continental margins”, section “Sedimentary cover of the Moroccan Atlas”, conducted during the 1980’s and early 1990’s by a research group of Freie Universität Berlin and generously financed by the Deutsche Forschungsgemeinschaft (DFG). H.-G. Herbig is obliged to the Ministère de l’Energie et des Mines, Service géologique du Maroc, Rabat, for working

permits and continous friendly support. O. Dragastan started to study *Halimeda* during a visit in Cologne, supported by the Institut für Geologie und Mineralogie, Universität zu Köln. The final draft of the paper was completed by H.-G. Herbig during a sabbatical granted by Universität zu Köln, and a second visit of O. Dragastan, kindly supported by Alexander-von-Humboldt Foundation. We are especially indebted to P. Enos, University of Kansas and I. Bucur, University of Cluj-Napoca, for thoughtful reviews. D. Bassi, Università de Ferrara, kindly commented a late version of the manuscript. Mrs. Christel Krings helped with the graphic artwork. Her efforts with the final electronic version of the plates were absolutely indispensable.

REFERENCES

AGARDH, J. G., 1887. Till algernes systematik. Nya bidrag (Femte afdelningen). *Acta Universitatis Lundensis*, 23 (2): 1-174.

AZMANY-FARKHANY, M., BOUJO, A. and SALVAN, H.M., 1986. *Géologie des gîtes mineraux marocains, vol. 3. Phosphates.* Notes et Mémoires du Service Géologique du Maroc, No. 276, 392 pp.

BADVE, R.M. and NAYAK, K.K., 1983. Occurrence and significance of the algal genus *Halimeda* from Nimar Sandstone, Bagh Beds, Jhabua District. M. P. *Biovigyanam*, 9: 137-148.

BADVE, R. M. and KUNDAL, P., 1986. Marine Cretaceous algae from the Baratang Formation, Andaman Islands, India. *Bulletin of the Geological, Mining and Metallurgical Society of India*, 54: 149-158.

BANDEIRA-PEDROSA, M. A., PEREIRA, S. M. B and OLIVEIRA, E. C., 2004. Taxonomy and distribution of the green algal genus *Halimeda* (Bryopsidales, Chlorophyta) in Brazil. *Revista Brasileira de Botânica*, 27 (2): 363-377.

BARATTOLO, F., 2002. Late Cretaceous – Paleogene Dasycladaceans and the K/T boundary problem. In: Bucur, I. I. and Filipescu, S., Eds. *Research advances in calcareous algae and microbial carbonates*, 17-40. Cluj: Cluj University Press.

BARTON, E. S., 1901. The genus *Halimeda*. *Monographs of the Siboga Expedition*, 60: 32 pp. Leiden: Brill.

BASSOULLET, J. P., BERNIER, P., DELOFFRE, R., GÉNOT, P., PONCET, J. and ROUX, A., 1983. Les algues udoteacées du Paléozoïque au Cénozoïque. *Bulletin des Centres de Recherche Exploration-Production Elf-Aquitaine*, 7(2): 449-621.

BECKMANN, J. P. and BECKMANN, R., 1966. Calcareous algae from the Cretaceous and Tertiary of Cuba. *Schweizerische Paläontologische Abhandlungen*, 85: 3-48.

BLAIR, S. M. and NORRIS, J. N., 1988. The deep-water species of *Halimeda* Lamouroux (Halimedaceae, Chlorophyta) from San Salvador Island, Bahamas: species composition, distribution and depth records. *Coral Reefs*, 6: 227-236.

BOSELLINI, F. R., RUSSO, A. and VESCOGNI, A., 2002. The Messinian reef complex of the Salento Peninsula (southern Italy): stratigraphy, facies and paleoenvironmental interpretation. *Facies*, 47: 91-112.

BOUJO, A., 1976. Contribution à l'étude géologique du gisement de phosphate crétacé-éocène des Ganntour (Maroc occidental). *Notes et Mémoires du Service Géologique du Maroc*, No. 262: 227 pp.

BRAGA, J. C, MARTIN, J. M. and RIDING, R., 1996. Internal structure of segment reefs: *Halimeda* algal mounds in the Mediterranean Miocene. *Geology*, 24: 35-38.

BUCUR, I. I., 1994. Lower Cretaceous Halimedaceae and Gymnocodiaceae from Southern Carpathians and Apuseni Mountains (Romania) and systematic position of the Gymnocodiaceae. *Beiträge zur Paläontologie*, 19: 13-37.

CAPPETTA, H., JAEGER, J.-J., SABATIER, M., SIGÉ, B., SUDRE, J. and VIANEY-LIAUD, M., 1987. Compléments et précisions biostratigraphiques sur la faune paléocène à mammifères et sélaciens du Bassin d'Ouarzazate (Maroc). - *Tertiary Research*, 8, (4): 147-157.

CHAPMAN, F. and MAWSON, D., 1906. On the importance of *Halimeda* as reef-forming organisms with description of the *Halimeda* limestones of the New Hebrides. *Quarterly Journal of the Geological Society London*, 62: 702-711.

CHOUBERT, G. and MARÇAIS, J., 1952. Aperçu structural. *Notes et Mémoires du Service Géologique du Maroc*, No. 100 (= *19ème Congrès Géologique International, Alger 1952, Monographies Régionales, 3ème Série, Maroc, N° 6: Géologie du Maroc*): 9-73.

———, 1956. Les grands traits de la géologie du Maroc. In: Choubert, G. and Faure-Muret, A., Eds., Lexique stratigraphique du Maroc. *Notes et Mémoires du Service Géologique du Maroc*, No. 134 (= *Lexique stratigraphique international, Vol. IX (Afrique), Fascicule 1a (Maroc)*, 5-38.

CHOUBERT, G. and FAURE-MURET, A., 1960-62. Evolution du domaine atlasique marocain depuis les temps paléozoiques. *Livre du Mémoire Paul Fallot, vol. 1* (*Mémoire hors Série de la Société Géologique du France*): 447-527.

CONARD, M. and RIOULT, M., 1977. *Halimeda elliotti* nov. sp., algue calcaire (Chlorophyceae) du Turonien des Alpes-Maritimes (S.E. France). *Géologie Méditerranéenne*, 4 (2): 83-98.

DAVIES, P.J. and MARSHALL, J. F., 1985. *Halimeda* bioherms – low energy reefs, Northern Great Barrier Reef. *Proceedings of the 5th International Coral Reef Congress, Tahiti 1985*, 5: 1-14.

DECAISNE, J. 1842. Mémoire sur les corallines ou polypiers calcifères. *Annales des sciences naturelles, Botanique*, série 2, 18: 96-128.

DELOFFRE, R., POIGNANT, A.F. et TEHERANI, K., 1977. Algues calcaires de l'Albo-Aptien au Paléocène de l'Iran central. *Bulletin des Centres de Recherche Exploration-Production Elf-Aquitaine*, 1 (1): 29-57.

DERCOURT, J., ZONENSHAIN, L. P., RICOU, L.-E, KAZMIN, V. G., LE PICHON, X., KNIPPER, A. L., GRANDJACQUET, C., SBORSHCHIKOV, I. M., BOULIN, J., SOROKHTIN, O., GEYSSANT, J., LEPVRIER, C., BIJU-DUVAL, B., SIBUET, J. C., SAVOSTIN, L. A., WESTPHAL, M. and LAUER, J.-P., 1985. Présentation de 9 cartes paléogeographiques au 1/20.000.000e s'étendant de l'Atlantique au Pamir pour la période du Lias à l'Actuel. *Bulletin de la Société Géoloquique de France*, 8ème série, 1: 637-652.

DRAGASTAN, O., RICHTER, D. K. , KUBE, B., POPA, E., SÂRBU, A. and CIUGULEA, I., 1997. A new family of Paleo-Mesozoic calcareous green siphons-algae (Order Bryopsidales, Class Bryopsidophyceae, Phylum Siphonophyta). *Revista Española de Micropaleontología*, 29: 69-136.

DRAGASTAN, O. and RICHTER, D. K., 1999. Late Jurassic oolites from Acrocorinth (NE-Peloponesus): calcareous micro-algae as an exceptional paleoecologic indicator. *Bochumer geologische und geotechnische Arbeiten*, 53: 149-172.

DRAGASTAN, O., KUBE, B. and RICHTER, D. K., 2000. New Late Triassic calcareous algae from Hydra, Greece. *Acta Palaeontologica Romaniae*, 2 (1999): 139-156.

DRAGASTAN, O., LITTLER, D. S. and LITTLER, M. M., 2002. Recent vs. fossil *Halimeda* species of Angaur Island, Palau and adjacent western Pacific areas. *Acta Palaeontologica Romaniae, Special Publication*, No. 1: 1-20.

DRAGASTAN, O. and SOLIMAN, A. H., 2002. Paleogene calcareous algae from Egypt. *Micropaleontology*, 48: 1-30.

DRAGASTAN, O., LITTLER, D. S. and LITTLER, M. M., 2003. Fossil siphonaceous green algal diversity of Key Largo and Miami limestone formations – South Florida (part I). *Analele Universitatii Bucuresti, Geologie, Special Publication*, No. 1: 5-35.

DREW, E. A., 1995. Diversity of the green algal genus *Halimeda* in the Chagos Archipelago, central Indian Ocean. *Aquatic Botany*, 52: 143-150.

DREW, E. A. and ABEL, K. M., 1985. Biology, sedimentology and geography of the vast inter-reefal *Halimeda* meadows within the Great Barrier Reef province. *Proceedings of the 5th International Coral Reef Congress, Tahiti 1985*, 5: 15-24.

———, 1988a. Studies on *Halimeda*. I. The distribution and species composition of *Halimeda* meadows throughout the Great Barrier Reef Province. *Coral Reefs*, 6: 195-205.

———, 1988b. Studies on *Halimeda*. II. Reproduction, particularly the seasonality of gametangia formation, in a number of species from the Great Barrier Reef Province. *Coral Reefs*, 6: 207-218.

ELLIOTT, G. F., 1955. Fossil calcareous algae from the Middle East. *Micropaleontology*, 1 (2): 125-130.

———, 1956. Algues calcaires Codiacées fossiles d'Iraq nouvelles et peu connues. *Bulletin de la Société Géologique de France*, *6ème Série*, 6: 789-795.

———, 1963. A Liassic *Pycnoporidium* (calcareous algae). *Eclogae Geologicae Helvetiae*, 56: 179-181.

———, 1965. The interrelationships of some Cretaceous Codiaceae (calcareous algae). *Palaeontology*, 8: 199-203.

———, 1968. Permian to Paleocene calcareous algae (Dasycladaceae) of the Middle East. *Bulletin of the British Museum (Natural History), Geology, Supplement*, 4: 1-111, 24 pls.

———, 1975. Transported algae as indicators of different marine habitats in the English Middle Jurassic. *Palaeontology*, 18: 351-366.

———, 1982. A new calcareous green alga from the Middle Jurassic of England. *Palaeontology*, 25: 431-437.

ELLIS, J., 1768. Extract of a letter from John Ellis Esquire, F. R. S. to Dr. Linneaus of Upsala, F. R. S. on the animal nature of the genus of zoophytes, called *Corallina*. *Philosophical transactions of the Royal Society of London*, 57 (1): 404-427.

ELLIS, J. and SOLANDER, D., 1786. *The Natural History of many curious uncommon zoophytes collected from various parts of the globe by John Ellis, systematically arranged and described by Daniel Solander.* London, 208 pp.

EMBERGER, L., 1968. *Les plantes dans leur rapports avec les vegetaux vivants*. Paris: Masson et Cie, 758 p.

ENOS, P., 1977. Holocene sediment accumulations of the South Florida shelf margin. In: Enos, P. and Perkins, R.D., Eds. *Quaternary sedimentation in South Florida.* Geological Society of America, Memoir, 147: v+130 pp.

FELDMANN, J., 1946. Sur l'hétéroplastie de certaines Siphonales et leur classification. *Compte Rendu Hebdomaire des Seances de l'Académie des Sciences, Paris*, 222: 752-753.

———, 1954. Sur la classification des Chlorophycées siphonées. *Rapports et communications, 8ème Congrès International de Botanique, Paris*: 17: 96-98

FLAJS, G. (1977). Die Ultrastrukturen des Kalkalgenskeletts. *Palaeontographica*, (B), 160: 69-128.

FLÜGEL, E., 1975. Kalkalgen aus Riffkomplexen der alpin-mediterranen Obertrias. *Verhandlungen der Geologischen Bundesanstalt Wien*, 1974: 297-346.

———, 1988. *Halimeda*: paleontological record and palaeoenvironmental significance. *Coral Reefs*, 6:123-130.

FORNOS, J. J., FORTEZA, V., JAUME, C. and MARTINEZ-TABERNER, A., 1992. Present-day *Halimeda* carbonate sediments in temperate Mediterranean embayments: Fornells, Balearic Islands. *Sedimentary Geology*, 75: 283-293.

GARWOOD, E. J., 1913. The Lower Carboniferous succession in the northwest of England. *Quarterly Journal of the Geological Society London*, 68: 449-586.

———, 1914. Some new rock-building organisms of the Lower Carboniferous beds of Westmorland. *Geological Magazine*, 51: 265-271.

GAUTHIER, H. 1957. Contribution à l'étude géologique des formations post-liasiques des bassins du Dadès et du Haut Todra (Maroc méridional). *Notes et Mémoires du Service Géologique du Maroc*, No. 119: 212 pp.

GEYER, G. and HERBIG, H. G., 1988. New Eocene oysters and the final regression at the southern rim of the central High Atlas (Morocco). *Geobios*, 21: 663-691.

GINSBURG, R. N., 1956. Environmental relationships of grain size and constituent particles in some South Florida carbonate sediments. *American Association of Petroleum Geologists Bulletin*, 40: 2384-2427.

GHEERBRANT, E., CAPPETTA, H., FEIST, M., JAEGER, J.-J., SUDRE, J., VIANEY-LIAUD, M. and SIGÉ, B., 1993. La succession des faunes de vertébrés d'âge paléocènce supérieur et éocène inférieur dans le bassin d'Ouarzazate, Maroc. Contexte géologique, portée biostratigraphique et paléogeographique. *Newsletter on Stratigraphy*, 28: 33-58.

GHEERBRANT, E., SUDRE, J., SEN, S., ABRIAL, C., MARANDAT, B., SIGÉ, B. and VIANEY-LIAUD, M., 1998. Nouvelles données sur les mammiferes du Thanétien et de l'Yprésien du Bassin d'Ouarzazate (Maroc) et leur contexte stratigraphique. *Palaeovertebrata*, 27 (3/4): 155-202.

GOREAU, T. F. and GOREAU, N. I., 1973. The ecology of Jamaican coral reefs II. Geomorphology, zonation and sedimentary facies. *Bulletin of Marine Science*, 23: 399-464.

GOREAU, T. F. and GRAHAM, E. A., 1967. A new species of *Halimeda* from Jamaica. *Bulletin of Marine Science*, 17: 432-441.

GOULD, S. J. and ELDREGDE, N, 1977. Punctuated equilibria: the tempo and mode of evolution reconsidered. *Paleobiology*, 3: 115-151.

GRADSTEIN, F. M., OGG, J. G., SMITH, A. G., AGTERBERG, F. P., BLEEKER, W., COOPER, R. A., DAVYDOV, V., GIBBARD, P., HINNOV, L. A., HOUSE, M. R., LOURENS, L., LUTERBACHER, H. P., McARTHUR, J., MELCHIN, M. J., ROBB, L. J.,

SHERGOLD, J., VILLENEUVE, M., WARDLAW, B. R., ALI, J., BRINKHUIS, H., HILGEN, F. J., HOOKER, J., HOWARTH, R. J., KNOLL, A. H., LASKAR, J., MONECHI, S., PLUMB, K. A., POWELL, J., RAFFI, I., RÖHL, U., SADLER, P., SANFILIPPO, A., SCHMITZ, B., SHACKLETON, N. J., SHIELDS, G. A., STRAUSS, H., VAN DAM, J., VAN KOLFSCHOTEN, T., VEIZER, J., and WILSON, D., 2004. A *Geologic Time Scale 2004*. Cambridge: Cambridge University Press, 589 pp.

HAQ, B. U., HARDENBOL, J. and VAIL, P. R., 1987. Chronology of fluctuating sea levels since the Triassic. *Science*, 235: 1156-1167.

HERBIG, H. G., 1986. Lithostratigraphisch-fazielle Untersuchungen im marinen Altertertiär südlich des zentralen Hohen Atlas (Marokko). *Berliner geowissenschaftliche Abhandlungen*, (A), 66: 343-380.

———, 1987. The Paleogene of the Atlas System (Morocco): Facies control by eustacy and synsedimentary tectonics. - In: Matheis, G. and Schandelmeier, H., Eds., *Current research in African Earth Sciences*, 253-256. (Extended Abstracts, 14th Colloquium on African Earth Sciences, Berlin 1987). Rotterdam: Balkema.

———, 1988. The Upper Cretaceous to Tertiary hammada west of Errachidia (SE Morocco): a continental sequence involving paleosol development. *Neues Jahrbuch für Geologie und Paläontologie, Abhandlungen*, 176: 187-212.

———, 1991. Das Paläogen am Südrand des zentralen Hohen Atlas und im Mittleren Atlas Marokkos. Stratigraphie, Fazies, Paläogeographie und Paläotektonik. *Berliner geowissenschaftliche Abhandlungen*, (A), 135: 289 pp.

HERBIG, H.-G. and GREGOR, H.-J., 1992. The mangrove-forming palm *Nypa* from the early Paleogene of southern Morocco. Paleoenvironment and paleoclimate. *Géologie mediterranéenne*, 27, 2 (1990): 123-137.

HERBIG, H. G. and TRAPPE, J., 1994. Stratigraphy of the Subatlas Group (Maastrichtian – Middle Eocene, Morocco). *Newsletters on Stratigraphy*, 30: 125-165.

HERBIG, H.-G. and DRAGASTAN, O., 2005. Die Grünalge *Halimeda* aus dem südmarokkanischen Alttertiär – Beiträge zur Phylogenie und Paläoökologie eines lebendes Fossils. *Berichte des Institutes für Erdwissenschaften, Karl-Franzens-Universität Graz*, 10: 40-43.

HILLIS, L. (as HILLIS-COLINVAUX, L.), 1980. Ecology and taxonomy of *Halimeda*: primary producer of coral reefs. *Advances in Marine Biology*, 17: 1-327.

———, 1984. Systematics of Siphonales. In: Irvine, D.E.G. and John, D.M., Eds., *Systematics of the Green Algae*, 271-296. Systematics Association, Special Volume, 27.

———, 2000. Phylogeny of *Halimeda* (Bryopsidales): linking paleontological, morphological and molecular data. *Acta Palaeontologica Romaniae*, 2: 183-189.

———, 2001. The calcareous reef alga *Halimeda* (Chlorophyta, Bryopsidales): a Cretaceous genus that diversified in the Cenozoic. *Palaeogeography, Palaeoclimatology, Palaeoecology*, 166: 89-100.

HILLIS, W. L., ENGMAN, J. A. and KOOISTRA, W. H. C. F., 1998. Morphological and molecular phylogenies of *Halimeda* (Chlorophyta, Bryopsidales) identify three evolutionary lineages. *Journal of Phycology*, 34: 669-681.

HINE, A. C., HALLOCK, P., HARRIS, M. W., MULLINS, H. T., BELKNAP, D. F. and JAAP, W. C., 1988. *Halimeda* bioherms along an open seaway: Miskito channel, Nicaraguan rise, SW Caribbean Sea. *Coral Reefs*, 6: 173-178.

HOWE, M. A., 1905. Phycological studies. I. New Chlorophyceae from Florida and Bahamas. *Bulletin of the Torrey Botanical Club*, 32: 563-586.

———, 1907. Phycological studies. III. Further notes on *Halimeda* and *Avrainvillea*. *Bulletin of the Torrey Botanical Club*, 34: 491-516.

JOHNS, H. D. and MOORE, C. H. 1988. Reef to basin sediment transport using *Halimeda* as a sediment tracer, Grand Cayman Island, West Indies. *Coral Reefs*, 6: 187-193.

JOHNSON, J. H. 1968. Lower Cretaceous algae from Texas. *Professional Contributions of the Colorado School of Mines*, 4: 1-71.

KEMPER, E., MARONDE, H. D. and STOPPEL, D. 1976. Triassic and Jurassic limestone in the region northwest and west of Si Sawat (Kanchanaburi province, western Thailand. *Geologisches Jahrbuch*, (B), 21: 93-127.

KOOISTRA, W.H.C.F., 2002. Molecular phylogenies of Udoteaceae (Bryopsidales, Chlorophyta) reveal non-monophyly for *Udotea, Penicillus* and *Chlorodesmis*. *Phycologia*, 41: 453-462.

KOOISTRA, W. H. C. F., CALDERON, M. and HILLIS, L. W., 1999. Development of the extant diversity in *Halimeda* is linked to vicariant events. *Hydrobiologia*, 398/399: 39-45.

KOOISTRA, W. H. C. F., COPPEJANS, E. G. G. and PAYRI, C., 2002. Molecular systematics, historical ecology, and phylogeography of Halimeda (Bryopsidales). *Molecular Phylogenetics and Evolution*, 24: 121-138.

KUSS, J. and HERBIG, H. G., 1993. Biogeography, facies and taxonomy of Early Tertiary green algae from Egypt and Morocco. In: Barattolo, F., De Castro, P. and Parente, M., Eds. *Studies on fossil benthic algae*, 249-280. Bollettino della Società Paleontologica Italiana, Special Volume 1.

LAMOUROUX, J. V. F., 1812. Sur la classification des polypiers coralligènes non entièrement pierreux. *Nouveaux Bulletin des Sciences, par la Societé philomatiques de Paris*, 3: 181-188.

———, 1816. *Histoire des polypiers coralligenes flexibles, vulgairenommes zoophytes*. Caen, 460 pp.

LEE, R. E. (1989). *Phycology*. Cambridge: Cambridge University Press, xv + 645 pp.

LE MAITRE, D., 1937. Études paléontologiques sur le Lias du Maroc. Nouvelles recherches sur les spongiomorphides et les algues du Lias et de l'oolithe inférieure. *Notes et Mémoires du Service géologique du Maroc*, 43: 1-25.

LITTLER, D. S. and LITTLER, M. M., 1990. Systematics of Udeotea species (Bryopsidales, Chlorophyta) in tropical western Atlantic. *Phycologia*, 29: 206-252.

———, 1992. Systematics of Avrainvillea (Bryopsidales, Chlorophyta) in tropical western Atlantic. *Phycologia*, 31: 206-252.

———, 1997. An illustrated marine flora of the Pelican Cays, Belize. *Bulletin of the Biological Society of Washington*, 9: 1-149.

———, 2000. *Carribean reef plants: an identification guide to the reef plants of the Caribbean, Bahamas, Florida, and Gulf of Mexico*. Washington D.C.: OffShore Graphics Inc., 542 pp.

———, 2003. *South Pacific Reef Plants: A divers guide to the plant life of South Pacific coral reefs*. Washington, D.C.: OffShore Graphics Inc., 331 pp.

LITTLER, D. S., LITTLER, M. M., BUCHER, K. E. and NORRIS, J. N., 1989. *Marine plants of the Caribbean. A field guide from Florida to Brazil*. Washington, D.C.: Smithsonian Institution Press, 263 pp.

MACINTYRE, G. I. and REID R. P., 1995. Crystal alteration in a living calcareous alga (*Halimeda*): Implications for studies in skeletal diagenesis. *Journal of Sedimentary Research*, A65: 143-153.

MARSHALL, J. F. and DAVIES, J. P., 1988. *Halimeda* bioherms of the northern Great Barrier Reef. *Coral Reefs*, 6: 139-148.

MARTIN, J. M., BRAGA, J. C. and RIDING, R., 1997. Late Miocene *Halimeda* alga-microbial segment reefs in the marginal Mediterranean Sorbas Basin, Spain. *Sedimentology*, 44: 441-456.

MASSIEUX, M., 1966. Les algues du Nummulitique égyptien et des terrains crétacés-éocènes de quelques régions mésogéennes. 2ème partie, étude critique. *Revue de Micropaléontologie*, 9: 135-146.

MATTOX, R. K. AND STEWART, D. K., 1984. Classification fo the Green Algae: a concept based on comparative cytology. In: Irvine, D.E.G. and John, D.M., Eds. *Systematics of the Green Algae*, 29-72. Systematic Association Special Volume 27.

MICHARD, A., 1976. Eléments de géologie marocaine. *Notes et Mémoires du Service Géologique du Maroc*, 252: 1-408 pp.

MILLIMAN, J. D., 1974. *Marine carbonates*. Berlin-Heidelberg-New York: Springer-Verlag, 375 pp.

MORELLET, L. and MORELLET, J., 1922. Contribution à l'étude paléontologique du genre *Halimeda* Lam. (Algue siphonée de la famille des Codiacées). *Bulletin de la Societé Géologique de France*, *4ème serie*, 22: 291-296.

———, 1940a. Les Dasycladacées et les Codiacées (algues vertes) du 'calcaire pisolitique'. *Compte Rendu Sommaire des Séances, Société Géologique de France*, 1940: 116-118.

———, 1940b. Étude sur les algues calcaires de l'Eocène de Cotentin. *Bulletin de la Societé Géologique de France*, 5ème Série, 10: 201-206.

MORET, L. 1931. Recherches géologiques dans l'Atlas de Marrakech. *Notes et Mémoires du Service Géologique du Maroc*, No. 18 [= *Travaux du Laboratoire de Géologie de la Faculté des Sciences de l'Université de Grenoble*, 16 (1)]: 262 pp.

———, 1938. Contribution à la paléontologie des couches crétacées et éocènes du versant sud de l'Atlas de Marrakech (Maroc). *Notes et Mémoires, Service des Mines et de la Carte Géologique du Maroc*, No. 49: 77 pp.

MOHR, B. and FECHNER, G. 1986. Eine eozäne Mikroflora (Sporomorphae und Dinoflagellaten-Zysten) aus der Südatlas-Randzone westlich Boumalne du Dadès (Marokko). *Berliner Geowissenschaftliche Abhandlungen*, (A), 66: 381-414.

MU, X., 1991. Fossil Udoteaceae and Gymnocodiaceae. In: Riding, R., Ed. *Calcareous algae and stromatolites*. Berlin-Heidelberg-New York: Springer Verlag, 146-166.

NEUMANN, A. C. and LAND, L. S., 1975. Lime mud deposition and calcareous algae in the Bight of Abaco, Bahamas: a budget. *Journal of Sedimentary Petrology*, 45: 763-786.

ORME, G. R. and SALAMA, M. S. 1988. Form and seismic stratigraphy of Halimeda banks in part of the northern Great Barrier Reef Province. *Coral Reefs*, 6: 131-137.

PAL, A. K., 1971. On the algal genera *Arabicodium*, *Boueina* and *Halimeda* (Codiacean algae) in the Bagh Group of Madhya Pradesh. *Quarterly Journal of the Geological, Mining and Metallurgical Society of India*, 43: 131-140.

PFENDER, J., 1940. Les algues du Numulitique égyptien et des terrains crétacés-éocènes de quelques regions mésogéenes. *Bulletin de la Institute d' Egypte*, 22: 225-250.

PFENDER, J. and MASSIEUX, M., 1966. Les algues du Nummulitique égyptien des terrains crétacés-éocènes des quelques régions mésogeennes (prèmiere partie). *Revue de Micropaléontologie*, 9: 111-132.

PIA, J., 1927. Thallophyta. In: Hirmer, E., Ed. *Handbuch der Paläobotanik*. München-Berlin: Oldenbourg Verlag, 31-136.

———, 1932. Remarques sur les algues calcaires. In: Pia, J., Pfender, J. and Termier, H., Etudes géologique sur les calcaires de Bekrit et Timhadit (Moyen Atlas). *Notes et Mémoires, Service des Mines et de la Carte Géologique du Maroc*, 20: 1-19.

PONCET, J., 1989. Présence du genre *Halimeda* Lamouroux, 1812 (algue verte calcaire) dans le Permian supérieur du sud Tunisien. *Revue de Micropaléontologie*, 32: 40-44.

RADOICIC, R., 1990. Paleogene Dasycladacean algae from subsurface of the western Iraqi desert. *Bulletin de l'Académie Serbe des Sciences et des Arts, Classe de Sciences Mathématiques et Naturelles, Sciences Naturelles*, 32: 91-103.

———, 1992. Paleocenska Mikroflora kreènajka Kamenjaka, SI Majevica (èetvrta Biljeska). *Radovi Geoinstituta Beograd* (Proceedings of Geoinstitute Belgrade), 26: 201-230.

———, 1998. *Halimeda elliotti* Conard and Rioult 1977, (Udoteacea, green algae) from the Kukes Cretaceous Unit (Mirdita Zone). *Glasnik Prirodnjackog Muzeja u Beogradu*, Serija A, Geoloske nauke (Bulletin of Natural History Museum in Belgrade, Serial A, Geological Sciences) 47-50 (1992-1998): 181-188.

RAHHALI, I., 1970. Foraminifères benthoniques et pélagiques du Crétacé supérieur du synclinal d'El-Koubbat (Moyen Atlas - Maroc). *Notes du Service Géologique du Maroc*, 30: 51-98.

ROBERTS, H.H., PHIPPS, C.V. and EFFENDI, L. 1987. *Halimeda* bioherms of the eastern Java Sea, Indonesia. *Geology*, 15: 371-374.

ROBERTS, H. H., AHARON, P. and PHIPPS, C. V. 1988. Morphology and sedimentology of *Halimeda* bioherms from the eastern Java Sea (Indonesia). *Coral Reefs*, 6: 161-172.

ROCH, E., 1939. Description géologique des montagnes à l'Est de Marrakech. *Notes et Mémoires du Service Géologique du Maroc*, No. 51: 438 pp.

ROTHPLETZ, A., 1913. Über die Kalkalgen, Spongiostromen und einige andere Fossilien aus dem Obersilur Gotlands. *Sveriges Geologiske Undersökning*, 10: 57 pp.

ROUND, E. F., 1963. The taxonomy of the Chlorophyta. *British Phycological Bulletin*, 2: 224-235.

———, 1984. The systematics of Chlorophyta: A historical review leading to some modern concepts (Taxonomy of the Chlorophyta III). In: Irvine, D. E. G. and John, D. M., Eds., *Systematics of the Green Algae,* 1-27. Systematic Association Special Volume 27.

SALVAN, H. 1960. Les phosphates de chaux sédimentaires du Maroc. Leurs caractéristiques et leurs problèmes (Essai de synthèse). *Notes Marocaines, Societé de Géographie du Maroc*, 14: 7-20.

SEGONZAC, G., 1979. Algues calcaires du Thanétien d'Esperanza (Aude). (Dasycladacées, Corallinacées). *Bulletin de la Société d'Histoire Naturelle de Toulouse*, 115 (3-4): 439-463.

SEGONZAC, G., PEYBERNÉS, B. and RAHHALI, I., 1986. Les algues du 'Calcaire rosé de Timahdite' (Eocène inférieur) dans le Moyen-Atlas (Maroc): description d'*Halimeda nana* Pia, 1932, dans sa localité-type et son paléoenvironnement. *Journal of African Earth Sciences*, 5: 501-507.

SHUYSKI, V. P., 1987. Zelenie Vodorosli (Chlorophyta). In: Chuvashov, B. I., Ed., *Iskopaemie izvestkoviie vodorosli*: 38-108.

SILVA, P.S., 1980. Names of classes and families of living algae with special reference to their use in the Index Nominum Genericorum (Plantarum). *Regnum Vegetabile*, 103: 1-156.

———, 1982. Chlorophyceae. In: Parker, S.P. , Ed. *Synopsis and classification of living organisms,* Vol. 1, 133-161. New York: McGraw-Hill.

SILVA, P. S., BASSON, P. W. and MOE, R. L., 1996. Catalogue of the benthic marine algae of the Indian Ocean. *University of California Publications in Botany*, 79: 1259 pp.

SIMMONS, M. D. and JOHNSTON, M. J., 1991. *Permocalculus iagifuensis* sp. nov.: a new Miocene gymnocodiacean alga from Papua-New Guinea. *Journal of Micropaleontology*, 9: 238-244.

STEINMANN, G. 1899. Über *Boueina*, eine fossile Alge aus der Familie der Codiaceen. *Berichte der Naturforschenden Gesellschaft Freiburg*, 11: 62-72.

TAPPAN, H. 1980. *The paleobiology of plant protists.* San Fransisco: W.H. Freeman and Co, 1028 pp.

TAYLOR, W. R., 1950. *Plants of Bikini and other northern Marshall Islands*. Ann Arbor: University of Michigan Press, xv+227 pp.

———, 1960. *Marine algae of the eastern tropical and subtropical coasts of the Americas*. Ann Arbor: University of Michigan Press, xi+870 pp.

TRAGELEHN, H., 1996. "Maastricht und Paläozän am Südrand der Nördlichen Kalkalpen (Niederösterreich, Steiermark) – Fazies, Stratigraphie, Paläogeographie, und Fossilführung des Kambühelkalkes und assoziierter Sedimente." Dissertation, Universität Erlangen. Vol. I: 1-216, Vol. II: pls. 1-67.

TRAPPE, J., 1989. "Das marine Alttertiär im westlichen Hohen Atlas. Mikrofazies, Paläogeographie, Phosphoritgenese." Dissertation, Universität Bonn: 219 pp.

———, 1991. Stratigraphy, facies distribution and paleogeography of the marine Paleogene from the western High Atlas, Morocco. *Neues Jahrbuch für Geologie und Paläontologie, Abhandlungen*, 180: 279-321.

———, 1992. Microfacies zonation and spatial evolution of a carbonate ramp: marginal Moroccan phosphate sea during the Paleogene. *Geologische Rundschau*, 81: 105-126.

VERBRUGGEN, H. and KOOISTRA, W. H. C. F., 2004. Morphological characterization of lineages within the calcified tropical seaweed genus *Halimeda* (Bryopsidales, Chlorophyta). *European Journal of Phycology*, 39: 213-228.

VERBRUGGEN, H., DE CLERCK, O., COCQUYT, E., KOOISTRA, W. H. C. F. and COPPEJANS, E. 2005a. Morphometric taxonomy of siphonous green algae: a methodological study within the genus Halimeda (Bryopsidales). *Journal of Phycology*, 41: 126-139..

VERBRUGGEN, H., DE CLERCK, O., KOOISTRA, W. H. C. F. and COPPEJANS, E., 2005b. Molecular and morphometric data pinpoint species boundaries in *Halimeda* Section Rhipsalis (Bryopsidales, Chlorophyta). *Journal of Phycology*, 41: 606-621.

WRAY, J. L., 1977. Calcareous Algae. *Developments in Palaeontology and Stratigraphy*, 4: 1-185.

YU-JING, W., 1976. Calcareous algae from the Late Cretaceous and Paleogene sediments in the Mount Jolmo Lungma region. Palaeontology II. Tibetan scientific team. *A report of scientific expedition in the Mount Jolmo Lungma (1966-1968)*, 425-457. Academia Sinica, Beijing: Science Press.

ZYLKA, R. and JACOBSHAGEN, V., 1986. Zur strukturellen Entwicklung am Südrand des zentralen Hohen Atlas (Marokko). *Berliner Geowissenschaftliche Abhandlungen*, (A), 66: 415-432.

Manuscript received December 15, 2005
Manuscript accepted March 25, 2007

APPENDIX 1

Halimeda-bearing sections, southern rim of central High Atlas, Morocco. Indicated are section code, geographic position, sheet of topographic map "Carte du Maroc 1 : 100.000," and Lambert coordinates (x/y) (from Herbig 1991)

SA-5 Oued Imassine, 0.8km N of height 1630. NH-29-XXIV-2 Qalaa't Mgouna. 403.6/73.8.

SA-7 Jbel Riguit, northern slope, 1.8km W Ait Youl, Dades valley). NH-29-XXIV-2 Qalaa't Mgouna. 440.5/92.0.

SA-8 Assif n'Ougalt, southern side, 7.0km W of Arg n'Sidi Ali ou Bourek. NH-30-XIX-1 Boumalne. 463.8/99.8

SA-10 1.6km N of Timadriouine, gravel road to Arg n'Sidi Ali ou Bourek,. NH-30-XIX-1 Boumalne. 469.8/91.9.

SA-11 5km N of Tinerhir, road to Todrha gorge. NH-30-XIX-3 Tinerhir. 483.9/104.7. Hypostratotype of Jbel Guersif Formation and Ait Ouarhitane Formation.

SA-12 4.5km N of Tinerhir, N of height 1478. NH-30-XIX-3 Tinerhir. 487.4/107.8.

SA-13 Akka Mellal plateau, 7km WSW of Tinerhir. NH-30-XIX-3 Tinerhir. 480.0/100.6.

SA-14 Jbel Tagount, southern foot 8.5km W of Tinerhir. NH-30-XIX-3 Tinerhir. 478.5/104.2. Stratotype of Ait Ouarhitane Formation and Jbel Tagount Formation.

SA-15 Jbel Bou Aissa, western end, 10km NW Imider. NH-30-XIX-1 Boumalne. 457.7/95.7.

SA-18 Jbel Istefane, 2.5km W of Arg n'Sidi Ali ou Bourek. NH-30-XIX-1 Boumalne. 468.5/98.5.

SA-19 Jbel Guersif, eastern end, 12.0km N of Qalaa't Mgouna. NH-29-XXIV-2 Qalaa't Mgouna. 431.8/84.0. Stratotype of Jbel Guersif Formation.

SA-20 Jbel Ta'louit, northern slope, gravel road to Bou Taghrar. NH-29-XXIV-2 Qalaa't Mgouna. 430.0/87.6. Hypostratotype of Ait Ouarhitane Formation and Jbel Tagount Formation.

SA-21 1.1km NW of Bou Taghrar. NH-29-XXIV-2 Qalaa't Mgouna. 429.4/89.7.

SA-22 5.0km W of Agouti et Tahtani. NH-29-XXIV-2 Qalaa't Mgouna. 420.8/85.8.

Sa-25a Jbel Tassa n'Tlerhoumt, 2.7km E of Ait Ouglif, Dades valley. NH-30-XIX-1 Boumalne. 448.8/95.4.

PLATE 1 (page 37)

Halimeda cylindracea Decaisne 1842. Jbel Guersif Formation (late Thanetian). Figures ×63.
Sample numbers refer to Herbig (1991, fig. 17). For location of sections see text-figure 2b and Appendix 1.

1 Longitudinal-oblique section. 130584/5, section SA-5 (GIK 1874a).

2 Detail in the transitional area between medullar and cortical zones showing the shape and disposition of 1st, 2nd, and 3rd cortical utricle series (see arrow). 130584/5, section SA-5 (GIK 1874a).

3 Longitudinal-oblique section. 180584/6, section SA-11(GIK 1886a).

4 Transverse sections showing empty medullar (m) area and cortex with three utricle series. 130584/5, section SA-5 (GIK 1874a).

5 Transverse section showing large medullar (m) area and cortex with three utricle series. 031085/5, section SA-13 (GIK 1897a).

6 Transverse section showing large medullar (m) area and cortex with three utricle series. 031085/5, section SA-13(GIK 1897a).

PLATE 2 (page 38)

Halimeda cylindracea Decaisne 1842. Jbel Guersif Formation (late Thanetian). Figures ×63.
Sample numbers refer to Herbig (1991, fig. 17). For location of sections see text-figure 2b and Appendix 1.

1 Longitudinal-oblique section showing the disposition of medullar siphons (m) and the cortical utricle series. 160584/8, section SA-8 (GIK 1879a).

2 Tangential-oblique section. 130584/5, section SA-5 (GIK 1874a).

3 Tangential-oblique section, detail and arrangement of cortical utricles, eight in number, small and round (see arrows). 130584/5, section SA-5 (GIK 1874a).

4-7 Transverse sections in medullar area (m) and the characteristic 1st, 2nd, 3rd, and 4th utricle series (note arrow in Fig. 6). 180584/6, section SA-11 (GIK 1886a).

PLATE 3 (page 39)

Halimeda nana Pia 1932. Jbel Guersif Formation (late Thanetian). Sample numbers refer to Herbig (1991, fig. 17).
For location of sections see text-fig. 2b and Appendix 1.

1 Longitudinal-oblique section. 180584/6, section SA-11 (GIK 1886b). ×63.

2 Longitudinal-oblique section. 180584/6, section SA-11 (GIK 1886b). ×27.

3 Longitudinal-oblique section and transverse section showing the two or three small, fine utricle series (arrow). 180584/6 (GIK 1886b), section SA-11. ×27.

4 Longitudinal-oblique section. 160584/12, section SA-8 (GIK 1881). ×63.

5 Longitudinal-oblique section. 180584/6, section SA-11 (GIK 1886b). ×63.

6 Longitudinal-oblique section showing the two or three small, fine utricle series (arrow). 180584/6, section SA-11 (GIK 1886b). ×27.

7 Longitudinal-oblique section. 130584/3, section SA-5 (GIK 1872a). ×63.

8 Longitudinal-oblique section showing segment with small lobe looking like a „lateral branch". 160584/12, section SA-8 (GIK 1881). ×63.

9 Longitudinal-oblique section showing the two or three small, fine utricle series (arrow). 031085/2, section SA-13 (GIK 1895a). ×27.

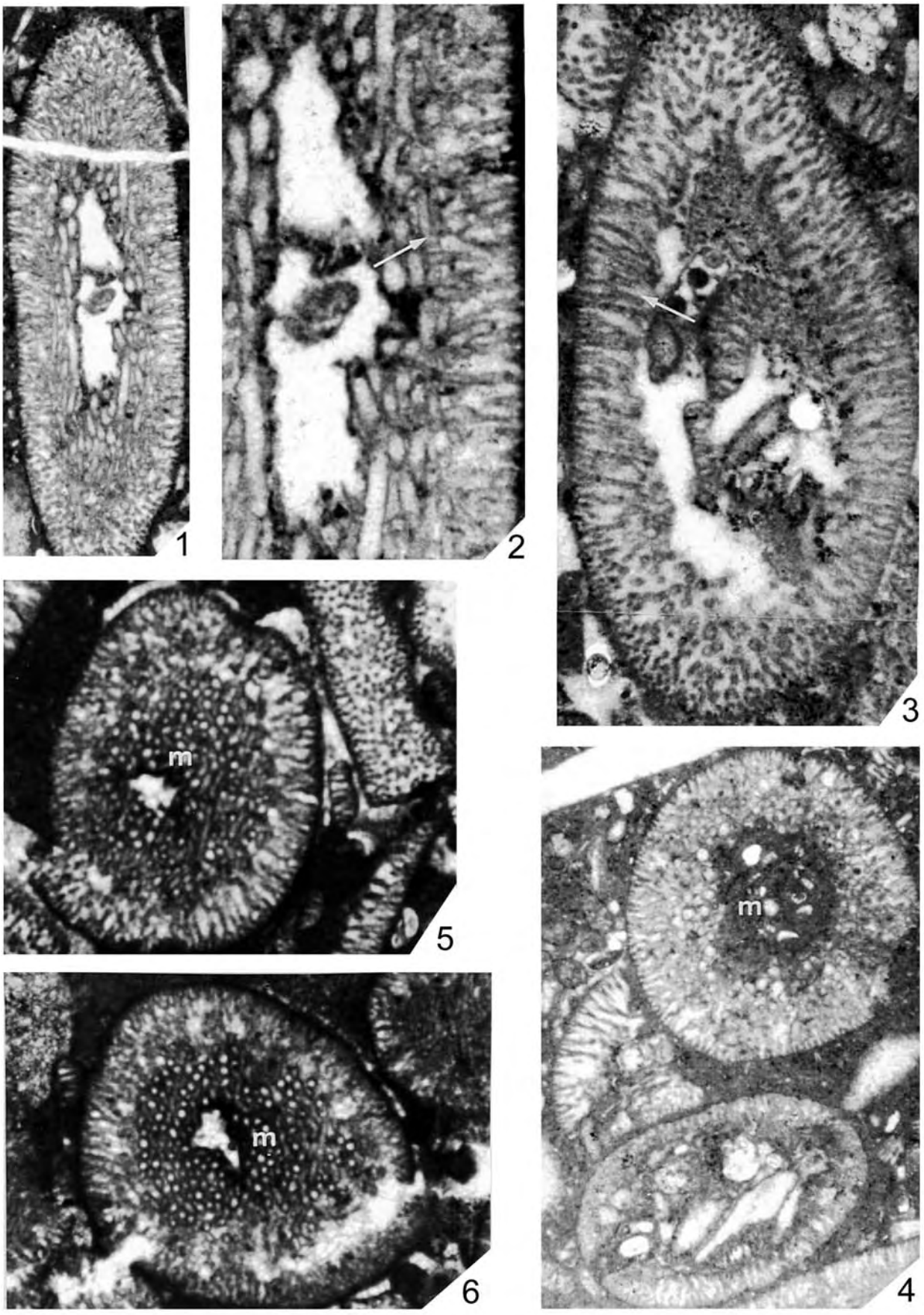
1
2
3
m
5
m
4
m
6

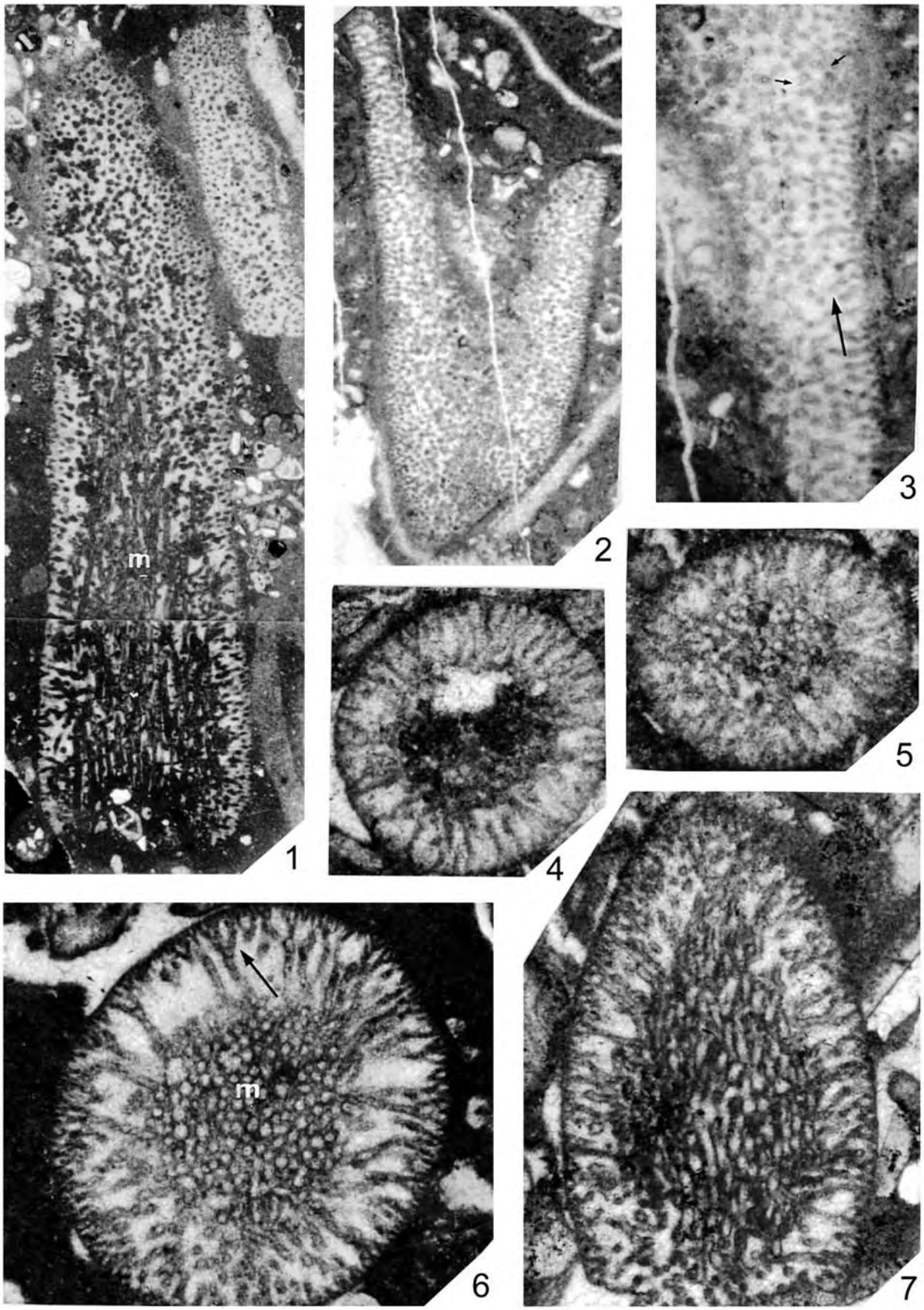
m
1
2
3
4
5
m
6
7

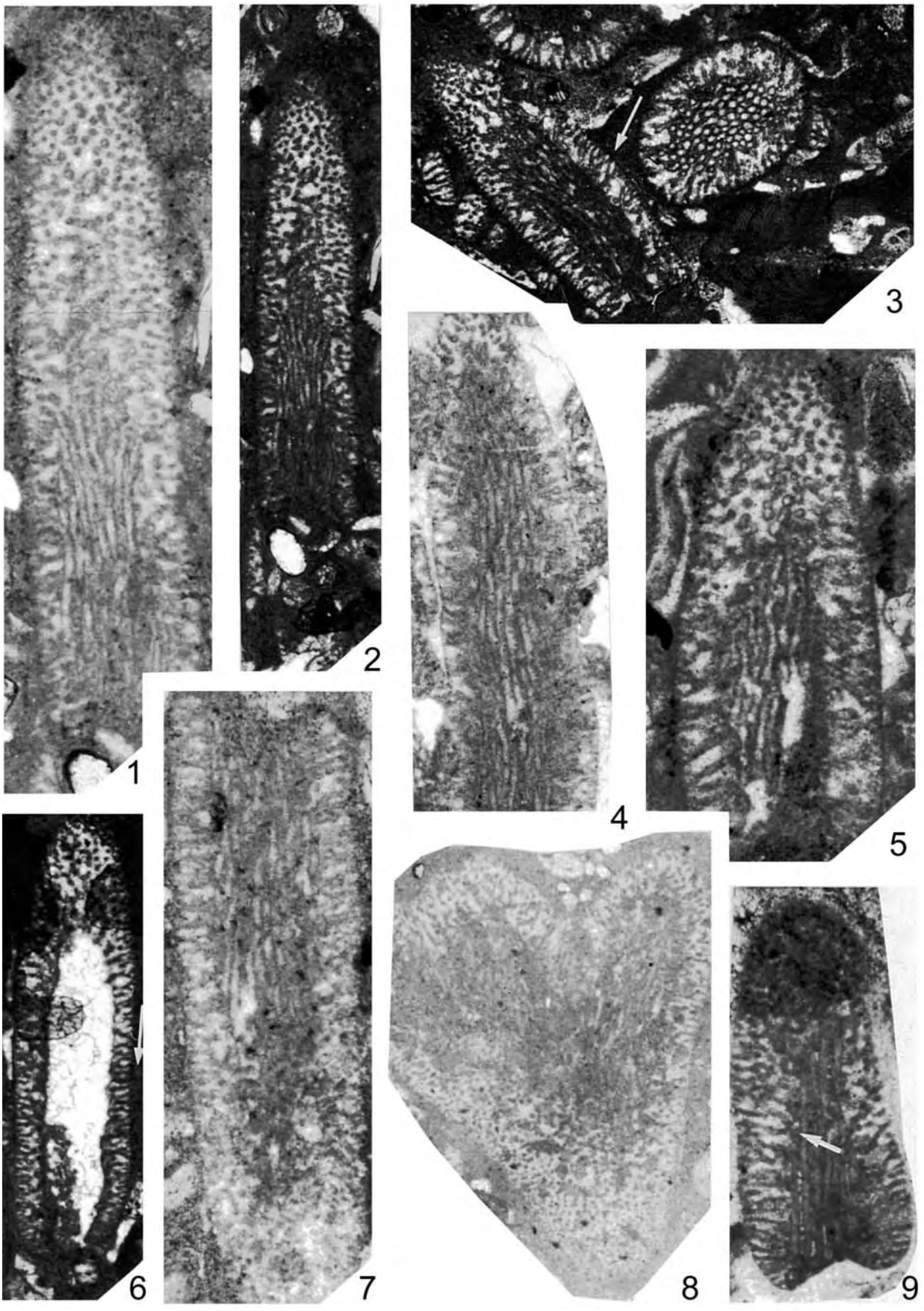
1
2
3
4
5
6
7
8
9

PLATE 4 (page 41)

Halimeda incrassata (J. Ellis) Lamouroux 1816. Figs. 1, 3-9: Jbel Guersif Formation (late Thanetian). Figures ×63 except Fig. 2a-b: Recent, scale bar: 50µm. Sample numbers refer to Herbig (1991, fig. 17). For location of sections see text-fig 2b and Appendix 1.

1 Longitudinal-oblique sections showing three utricle series (arrows). 160584/11, section SA-8 (GIK 1880a).

2 Transverse (a) and longitudinal (b) sections from a Recent specimen. fm: medullar siphons, uI –uIV: cortical utricle series (from Dragastan and Soliman, 2002).

3 Tangential section showing the disposition of six cortical utricles in a rosette-like bundle (arrow). 131085/16, section SA-22 (GIK 1917a).

4 Longitudinal-oblique sections showing three utricle series (arrow). 031085/4, section SA-13 (GIK 1896a).

5 Transverse section showing cortex with typical three up to four utricle series (arrow). 130584/5, section SA-5 (GIK 1874b).

6 Transverse section showing cortex with typical three up to four utricle series (arrow). 160584/8, section SA-8 (GIK 1879).

7 Transverse section showing cortex with typical three up to four utricle series (arrow). 031085/4, section SA-13 (GIK 1896a).

8 Fragment of cortex showing up to five utricle series (arrow). 130584/4, section SA-5 (GIK 1873a).

9 Fragment of cortex showing up to five utricle series (arrow). 170584/31, section SA-10 (GIK 1885).

PLATE 5 (page 42)

Halimeda incrassata (J. Ellis) Lamouroux 1816 (Figs. 1-4) and, for comparison, *Halimeda nana* Pia 1932 (Figs. 5-6). Jbel Guersif Formation (late Thanetian). Figures ×63. Sample numbers refer to Herbig (1991, fig. 17). For location of sections see text-fig 2b and Appendix 1.

1 *Halimeda incrassata* (J. Ellis) Lamouroux 1816. Longitudinal-oblique section with four utricle series. 031085/5, section SA-13 (GIK 1897b).

2 *Halimeda incrassata* (J. Ellis) Lamouroux 1816. Transverse section with medullar area (m) and thick cortex. 130584/4, section SA-5 (GIK 1873a).

3 *Halimeda incrassata* (J. Ellis) Lamouroux 1816. Longitudinal-oblique section with three utricle series. 160584/8, section SA-8 (GIK 1879).

4 *Halimeda incrassata* (J. Ellis) Lamouroux 1816. Broken segment showing cortex with four utricle series (arrow). 130584/5, section SA-5 (GIK 1874b).

5-6 *Halimeda nana* Pia 1932. Specimens illustrated in plate 3, figure 3 for comparison with *H. incrassata* showing the cortex with two up to three utricle series. 180584/6, section SA-11 (GIK 1886b).

PLATE 6 (page 43)

Halimeda opuntia (Linnaeus) Lamouroux 1816 (Fig. 1), *Halimeda monile* (J. Ellis and Solander) Lamouroux 1816 (Figs. 2-5) and *H. erikfluegeli* n. sp. (Figs. 6-7) from Jbel Guersif Formation (late Thanetian). Figures ×63. Sample numbers refer to Herbig (1991, fig. 17). For location of sections see text-fig 2b and Appendix 1.

1 *Halimeda opuntia* (Linnaeus) Lamouroux 1816. Tangential oblique section in a disc-like segment showing large medullar area (m)and the cortex (c). 180584/6, section SA-11 (GIK 1886c).

2 *Halimeda monile* (J. Ellis and Solander) Lamouroux 1816. Oblique-transverse section showing three utricle series (arrow). Note arrangement of medullar siphons in round bundle in lowest part of medulla. 131085/16, section SA-22 (GIK 1917b).

3-5 *Halimeda monile* (J. Ellis and Solander) Lamouroux 1816. Transverse-oblique and transverse section showing few medullar siphons and in the cortex three utricle series (arrows). 130584/4, section SA-5 (GIK 1873b).

6 *Halimeda erikfluegeli* n.sp. Holotype. Longitudinal section. 021085/7, section SA-12 (GIK 1894a).

7 *Halimeda erikfluegeli* n.sp. Paratype. (GIK). Transverse section. 031085/2, section SA-13 (GIK 1895b).

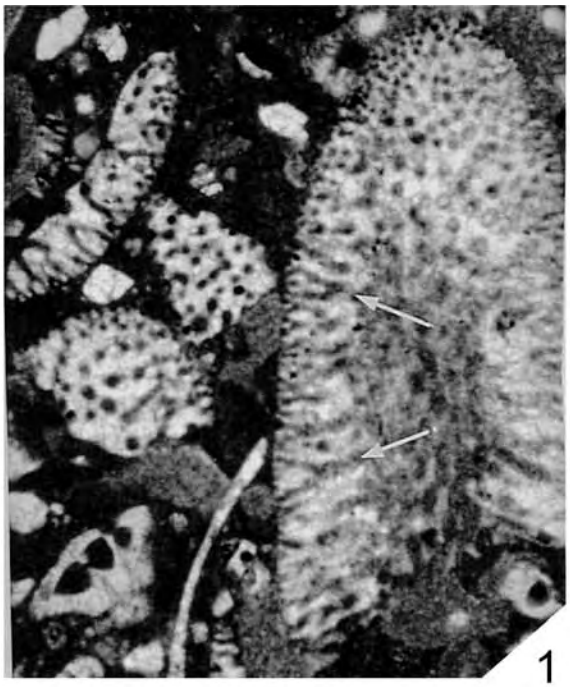

1

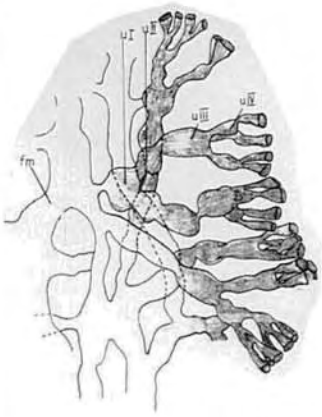

2b

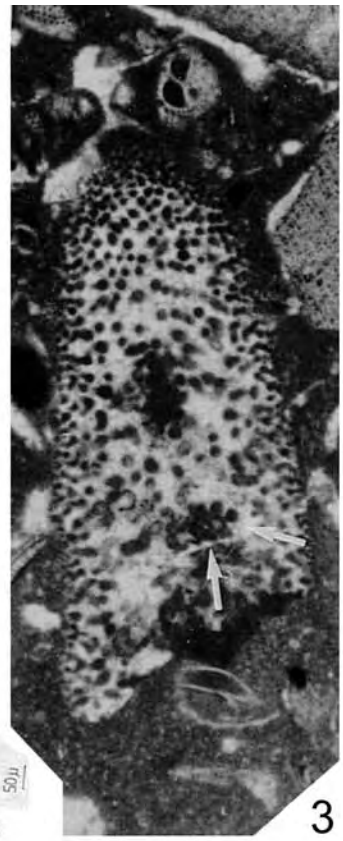

3

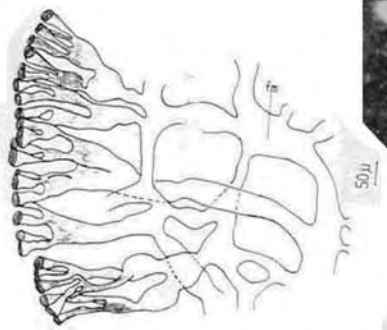

2a

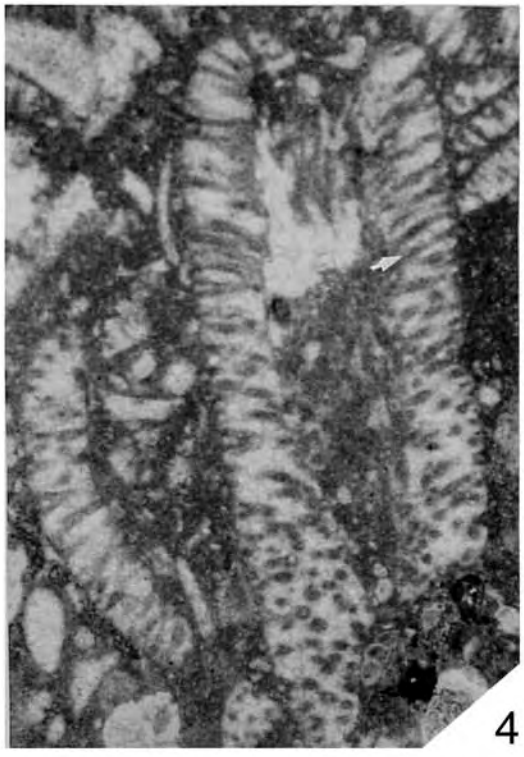

4

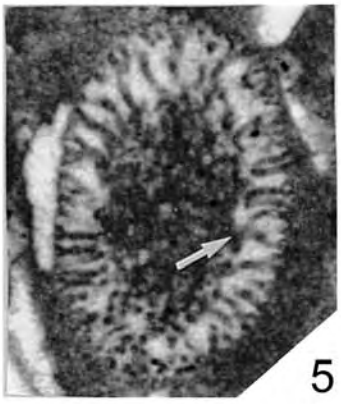

5

6

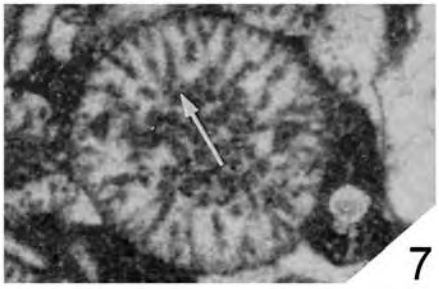

7

8

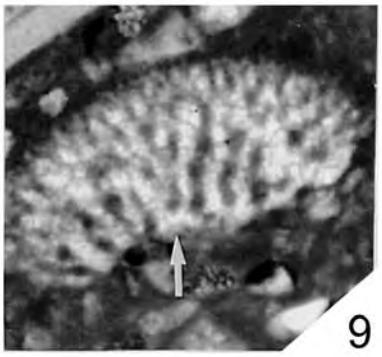

9


1

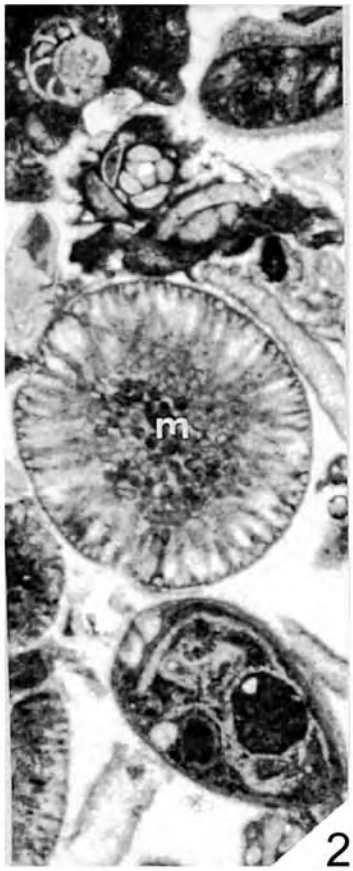

2

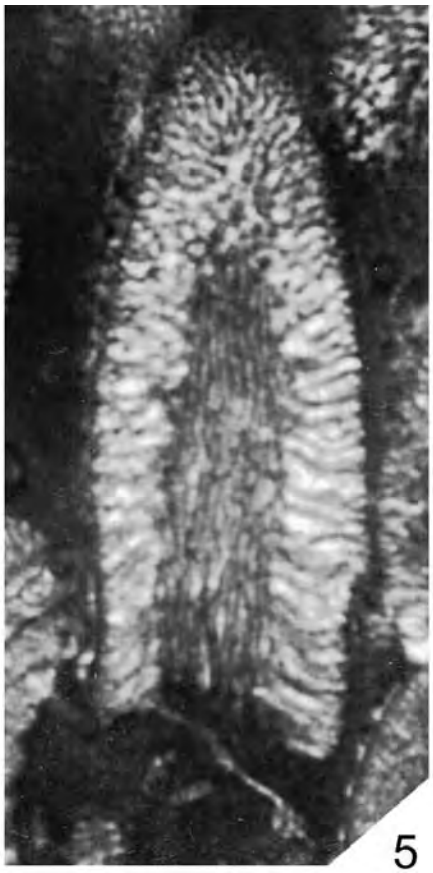
5

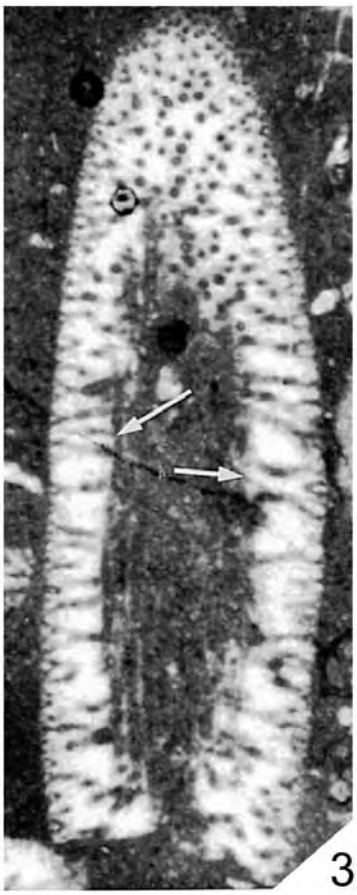
3


4

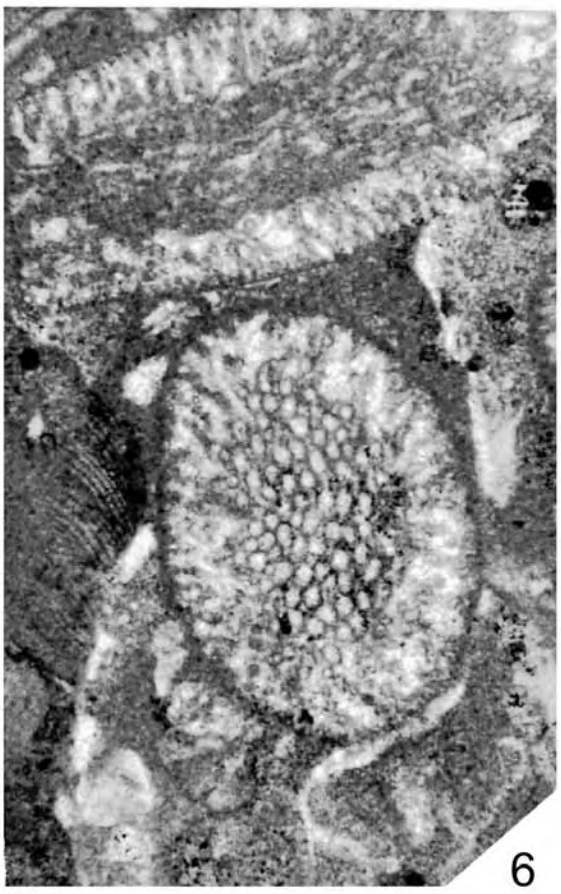
6

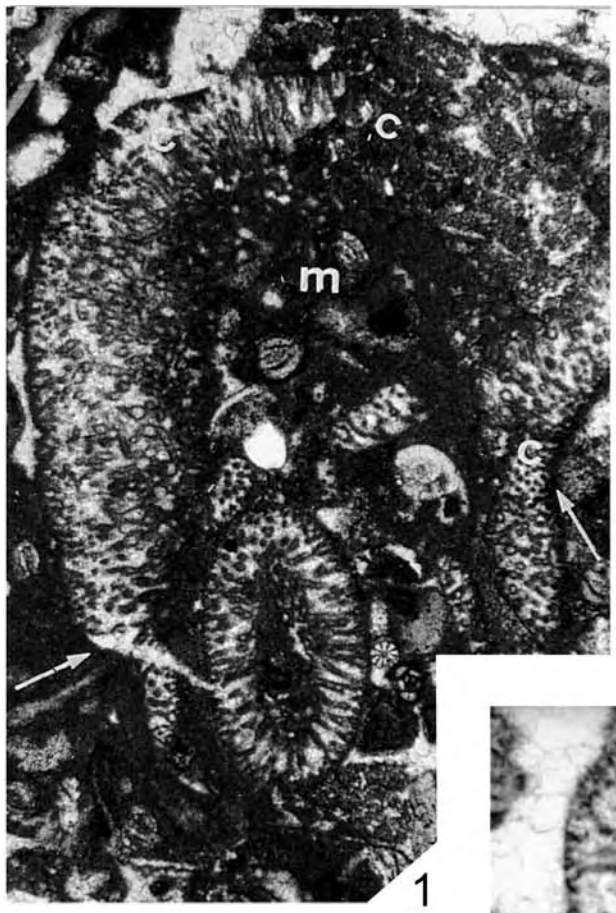

1

2

3

4

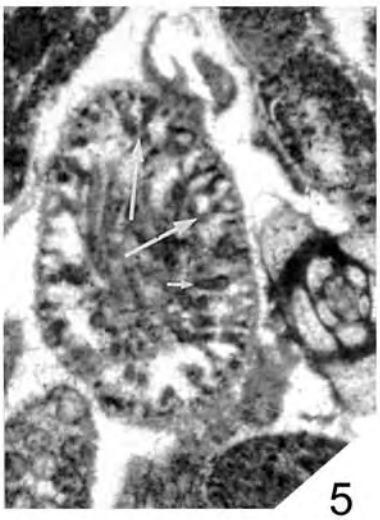

5

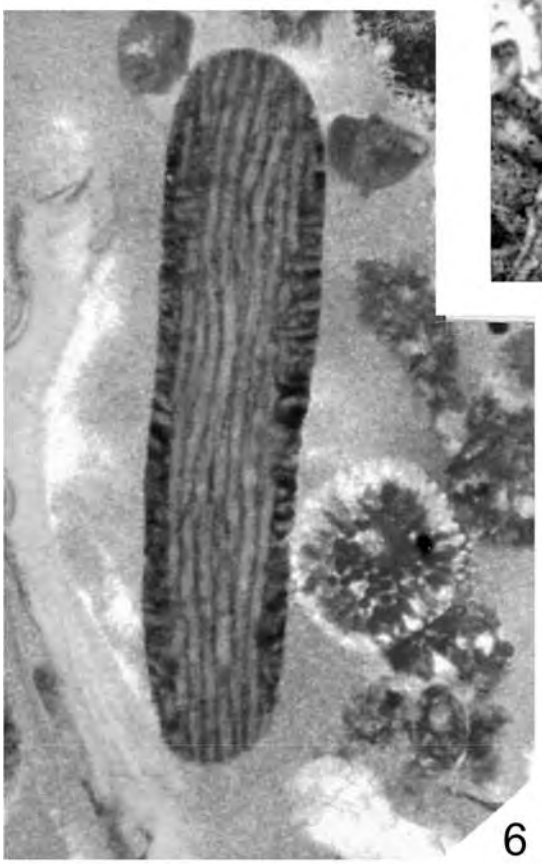

6

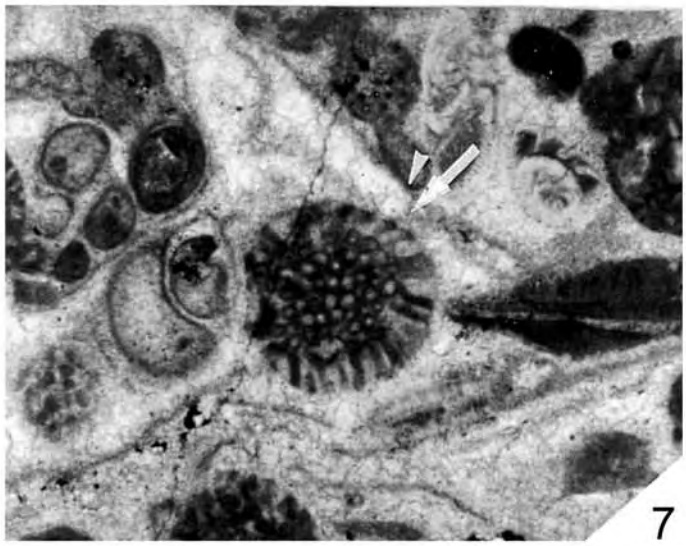

7

PLATE 7 (page 45)

Halimeda lacunosa n. sp (Fig. 1-3) and *Halimeda barbata* n.sp. (Fig. 4-5) from Jbel Guersif Formation (late Thanetian). Figures ×63. Sample numbers refer to Herbig (1991, fig. 17). For location of sections see text-fig 2b and Appendix 1.

1 *Halimeda lacunosa* n.sp. Holotype. Longitudinal-oblique section showing utricular gamentangial (s) cavities (arrow). 031085/4, section SA-13 (GIK 1896b).

2 *Halimeda lacunosa* n.sp. Paratype. Tangential-oblique section with gamentangial cavities disposed intracortical as well as utricular (arrows). From holotype sample 031085/4, section SA-13 (GIK 1896c).

3 *Halimeda lacunosa* n.sp. Additional material. Broken segment showing three to four utricle-series (arrow), and intracortical gamentangial cavities (s). 160584/11, section SA-8 (GIK 1880b).

4 *Halimeda barbata* n.sp. Holotype. Longitudinal-oblique section showing four to five (?) utricle series (arrows). 160584/11, section SA-8 (GIK 1880c).

5 *Halimeda barbata* n.sp. Paratype. Broken segment in large intraclast showing the cortex with tiny utricles, especially to the periphery (arrow). From holotype sample 160584/11, section SA-8 (GIK 1880d).

PLATE 8 (page 46)

Halimeda marcconradi n.sp. Jbel Guersif Formation (late Thanetian). Figures ×63. Sample 21085/7, section SA-12 (sample number refers to Herbig 1991, fig. 17). For location of section see text-fig 2b and Appendix 1.

1 Holotype. Longitudinal-oblique section. 021085/7, section SA-12 (GIK 1894b).

2 Paratype. Longitudinal oblique section. From holotype sample 021085/7, section SA-12 (GIK 1894c).

3 Paratype. Transverse section in broken segment showing only medullar siphons (m) and longitudinal section (left) showing the cortex. From holotype sample 021085/7, section SA-12 (GIK 1894d).

4 Paratype. Transverse section showing the medullar area (m) and the abraded cortex; longitudinal-oblique section above. From holotype sample 021085/7, section SA-12 (GIK 1894e).

5 Paratype. Two longitudinal-oblique section showing medullar siphons (m) and thin cortex (c). From holotype sample 021085/7, section SA-12 (GIK 1894f).

PLATE 9 (page 47)

Halimeda praetaenicola n.sp. Jbel Guersif Formation (late Thanetian). Figures ×63. Sample numbers refer to Herbig (1991, fig. 17). For location of sections see text-fig 2b and Appendix 1.

1 Holotype. Longitudinal-oblique section with large, empty medullar area and two utricle series. 021085/7, section SA-12 (GIK 1894g).

2 Additional material. Transverse section showing a long fertile siphon as pedunculate gamentangium (g). 031085/2, section SA-13 (GIK 1895c).

3 Additional material. Broken segment showing the cortex with three utricle series (arrows). 031085/2, section SA-13 (GIK 1895c).

4 Additional material. Transverse sections. 130584/3, section SA-5 (GIK 1872b).

5 Paratype. Broken segment showing the cortex with three utricle series (arrows). From the holotype sample 021085/7, section SA-12 (GIK 1894h).

6 Additional material. Transverse section. 130584/3, section SA-5 (GIK 1872b).

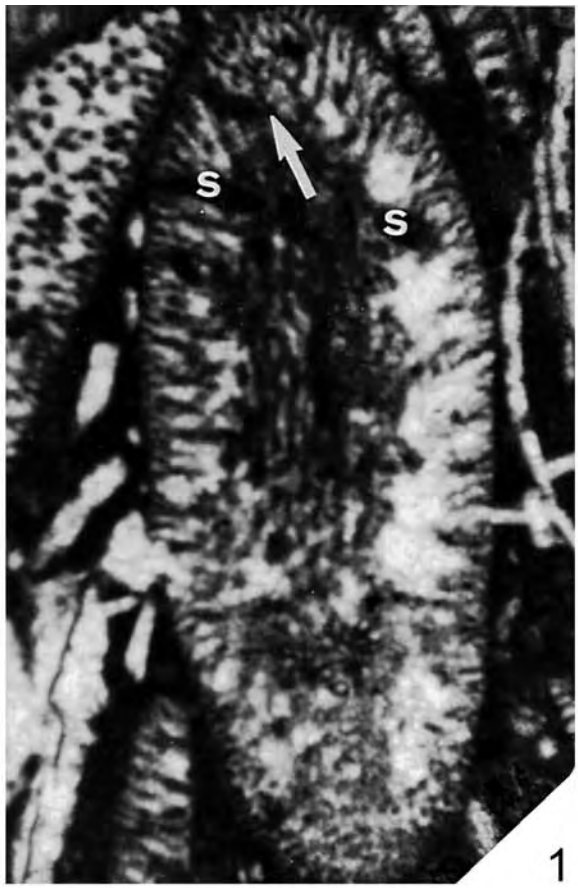
S
S
1


2

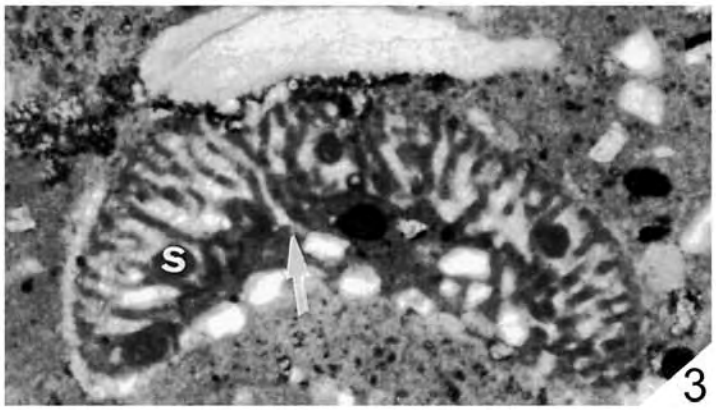
S
3

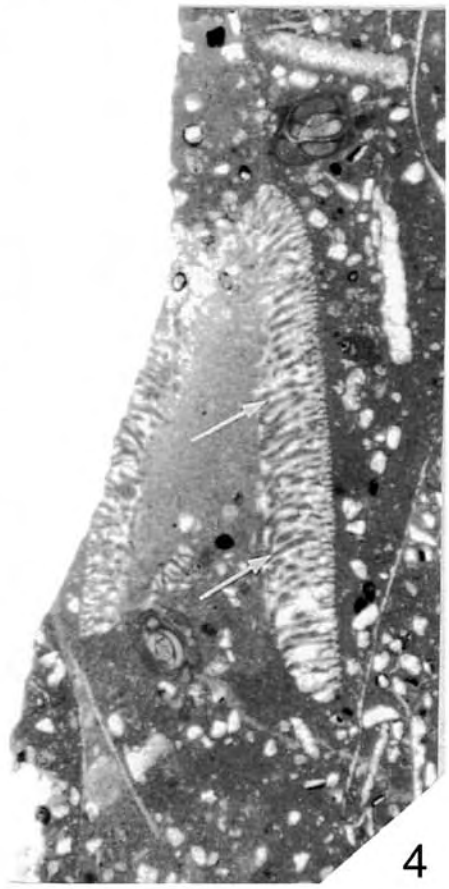
4

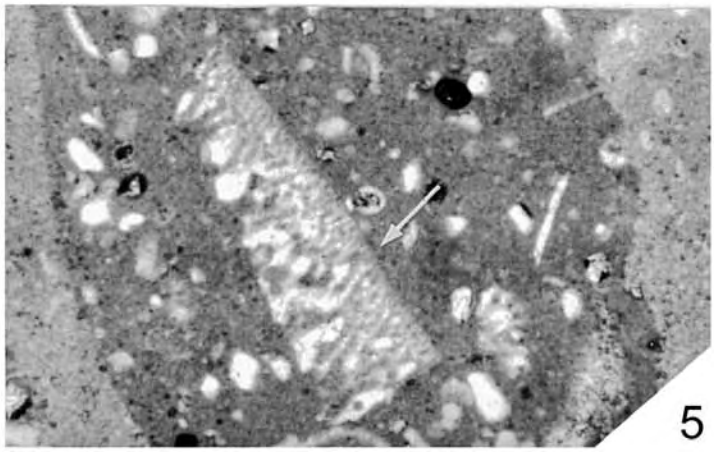
5


1

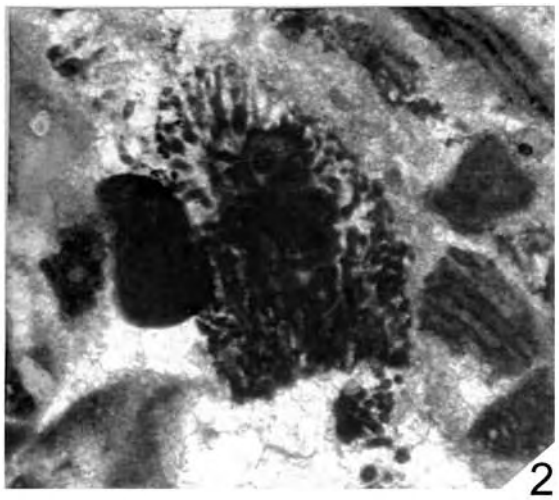
2

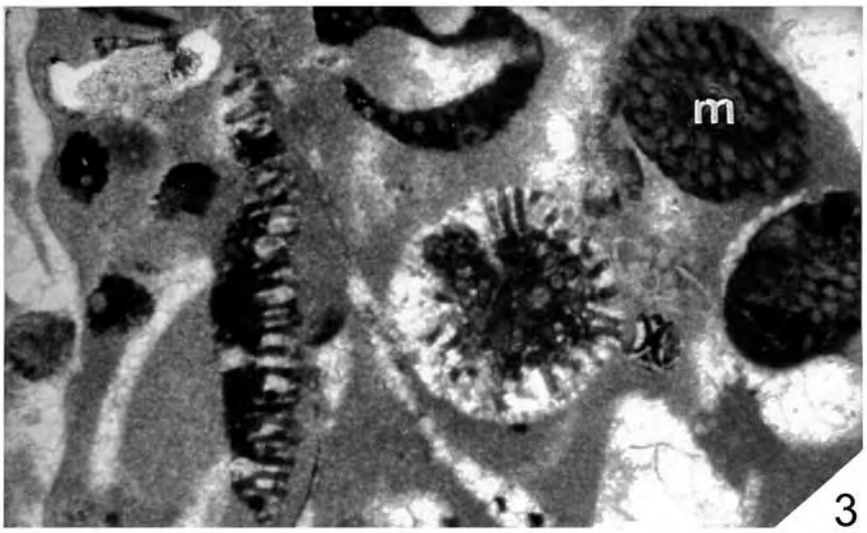
m
3

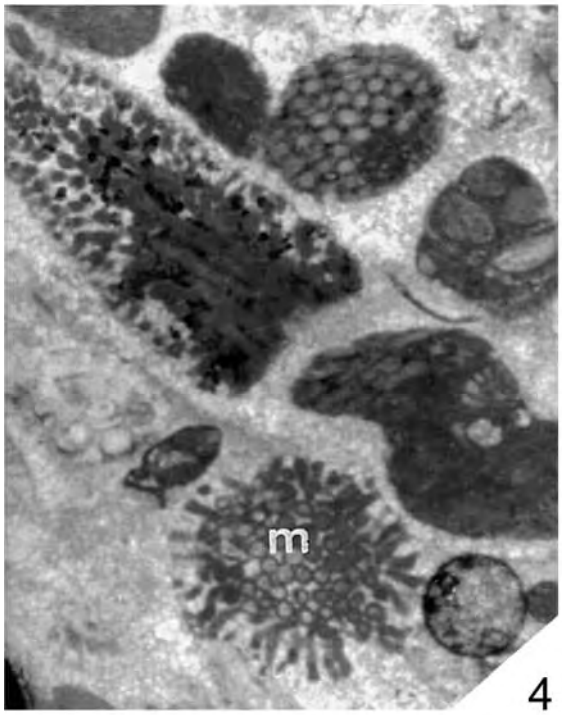
m
4

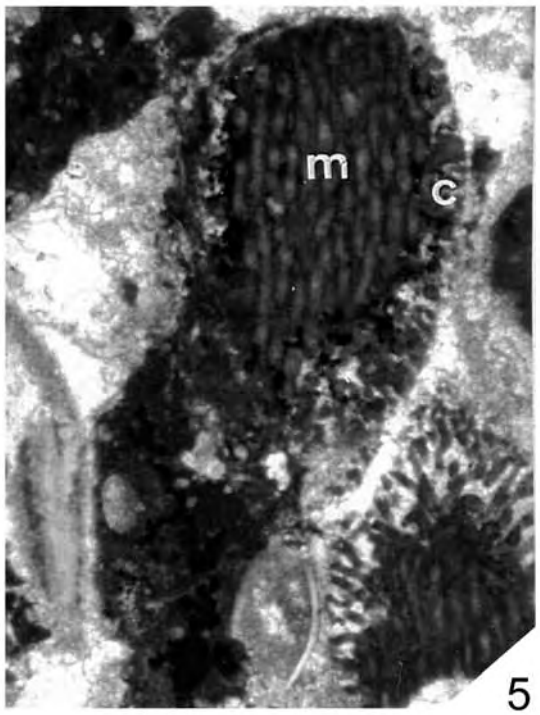
m
c
5


1

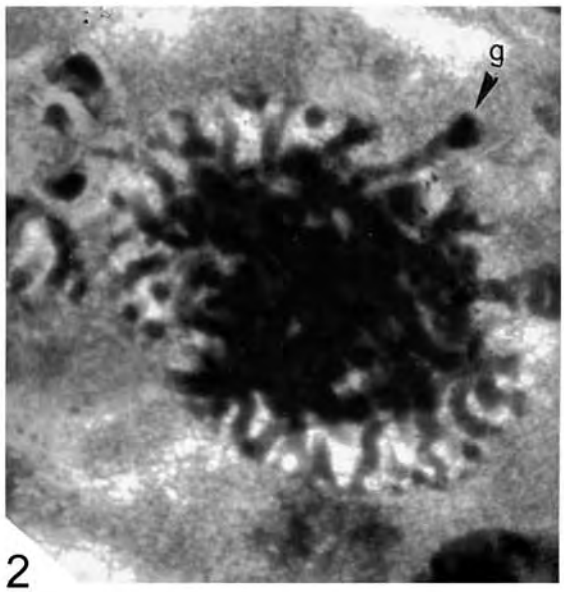

2

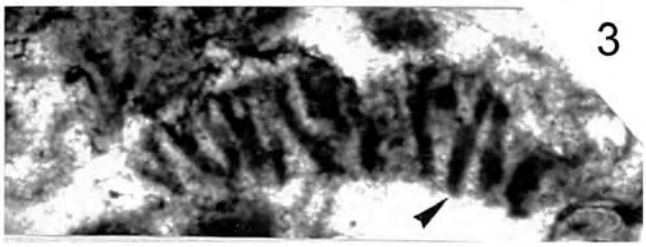
3


4

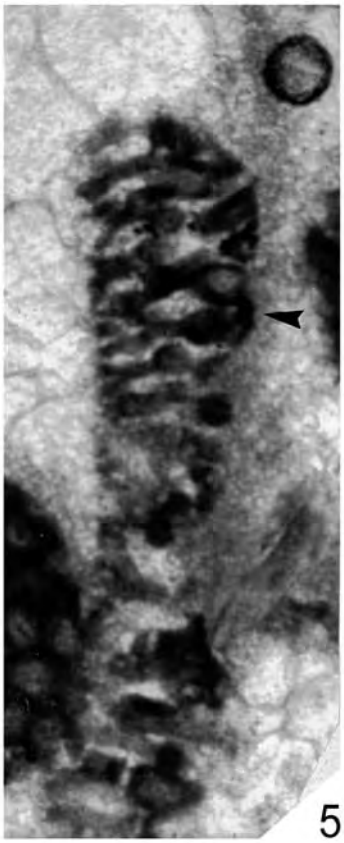
5


6

PLATE 10 (page 49)

Halimeda unica n.sp. Jbel Guersif Formation (late Thanetian). Figures ×45. Sample numbers refer to Herbig (1991, fig. 17). For location of sections see Text-Fig. 2b and Appendix 1.

1 Holotype. Longitudinal-oblique section showing medullar area crossed by tiny, medium long siphons (m) and cortex with three utricle series (c). 031085/5, section SA-13 (GIK 1897c).

2 Paratype. Longitudinal-oblique section. From the holotype sample 031085/5, section SA-13 (GIK 1897d).

3 Paratype. Tangential section showing the dense distribution of outermost, third utricle series. From the holotype sample 031085/5, section SA-13 (GIK 1897e).

4-6 Paratypes. Transverse sections showing the medullar siphons or empty medullar area and the cortex with clear shapes of utricles. From the holotype sample 031085/5, section SA-13 (GIK 1897f-h).

7 Paratypes. Longitudinal-oblique section showing a large empty medullar area. From the holotype sample 031085/5, section SA-13. (GIK 1897i)

PLATE 11 (page 50)

Halimeda opuntia (Linnaeus) Lamouroux 1816. Fig. 1-10: Ait Ouarhitane Formation (mid to late Ypresian). Figures1-5, 7-10 ×54; Fig. 11: reconstructed idealised segment. Fig. 12: Cortex system of Recent *H. opuntia*. Sample numbers refer to Herbig (1991, fig. 27). For location of sections see text-fig 2b and Appendix 1.

1-9 11 Idealised thallus segment in Fig. 11 reconstructed after different planes of the sections crossing many flat disc-like, ribbed thalli segments as follows: 1, 2, 5, transverse, slightly oblique sections in the basal and lateral parts of the segments; 3-4, 9, transverse sections in the middle and upper part of the segments showing some ribs like small „horns"; 6, magnified area from figure 5 showing the morphology of the utricle series in the cortex; 7-8, longitudinal oblique sections in the middle and lateral areas. Figs. 1-8 from 061085/2, section SA-15 (GIK 1905b), Fig. 9 from 091085/9, section SA-18 (GIK 1908).

10 Transverse sections in disc-like segments showing internal projections separating medullar siphonal bundles. 091085/9, section SA-18 (GIK 1908).

12 Recent *H. opuntia* (after Littler and Littler 2000) showing typical morphology of the utricle series. Scale bar 100µm.

PLATE 12 (page 51)

Halimeda opuntia (Linnaeus) Lamouroux 1812 (Figs. 1-4) and *Halimeda opuntia* f. *triloba* (Decaisne) Agardh,1887 (Fig. 5). Ait Ouarhitane Formation (mid to late Ypresian). Sample numbers refer to Herbig (1991, fig. 27). For location of sections see text-fig 2b and Appendix 1.

1 *Halimeda opuntia* (Linnaeus) Lamouroux 1816. Transverse-oblique section. 091085/10, section SA-18 (GIK 1909a). ×54.

2 *Halimeda opuntia* (Linnaeus) Lamouroux 1816. Same specimen as in Figure 1, magnified to show rib-like protuberances and the shape of utricles. 091085/10, section SA-18 (GIK 1909a). ×90.

3 *Halimeda opuntia* (Linnaeus) Lamouroux 1816. Transverse section of a protuberance that sustains another segment. 160584/22, section SA-8 (GIK 1883a). ×90.

4 *Halimeda opuntia* (Linnaeus) Lamouroux 1816. Magnified part of the cortex crossed by three utricle series (1, 2, 3). 061085/2, section SA-15 (GIK 1905b). ×90.

5 *Halimeda opuntia* f. *triloba* (Decaisne) Agardh 1887. Slightly oblique transverse section showing three lobes at middle part, left margin and right margin (arrows) of segment. Note medullary siphons (m) and strongly calcified cortex crossed by four utricle series. 150584/12, section SA-7 (GIK 1878a). ×54.

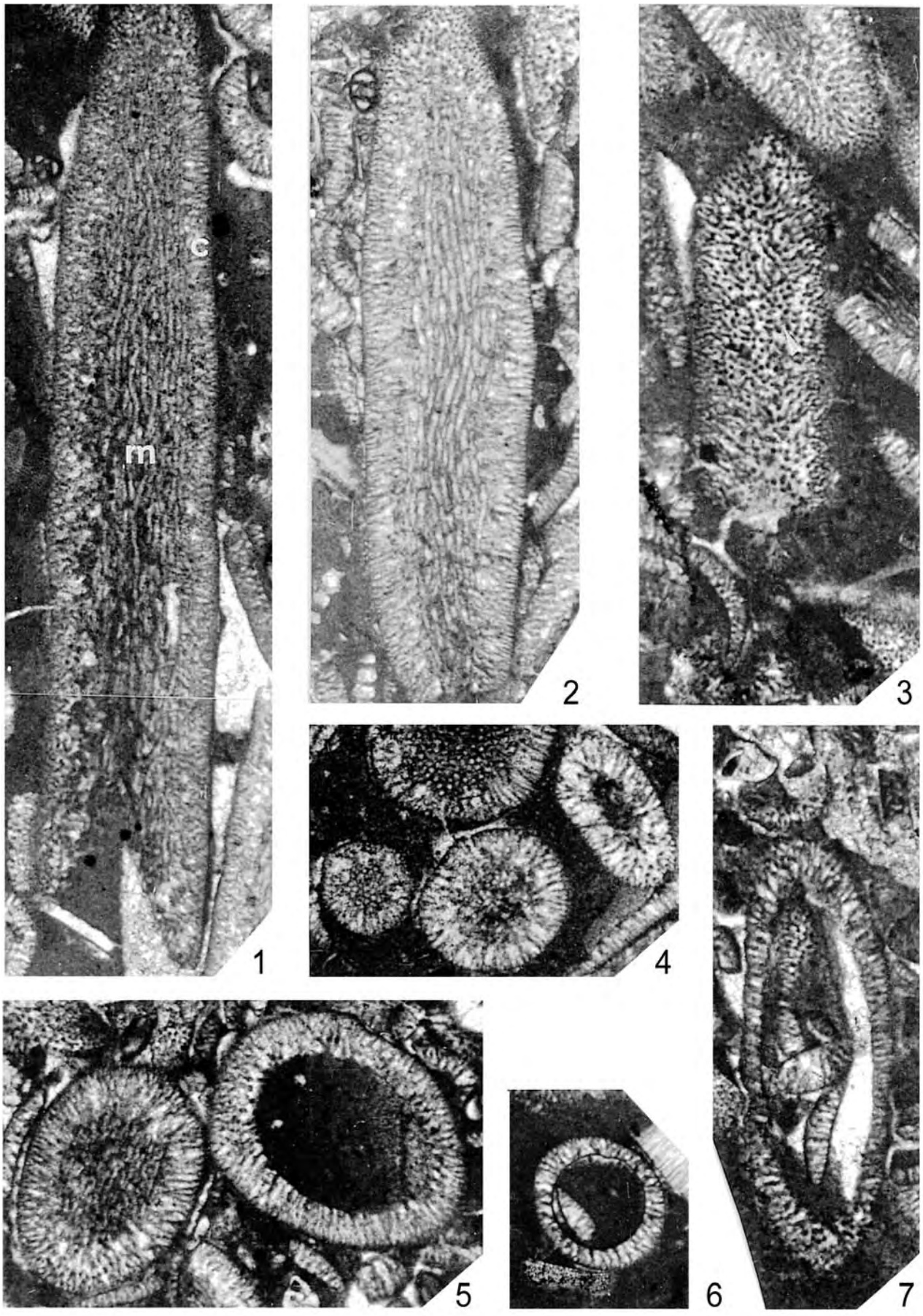
c
m
1
2
3
4
5
6
7

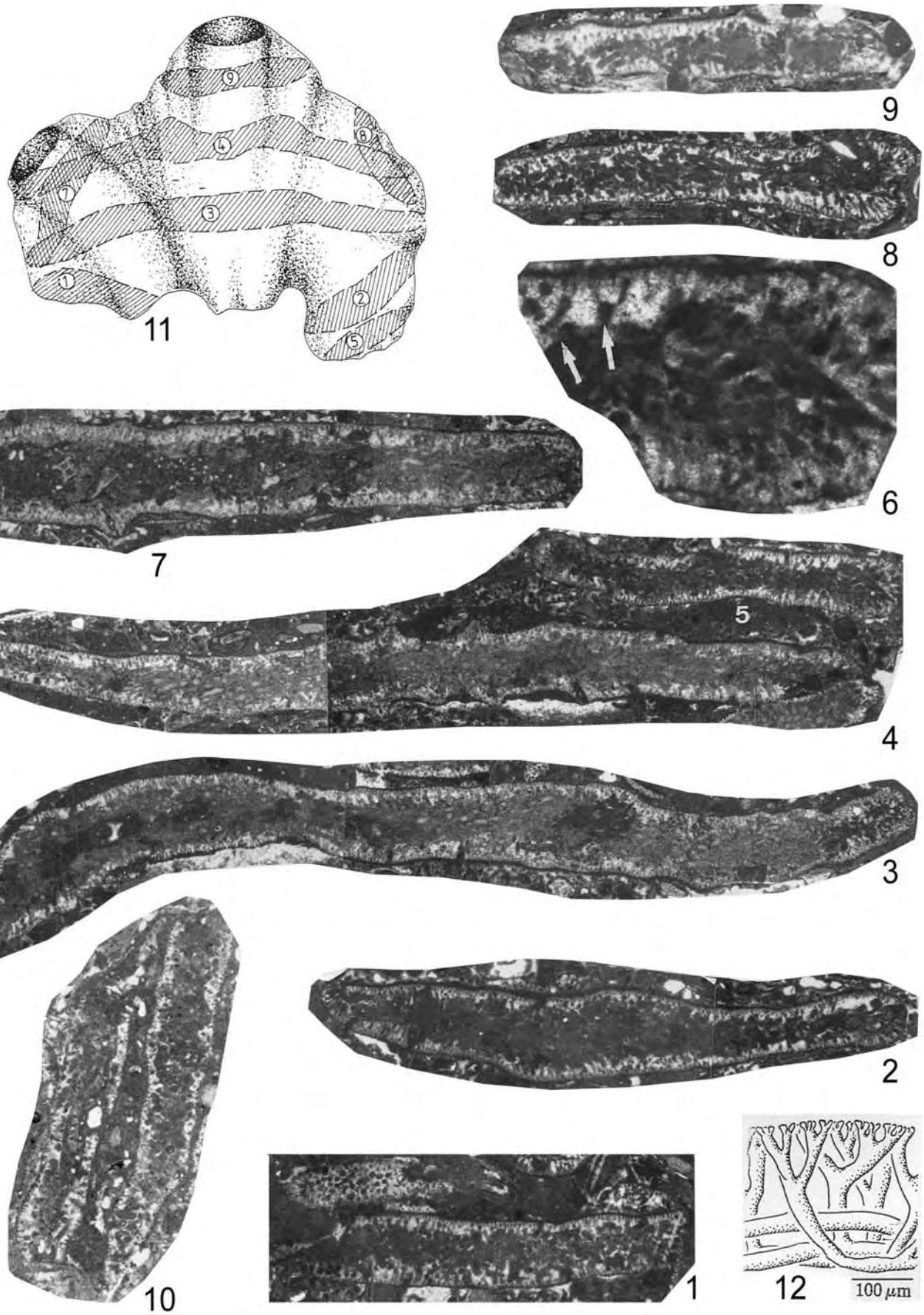
11
9
8
6
7
5
4
3
2
10
1
12
100 µm

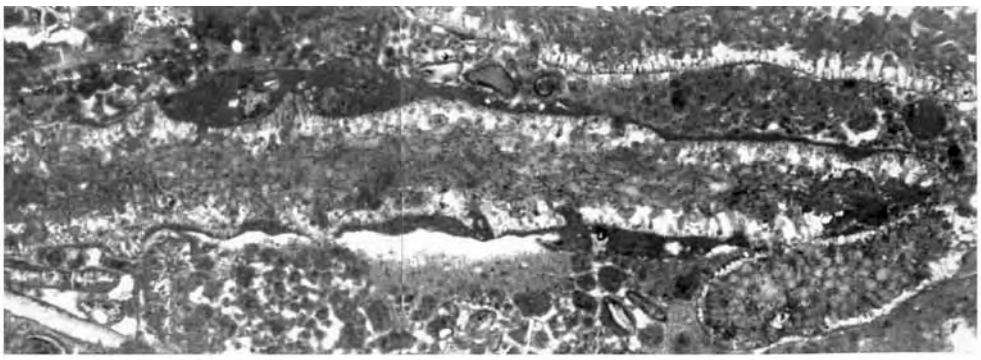

1

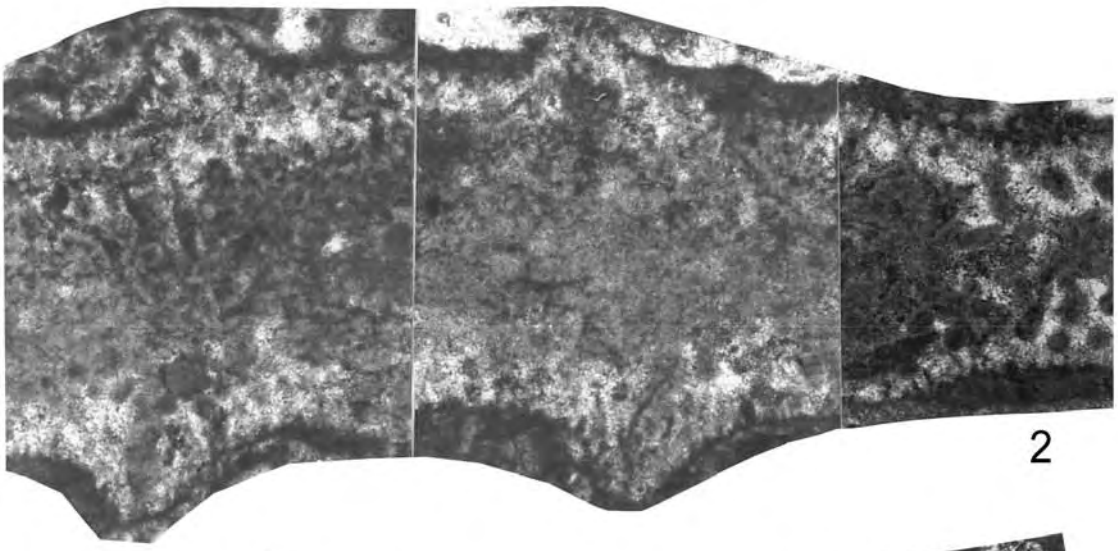

2

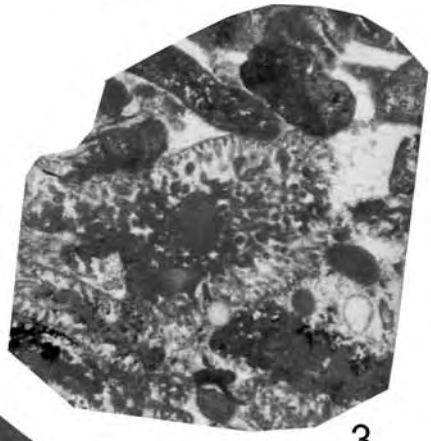

3

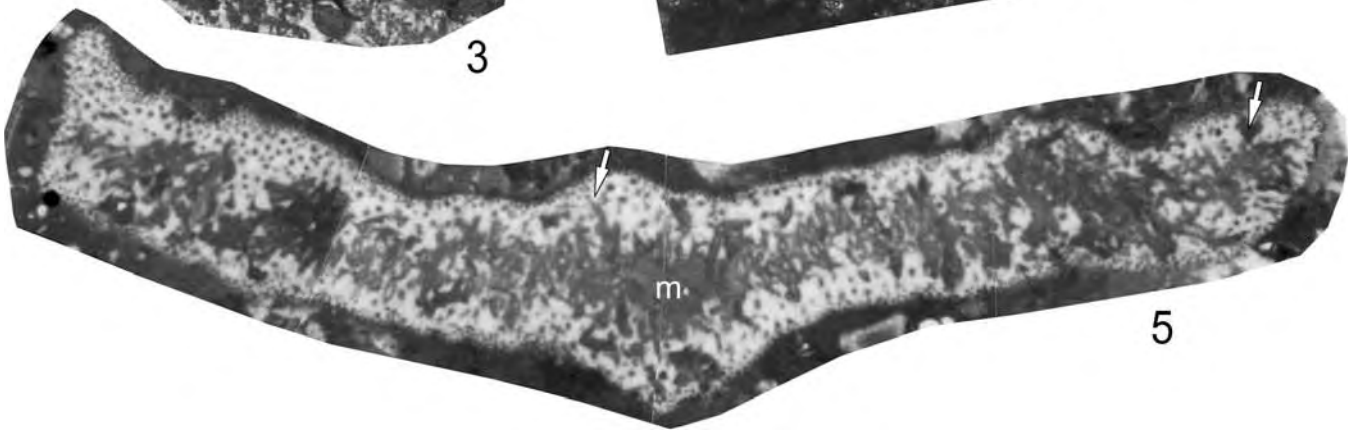

5

PLATE 13 (page 53)

Halimeda simulans Howe 1907. Ait Ouarhitane Formation (mid to late Ypresian).
Figures ×63. Sample numbers refer to Herbig (1991, fig. 27). For location of sections see text-fig 2b and Appendix 1.

1 Longitudinal section crossed by few medullary siphons (m) and cortex having three utricle series (arrow). 031085/12, section SA-13 (GIK 1899).

2 Longitudinal section crossed by few medullary siphons (m) and cortex having three utricle series. 150584/11, section SA-7 (GIK 1877a).

3 Longitudinal section crossed by few medullary siphons and cortex having three utricle series (arrow). 150584/11, section SA-7 (GIK 1877a).

4 Oblique-longitudinal section showing cortex with three utricle series (arrow). 150584/11, section SA-7 (GIK 1877a).

5 Transverse section. 150584/11, section SA-7 (GIK 1877a).

6 Longitudinal section crossed by few medullary siphons (m) and cortex having three utricle series. 061085/2, section SA-15 (GIK 1905c).

7 Transverse section. Arrow indicates morphology of the utricle series). 041085/4, section SA-14 (GIK 1900b).

PLATE 14 (page 54)

Halimeda monile (J. Ellis and Solander) Lamouroux 1816. Figs. 1-2, 4-6 from Ait Ouarhitane Formation (mid to late Ypresian), Fig. 3 from Jbel Tagount Formation (latest Ypresian to late Lutetian or latest Bartonian). Figures ×63. Sample numbers refer to Herbig (1991, figs. 27, 30). For location of sections see text-fig 2b and Appendix 1.

1 Transverse section in disc-like segment. 121085/8, section SA-21 (GIK 1916b).

2 Longitudinal-oblique section in a broken, disc-like, trilobed(?) segment. 180584/23, section SA-11 (GIK 1888).

3 Transverse section in a flat, disc-like segment crossed by medullar area. Typical utricles disposed in three series (arrows); note the round gametangial cavities located on secondary and tertiary utricles. 110988/3, section SA-5 (GIK 1875a).

4 Broken thallus segment showing in the cortex characteristic shape of three utricle series (arrow). 121085/8, section SA-21 (GIK 1916b).

5 Transverse section in disc-like segment showing the typical disposition of medullar siphons. 180584/28b, section SA-11 (GIK 1890b).

6 Transverse section in a basal cylindrical segment. 180584/23, section SA-11 (GIK 1888).

PLATE 15 (page 55)

Halimeda praeopuntia J and L. Morellet 1922. Ait Ouarhitane Formation (mid to late Ypresian).
Figures ×63. Sample numbers refer to Herbig (1991, fig. 27). For location of sections see text-fig 2b and Appendix 1.

1 Longitudinal-oblique sections, showing large, irregular medullar area (m) and thin cortex crossed by two or three utricle series (arrow). 091085/10, section SA-18 (GIK 1909b).

2 Longitudinal-oblique section, showing large, irregular medullar area (m) and thin cortex crossed by two or three utricle series. 091085/10, section SA-18 (GIK 1909b).

3 Transverse-oblique section showing typical utricle series (arrows). 111085/18, section SA-20 (GIK 1914).

4 Longitudinal section with medullar siphons (m). In the cortex two or three utricle series are visible (arrows). 121085/6, section SA-21 (GIK 1915a).

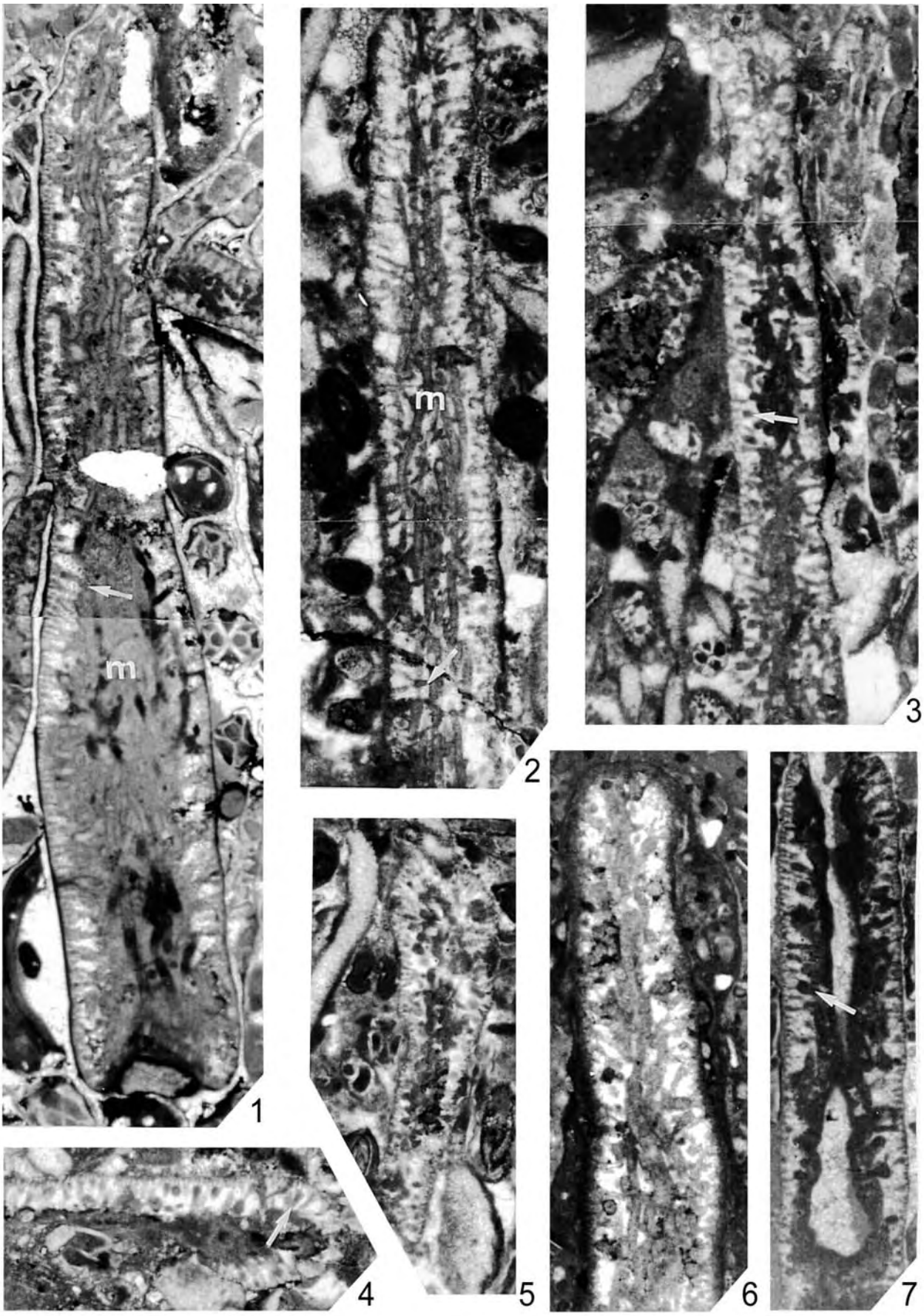
m
1
m
2
3
4
5
6
7

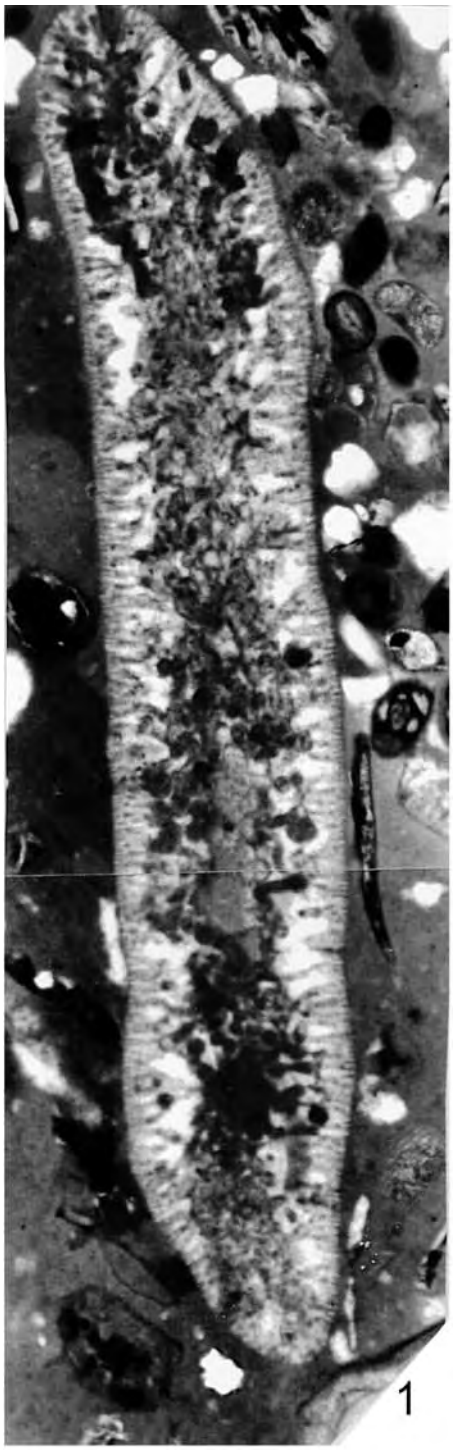
1

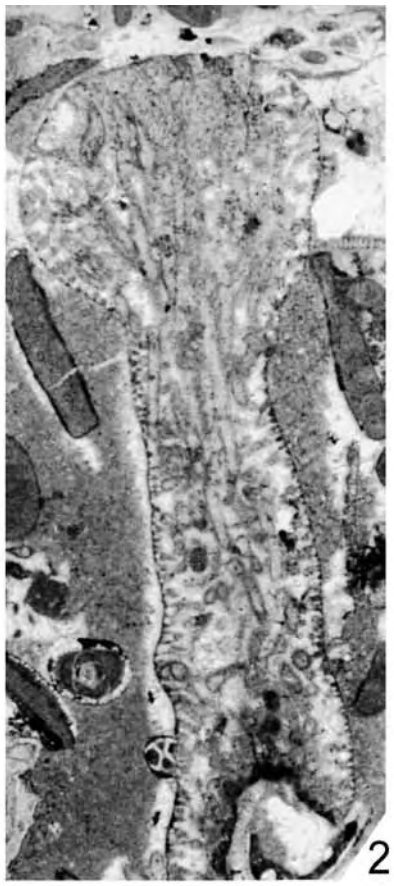
2

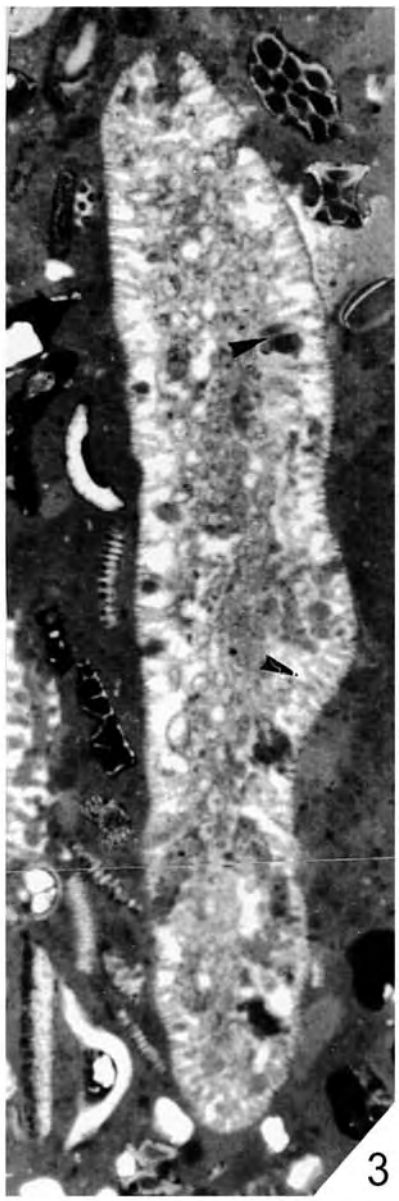
3

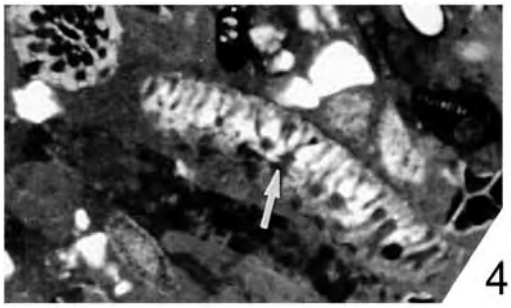
4

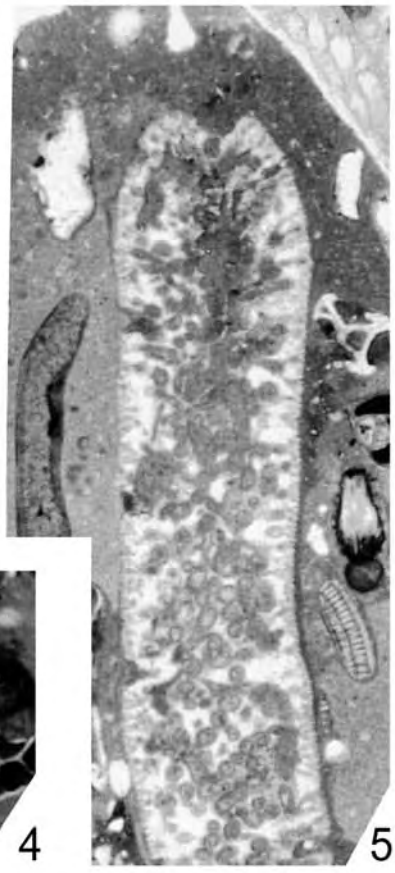
5


6


m
1
m
2
m
3
m
4

PLATE 16 (page 57)

Halimeda cylindracea Decaisne 1842 (Fig. 1-4) and *Halimeda incrassata* (J. Ellis) Lamouroux 1816 (Fig. 5-6). Ait Ouarhitane Formation (mid to late Ypresian). Figures ×63. Sample numbers refer to Herbig (1991, fig. 27). For location of sections see text-fig 2b and Appendix 1.

1 *Halimeda cylindracea* Decaisne 1842. Tangential (subcortical) oblique-longitudinal section with medullar area (m) and cortex with three utricle series. 180584/28b, section SA-11 (GIK 1890a).

2 *Halimeda cylindracea* Decaisne 1842. Longitudinal section at the transition between medulla and cortex, large medullar area (m) and cortex crossed by three up to four utricle series. 180584/26b, section SA-11 (GIK 1889).

3 *Halimeda cylindracea* Decaisne 1842. Longitudinal-oblique section with clear, medullar area (m) and cortex with three up to four utricle series (arrows). 121085/8, section SA-21 (GIK 1916a).

4 *Halimeda cylindracea* Decaisne 1842. Transverse section showing the large medullar area. 160584/16, section SA- 8 (GIK 1882a).

5 *Halimeda incrassata* (J.Ellis) Lamouroux 1816. Transverse section showing medullar area (m) and cortex with three utricle series (arrow). 041085/4, section SA-14 (GIK 1900a).

6 *Halimeda incrassata* (J.Ellis) Lamouroux 1816. Longitudinal-oblique section showing the typical shape of utricle series (arrows). 061085/2, section SA-15 (GIK 1905a).

PLATE 17 (page 58)

Halimeda tuna (Ellis and Solander) Lamouroux 1816. Ait Ouarhitane Formation (mid to late Ypresian). Figures ×54. Sample numbers refer to Herbig (1991, fig. 27). For location of sections see text-fig 2b and Appendix 1.

1-9 Transverse or transverse-oblique sections in disc-like, contorted segments. Narrow, medullar area with siphons disposed in round bundles in Figs. 1, 3, 6 (arrows) and cortex crossed by two or three utricle series. Figs. 1, 5 from 061085/4, section SA-15 (GIK 1906); Fig. 2 from 121085/6, section SA-21 (GIK 1915b); Figs. 4 ,8 from 150584/11, section SA-7 (GIK 1877b); Figs. 3, 7 from 061085/2, section SA-15 (GIK 1905d); Figs. 6, 9 from 031085/10, section SA-13 (GIK 1898).

10 Longitudinal-oblique lateral section. 041085/4, section SA-14 (GIK 1901).

PLATE 18 (page 59)

Halimeda tuna (Ellis and Solander) Lamouroux 1816. Ait Ouarhitane Formation (mid to late Ypresian). Sample numbers refer to Herbig (1991, fig. 27). For location of sections see text-fig 2b and Appendix 1.

1-2,4, 6-15 Different transverse and transverse oblique sections, some in broken segments. Figs. 2, 9 11 12 show medullar siphons, which are partially arranged in clearly visible round bundles (arrows). Fig.1 from 031085/10, section SA-13 (GIK 1898); Figs. 2 14 from 160584/16, section SA-8 (GIK 1882b); Figs. 4 12 from 041085/16, section SA-14 (GIK 1901); Figs. 6, 8 from 041085/4, section SA-14 (GIK 1900c); Figs. 7, 9 from 150584/11, section SA-7 (GIK 1877b); Figs. 10 11 from 150584/12, section SA-7 (GIK 1878b); Fig. 13 15 from 160584/22, section SA-8 (GIK 1883b). All ×54.

3 Transverse section in a flat, disc-like segment with two lateral lobes. 091085/10, section SA-18 (GIK 1909c). ×63.

5 Magnified part of Figure 4 showing typical three utricle series (arrow). ×90.

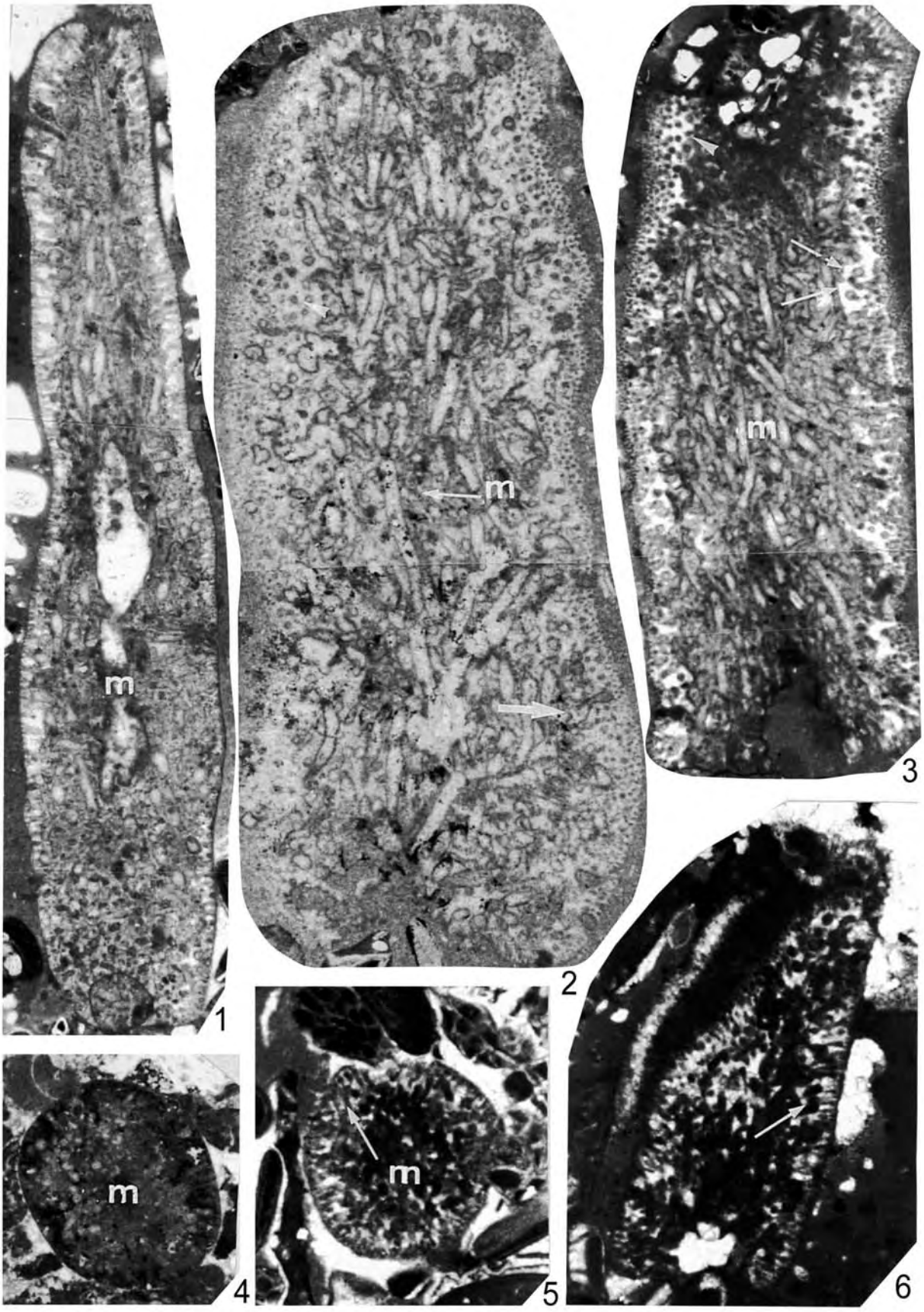
m
1
m
2
m
3
m
4
m
5
6

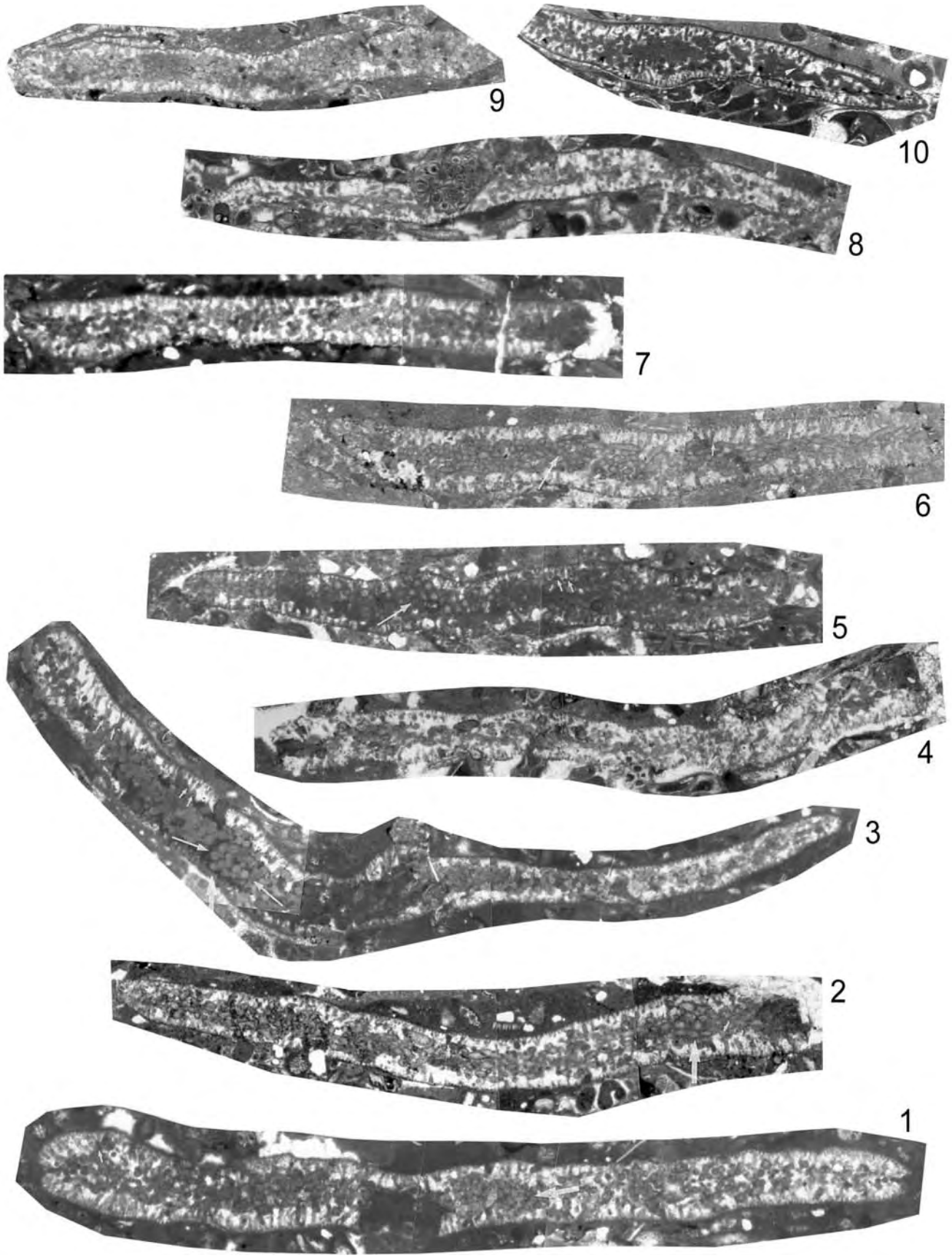
9
10
8
7
6
5
4
3
2
1

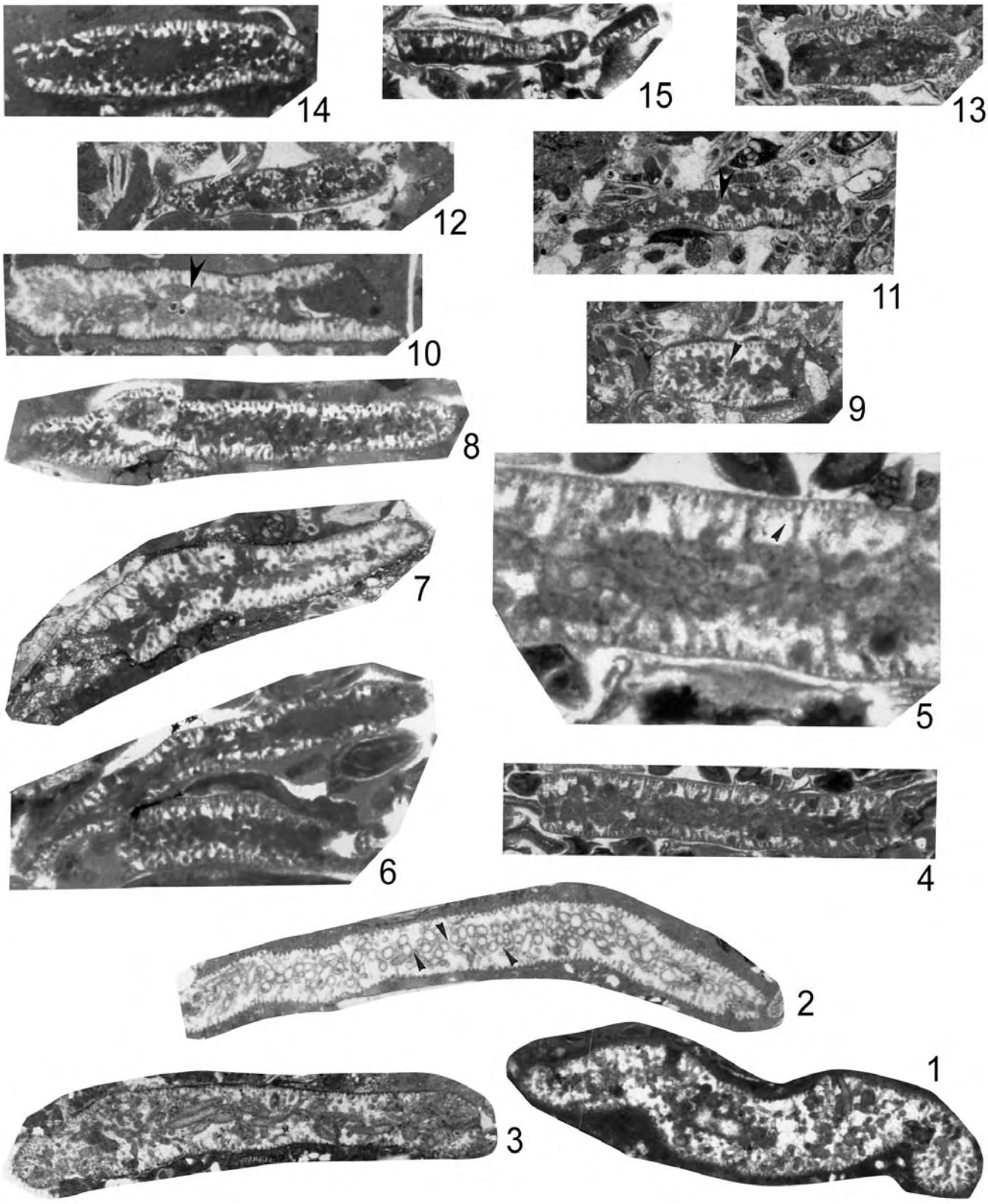
14
15
13
12
11
10
9
8
7
5
6
4
2
1
3

PLATE 19 (page 61)

Halimeda gracilis Harvey ex Agardh 1887 (Fig. 1-3) and *Halimeda praemacroloba* n. sp. (Fig. 4-8).
Ait Ouarhitane Formation (mid to late Ypresian). Figures ×63. Sample numbers refer to Herbig (1991, fig. 27).
For location of sections see text-fig 2b and Appendix 1.

1 *Halimeda gracilis* Harvey ex Agardh 1887. Longitudinal section in a very flat disc-like segment with narrow medullar area and cortex with two utricle series. 061085/2, section SA-15 (GIK 1905e).

2 *Halimeda gracilis* Harvey ex Agardh 1887. Longitudinal section in the central part of a broken disc-like segment; note typical shape of cortical siphons (arrows). 061085/2, section SA-15 (GIK 1905e).

3 *Halimeda gracilis* Harvey ex Agardh 1887. Longitudinal-oblique section in the lateral part of a broken disc-like segment. 061085/2, section SA-15 (GIK 1905e).

4 *Halimeda praemacroloba* n. sp. Holotype. Longitudinal-oblique section in a broken disc-like segment, narrow medullar area (m) and cortex with two or three utricle series (arrow). 061085/2, section SA-15 (GIK 1905f).

5 *Halimeda praemacroloba* n. sp. Paratype. Transverse section in a cylindrical basal segment. From holotype sample 061085/2, section SA-15 (GIK 1905g).

6 *Halimeda praemacroloba* n. sp. Paratype. Transverse-oblique section in a broken cylindrical or slightly compressed basal segment. From holotype sample 061085/2, section SA-15 (GIK 1905h).

7 *Halimeda praemacroloba* n. sp. Additional material. Broken thallus segment with three utricle series in the cortex (arrow). 160584/16, section SA-8 (GIK 1882c).

8 *Halimeda praemacroloba* n. sp. Additional material. Broken thallus segment with three utricle series in the cortex (arrow). 150584/12, section SA-7 (GIK 1878c).

PLATE 20 (page 62)

Halimeda copiosa Goreau and Graham 1967 (Fig. 1-3) and *Halimeda tuna* f. *platydisca* (Decaisne) Barton 1901 (Fig. 4).
Ait Ouarhitane Formation (mid to late Ypresian). Figures ×63. Sample numbers refer to Herbig (1991, fig. 27).
For location of sections see text-fig 2b and Appendix 1.

1 *Halimeda copiosa* Goreau and Graham 1967. Transverse section of a broken segment showing medullar siphons and cortex crossed by three utricle series (arrow). 091085/8, section SA-18 (GIK 1907).

2 *Halimeda copiosa* Goreau and Graham 1967. Transverse section of a disc showing large medullar siphons and thin cortex. 180584/22, section SA -11 (GIK 1887).

3 *Halimeda copiosa* Goreau and Graham 1967. Transverse-oblique section of a broken segment showing large medullar siphons and cortex crossed by three utricle series. 180584/22, section SA-11 (GIK 1887).

4 *Halimeda tuna* f. *platydisca*(Decaisne) Barton 1901. Transverse-oblique section showing shape and disposition of utricle series (arrow) in the cortex. 160584/16, section SA-8 (GIK 1882d).

PLATE 21 (page 63)

Halimeda tuna (Ellis and Solander) Lamouroux 1816. Jbel Tagount Formation (latest Ypresian to late Lutetian or latest Bartonian).
Figures ×63 except Fig. 7 (x 90). Sample 041085/20, section SA-14 (sample number refers to Herbig 1991, fig. 30) (GIK 1903).
For location of section see text-fig 2b and Appendix 1.

1 Longitudinal section in a disc-like segment showing the short medullar siphon and thin cortex..

2-6 Transverse and transverse oblique sections at different levels of disc-like segments showing the regular disposition of the medullar siphon in round clusters with six siphons each.

7-8 Like 2-6, but note clear tendency to constrict the medullar area by short projections of the cortex (i).

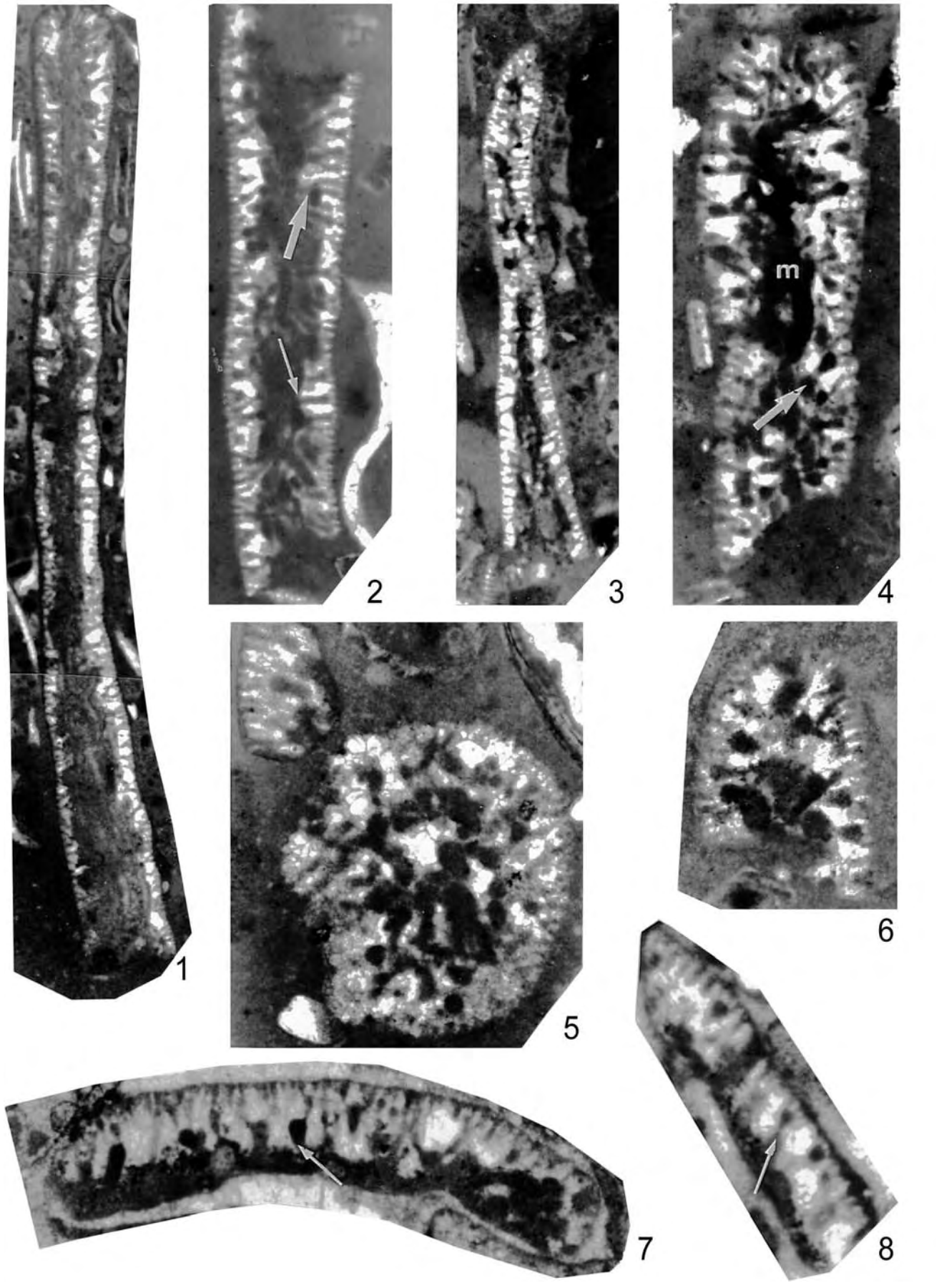
1
2
3
4
m
5
6
7
8

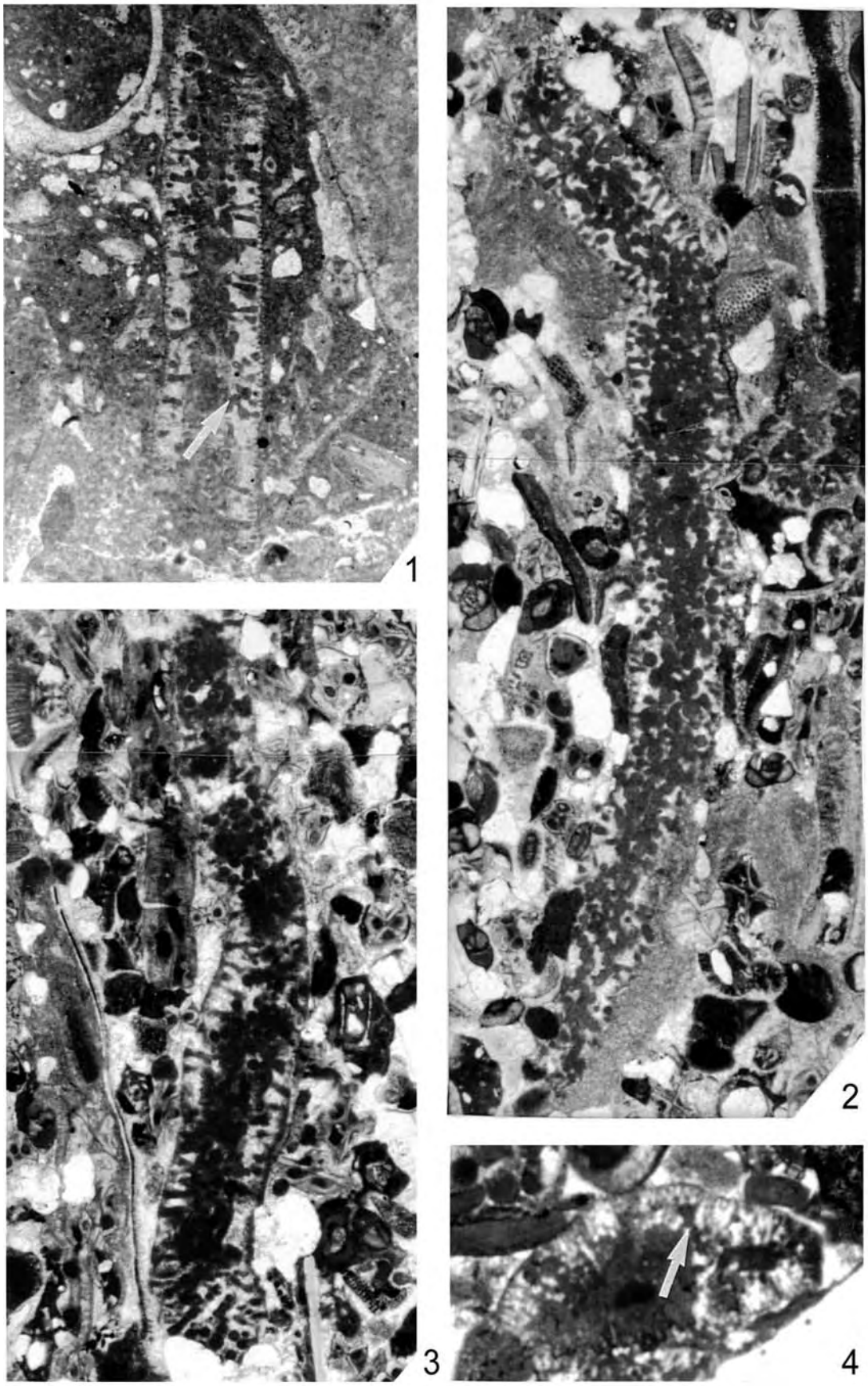
1
2
3
4

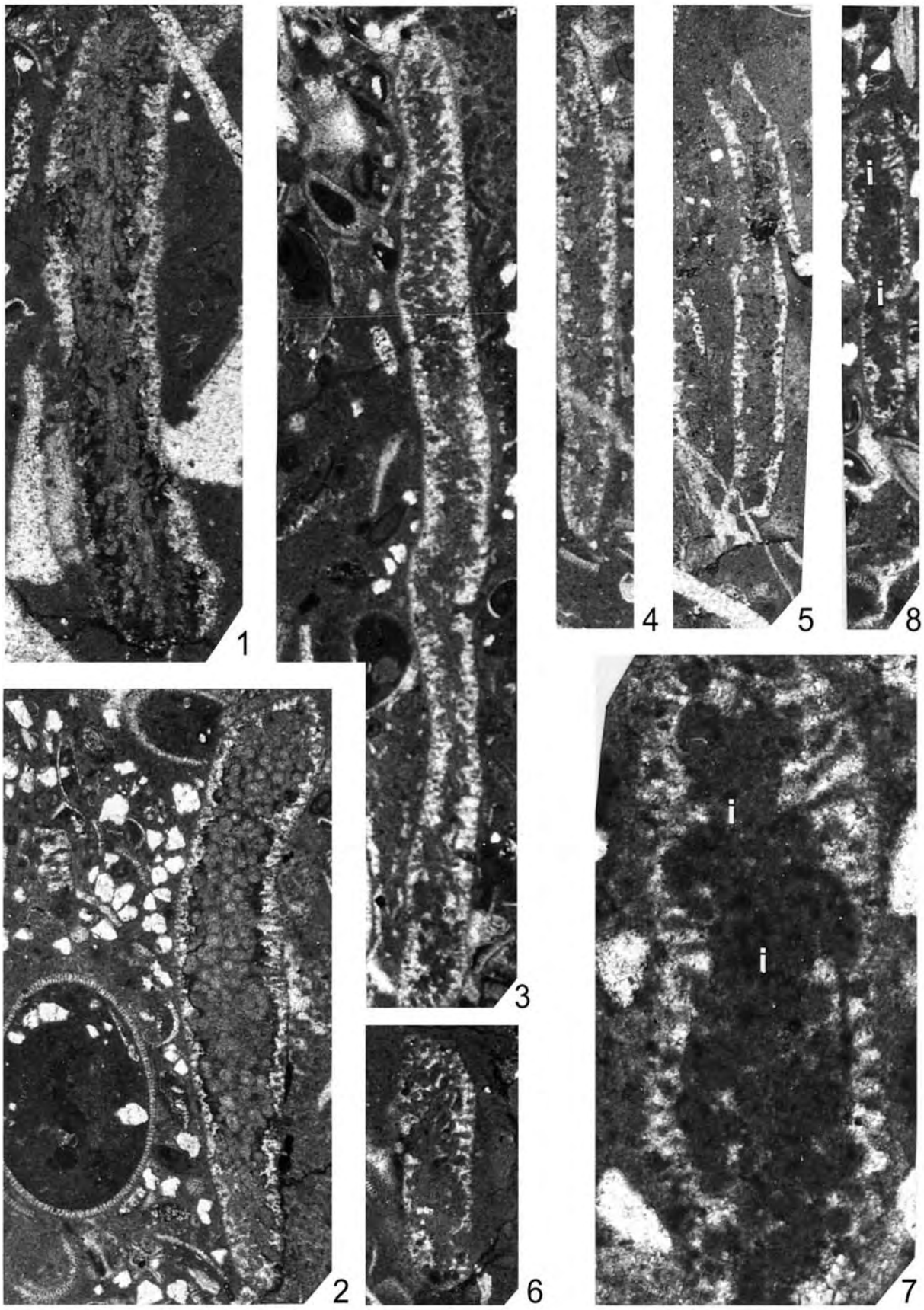
1
2
3
4
5
6
7
8
i
i
i
i

PLATE 22 (page 65)

Halimeda tuna (Ellis and Solander) Lamouroux 1816. Jbel Tagount Formation (latest Ypresian to late Lutetian or latest Bartonian). Figures ×54 except Fig 1a (×90). Sample numbers refer to Herbig (1991, fig. 30). For location of sections see text-fig 2b and Appendix 1.

1 Longitudinal-oblique section of a small disc-like segment with small lobes (d) and a transverse section in a lateral part of a broken segment (b). 1a – detail of cortex showing shape and disposition of utricle series (arrow). 041085/18, section SA-14 (GIK 1902b).

2-6,8 Transverse sections in different disc-like segments showing disposition of medullar siphons in round bundles and thin cortex. Fig. 2 from 110988/3, section SA-5 (GIK 1875c); Figs. 3, 5-6 from 091085/14, section SA-18 (GIK 1911a); Fig. 4 from 110988/5, section SA-5 (GIK 1876); Fig.8 from 041085/21, section SA-14 (GIK 1904).

7 \Various longitudinal and transverse sections mostly in broken thalli segments. 101085/13, section SA-19 (GIK 1913).

9 Transverse-oblique section showing the medullar siphons disposed in round bundles (arrows). 161086/7, section SA-25a (GIK 1919b).

10 Longitudinal section crossing the upper lateral part of a disc-like segment with narrow medullar area and short medullar siphons because of frequent dichotomic branching; cortex crossed by two or three utricle series. 091085/14, section SA-18 (GIK 1911a).

PLATE 23 (page 66)

Halimeda gracilis Harvey ex Agardh 1887 (Fig. 1), *Halimeda praegoreaui* n. sp. (Fig. 2-3), *Halimeda scabra* Howe 1905 (Fig. 4), and *Halimeda fragilis* Taylor 1950 (Fig. 5-7). Jbel Tagount Formation (latest Ypresian to late Lutetian or latest Bartonian). Figures ×63. Sample numbers refer to Herbig (1991, fig. 30). For location of sections see text-fig 2b and Appendix 1.

1 *Halimeda gracilis* Harvey ex Agardh 1887. Longitudinal section of a broken disc-like segment showing long medullar siphons; cortex crossed by two or three utricle series. 091085/13, section SA-18 (GIK 1910a).

2 *Halimeda praegoreaui* n. sp. Additional material. Transverse-oblique section of a disc-like segment with large medullar area and thin cortex crossed only by two utricle series. 110988/3, section SA-5 (GIK 1875d).

3 *Halimeda praegoreaui* n. sp. Holotype. Transverse section in a long, flat, subcuneate segment, cut in the lateral of the upper part of the segment. 180584/36, section SA-11 (GIK 1893d).

4 *Halimeda scabra* Howe 1905. Transverse-oblique section of a thallus segment showing sparse medullar siphons and cortex crossed by three utricle series. The third series is tiny, hair-like (arrows). 091085/14, section SA-18 (GIK 1911b).

5 *Halimeda fragilis* Taylor 1950. Transverse section of thallus fragment showing disposition of medullar siphons and cortex with three utricle series. 091085/13, section SA-18 (GIK 1910b).

6 *Halimeda fragilis* Taylor 1950. Longitudinal section of thallus segment showing medium long medullar siphon and cortex. 091085/13, section SA-18 (GIK 1910b).

7 *Halimeda fragilis* Taylor 1950. Longitudinal-oblique section of thalli segments showing medullar area and shape of the utricle series. 161086/7, section SA-25a (GIK 1919c).

PLATE 24 (page 67)

Halimeda opuntia (Linnaeus) Lamouroux 1816. Jbel Tagount Formation (latest Ypresian to late Lutetian or latest Bartonian). Figures ×63. Sample numbers refer to Herbig (1991, fig. 30). For location of sections see text-fig 2b and Appendix 1.

1 Longitudinal-tangential section of a disc-like segment with two lobes. 110988/3, section SA-5 (GIK 1875b).

2 Transverse-oblique section in a lobe of a disc-like segment. 180584/36, section SA-11 (GIK 1893a).

3 Longitudinal section in a disc-like segment (above) showing three lobes , the large medullar area and thin cortex. Below another oblique-transverse section in the lateral part of the segment. 041085/18, section SA-14 (GIK 1902a).

4 Transverse-oblique section in the lobe of a disc-like segment. 041085/18, section SA-14 (GIK 1902a).

5 Transverse section in the middle part of a disc-like segment. 041085/18, section SA-14 (GIK 1902a).

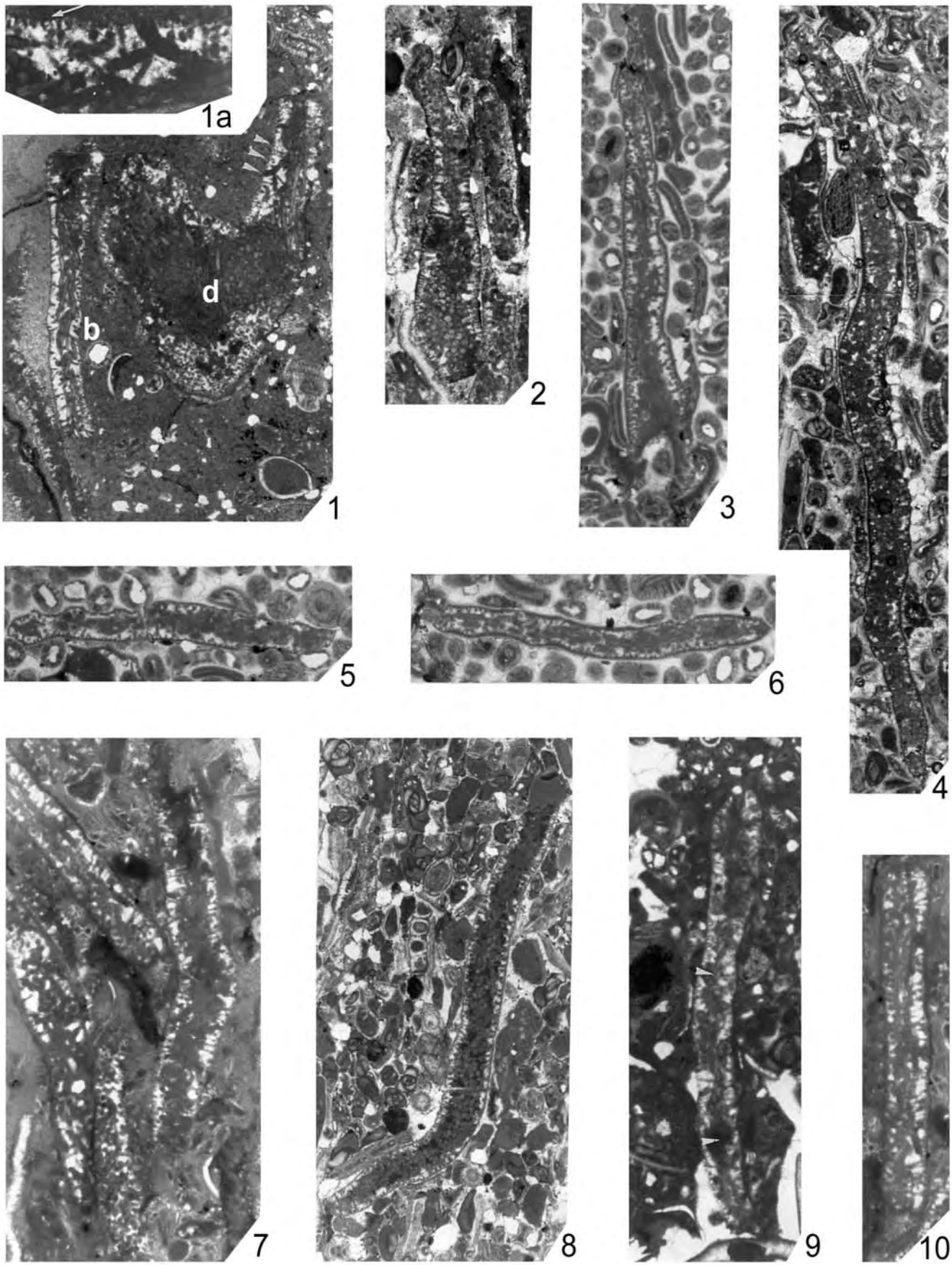
1a
d
b
1
2
3
4
5
6
7
8
9
10

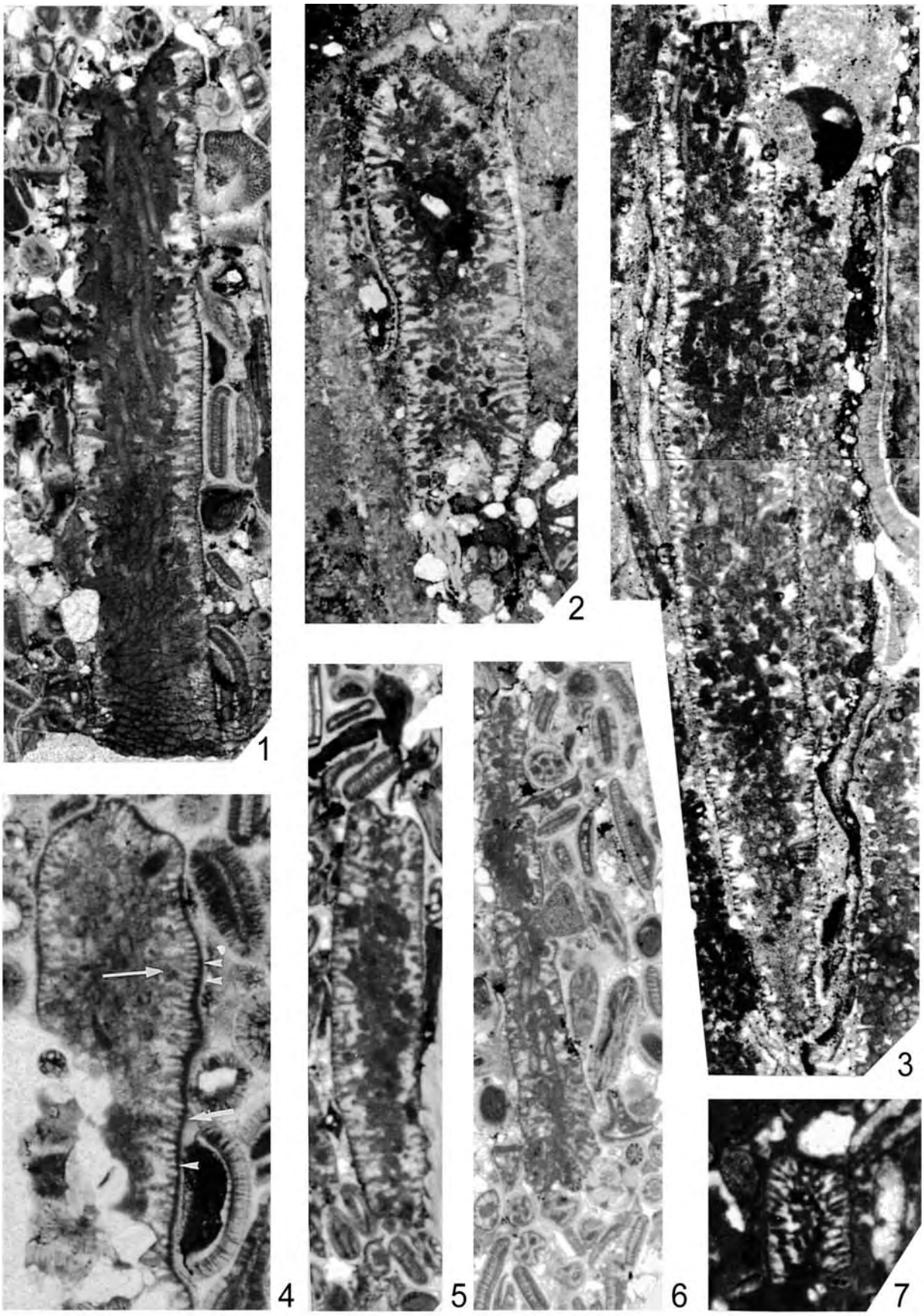
1
2
3
4
5
6
7

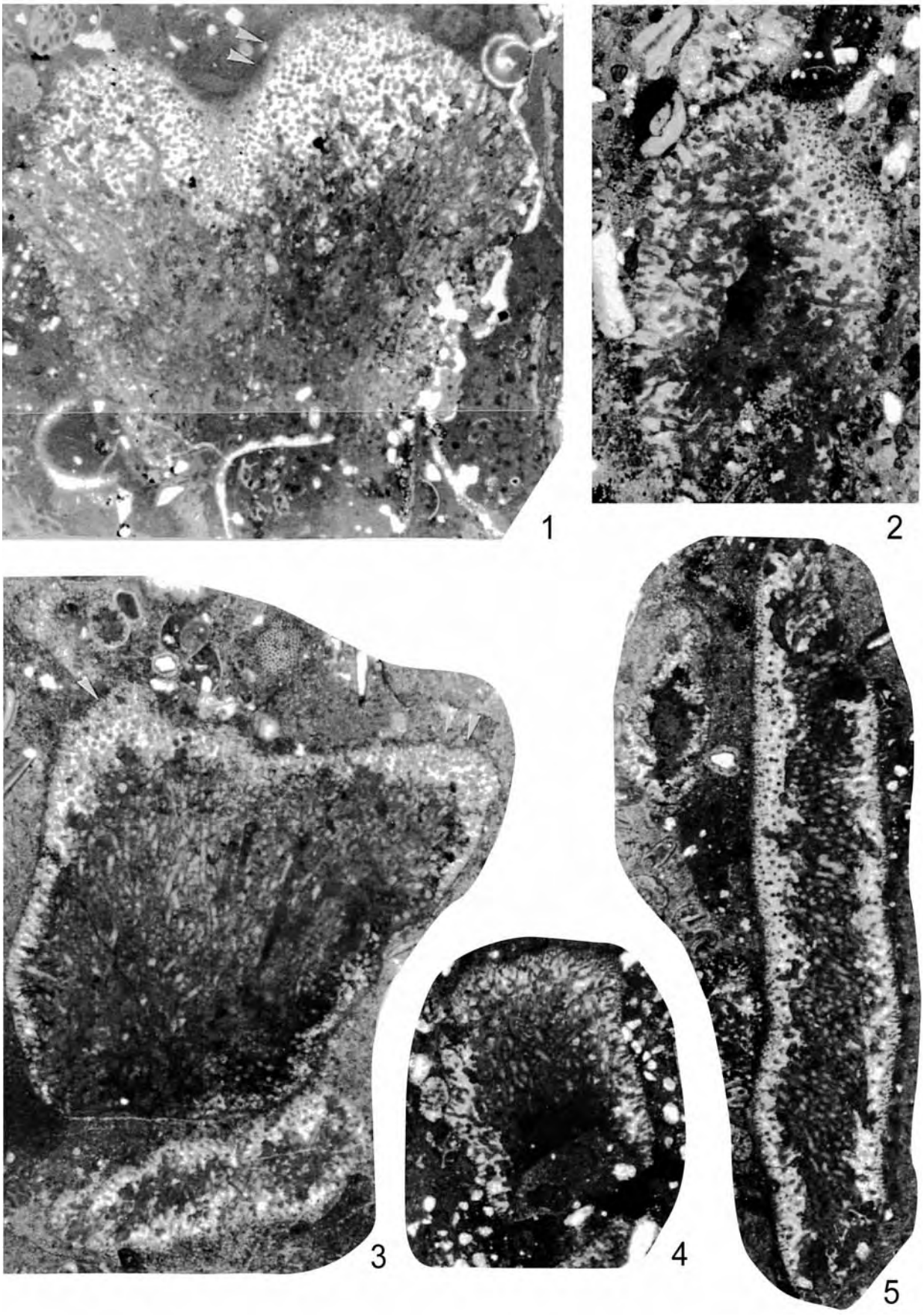
1
2
3
4
5

PLATE 25 (page 69)

Halimeda tuna f. *platydisca* (Decaisne) Barton 1901. Jbel Tagount Formation (latest Ypresian to late Lutetian or latest Bartonian). Figures ×63. Sample numbers refer to Herbig (1991, fig. 30). For location of sections see text-fig 2b and Appendix 1.

1-4 Transverse sections crossing various levels of disc-like segments, showing large medullar siphons (m) and cortex with three utricle series (arrows). Segments are not well preserved. Cortices are partially destroyed during reworking (especially in Figures 2-3). Fig. 1 from 180584/31, section SA-11 (GIK 1891b); Fig.2 from 091085/15, section SA-18 (GIK 1912b); Figs.3-4 from 180584/36, section SA-11 (GIK 1893c).

PLATE 26 (page 70)

Halimeda simulans Howe 1907. Jbel Tagount Formation (latest Ypresian to late Lutetian or latest Bartonian). Figures ×63. Sample numbers refer to Herbig (1991, fig. 30). For location of sections see text-fig 2b and Appendix 1.

1-2,4,7 Transverse sections crossing at different levels in disc-like segments, showing large medullar siphons (m, Fig. 2) and cortex crossed by two utricle series (arrows in Figs. 2, 4). Figs. 1, 4, 7 from 180584/36, section SA-11 (GIK 1893b); Fig. 2 from 180584/31, section SA-11 (GIK 1891a).

3,5-6 Longitudinal sections showing large, medullar siphons (m, Fig. 3). 180584/36, section SA-11 (GIK 1893b).

PLATE 27 (page 71)

Halimeda cylindracea Decaisne 1842. Jbel Tagount Formation (latest Ypresian to late Lutetian or latest Bartonian). Figures ×27. Sample numbers refer to Herbig (1991, fig. 30). For location of sections see text-fig 2b and Appendix 1.

1 Longitudinal-oblique section. Arrows point to characteristic long cylindrical primary utricles. 161086/6, section SA-25a (GIK 1918).

2 Transverse section of cylindrical, slightly compressed segment showing large medullar area (m) and cortex with three utricle series (arrow). 161086/6, section SA-25a (GIK 1918).

3 Longitudinal oblique section showing three utricle series (arrow). 161086/7, section SA-25a (GIK 1919a).

4 Transverse section of a broken thallus segment showing the cortex and utricle series (arrow). 091085/15, section SA-18 (GIK 1912a).

PLATE 28 (page 72)

Halimeda praecuneata n. sp. Jbel Tagount Formation (latest Ypresian to late Lutetian or latest Bartonian). Figures ×63. Sample numbers refer to Herbig (1991, fig. 30). For location of sections see text-fig 2b and Appendix 1.

1 Holotype. Transverse section of a cuneate, discoid segment showing uneven, large medullar area (m) and cortex crossed by three utricle series (arrows). 180584/35, section SA-11 (GIK 1892).

2 Additional material. Transverse sections at different levels in cuneate disc-like segments. 041085/18, section SA-14 (GIK 1902c).

3 Additional material. Above, transverse-oblique section in the lateral part of the segment. Below, transverse section of badly preserved, transported segment.

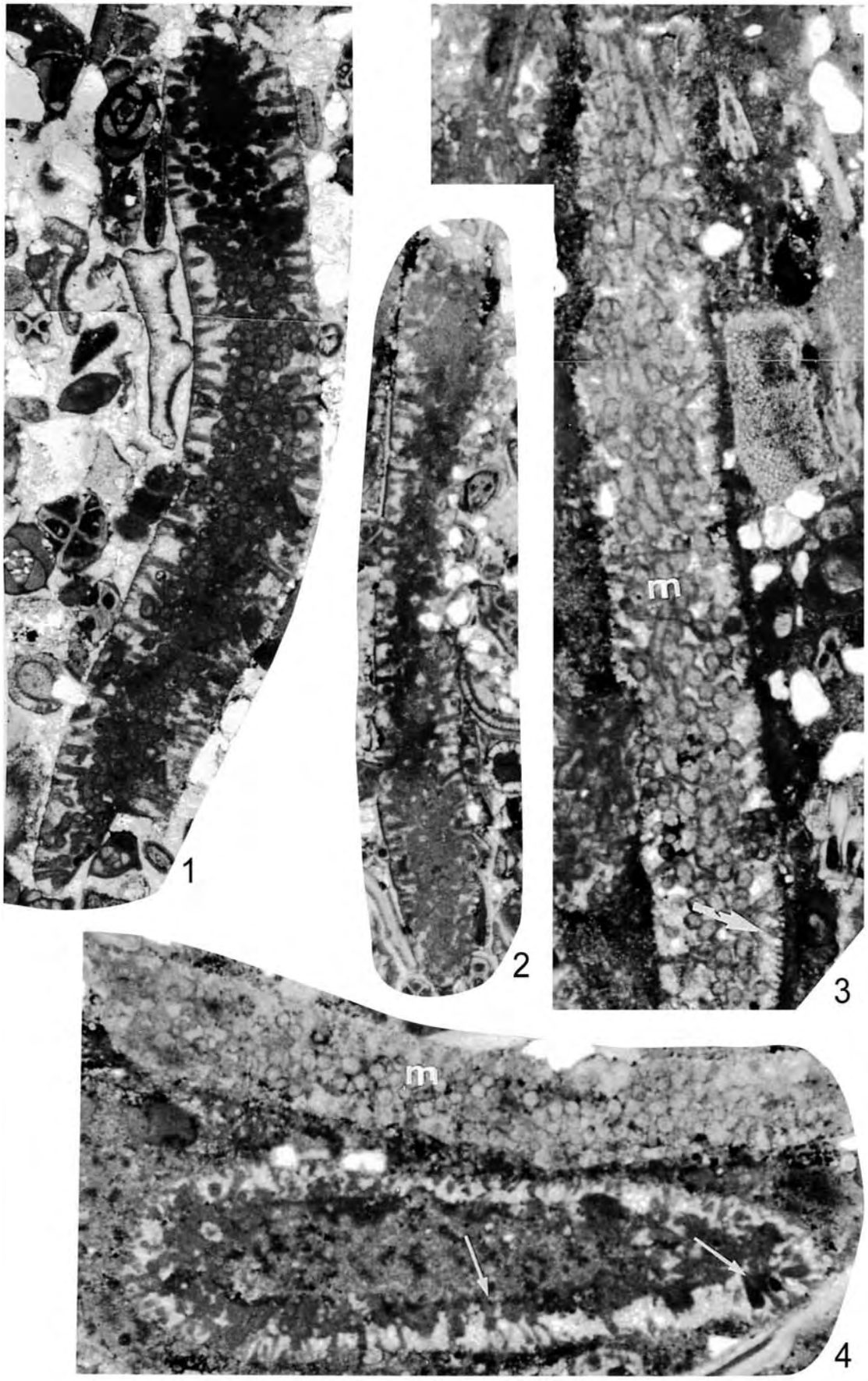
1
2
m
3
m
4

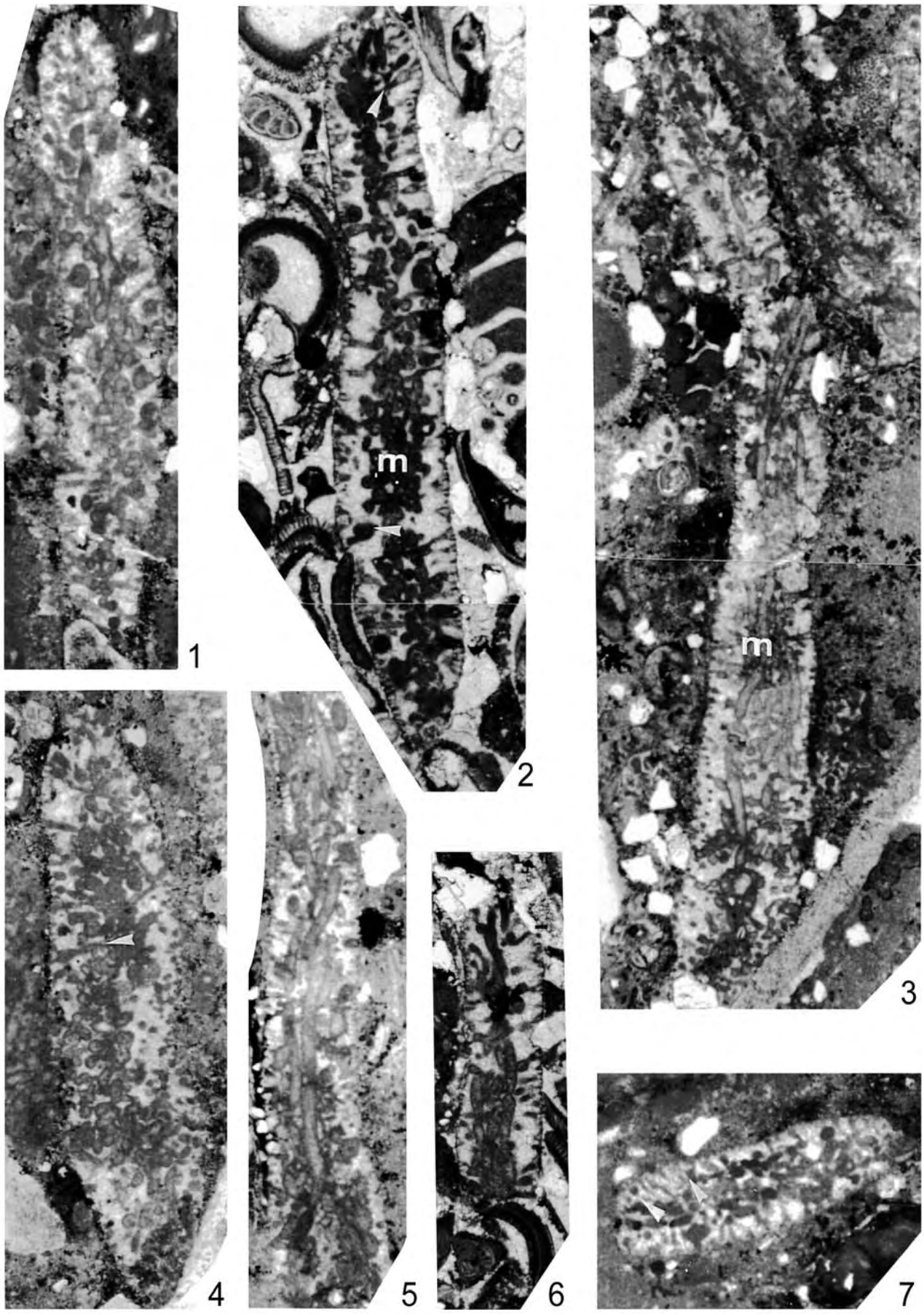
1
m
2
m
3
4
5
6
7

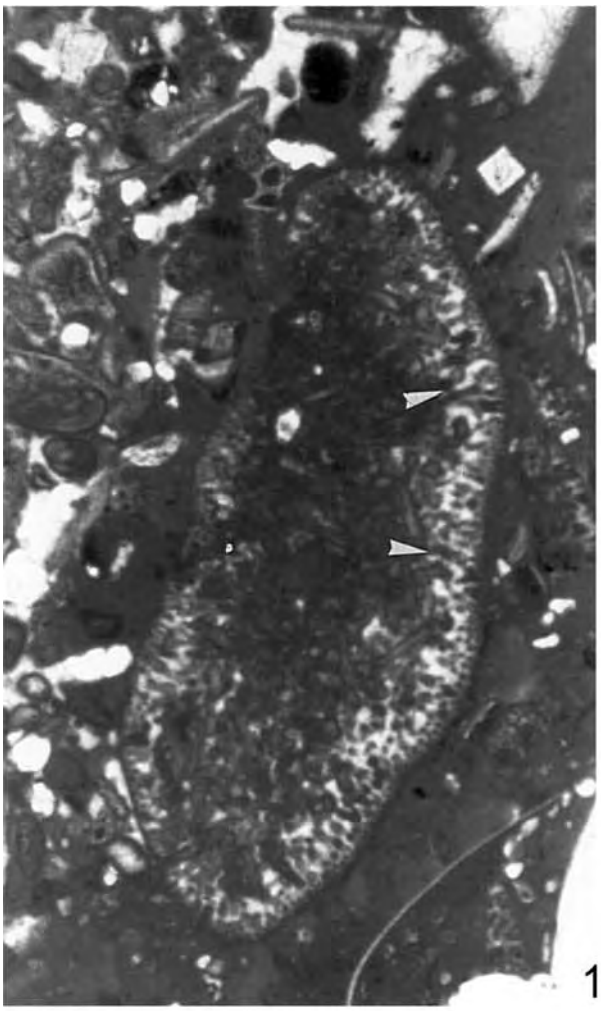

1

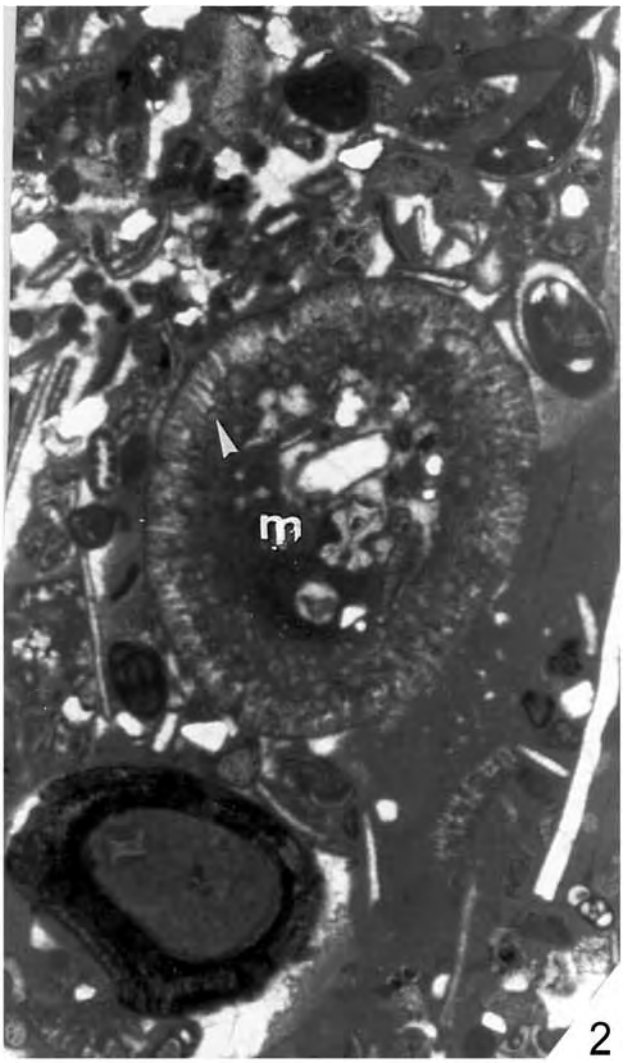

2

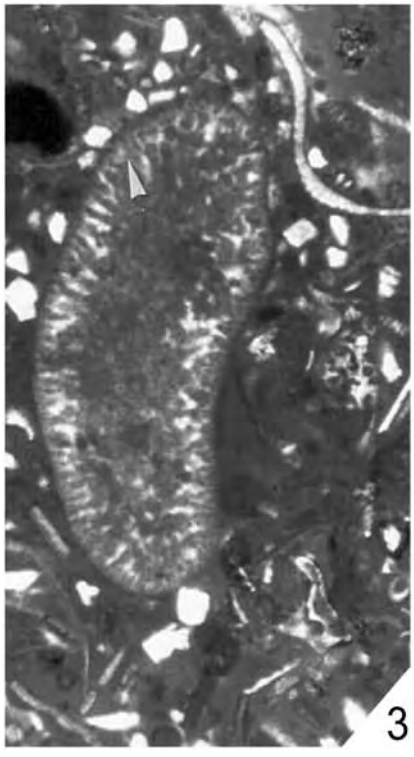

3

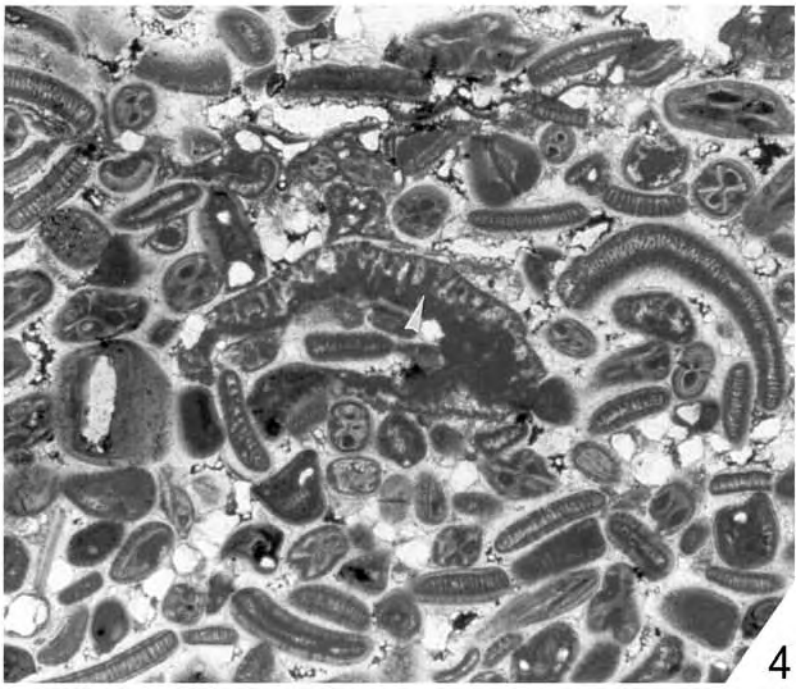

4

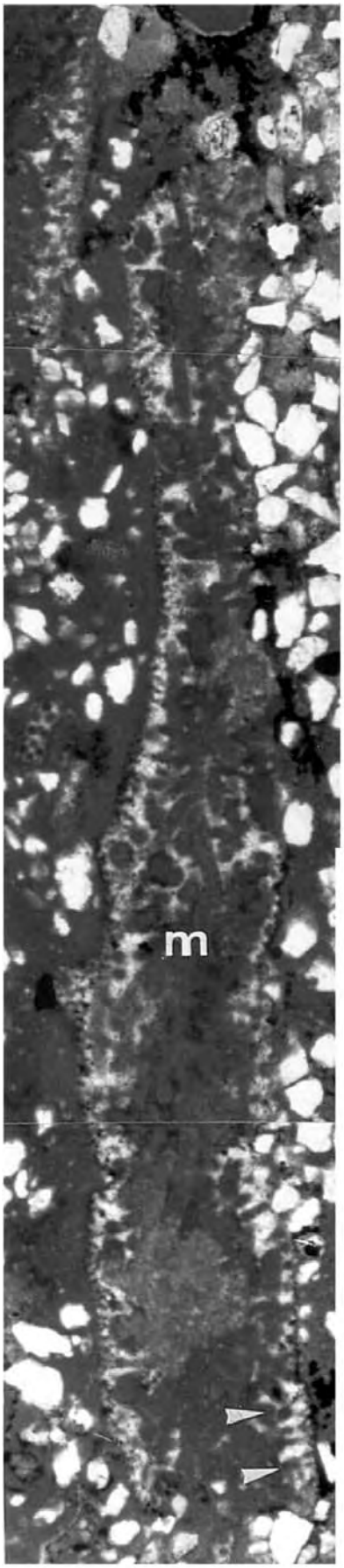

1

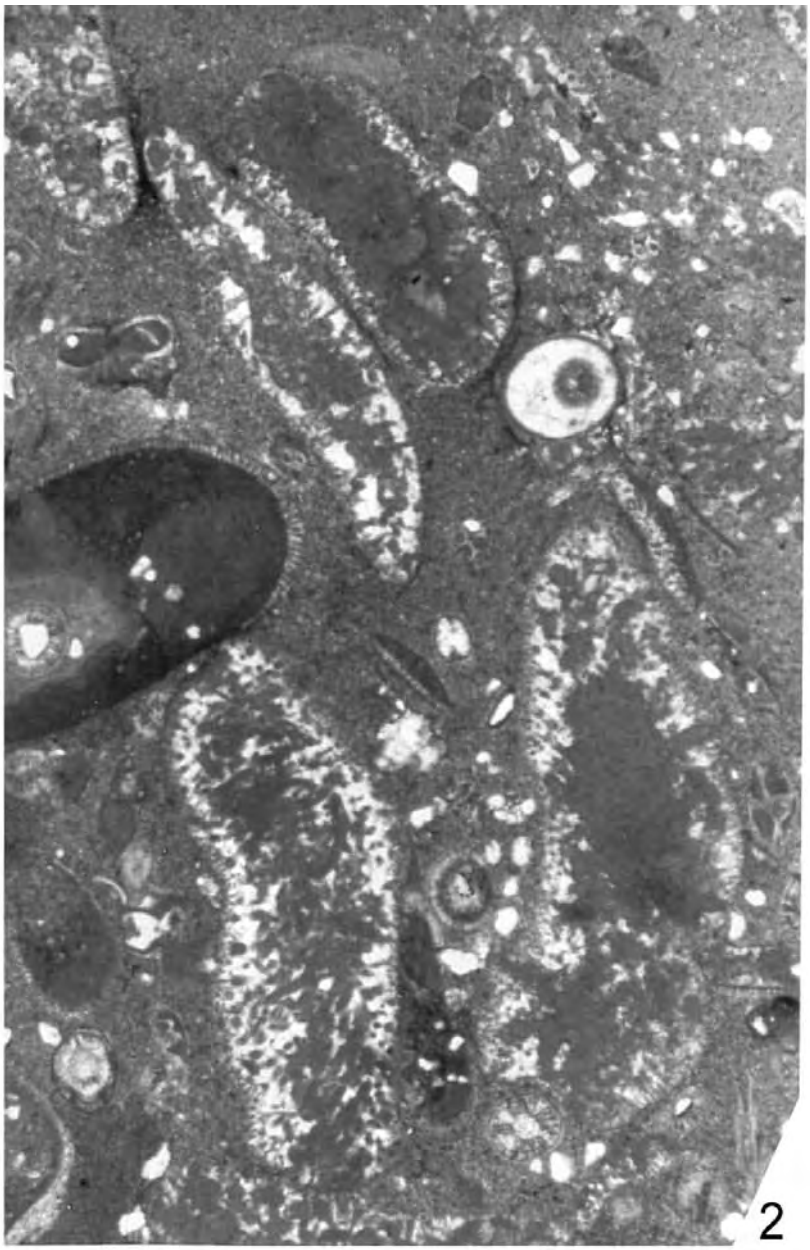

2

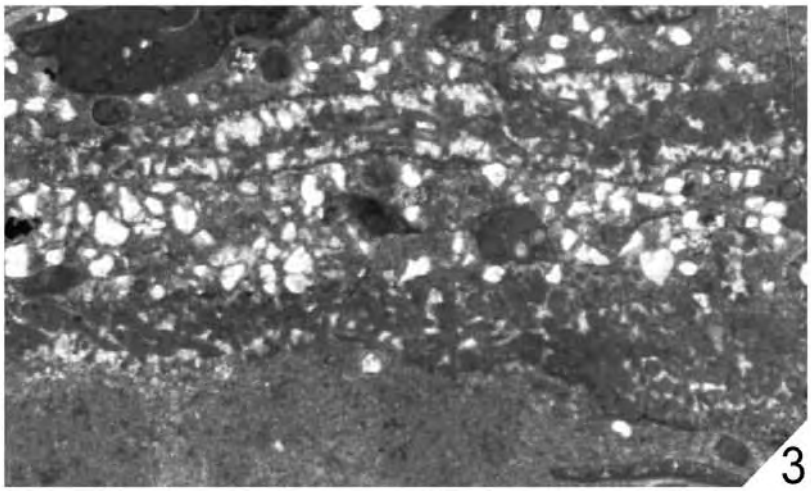

3

Emendation of the genus *Streptochilus* Brönnimann and Resig 1971 (Foraminifera) and new species from the lower Miocene of the Atlantic and Indian Oceans

Christopher W. Smart[1] and Ellen Thomas[2]

[1]*School of Earth, Ocean and Environmental Sciences, University of Plymouth, Drake Circus, Plymouth, Devon, PL4 8AA, UK*

[2]*Department of Geology and Geophysics, Yale University, P. O. Box 208109, New Haven, CT 06520-8109, USA and Department of Earth and Environmental Sciences, Wesleyan University, Middletown, CT 06459, USA*

email: csmart@plymouth.ac.uk; ellen.thomas@yale.edu

ABSTRACT: Three new species of *Streptochilus*, a biserial planktic foraminiferal genus, were recognized in the lower Miocene of the eastern Atlantic and western Indian Oceans. These species had been formerly thought to be benthic species of the genus *Bolivina*, but evidence on their apertural morphology and stable isotopic composition indicates that they lived as plankton and should be assigned to the genus *Streptochilus*. The observation that three morphological species occurred in different regions of the oceans during the same short period of time (18.9-17.2 Ma) suggests that these biserial planktic species may have evolved polyphyletically, either from biserial planktic or from benthic ancestors, possibly in response to the occurrence of relatively eutrophic environmental conditions caused by intermittent upwelling, leading to high algal growth rates but low transport efficiency of organic matter to the sea floor. The new species of *Streptochilus* are described, illustrated and named: *S. rockallkiddensis* sp. nov. (from the northeastern Atlantic), *S. cetacensis* sp. nov. (from the equatorial and southeastern Atlantic) and *S. mascarenensis* sp. nov. (from the western equatorial Indian Ocean) and the description of the genus is emended.

INTRODUCTION

High abundances of small biserial foraminifera assigned to the benthic genus *Bolivina* have been observed in lower Miocene sediments in the northeastern Atlantic and western Indian Oceans (~18.9-17.2 Ma) (Thomas 1986, 1987; Smart 1992; Smart and Murray 1994; Smart and Ramsay 1995). The early Miocene 'High Abundance of Bolivinid (HAB) event', as it was called, was not observed in sediments in the western equatorial Atlantic, eastern equatorial Pacific Ocean (Thomas 1985) and the Weddell Sea (Thomas 1990), although the correct size fraction and time interval were studied (text-fig. 1). These foraminifera occur dominantly in the small size fraction (>63µm) which has not been studied at many locations. At DSDP Site 608 (Northern Atlantic Ocean), Pagani et al. (1999, 2000) identified an increase in the carbon isotopic composition of alkenones coeval with the HAB event. This increase was interpreted as resulting from increased algal growth rates, possibly in response to increased local availability of nutrients. The calcareous nannoplankton record for that site (Olafsson 1991) shows a peak in the relative abundance of the *incertae sedis* marker species *Sphenolithus belemnos* coeval with the lower part of the event and of *Sphenolithus heteromorphus* in its higher part. Nannofossil events have been dated in the orbitally tuned Neogene time scale (Lourens et al. 2004), with the Lowest Occurrence (LO) of *S. belemnos* at 18.92 Ma, its Highest Occurrence (HO) at 17.89 Ma and the LO of *S. heteromorphus* at 17.66 Ma (Zachos et al. 2004).

The HAB event was hard to explain. In the modern oceans such high abundances of bolivinids occur only where an oxygen minimum zone impinges on the sea floor, e.g., under upwelling regions along continental margins and in silled basins (e.g., Bernhard 1986; Bernhard and Sen Gupta 1999). Thomas (1986, 1987), Smart (1992) and Smart and Murray (1994) speculated that the HABs could have occurred in a period of low oxygen conditions associated with sluggish circulation, although the sites are in the open ocean, and there is no sedimentological evidence for dysoxic conditions (e.g., high organic carbon concentration, laminated sediment). Smart and Ramsay (1995) and Ramsay et al. (1998) suggested that the event was associated with an oxygen depleted water mass restricted to the Atlantic and western Indian Oceans. How did the early Miocene world look during the HAB event?

During the early Miocene a continental ice sheet was present on East Antarctica, and possibly on Greenland (Eldrett et al. 2007). The volume of the East Antarctic Ice Sheet fluctuated (Lear et al. 2004; Hannah 2006; Pekar and DeConto 2006), with smallest ice volume and highest temperatures towards the end of the early Miocene (text-fig. 2), followed by deep-water cooling, increasing latitudinal temperature gradients (e.g., Nikolaev et al. 1998), increasing vertical water mass stratification, and the transition to a permanent, continent-wide East Antarctic Ice Sheet (e.g., Zachos et al. 2001; Miller et al. 2005; Vlastelic et al. 2005). These changes were accompanied by turnover in oceanic biota, possibly due to increasing vigor of upwelling, increased nutrient levels and oceanic productivity (e.g., Hallock et al. 1991; Halfar and Mutti 2005). Early Miocene pCO_2 levels may have been similar to pre-industrial ones, as estimated from alkenone carbon isotopes (Pagani et al. 1999), boron isotopes (Pearson and Palmer 2000), and leaf stomates (Royer et al. 2001), suggesting ocean circulation might have been at least a contributing factor in forcing the warm climate.

Substantial changes in circulation, oceanic productivity and the oceanic carbon cycle may have occurred during the early-middle Miocene (e.g., Woodruff and Savin 1989; Ramsay et al.

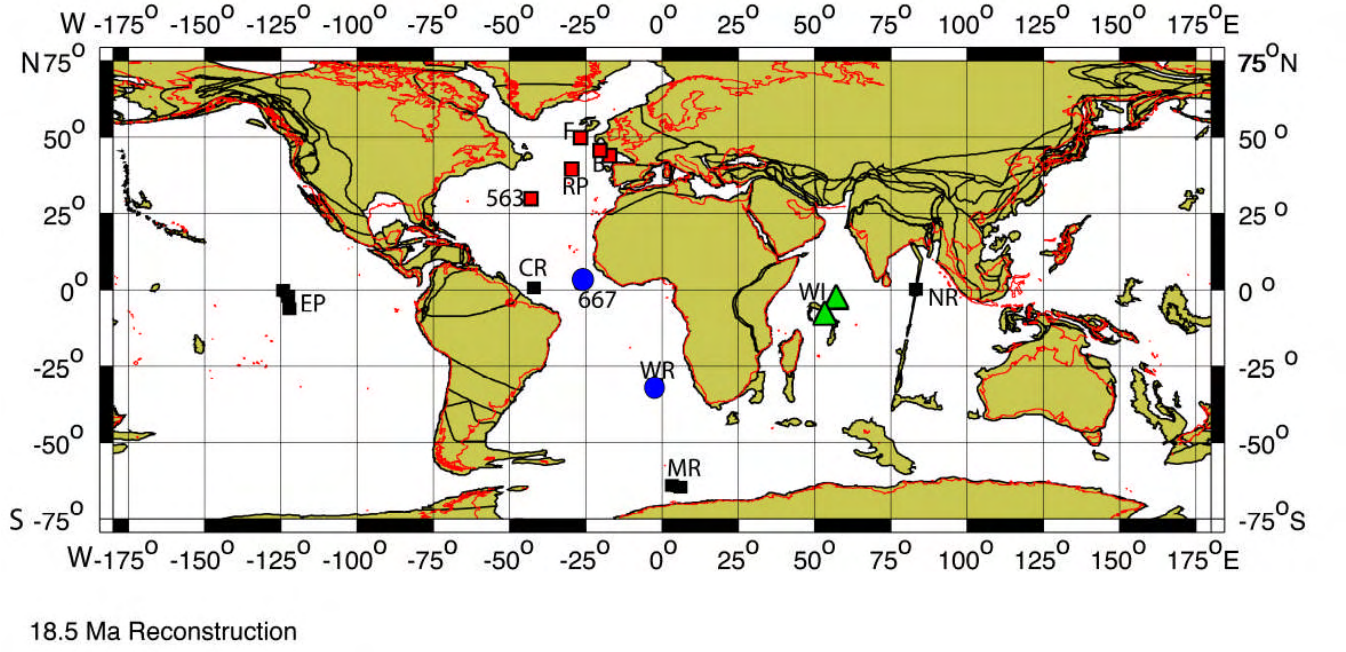

TEXT-FIGURE 1
Occurrence of early Miocene biserial foraminifera. Red squares: *S. rockallkiddensis* at F: Feni Drift (DSDP Site 610); B: Bay of Biscay (DSDP Sites 400, 548); RP: Rockall Plateau (DSDP Site 608); 563: DSDP Site 563. Blue circles: *S. cetacensis* at 667: ODP Site 667; and WR: Walvis Ridge (DSDP Site 529; ODP Sites 1264, 1265). Green triangles: *S. mascarenensis* at WI: Western Indian Ocean (DSDP Site 237, ODP Site 709). No biserial foraminifera (black squares): CR: Ceara Rise (ODP Site 926) (Smart, unpub. data); MR: Maud Rise (ODP Sites 689, 690) (Thomas 1990); NR: Ninetyeast Ridge (ODP Site 758) (Thomas, unpub. data); EP: Equatorial Pacific Ocean (DSDP Sites 573, 574, 575) (Thomas 1985). http://www.odsn.de/odsn/services/paleomap/paleomap.html. (Modified after Smart and Thomas 2006).

1998; Sykes et al. 1998; Wright 1998; Wright and Miller 1996; Lear et al. 2003, 2004; Poore et al. 2006). Benthic foraminiferal carbon isotope values shifted to more positive values starting at ~19 Ma, peaking between ~16.3 and ~13.5 Ma (Zachos et al. 2001; text-fig. 2). This positive excursion has been linked to organic carbon deposition in marine sediments around the Pacific Rim ('Monterey Event', Vincent and Berger 1985), or in lignites on land (Föllmi et al. 2005). Biogenic silica deposition moved from the Atlantic to the Pacific Ocean near the end of the early Miocene (Baldauf and Barron 1990). Deep-water exchange between the Indian and Atlantic Oceans through the eastern Mediterranean became limited at ~21-19 Ma, with a shallow connection persisting until ~17 Ma (Harzhauser et al. 2002), and closed by ~14 Ma (Woodruff and Savin 1989). The closure of the eastern Mediterranean has been argued to have ended the influx of warm, relatively salty Tethyan Outflow Water (TOW, Wright et al. 1992; called Tethyan/Indian Saline Water [TISW] by Woodruff and Savin 1989) into the northwestern Indian Ocean, with the possible effect of global cooling, but the existence of a significant volume of such outflow has not been confirmed (Smart et al. 2007).

Formation of Northern Component Water (NCW, a precursor of North Atlantic Deep Water) has been alleged to have started at ~19 Ma and reached an early peak at about ~17 Ma (Flower et al. 1997; Wright and Miller 1996; Wright 1998), but there is serious doubt about its significant presence before about 12 Ma (Zachos et al. 2001; Poore et al. 2006). The opening of Drake Passage and subsequent establishment of the Antarctic Circumpolar Current (ACC) has been linked to the middle Miocene global cooling (e.g., Pagani et al. 2000; Vlastelic et al. 2005). A deep-reaching ACC may be necessary for the formation of NCW (e.g., Sijp and England 2004), and may not have existed before ~20 Ma (Anderson and Delaney 2005). Age estimates for the initiation of the ACC, however, vary from late Miocene to middle Eocene (e.g., Barker and Thomas 2004).

In conclusion, there is no agreement on early-middle Miocene ocean circulation patterns and the cause of the rapid middle Miocene intensification of glaciation. Recent papers argue that orbitally driven changes in insolation may have been the main trigger (Abels et al. 2005; Holbourn et al. 2005), reinforcing the effects of declining levels of atmospheric greenhouses gases (Holbourn et al. 2005). Presently available records of such gases do not confirm this hypothesis (Pagani et al. 1999; Zachos et al. 2001), possibly because of their lack of time resolution (Holbourn et al. 2005).

We (Smart and Thomas 2006) used information on apertural morphology, accumulation rates and isotopic composition of the tests to show that the abundant early Miocene biserial foraminifera, assigned to the benthic genus *Bolivina*, are in fact planktic foraminifera and should be assigned to the genus *Streptochilus*. We suggested that the widespread, but not global, events during which the *Streptochilus* were abundant may reflect vigorous but variable upwelling of nutrient-rich waters, inducing high growth rates of phytoplankton. Export production as estimated from benthic foraminiferal accumulation rates, however, was low during episodes of abundant *Streptochilus*, possibly because of high regeneration rates of organic matter in an expanded thermocline. The upwelled waters may have been

an analog to the present Subantarctic Mode Waters, carrying nutrients into the eastern Atlantic and western Indian Oceans, as the result of the initiation of a deep-reaching Antarctic Circumpolar Current and active Agulhas Leakage, thus vigorous vertical mixing of nutrient-rich waters in the Southern Oceans, while there was no significant, continuous inflow of NCW (Poore et al. 2006).

In this paper we compile information on fossil and living species of *Streptochilus*, describe the morphology of the early Miocene biserial planktic species in detail, and recognize several species, each with a restricted geographic distribution. The early Miocene biserial foraminifera described here have apertures similar to those of species described as *Streptochilus*, with an internal plate formed by the infolding and downward extension of one margin of the rimmed aperture (Brönnimann and Resig 1971; Resig and Kroopnick 1983; Poore and Gosnell 1985; Resig 1989). Their walls are relatively smooth to somewhat granular in the earlier chambers and their chambers are less globose than in all described species of *Streptochilus*. Their morphology varies between sites in the North Atlantic and Indian Oceans, and we consider them to belong to three morphological species that, until now, have not been described.

BISERIAL PLANKTIC FORAMINIFERA

Bi- and triserial planktic foraminifera were common during the Late Cretaceous, with triserial forms among the rare survivors of the end Cretaceous mass extinction (e.g., Kroon and Nederbragt 1990; Olsson et al. 1999). Biserial forms, usually assigned to the genus *Chiloguembelina*, were common to abundant in the Paleogene (e.g., Olsson et al. 1999; Huber et al. 2006), and abundant occurrence of such taxa is commonly seen as reflecting relatively high productivity (e.g., Hallock et al. 1991). The genus *Chiloguembelina* was generally considered to have become extinct during the Oligocene, and the genus *Streptochilus* was seen as its descendant (Kennett and Srinivasan 1983), ranging from late early Miocene through Pleistocene (Brönniman and Resig 1971; Resig 1989). Poore and Gosnell (1985), however, argued that some species usually assigned to *Chiloguembelina* (e.g., *C. martini*) should be included in *Streptochilus* because of the presence of a toothplate (see below), as agreed by Huber et al. (2006) and Sexton et al. (2006). Huber at al. (2006) suggested that *Streptochilus martini* evolved in the middle Eocene from *Chiloguembelina ototara*. There is a stratigraphic gap in the upper Oligocene from which no biserial planktics have been described (Kennett and Srinivasan 1983; De Klasz et al. 1989).

The relations of the genus *Streptochilus* to other genera are not clear, however, and there is a remarkable morphological resemblance between the forms of *Streptochilus* described below and the Maastrichtian species *Zeauvigerina waiparaensis*, especially the forms called *Z. waiparaensis* sensu stricto (Huber and Boersma 1994). There is great similarity in the ontogenetic chamber morphologies, the adult and pre-adult apertural morphologies, the toothplate, and the stable isotopic signature. In addition, *Z. waiparaensis* is, as the *Streptochilus* species described below, characterized by high morphological variability and an unusually limited geographic distribution for a planktic form. If the species *Z. waiparaensis* with an earliest described occurrence in the middle Maastrichtian (Huber and Boersma 1994) should be assigned to the genus *Streptochilus*, the genus would have a much longer history than recorded by e.g. Huber et al. (2006). Alternatively, the phylogeny might be more complicated, and evolution of biserial planktic species might have been polyphyletic (see below).

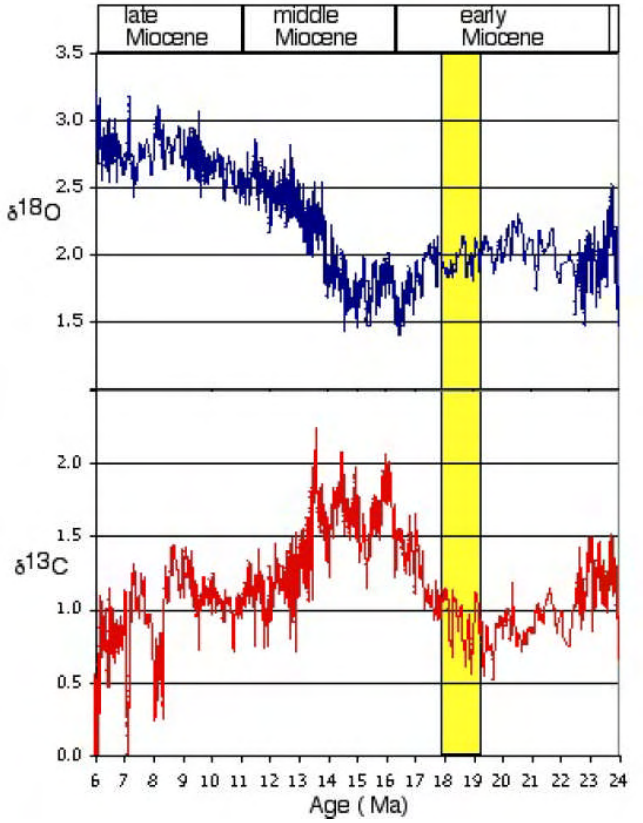

TEXT-FIGURE 2
Duration of the high abundance of biserial foraminifera event (yellow bar), plotted over carbon and oxygen data in Zachos et al. (2001), using the time scale of Berggren et al. (1995). Age of abundant biserial event at Site 608 using the time scale of Lourens et al. (2004): 18.9-17.2 Ma (Lowest Occurrence [LO] of *Sphenolithus belemnos* at 18.92 Ma, Highest Occurrence at 17.89 Ma; LO of *S. heteromorphus* at 17.66 Ma (Zachos et al. 2004); using the time scale of Berggren et al. (1995): 19.3-17.6 Ma.

Several Mio- and Pliocene *Streptochilus* species were originally described as *Bolivina*, until isotope and distributional data were collected indicating a planktic mode of life, and the name *Streptochilus* was used for planktic species, the names *Bolivina* and *Brizalina* reserved for benthic ones (Brönnimann and Resig 1971; Resig and Kroopnick 1983; Resig 1989). Late Eocene *Streptochilus* species have stable isotopic signatures similar to those of the Miocene ones (Sexton et al. 2006), and are characterized by light oxygen isotope values indicating high (surface) water temperatures. Carbon isotope values, however, are also light, even lighter than those of benthics in the same samples (Smart and Thomas 2006). Resig and Kroopnick (1983) argued that this isotope signature indicated a 'deep planktonic habitat within the oxygen minimum layer', but in such a habitat $\delta^{18}O$ values would be much more positive than observed. Nikolaev et al. (1998) classified *Streptochilus* as an intermediate-dwelling species (75–150 m depth). Smart and Thomas (2006) explained the light carbon isotope signature as resulting from rapid calcification in a region with variable upwelling conditions, as such isotope signatures are seen in Recent surface dwellers in regions with intermittent upwelling, e.g. monsoonal areas in the Ara-

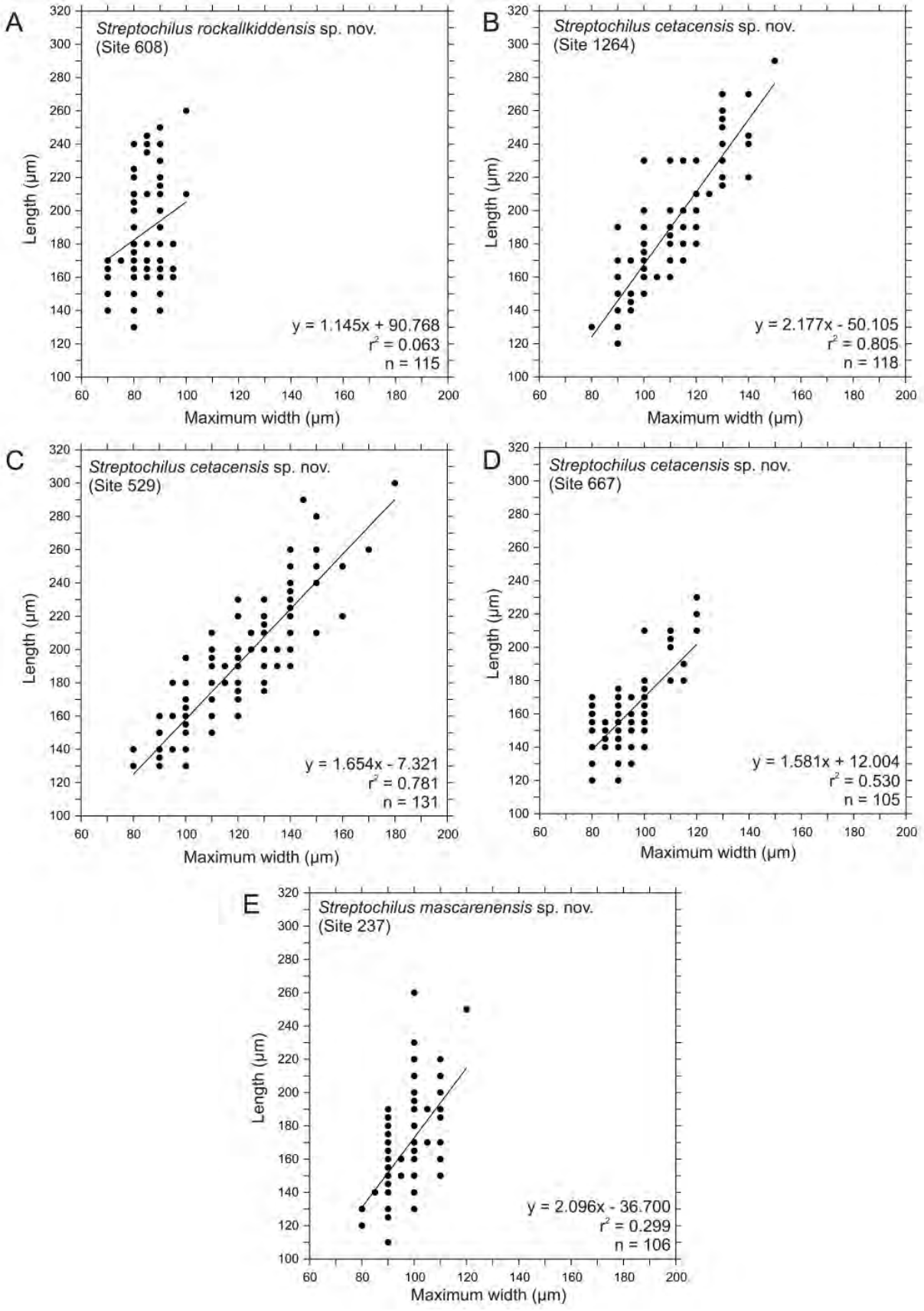

TEXT-FIGURE 3
Scatter plots of length versus maximum width of the three new *Streptochilus* spp. measured in random samples. Regression lines, equations of lines, coefficients of determination (r^2) and number (n) of specimens examined are also shown.

TABLE 1
Lower Miocene occurrences of high abundances of *Streptochilus* spp.

Hole	Latitude	Longitude	Present water depth (m)	Size-fraction (µm)	Ref.	*Streptochilus* new species names
Atlantic Ocean						
400A	47°22'N	09°11'W	4399	>63	1	*S. rockallkiddensis*
529	28°55'S	02°46'E	3035	>63	1, 2	*S. cetacensis*
548A	48°54'N	12°09'W	1251	>74	3	*S. rockallkiddensis*
563	33°38'N	43°46'W	3786	>63	1	*S. rockallkiddensis*
608	42°50'N	23°05'W	3534	>63	4, 5	*S. rockallkiddensis*
610	53°13'N	18°53'W	2427	>63	4, 5	*S. rockallkiddensis*
667A	04°34'N	21°54'W	3529	>63	1	*S. cetacensis*
1264A, B	28°31'S	02°50'E	2505	>63	6	*S. cetacensis*
1265A	28°50'S	2°38'E	3060	>63	6	*S. cetacensis*
Indian Ocean						
237	07°05'S	58°08'E	1623	>63	7	*S. mascarenensis*
709C	03°54'S	60°33'E	3040	>63	7	*S. mascarenensis*

References: 1 = Smart and Murray (1994), 2 = Smart (1992), 3 = Poag and Low (1985), 4 = Thomas (1986), 5 = Thomas (1987), 6 = Zachos et al. (2004), 7 = Smart and Ramsay (1995).

bian Sea (e.g., Kroon and Ganssen 1989; Naidu and Niitsuma 2004). Such a habitat would be in agreement with inferences that Paleogene biserial forms generally indicate eutrophic conditions (e.g., Hallock et al. 1991; Smart and Thomas 2006).

Streptochilus was thought to be extinct when the genus was first described (Brönnimann and Resig 1971), but found to be common (up to 15%) as living forms in plankton tows south of India, where intermittent upwelling causes highly variable conditions close to the shelf edge (Kroon and Nederbragt 1990). The spatial and temporal distribution of living *Streptochilus* are poorly known because they are minute and their size fraction rarely studied. They were found as rare specimens in plankton tows in the northern Atlantic and Caribbean (Hemleben et al. 1989; Schmuker and Schiebel 2002). According to Hemleben et al. (1989), *Streptochilus globigerus* is a deep-dwelling species in highly productive, commonly coastal waters, but also occurs as rare forms in the northern Atlantic near Bermuda, where they consume diatoms, being warm-temperate forms (Hemleben et al. 1989). Schmuker and Schiebel (2002) listed *S. globigerus* as rare in the higher productivity regions of the eastern Caribbean. Miocene *Streptochilus* spp. have been described as tropical to warm-subtropical (Brönnimann and Resig 1971; Kennett and Srinivasan 1983; Resig 1989), but they are abundant in few samples (thus reflecting a limited time-range) from the northernmost Atlantic Ocean (Flower 1999) through the Bahama Bank (Kroon et al. 2000), the equatorial western Pacific (Premoli-Silva and Violanti 1981; Resig 1989) and the eastern Indian Ocean (Resig 1989).

Biserial planktic foraminifera have been said to be represented by only one living species, *Streptochilus globigerus* (Hemleben et al. 1989), but there might be more than one morphological species. Some *Streptochilus* species have a fairly smooth wall (e.g., the type species of the genus, *S. globulosus*). Others have a macroperforate, cancellate wall, with large pores inside a hexagonal system of ridges (e.g., *S. globigerus*). An extinct species, *S. subglobigerum*, was described as being partially cancellate-walled, but having smooth-walled later chambers (Resig 1989). Note that the description of macroperforate species as belonging to the genus *Streptochilus* (Hemleben et al. 1989) could be seen as problematic, since the genus is classified as microperforate (Huber et al. 2006). Kroon and Nederbragt (1990) observed living species (*Streptochilus* spp.) south of India, but they were not named, not described at the species level, and not figured. De Klasz et al. (1989) named that species *S. globulosus*, a smooth-walled species, which had been thought to have a Plio-Pleistocene range (Kennett and Srinivasan 1983; Resig 1989). In contrast, Hemleben et al. (1989) and Schmuker and Schiebel (2002) state that there is only one living species, which

they call *S. globigerus*, a macroperforate species with a cancellate wall, originally said to have a Mio-Pliocene range (Kennett and Srinivasan 1983; Resig 1989). None of these authors shows a picture or includes a detailed description, and it thus is not clear whether there is one living morphological species or at least two, one smooth-walled and one cancellate. Living *Streptochilus* specimens collected in the Indian Ocean by K. Darling (pers. comm., 2005) have a cancellate wall and are macroperforate, and thus should be assigned to the species *S. globigerus*.

In conclusion, we argue that the present taxonomic status of the genus *Streptochilus* is not satisfactory, and that there is uncertainty regarding the taxonomic and/or habitat status of biserial species that have not been studied in detail. It is thus surprisingly difficult to ascertain whether biserial foraminifera are planktic or benthic based on morphology only. Most biserial planktics have more inflated chambers than benthics, and possess a wide, arched aperture without an internal toothplate, as in *Chiloguembelina.* The genus *Streptochilus,* however, is characterized by an aperture bordered by a collar, with a connecting internal plate superficially resembling the bolivinid toothplate (e.g., Huber et al. 2006), but this toothplate in *Streptochilus* does not extend freely outside the aperture (Brönnimann and Resig 1971; Resig and Kroopnick 1983; see also Smart and Thomas 2006). The name *Streptochilus* was derived from *streptos*, Greek (στρεπτοσ) for 'twisted' and *cheilos*, Greek (χειλοσ) for 'lip', indicating the change to an inward directed lip (Brönnimann and Resig 1971). The exact nature of the toothplate, however, is not easily observed in a light microscope because of the small size. In addition, in some specimens the toothplate is missing, and many published figures do not show this feature. Brönnimann and Resig (1971) did not specify a wall-type for the genus, and Resig (1989) included both smooth and cancellate-walled species in the genus. Huber et al. (2006) said that 'smooth to granular, rather than pustulose to costate surface texture' belongs to the distinguishing feature of the genus, but since they describe only the Eocene-Oligocene *S. martini* they do not discuss the exclusively Neogene cancellate wall type.

We are of the opinion that there is no solid evidence that a planktic or benthic lifestyle reflects phylogenetic relationships of biserial taxa. Non-morphological (e.g., stable isotopic) information on lifestyle, as described above, possibly should not be used in assigning biserial species to a genus, and morphology might not always be a foolproof way of defining lifestyle. Many biserial taxa have been assigned to the genera *Bolivina* or *Brizalina*, and thus are assumed to be benthic forms by definition, not because of the existence of evidence that they actually live or have lived in a benthic environment. Biserial forms thought to have been planktic have been seen as a monophyletic group, with all Cenozoic forms descended from a survivor group of the Cretaceous-Paleogene extinction (e.g., Kennett and

---

PLATE 1

Scanning electron micrographs of *Streptochilus rockallkiddensis* sp. nov.; 1 holotype; 2-13 paratypes.
Note smooth wall in 2 and 4-7, and varying degrees of granular surface texture in 3, 8-13.
Note parallel-sided shape of 4-6 and 11, and tending to uniserial in 13.

1 a, Side view of holotype, reg. no. BM(NH) PF 67972, uncoated, note half of test with granular surface texture and parallel-sided shape, scale bar = 50µm; b, detail of wall, scale bar = 10µm (DSDP 94-608-37X-4, 38-40cm, 343.78 mbsf).

2-13 Side views of paratypes, all uncoated, all scale bars = 50µm;

2 reg. no. BM(NH) PF 67973, from DSDP 94-608-37X-6, 38-40cm, 346.78 mbsf

3 reg. no. BM(NH) PF 67974, from DSDP 94-608-37X-4, 38-40cm, 343.78 mbsf

4 reg. no. BM(NH) PF 67975, from DSDP 94-608-37X-6, 38-40cm, 346.78 mbsf

5 reg. no. BM(NH) PF 67976, from DSDP 94-608-37X-4, 38-40cm, 343.78 mbsf

6 reg. no. BM(NH) PF 67977, from DSDP 94-608-37X-6, 38-40cm, 346.78 mbsf

7 reg. no. BM(NH) PF 67978, from DSDP 94-608-37X-6, 38-40cm, 346.78 mbsf

8 reg. no. BM(NH) PF 67979, from DSDP 94-608-37X-6, 38-40cm, 346.78 mbsf

9 reg. no. BM(NH) PF 67980, from DSDP 94-608-37X-4, 38-40cm, 343.78 mbsf;

10 reg. no. BM(NH) PF 67981, from DSDP 94-608-37X-6, 38-40cm, 346.78 mbsf

11 reg. no. BM(NH) PF 67982, from DSDP 94-608-37X-6, 38-40cm, 346.78 mbsf

12 reg. no. BM(NH) PF 67983, from DSDP 94-608-37X-6, 38-40cm, 346.78 mbsf

13 reg. no. BM(NH) PF 67984, from DSDP 94-608-37X-6, 38-40cm, 346.78 mbsf.

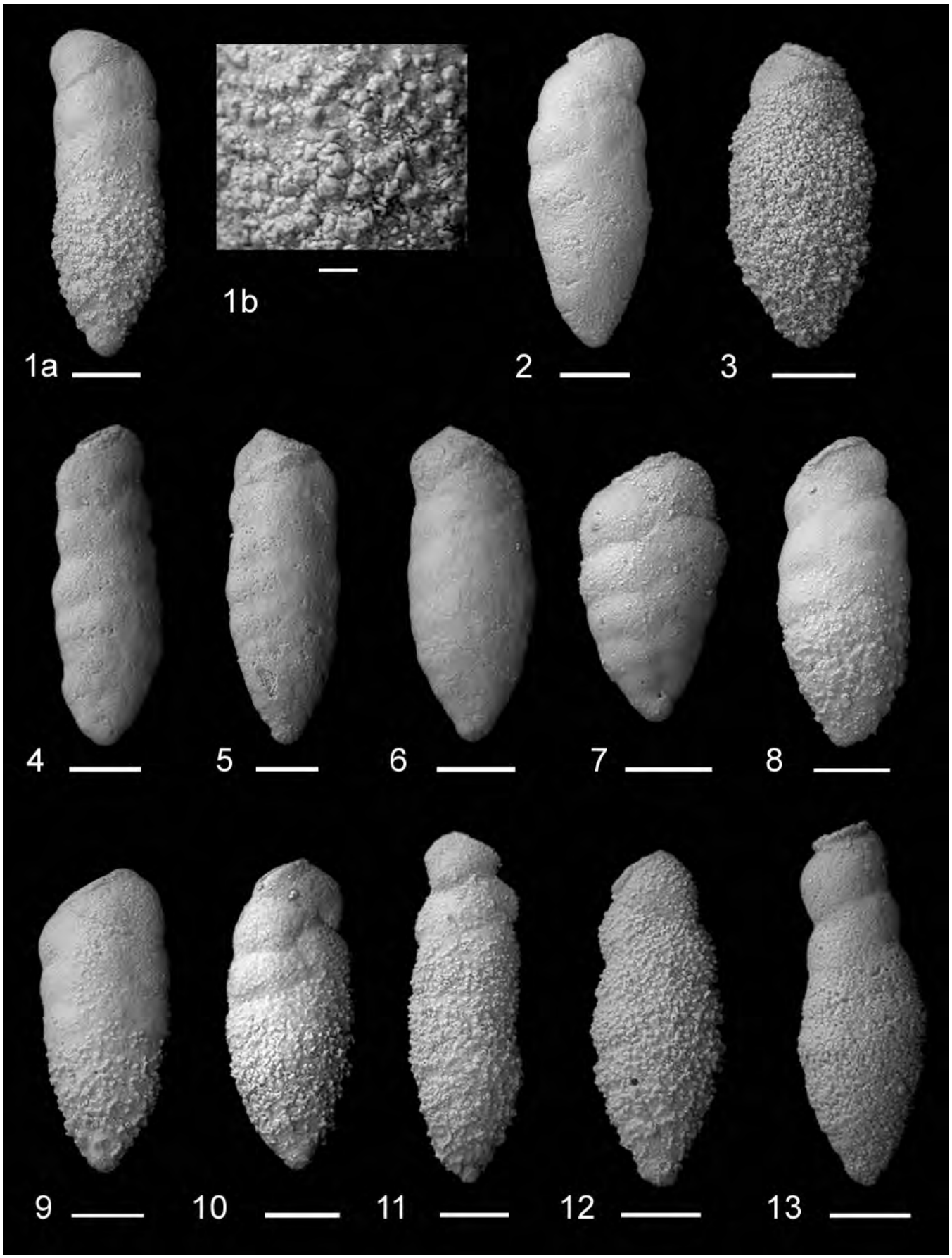
1a
1b
2
3
4
5
6
7
8
9
10
11
12
13

Srinivasan 1983; De Klasz et al. 1989; Olsson et al. 1999; Huber et al. 2006). Benthic biserial specimens assigned to the genus *Bolivina*, however, are commonly seen in plankton tows (Lidz 1966; Hueni et al. 1978, D. Kroon, pers. comm.. 2005; R. Schiebel, pers. comm. 2005), and are abundant among species transported off the shelves into open ocean during storms (e.g., Brunner and Biscaye 1997). Some of the shelf dwelling *Bolivina,* e.g., *Bolivina variabilis* (Williamson 1858) have cancellate walls resembling those of *S. globigerus*, with large pores in hexagonal depressions. The exact shape of the aperture of this species and its toothplate have not been described, because the type figure of *B. variabilis* shows an aperture without a toothplate: either the figure is incorrect or the toothplate has been broken. A plesiotype at the Smithsonian Museum of Natural History (Washington DC, USA; Cushman Collection # 23807) also lacks the toothplate. This species therefore could be a *Streptochilus* rather than a *Bolivina*, with its apertural structure strongly resembling that of *Streptochilus* in photographs of some specimens assigned to this species (Murray 1971; Boltovskoy et al. 1980). Since details of toothplates have not been commonly described, biserial benthic species might have different types of toothplate, and the toothplate type described in the type species of *Streptochilus* could thus possibly occur in some benthic species. The genus *Laterostomella* has an aperture similar to that of *Streptochilus*, and at least some species placed in this genus have a macro-perforate, cancellate wall (De Klasz et al. 1989). Loeblich and Tappan (1987) considered *Laterostomella* to be a morphological synonym of *Streptochilus*, but oxygen isotope data indicate it had a benthic life style, the reason for De Klasz et al. (1989) to argue that this name can not be synonymous to the planktic *Streptochilus*.

As mentioned above, we are not fully convinced that this argument from habitat (rather than from morphology) is valid. It could be speculated that at least some bolivinids might live tychopelagically as some diatom species do, rather than exclusively as part of the benthos. If this is correct, benthic specimens of *Bolivina* swept out to the open ocean might survive and live and even reproduce within the planktic habitat, hence having a planktic lifestyle as indicated by their oxygen isotopic and trace element signature. Such bolivinids, a group generally adapted to high-food conditions (e.g., Jorissen et al., in press), would be expected to be most successful in survival in regions with a high food supply, i.e., upwelling regions. One taxonomic group (e.g., *Bolivina*) would then have either a benthic or a planktic lifestyle, depending upon the circumstances. One could go a step further in speculation, and argue that a planktic-living population could survive and evolve into a purely planktic species. In that case, there might be no close phylogenetic linkage between different biserial planktic groups, with polyphyletic evolution of planktic from benthic biserial groups occurring several times, thus explaining such a feature as the lack of biserial taxa in the late Oligocene. If such were true, taxonomic affiliation may not give clear information on planktic or benthic status. We argue that more detailed, morphological as well as stable isotopic investigations are needed, in addition to genetic investigations of

---

PLATE 2

Scanning electron micrographs of *Streptochilus rockallkiddensis* sp. nov.; paratypes.

1 Side view of paratype (reg. no. BM(NH) PF 67985), uncoated, note elongate shape becoming uniserial, scale bar = 50µm (DSDP 94-608-37X-4, 38-40cm, 343.78 mbsf).

2 Side view of paratype (reg. no. BM(NH) PF 67986), uncoated, note becoming uniserial towards apertural end, scale bar = 50µm (DSDP 94-608-37X-4, 38-40cm, 343.78 mbsf).

3 a, Edge view of paratype (reg. no. BM(NH) PF 67987), uncoated, showing aperture, scale bar = 50µm; b, detail of aperture showing infolded rimmed margin, scale bar = 10µm (DSDP 94-608-37X-6, 38-40cm, 346.78 mbsf).

4 a, Edge view of paratype (reg. no. BM(NH) PF 67988), uncoated, showing aperture, scale bar = 50µm; b, detail of aperture, scale bar = 10µm (DSDP 94-608-37X-6, 38-40cm, 346.78 mbsf).

5 a, Edge view of paratype (reg. no. BM(NH) PF 67989), uncoated, showing aperture, scale bar = 50µm; b, detail of aperture, note thickened rim of final chamber, scale bar = 10µm (DSDP 94-608-37X-6, 38-40cm, 346.78 mbsf).

6 a, Edge view of paratype (reg. no. BM(NH) PF 67990), gold coated, showing aperture, scale bar = 50µm; b, detail of aperture, note aperture obscured by thickening and thickened rim of final chamber, scale bar = 10µm (DSDP 94-608-37X-6, 38-40cm, 346.78 mbsf).

7 a, Oblique view of paratype (reg. no. BM(NH) PF 67991), gold coated, showing aperture, scale bar = 50µm; b, detail of aperture, note aperture obscured by thickening and thickened rim of final chamber, scale bar = 10µm (DSDP 94-608-37X-6, 38-40cm, 346.78 mbsf).

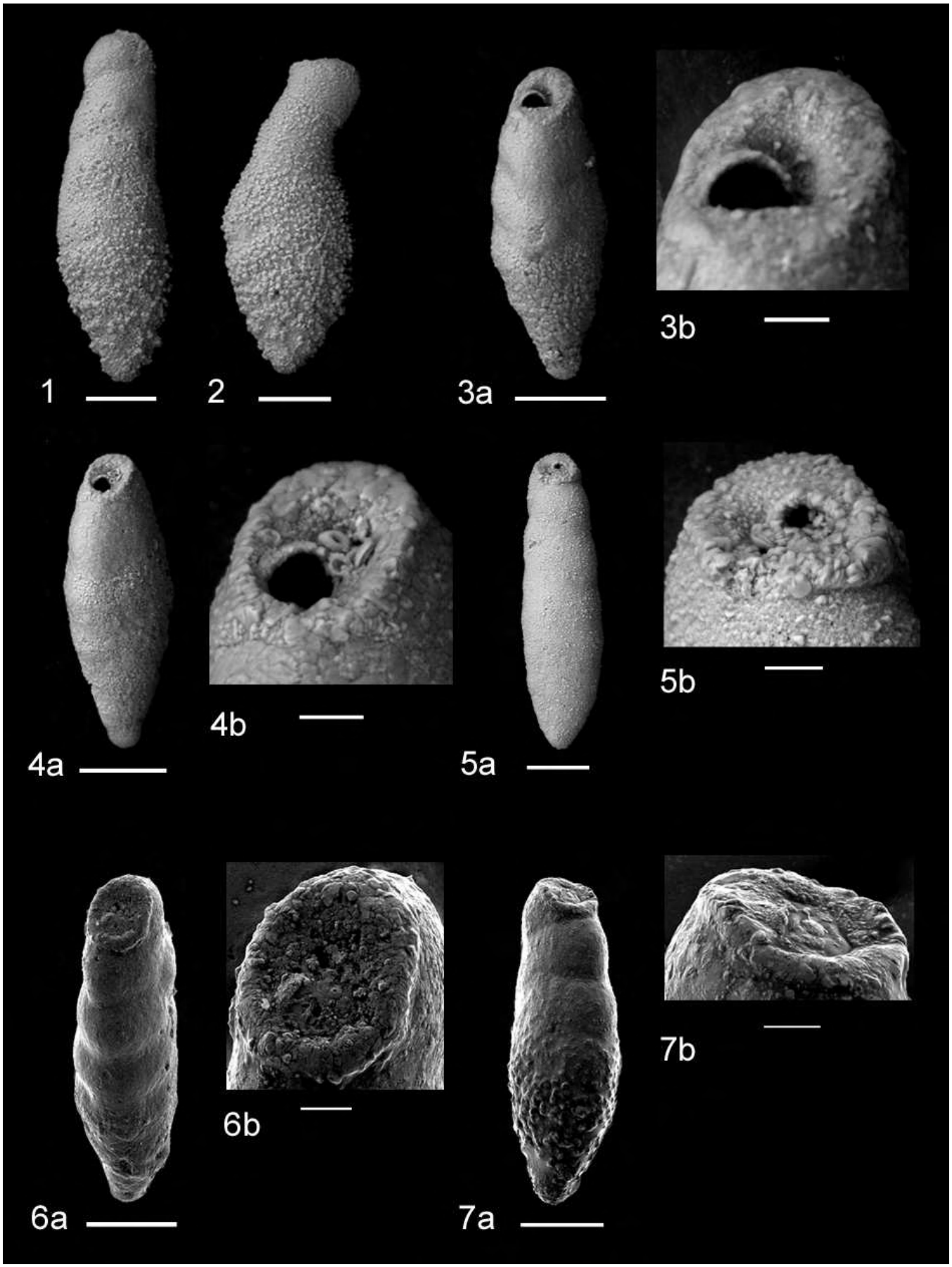
1
2
3a
3b
4a
4b
5a
5b
6a
6b
7a
7b

living biserial taxa, in order to solve the question of phylogenetic relations between biserial taxa, and whether biserial planktic foraminifera constitute a monophyletic group. Such information is also needed in order to solve the question whether detailed morphological information can be sufficient to determine the planktic or benthic lifestyle of biserial taxa, or whether this must be resolved by non-morphological (e.g., stable isotopic) data.

METHODS

For each sample, foraminifers were picked from the >63µm size-fraction, because *Streptochilus* spp. are absent in larger size-fractions. A random sample of specimens was chosen for size measurements. Specimen length, width and thickness were determined using a micrometer eyepiece (accuracy 10µm) fitted to a reflected-light microscope. For scanning electron microscope (SEM) analysis, specimens were mounted on small metal stubs with gummed adhesives and, in some cases, were sputter-coated with a thin layer of gold. Specimens were studied and photographed using a JEOL JSM-5600LV SEM at the University of Plymouth, UK. Gold-coated specimens were observed in high vacuum mode and uncoated specimens were examined in low vacuum mode. Specimens to be sectioned were embedded in epoxy resin and set. They were then manually polished and studied in low vacuum mode under the SEM.

Light photograph digital images were taken of various specimens by A. S. Henderson at the Natural History Museum, London. High-resolution digital photography and an image manipulation application are used to produce focused (and color) composite images of specimens. This technique (known as *PalaeoVision*), developed at the Natural History Museum, London, UK, provides detailed digital images that closely represent how the specimens look under a light microscope (e.g., Holbourn and Henderson 2002). Apart from one specimen (plate 7, fig. 11b), the specimens were too small to obtain clear focused images. All type specimens are deposited in the Department of Palaeontology, The Natural History Museum, Cromwell Road, London, UK.

SYSTEMATIC DESCRIPTIONS

The suprageneric classification scheme follows Loeblich and Tappan (1992).

Class FORAMINIFEREA Lee 1990
Order GLOBIGERINIDA Lankester 1885 (as Globigerinidea; nom. corr. Calkins 1909)
Superfamily HETEROHELICACEA Cushman 1927
Family CHILOGUEMBELINIDAE Reiss 1963

Genus ***Streptochilus*** Brönnimann and Resig 1971, emend. Smart and Thomas this paper

We propose that the original description of *Streptochilus* given by Brönnimann and Resig (1971) should be emended as follows, due to features of the new species *S. rockallkiddensis* (see below), i.e. the test may become staggered uniserial, and the aperture may be obscured by a thickening of the wall including the rim of the aperture:

PLATE 3

Scanning electron micrographs of *Streptochilus rockallkiddensis* sp. nov.; paratypes.

1 a, Oblique view of paratype (reg. no. BM(NH) PF 67992), gold coated, showing aperture, scale bar = 50µm; b, detail of aperture, note aperture obscured by thickening and thickened rim of final chamber, scale bar = 10µm (DSDP 94-608-37X-6, 38-40cm, 346.78 mbsf).

2 a, Edge view of paratype (reg. no. BM(NH) PF 67993), gold coated, showing aperture, scale bar = 50µm; b, detail of aperture, note aperture obscured somewhat by thickening and thickened rim of final chamber, scale bar = 10µm (DSDP 94-608-37X-6, 38-40cm, 346.78 mbsf).

3 a, Edge view of paratype (reg. no. BM(NH) PF 67994), gold coated showing aperture, note slight twisting, scale bar = 50µm; b, detail of aperture, note thickened rim of final chamber, scale bar = 10µm (DSDP 94-608-37X-6, 38-40cm, 346.78 mbsf).

4 a, Edge view of paratype (reg. no. BM(NH) PF 67995), dissected specimen, gold coated, scale bar = 50µm; b, detail of aperture, note internal plate connecting with apertural rim, scale bar = 10µm (DSDP 94-608-37X-6, 38-40cm, 346.78 mbsf).

5 a, Oblique view of paratype (reg. no. BM(NH) PF 67996), dissected specimen, gold coated, scale bar = 50µm; b, detail of aperture, note internal plate connecting with apertural rim, scale bar = 10µm (DSDP 94-608-37X-6, 38-40cm, 346.78 mbsf).

6 a, Edge view of paratype (reg. no. BM(NH) PF 67997), dissected specimen, gold coated, scale bar = 50µm; b, detail of aperture, note internal plate connecting with apertural rim, scale bar = 10µm (DSDP 94-608-37X-6, 38-40cm, 346.78 mbsf).

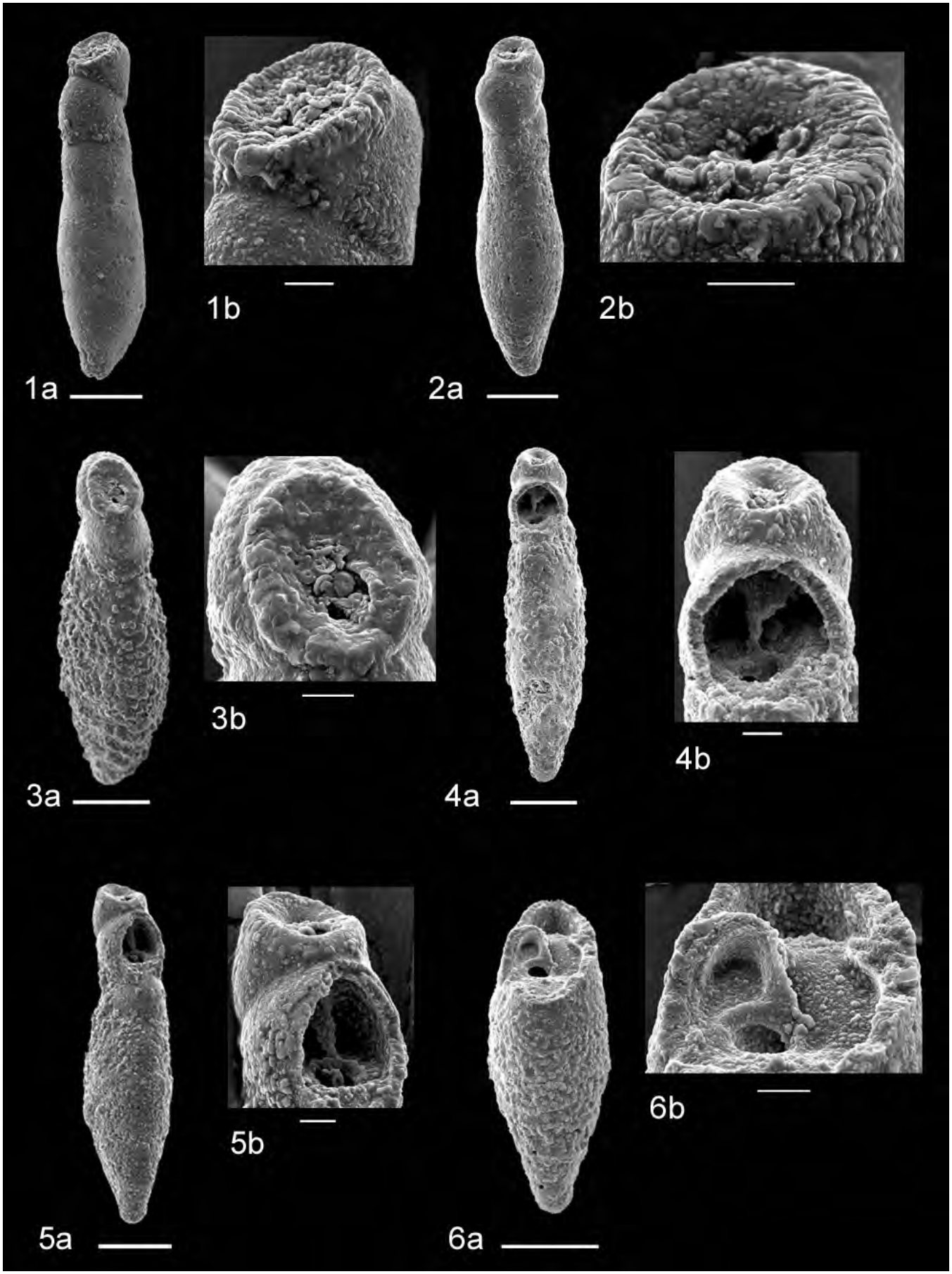
1a
1b
2a
2b
3a
3b
4a
4b
5a
5b
6a
6b

Test biserial, may become staggered uniserial, sometimes twisted; wall calcareous, perforate; aperture a high arch, eccentric in position, extending from the base of the last chamber onto the apertural face. On the outside margin, a collar borders the aperture. Near the base of the inside margin, the collar and apertural edge are turned inward, producing a plate-like connection with the proximal margin of the collar of the previous aperture. Aperture may be obscured by a thickening of the wall including the rim of the aperture. The length of the test varies between 75 and 300µm.

Streptochilus rockallkiddensis Smart and Thomas **n. sp.**
Plates 1-5

Bolivina sp. 9 – POAG and LOW 1985, pl. 1, figs. 16-18
Bolivina spathulata (Williamson). – THOMAS 1987, Tables 1-2
Bolivina sp. – SMART AND MURRAY 1994, fig. 2, no. 1. – SMART and RAMSAY 1995, fig. 2

Diagnosis. Test small, elongate, laterally slightly compressed, biserial becoming staggered uniserial, commonly rectilinear and often narrower towards apertural end, aperture with thickened rim and often obscured, surface ornamentation varying from smooth to granular.

Description. Test small, elongate, laterally slightly compressed, periphery rounded and non-lobulate, shape variable, commonly elongate, parallel-sided and rectilinear, occasionally flared, in some elongate specimens the later formed part of the test may narrow towards the apertural end, biserial tending to staggered uniserial in some elongate specimens, rarely twisted; most specimens have 6 pairs of chambers but the number of pairs varies from 5-8 or more, chambers increase regularly in size as added, slightly wider than high, initial chambers small and often obscured by granular surface ornamentation; sutures slightly curved and depressed; final chamber often has thickened rim; aperture low-arch shaped, offset to one side of test, with an internal plate formed by the infolding and downward extension of one margin of the rimmed aperture, often small and obscured by thickening; wall uniformly very finely perforate, surface ornamentation varies from smooth to finely granular to coarsely granular and, where present, ornamentation constitutes half or more of the test occurring from proloculus towards apertural end; no obvious differences between micro- and megalospheric specimens.

Dimensions. Length, 260-130µm (mean 187µm, St. Dev. 28, n = 115); maximum width, 100-70µm (mean 84 µm, St. Dev. 6, n = 115); thickness, 70-60µm (mean 63 µm, St. Dev. 4, n = 20).

Etymology. Named after the area where it has been found, i.e. Rockall Plateau, NE Atlantic Ocean and in honor of the late Professor Robert B. Kidd (1947-1996), a marine geologist and colleague who was one of the co-chief scientists on DSDP Leg 94 responsible for drilling DSDP Site 608, the site from which the highest abundances of the species have been reported to date.

Type locality and distribution. Lower Miocene, NE Atlantic Ocean, DSDP Site 608. Also reported from North Atlantic DSDP Sites 400, 548, 563 and 610 (Table 1).

Type specimens. The figured holotype, figured paratypes and unfigured paratypes are deposited in the Department of Palaeontology, The Natural History Museum, Cromwell Road, London, UK. The holotype (reg. no. BM(NH) PF 67972) is from DSDP 94-608-37X-4, 38-40cm, 343.78 mbsf [Deep Sea Drilling Project Leg-Hole-Core-Section-Interval, meters below sea floor] (Plate 1, Fig. 1a,b). All other examined and illustrated

---

PLATE 4
Scanning electron micrographs of *Streptochilus rockallkiddensis* sp. nov.; paratypes.

1 a, Edge view of paratype (reg. no. BM(NH) PF 67998), dissected specimen, gold coated, scale bar = 50µm; b, detail of aperture, note internal plate connecting with apertural rim, scale bar = 10µm (DSDP 94-608-37X-6, 38-40cm, 346.78 mbsf).

2 a, Side view of paratype (reg. no. BM(NH) PF 67999), gold coated, note smooth wall, scale bar = 50µm; b, detail of wall, scale bar = 10µm (DSDP 94-608-37X-6, 38-40cm, 346.78 mbsf).

3 a, Side view of paratype (reg. no. BM(NH) PF 68000), gold coated, note smooth wall, scale bar = 50µm; b, detail of wall, scale bar = 10µm; c, greater detail of wall showing fine pores, scale bar = 5µm (DSDP 94-608-37X-6, 38-40cm, 346.78 mbsf).

4 a, Side view of paratype (reg. no. BM(NH) PF 68001), gold coated, note coarse granular wall texture, scale bar = 50µm; b, detail of wall, scale bar = 10µm; c, greater detail of wall, scale bar = 5µm (DSDP 94-608-37X-6, 38-40cm, 346.78 mbsf).

5 a, Side view of paratype (reg. no. BM(NH) PF 68002), gold coated, note granular wall texture, scale bar = 50µm; b, detail of wall, scale bar = 10µm (DSDP 94-608-37X-6, 38-40cm, 346.78 mbsf).

6 a, Side view of paratype (reg. no. BM(NH) PF 68003), gold coated, note granular wall texture, scale bar = 50µm; b, detail of wall, scale bar = 10µm (DSDP 94-608-37X-6, 38-40cm, 346.78 mbsf).

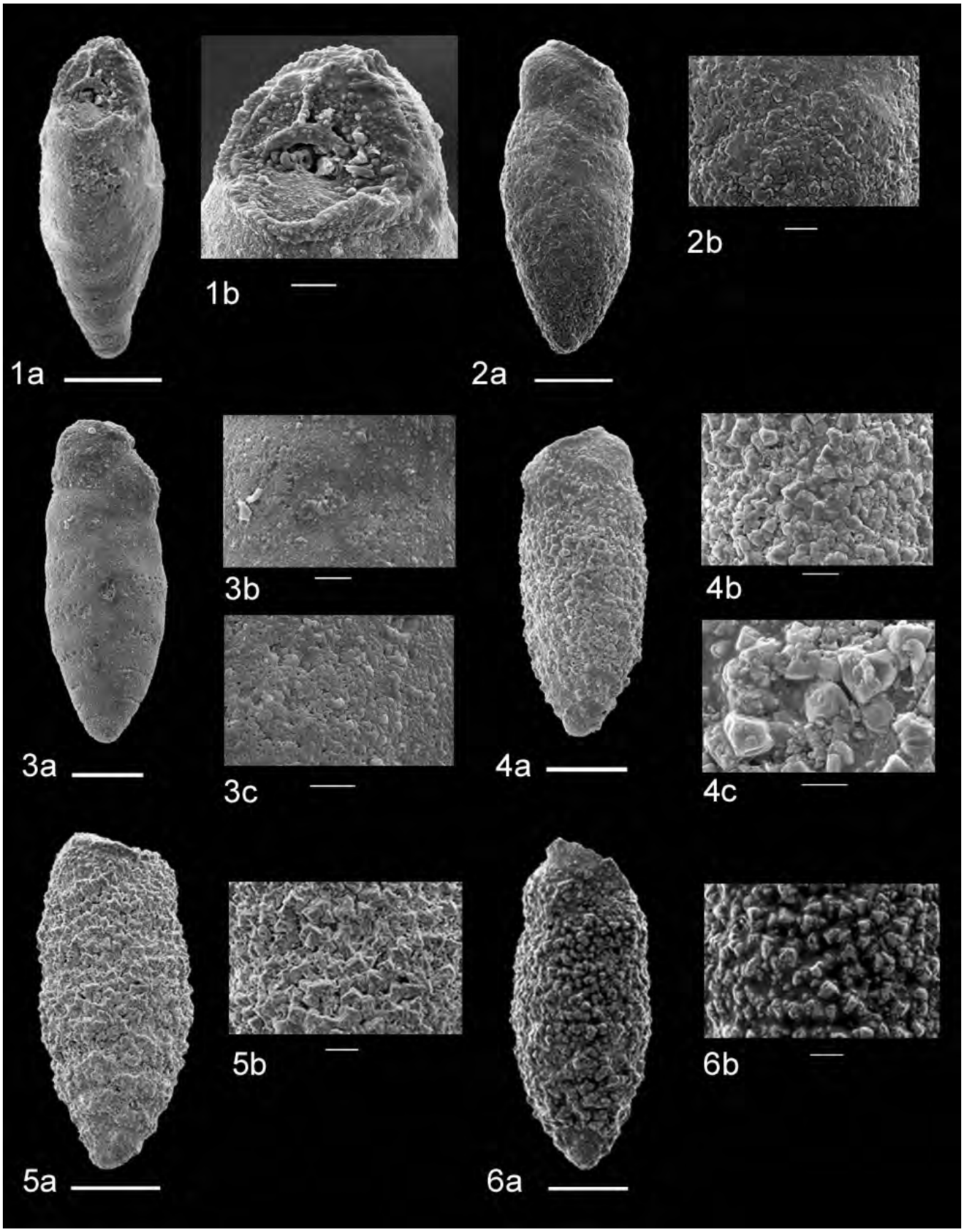
1a
1b
2a
2b
3a
3b
3c
4a
4b
4c
5a
5b
6a
6b

specimens are designated paratypes (reg. no. BM(NH) PF 67973-68061, BM(NH) PF 68192-68221) and are from DSDP 94-608-37X-4, 38-40cm, 343.78 mbsf; DSDP 94-608-37X-6, 38-40cm, 346.78 mbsf; and DSDP 82-563-11-5, 19-21cm, 257.69 mbsf (Plate 1, Figs. 2-13; Plates 2-5).

Remarks. The granular surface texture displayed by a high proportion of specimens can be difficult to discern under a light microscope, but becomes clear when specimens are viewed under a SEM. The degree of roughness of the test varies from specimen to specimen and from sample to sample. In the specimens examined from Site 608, the percentage of roughened specimens varies from ~68% (sample DSDP 608-37X-4, 38-40cm, n = 110) to ~37% (sample DSDP 608-37X-6, 38-40cm, n = 115). Specimens from DSDP Sites 400 and 563 often have a roughened appearance. Typically the roughened appearance makes up half of the test, although in some specimens this may be one-third, two-thirds, three-quarters or more of the test. The number of parallel-sided and flared tests varies between specimens and between samples, although parallel-sided individuals are generally more common. The roughened appearance obscures the chambers, although these are discernible when specimen is wetted.

Streptochilus rockallkiddensis sp. nov. closely resembles *Bolivina* sp. 9 of Poag and Low (1985, pl. 1, figs 16, 17, 18) reported from DSDP Site 548. Their illustrations clearly show the variability of test roughness ranging from smooth (pl. 1, fig. 16), to one-third roughened (pl. 1, fig. 17) to three-quarters roughened (pl. 1, fig. 18).

Thomas (1986, 1987) referred to *Streptochilus rockallkiddensis* sp. nov. as *Bolivina spathulata* (Williamson). A specimen from Site 563 has been illustrated in Smart and Murray (1994, Fig. 2, 1) and Smart and Ramsay (1995, Fig. 2). For a description of the differences between the three new Miocene *Streptochilus* spp., see differential analysis (below).

Streptochilus cetacensis Smart and Thomas **n. sp.**
Plates 6-11

Bolivina sp. – SMART and MURRAY 1994, fig. 2, no. 2, – SMART and RAMSAY 1995, fig. 2
Streptochilus sp. – SMART and THOMAS 2006, fig. 2, A, B

Diagnosis. Test elongate, laterally slightly compressed, flared and typically 'triangular' in shape with curved and depressed sutures, with many specimens covered with evenly distributed pores.

Description. Test small to medium sized, elongate, increasing regularly in size, flared and typically 'triangular' in shape, laterally slightly compressed, periphery broadly rounded to somewhat lobulate, sometimes twisted, biserial; 5-8 pairs of chambers, slightly inflated, wider than high, increasing regularly in size as added; sutures curved and depressed; aperture high arch-shaped, offset slightly to one side of test, extending from the base of the last chamber onto apertural face, bordered by a thickened rim/collar along the top and outer side of the arch, the opposite side is turned inward to a plate connecting with the top of the collar and the inturned portion of the preceding foramen; wall smooth to finely granular, commonly affected by dissolution, finely perforate although mostly obscured by dissolution, chambers often show numerous, small pores evenly distributed over test, in some specimens enlarged by dissolution; no obvious differences between micro- and megalospheric specimens.

Dimensions. Specimens at the two sites (529 and 1264) on Walvis Ridge: length, 300-120µm (mean 188µm, St. Dev. 39, n = 249); maximum width, 180-80µm (mean 114µm, St. Dev. 19,

---

PLATE 5

Scanning electron micrographs of *Streptochilus rockallkiddensis* sp. nov.; paratypes.

1 a, Side view of paratype (reg. no. BM(NH) PF 68004), gold coated, note granular wall texture, scale bar = 50µm; b, detail of wall, scale bar = 10µm (DSDP 94-608-37X-6, 38-40cm, 346.78 mbsf).

2 a, Side view of paratype (reg. no. BM(NH) PF 68005), gold coated, note granular wall texture, scale bar = 50µm; b, detail of wall, scale bar = 10µm (DSDP 94-608-37X-6, 38-40cm, 346.78 mbsf).

3 a, Side view of paratype (reg. no. BM(NH) PF 68204), polished microspheric specimen, uncoated, scale bar = 50µm; b, detail of initial part, scale bar = 10µm (DSDP 94-608-37X-4, 38-40cm, 343.78 mbsf).

4 a, Side view of paratype (reg. no. BM(NH) PF 68206), polished microspheric specimen, uncoated, scale bar = 50µm; b, detail of initial part, scale bar = 10µm (DSDP 94-608-37X-4, 38-40cm, 343.78 mbsf).

5 Side view of paratype (reg. no. BM(NH) PF 68200), polished megalospheric specimen, uncoated, scale bar = 50µm (DSDP 94-608-37X-4, 38-40cm, 343.78 mbsf).

6 Side view of paratype (reg. no. BM(NH) PF 68203), polished microspheric specimen, uncoated, scale bar = 50µm (DSDP 94-608-37X-4, 38-40cm, 343.78 mbsf).

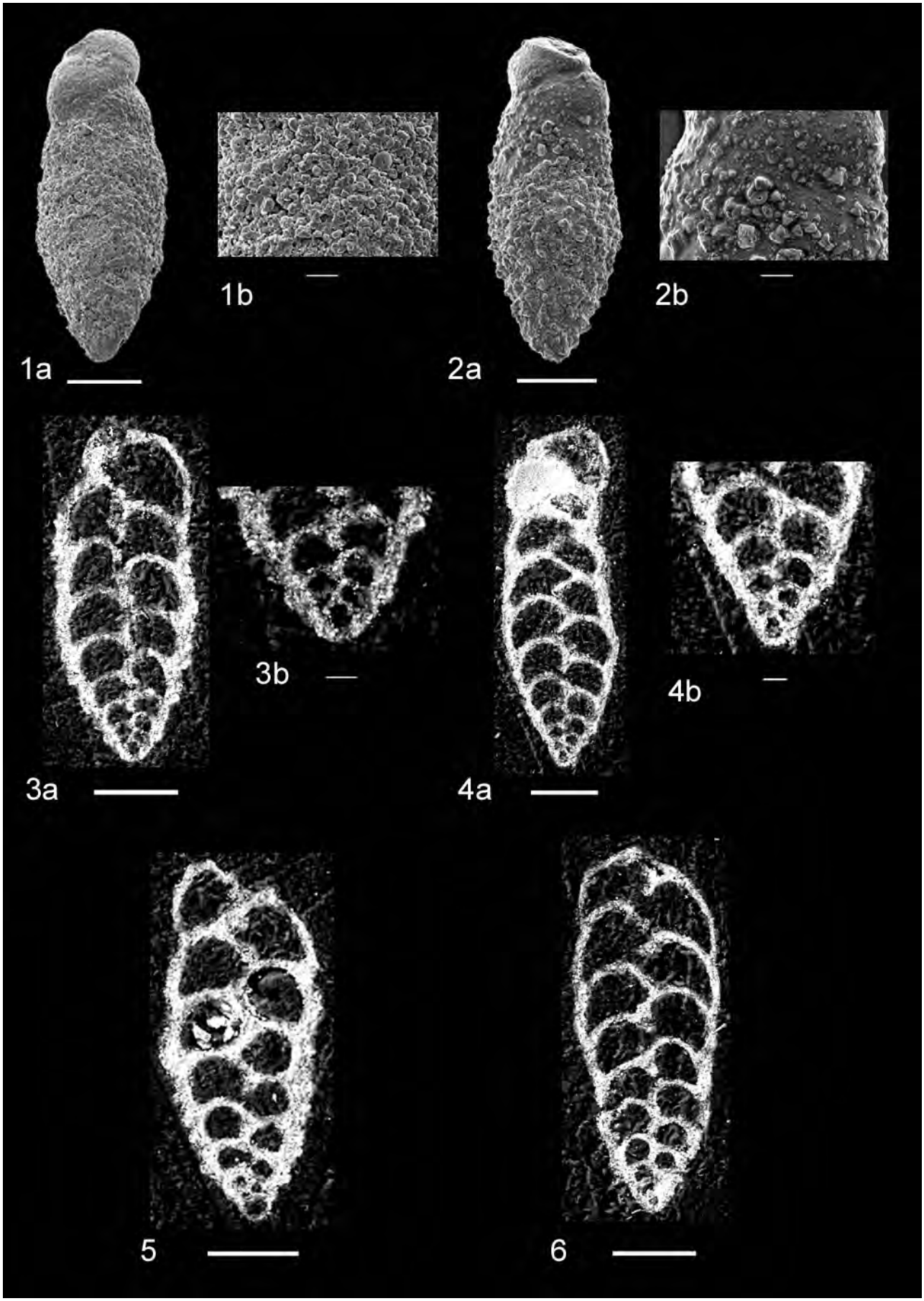
1a
1b
2a
2b
3a
3b
4a
4b
5
6

n = 249); thickness, 75-50µm (mean 62 µm, St. Dev. 6, n = 40). Specimens at Site 667: length, 230-120µm (mean 157µm, St. Dev. 21, n = 105); maximum width, 120-80 µm (mean 91 µm, St. Dev. 10, n = 105); thickness, 65-45 µm (mean 55 µm, St. Dev. 6, n = 20).

Etymology. Named after the Latin for a large marine animal such as a whale, *cetus*, after the area where it has been found (Walvis Ridge [Walvis = Dutch for whale], SE Atlantic Ocean, ODP Sites 1264 and 1265 and DSDP Site 529).

Type locality and distribution. Lower Miocene, SE Atlantic Ocean, ODP Site 1264 (Table 1); equatorial Atlantic Ocean, ODP Site 667.

Type specimens. The figured holotype, figured paratypes and unfigured paratypes are deposited in the Department of Palaeontology, The Natural History Museum, Cromwell Road, London, UK. The holotype (reg. no. BM(NH) PF 68062) is from ODP 208-1264B-21-1, 78-80cm, 210.60 mcd [Ocean Drilling Program Leg-Hole-Core-Section-Interval, meters coring depth] (Plate 6, Fig. 1a,b). All other examined and illustrated specimens are designated paratypes (reg. no. BM(NH) PF 68063-68151, BM(NH) PF 68222-68251) and are from ODP 208-1264B-21-1, 78-80cm, 210.60 mcd; DSDP 74-529-8-4, 72-74cm, 70.72 mbsf [Deep Sea Drilling Project Leg-Hole-Core-Section-Interval, meters below sea floor]; DSDP 74-529-8-3, 74-76cm, 69.24 mbsf; and ODP 108-667A-22H-7, 6-8cm, 200.36 mbsf (Plate 6, Figs. 2-11; Plates 7-11).

Remarks. Dissolution of tests commonly obscures detail; fine pores observable in later chambers unaffected by dissolution. Specimen size is variable with some specimens being relatively large, e.g., in sample DSDP 74-529-8-3, 74-76cm (69.24 mbsf) the size of the specimens examined was: length, 300-130µm (mean 211µm, St. Dev. 38, n = 62); maximum width, 180-80µm (mean 131µm, St. Dev. 19, n = 62). In contrast, specimens in sample DSDP 74-529-8-4, 72-74cm (70.72 mbsf) were consistently smaller: length, 260-130µm (mean 168µm, St. Dev. 29, n = 69); maximum width, 140-80µm (mean 107µm, St. Dev. 17, n = 69). Specimens from Site 667 (equatorial Atlantic Ocean) are overall smaller (text-fig. 3d) than those from the Walvis Ridge sites, and tend to have pores over all chambers of the test. We have included specimens from this location in *S. cetacensis* because they resemble the specimens from Walvis Ridge strongly, and the differences in size and pore distribution and size might be due to differential dissolution. Detailed morphological information from more locations is necessary in order to evaluate whether the equatorial group could be a different morphological species, or whether the variability is within the intra-group morphological variability of the species within the larger geographic region.

Streptochilus cetacensis sp. nov. resembles *Streptochilus* sp. aff. *S. martini* (Pijpers) as illustrated in Poore and Gosnell (1985; Plate 1, figs. 8-16). *Streptochilus cetacensis* resembles *Streptochilus globulosum* (Cushman), but the latter is much more globose. Originally, the size of the holotype (Holotype USNM26172 in the Smithsonian Museum of Natural History, USA) was given as: length, 700µm; width, 400µm; thickness, 150µm (Cushman 1933), which would have been much larger than our species, but these measurements were incorrect; the size of the holotype is length, 300µm and width, 130µm (Cushman et al. 1954), as checked by E. Thomas. For a description of the differences between the three new Miocene *Streptochilus* spp., see differential analysis (below).

Streptochilus mascarenensis Smart and Thomas **n. sp.**
Plates 12-13

PLATE 6

Scanning electron micrographs of *Streptochilus cetacensis* sp. nov.; 1 holotype, 2-11 paratypes.
All specimens are from ODP 208-1264B-21-1, 78-80cm, 210.60 mcd.

1 a, Side view of holotype, reg. no. BM(NH) PF 68062, uncoated, scale bar = 50µm; b, detail of wall, scale bar = 10µm (ODP 208-1264B-21-1, 78-80cm, 210.60 mcd);

2-11 Side views of paratypes, uncoated, all scale bars = 50µm

2 reg. no. BM(NH) PF 68063;

3 reg. no. BM(NH) PF 68064;

4 reg. no. BM(NH) PF 68065, slightly curved specimen;

5 reg. no. BM(NH) PF 68066;

6 reg. no. BM(NH) PF 68067;

7 reg. no. BM(NH) PF 68068;

8 reg. no. BM(NH) PF 68069;

9 reg. no. BM(NH) PF 68070;

10 reg. no. BM(NH) PF 68071, slightly curved specimen;

11 reg. no. BM(NH) PF 68072, slightly curved specimen.

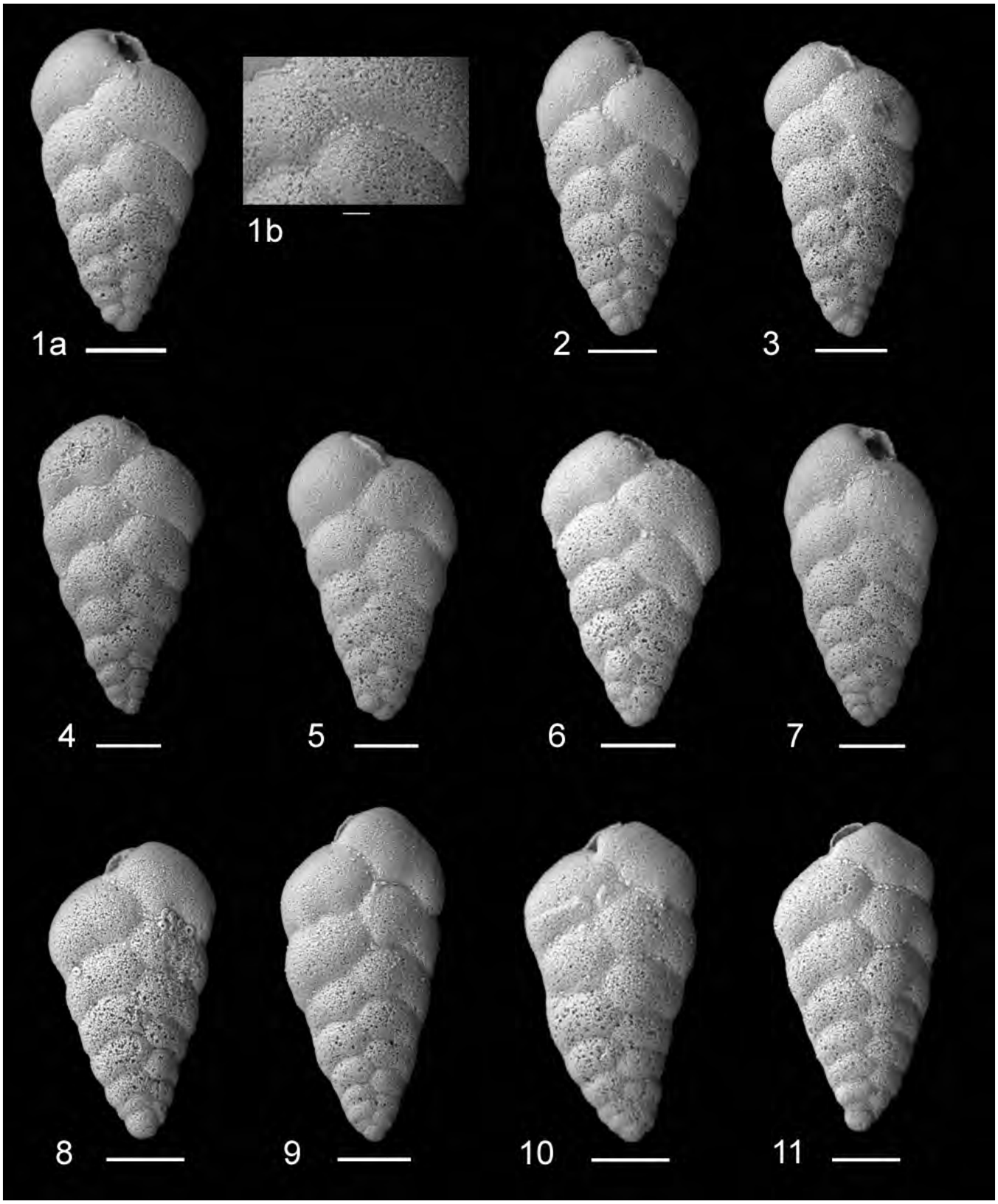
1a
1b
2
3
4
5
6
7
8
9
10
11

Bolivina sp. – SMART 2002, fig. 3.1, no. 2
Streptochilus sp. – SMART and THOMAS 2006, fig. 2, C, D

Diagnosis. Test small, elongate, laterally compressed, commonly flared with distinct chambers and curved and depressed sutures.

Description. Test small, elongate, increasing regularly in size, flared and occasionally almost parallel-sided, laterally compressed, periphery broadly rounded and lobulate, rarely twisted, biserial; 5-7 pairs of chambers, wider than high, increasing gradually in size as added; sutures distinct, curved and slightly depressed; aperture high arch-shaped, offset slightly to one side of test, extending from the base of the last chamber onto apertural face, bordered by a thickened rim/collar along the top and outer side of the arch, the opposite side is turned inward to a plate connecting with the top of the collar and the inturned portion of the preceding foramen; wall smooth to finely granular, very finely perforate; no obvious differences between micro- and megalospheric specimens.

Dimensions. Length, 260-110µm (mean 169µm, St. Dev. 30, n = 106); maximum width, 120-80µm (mean 98µm, St. Dev. 8, n = 106); thickness, 60-45µm (mean 50µm, St. Dev. 3, n = 20).

Etymology. Named after the area where it has been found, i.e. the Mascarene Plateau, NW Indian Ocean (DSDP Site 237).

Type locality and distribution. Lower Miocene, NW Indian Ocean, DSDP Site 237 (Table 1). Also reported from ODP Site 709.

Type specimens. The figured holotype, figured paratypes and unfigured paratypes are deposited in the Department of Palaeontology, The Natural History Museum, Cromwell Road, London, UK. The holotype (reg. no. BM(NH) PF 68152) is from DSDP 24-237-18-6, 69-71cm, 166.69 mbsf [Deep Sea Drilling Project Leg-Hole-Core-Section-Interval, meters below sea floor] (Plate 12, Figs. 1a,b,c). All other examined and illustrated specimens are designated paratypes (reg. no. BM(NH) PF 68153-68191, BM(NH) PF 68252-68279) and are from DSDP 24-237-18-3, 72-74cm, 162.22 mbsf; and DSDP 24-237-18-6, 69-71cm, 166.69 mbsf (Plate 12, Figs. 2-8; Plate 13).

Remarks. *Streptochilus mascarenensis* sp. nov. was called *Bolivina* sp. and specimens from DSDP Site 237 are illustrated in Smart (2002, Fig. 3.1, 2) and Smart and Thomas (2006, fig. 2, C, D). For a description of the differences between the three new Miocene *Streptochilus* spp., see differential analysis (below).

DIFFERENTIAL ANALYSIS

Early Miocene *Streptochilus* spp. occurred coevally at various sites in the Atlantic and Indian Oceans, but the species differ morphologically from site to site. *Streptochilus rockall-kiddensis* sp. nov. is the most variable species and differs from all other species in its typically parallel-sided/rectilinear shape which often narrows towards the apertural end, the tendency to become staggered uniserial, and thickening of the wall including the rim of the aperture which may obscure the aperture. The variability of surface ornamentation is a feature of this species which varies from smooth to granular, the granular nature constituting typically half or more of the test occurring from proloculus to apertural end.

Streptochilus mascarenensis sp. nov. closely resembles *Streptochilus cetacensis*, but *Streptochilus mascarenensis* sp. nov. is consistently more laterally compressed (thickness 50µm compared with 62µm), its periphery is more lobulate, and its pores are smaller. *Streptochilus cetacensis* sp. nov. is typically 'triangular' in shape and flared, and is clearly different from *S.*

PLATE 7

Scanning electron micrographs of *Streptochilus cetacensis* sp. nov.; paratypes.

1 Side view of paratype (reg. no. BM(NH) PF 68073), uncoated, slightly twisted specimen, scale bar = 50µm (ODP 208-1264B-21-1, 78-80cm, 210.60 mcd).

2 Side view of paratype (reg. no. BM(NH) PF 68074), uncoated, twisted specimen, scale bar = 50µm (ODP 208-1264B-21-1, 78-80cm, 210.60 mcd).

3-11 Side views of paratypes, all uncoated, all scale bars = 50µm;

3 reg. no. BM(NH) PF 68075, from DSDP 74-529-8-4, 72-74cm, 70.72 mbsf;

4 reg. no. BM(NH) PF 68076, from DSDP 74-529-8-4, 72-74cm, 70.72 mbsf;

5 slightly twisted specimen, reg. no. BM(NH) PF 68077, from DSDP 74-529-8-4, 72-74cm, 70.72 mbsf;

6 reg. no. BM(NH) PF 68078, from DSDP 74-529-8-4, 72-74cm, 70.72 mbsf;

7 reg. no. BM(NH) PF 68079, from DSDP 74-529-8-4, 72-74cm, 70.72 mbsf;

8 reg. no. BM(NH) PF 68080, from DSDP 74-529-8-3, 74-76cm, 69.24 mbsf;

9 reg. no. BM(NH) PF 68081, from DSDP 74-529-8-3, 74-76cm, 69.24 mbsf;

10 curved specimen, reg. no. BM(NH) PF 68082, from DSDP 74-529-8-4, 72-74cm, 70.72 mbsf;

11 a, SEM micrograph and b, light photograph (using *PalaeoVision* System) of same specimen; reg. no. BM(NH) PF 68083, from DSDP 74-529-8-4, 72-74cm, 70.72 mbsf.

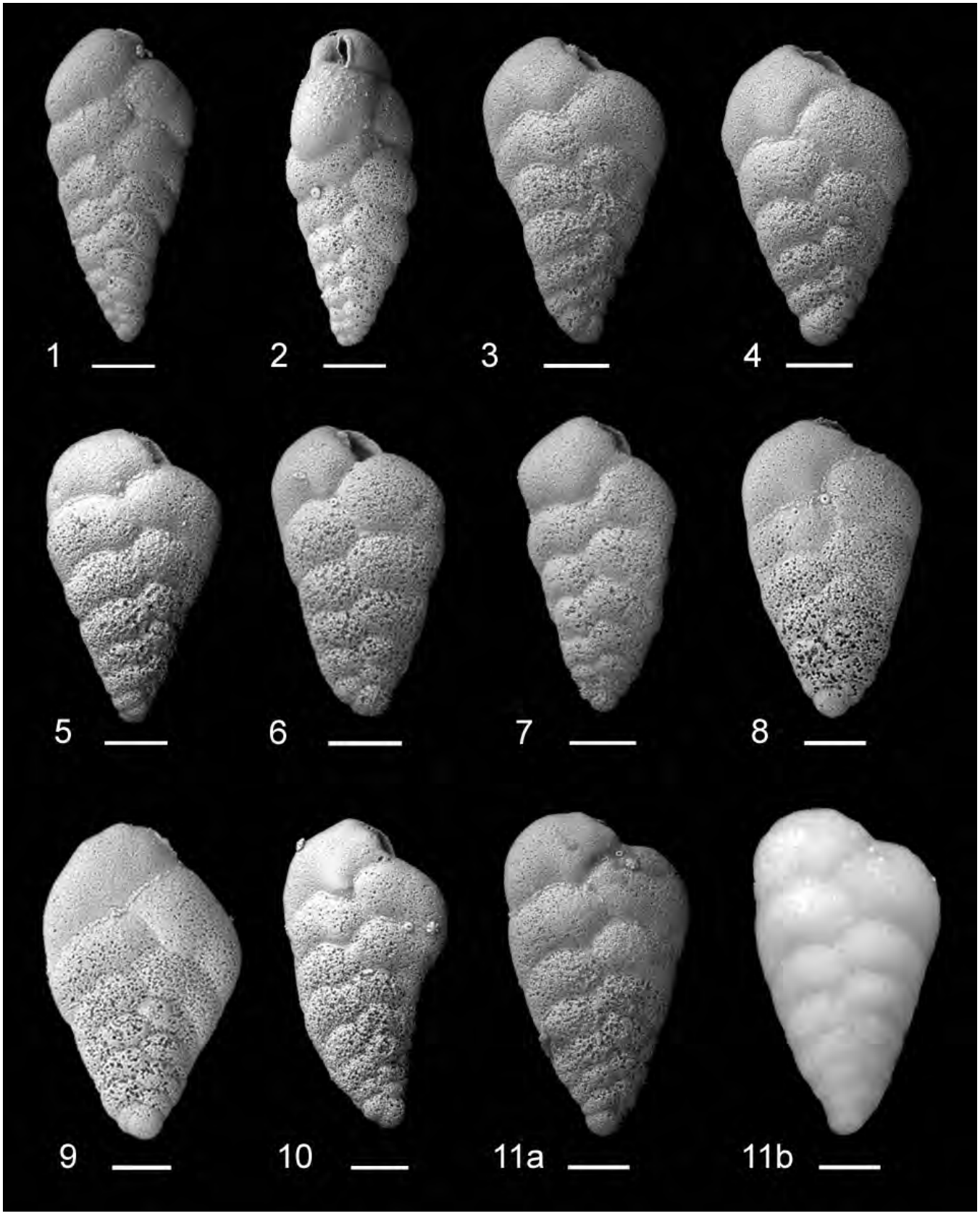
1
2
3
4
5
6
7
8
9
10
11a
11b

rockallkiddensis sp. nov. (text-fig. 3). Specimens of *S. cetacensis* at Site 667 are overall smaller than those from the southeastern Atlantic (Sites 529 and 1264) (text-fig. 3), and have distinctive pores over all chambers of the test. The differences in pore distribution and size of *S. cetacensis* between the equatorial Atlantic specimens (Site 667) and southeastern Atlantic specimens might be due to differential dissolution. *Streptochilus cetacensis* sp. nov. closely resembles *S. mascarenensis* sp. nov., but *S. cetacensis* sp. nov. is consistently less laterally compressed (thickness 62µm compared with 50µm), becomes thicker towards the apertural end, its periphery is less lobulate, and is more 'triangular' in shape. *S. mascarenensis* sp. nov. is clearly different from *S. rockallkiddensis* sp. nov. in its general shape, its more pronounced chambers, and absence of a coarsely roughened test. For all three new species, differentiating between microspheric and megalospheric specimens in non-sectioned specimens is often unclear and speculative, although in sectioned/polished specimens it is possible to distinguish between specimens that have relatively small (microspheric) or large (megalospheric) proloculi.

CONCLUSIONS

Several morphological species of *Streptochilus* (Foraminifera) occur in the lower Miocene in the eastern Atlantic and western Indian Oceans (18.9-17.2 Ma in the Lourens et al. 2004 time scale; 19.3-17.6 Ma in the Berggren et al. 1995 time scale). They had previously been assigned to the benthic genus *Bolivina*, but evidence on their apertural morphology, together with accumulation rate data and isotopic composition show that they lived as plankton, and should be assigned to the planktic genus *Streptochilus* (Smart and Thomas 2006). Three new species are described, illustrated and named: *S. rockallkiddensis* sp. nov. (from the northeastern Atlantic), *S. cetacensis* sp. nov. (from the equatorial and southeastern Atlantic), and *S. mascarenensis* sp. nov. (from the western equatorial Indian Oceans). The description of the genus *Streptochilus* is emended to include the observation that in some specimens of *S. rockallkiddensis* sp. nov. the test occasionally becomes staggered uniserial, typically parallel-sided/rectilinear in shape and the aperture is often obscured by a thickening of the wall including the rim of the aperture. The three species occurred in different regions of the oceans during the same short period of time (18.9-17.2 Ma) which suggests that they may have evolved (either from biserial planktic or from benthic ancestors) polyphyletically. If they evolved from benthic ancestors, e.g., from specimens swept out to sea during storms, their evolution may have been made possible by relatively eutrophic conditions in the surface waters (Smart and Thomas 2006), during which there were high algal growth rates but low transport efficiency of organic matter to the sea floor, possibly in a deep thermocline. There are no modern analog environments over such large areas of the eastern Atlantic and western Indian Oceans.

ACKNOWLEDGMENTS

CWS gratefully acknowledges financial support from a NERC/UK IODP Rapid Response Award. This research used samples provided by the Ocean Drilling Program (ODP). The ODP was sponsored by the US National Science Foundation (NSF) and participating countries (including the UK) under the management of the Joint Oceanographic Institutions (JOI), Inc. CWS would like to thank Roy Moate, Peter Bond and Glenn Harper (EM Unit, University of Plymouth, UK) for their assistance in scanning electron microscopy. ET recognizes funding by the USSSP for post-cruise research related to Leg 208. Thanks also go to Andy Henderson (Natural History Museum,

PLATE 8

Scanning electron micrographs of *Streptochilus cetacensis* sp. nov.; paratypes.

1 a, Edge view of paratype (reg. no. BM(NH) PF 68084), uncoated, scale bar = 50µm; b, detail of aperture showing infolded rimmed margin, scale bar = 10µm (DSDP 74-529-8-4, 72-74cm, 70.72 mbsf).

2 a, Oblique view of paratype (reg. no. BM(NH) PF 68085), uncoated, scale bar = 50µm; b, detail of aperture showing rimmed margin, scale bar = 10µm (DSDP 74-529-8-4, 72-74cm, 70.72 mbsf).

3 a, Oblique view of paratype (reg. no. BM(NH) PF 68086), gold coated, scale bar = 50µm; b, detail of aperture showing infolded rimmed margin, scale bar = 10µm; c, detail of wall showing fine granular texture and small pores, scale bar = 10µm (ODP 208-1264B-21-1, 78-80cm, 210.60 mcd).

4 a, Edge view of paratype (reg. no. BM(NH) PF 68087), dissected specimen, gold coated, scale bar = 50µm; b, detail of aperture, note internal plate connecting with apertural rim, scale bar = 10µm (ODP 208-1264B-21-1, 78-80cm, 210.60 mcd).

5 a, Oblique view of paratype (reg. no. BM(NH) PF 68088), dissected specimen, gold coated, scale bar = 50µm; b, detail of aperture, note internal plate connecting with apertural rim, scale bar = 10µm (ODP 208-1264B-21-1, 78-80cm, 210.60 mcd).

6 a, Side view of paratype (reg. no. BM(NH) PF 68089), uncoated, scale bar = 50µm; b, detail of wall showing fine granular texture and small pores, scale bar = 10µm (ODP 208-1264B-21-1, 78-80cm, 210.60 mcd).

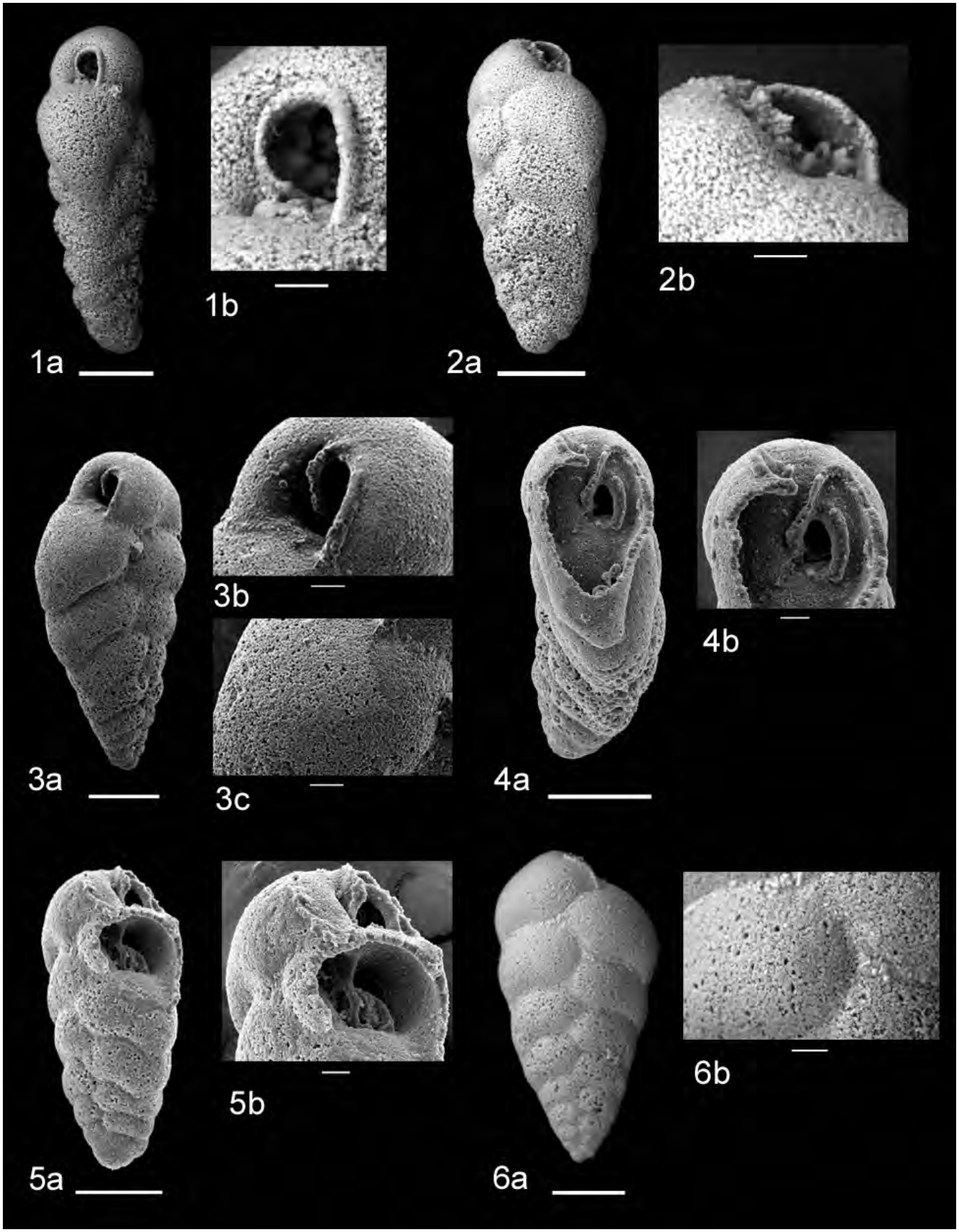
1a
1b
2a
2b
3a
3b
3c
4a
4b
5a
5b
6a
6b

London) for carrying out the *PalaeoVision* images. Stefan Revets is thanked for his constructive comments on an earlier version of the manuscript. We also thank Brian Huber and Dick Olsson for their helpful comments.

REFERENCES

ABELS, H. A., HILGEN, F. J., KRIJGSMAN, W., KRUK, R. W., RAFFI, I., TURCO, E., and ZACHARIASSE, W. J., 2005. Long-period orbital control on middle Miocene global cooling: integrated stratigraphy and stronomical tuning of the Blue Clay Formation on Malta. *Paleoceanography* 20: PA4012, doi: 10.1029/2004PA001129.

ANDERSON, L. D., and DELANEY, M. L., 2005. Use of multiproxy records on the Agulhas Ridge, Southern Ocean (Ocean Drilling Project Leg 177, Site 1090) to investigate sub-Antarctic hydrography from the Oligocene to the early Miocene. *Paleoceanography*, 20, PA3011, doi: 10.1029/2004PA001082

BALDAUF, J. G. and BARRON, J. A., 1990, Evolution of biosiliceous sedimentation patterns – Eocene through Quaternary: paleoceanographic response to polar cooling. In: Bleil, U. and Thiede, J., Eds., *Geological History of the Polar Ocean: Arctic versus Antarctic*, 575-607. Kluwer Academic Publishers, Dordrecht, Netherlands.

BARKER, P.F. and THOMAS, E., 2004. Origin, signature and palaeoclimatic influence of the Antarctic Circumpolar Current. *Earth Science Reviews*, 66: 143-162.

BERGGREN, W.A., KENT, D.V., SWISHER, C. C., III and AUBRY, M.-P., 1995. A revised Cenozoic geochronology and chronostratigraphy. In: Berggren, W.A., Kent, DV., Aubry, M.-P. and Hardenbol, J., Eds., *Geochronology, time scales and global stratigraphic correlation*, 129-212. SEPM Special Publication, 54.

BERNHARD, J. M., 1986. Characteristic assemblages and morphologies of benthic foraminifera from anoxic, organic-rich deposits. *Journal of Foraminiferal Research*, 16: 207-215.

BERNHARD, J. M. and SEN GUPTA, B.K., 1999. Foraminifera of oxygen-depleted environments. In: Sen Gupta, B.K., Ed., *Modern Foraminifera*, 141-160. Dordrecht: Kluwer Academic Publishers.

BOLTOVSKOY, E., GIUSSANI, G.; WATANABE, S. and WRIGHT, R. 1980. *Atlas of benthic shelf foraminifera of the Southwest Atlantic*. The Hague: Dr. W. Junk Publs., 147p.

BRÖNNIMANN, P. and RESIG, J., 1971. A Neogene globigerinacean biochronologic time-scale of the southwestern Pacific. In: Winterer, E., Riedel, W., et al., *Initial Reports of the Deep Sea Drilling Project*, volume 7: 1235-1469. Washington, DC: US Government Printing Office, .

BRUNNER, C. and BISCAYE, P., 1997. Storm-driven transport of foraminifers from the shelf to the upper slope, southern middle Atlantic Bight. *Continental Shelf Research*, 17: 491-508.

CALKINS, G. N., 1909. *Protozoology.* New York: Lea and Febiger.

CUSHMAN, J. A., 1927. An outline of reclassification of the Foraminifera. *Cushman Laboratory for Foraminiferal Research, Contributions*, 3 (1): 1-105.

———, 1933. Some new Recent foraminifera from the tropical Pacific. *Contributions from the Cushman Laboratory for Foraminiferal Research*, 9: 77-95.

CUSHMAN, J.A., TODD, R. and POST, R.J., 1954. Recent foraminifera of the Marshall Islands, Bikini and nearby Atolls, Part 2, Oceanography (Biologic). *US Geological Survey Professional Papers* , 260-H: 319-384.

DE KLASZ, I., KROON, D. and VAN HINTE, J. E., 1989. Notes on the foraminiferal genera *Laterostomella* de Klasz and Rerat and *Streptochilus* Brönnimann and Resig. *Journal of Micropaleontology*, 8: 215-226.

ELDRETT, L., HARDING, I. C., WILSON, P. A. and ROBERTS, A. P., 2007. Continental ice in Greenland during the Eocene and Oligocene. *Nature* 446: 176-179.

FLOWER, B. P., ZACHOS, J. C. and MARTIN, E., 1997. Latest Oligocene through early Miocene isotopic stratigraphy and deep-water paleoceanography of the western equatorial Atlantic Sites 926 and 929. In: Shackleton, N.J., Curry, W.B., Richter, C. and Bralower, T.J., Eds., *Proceedings of the Ocean Drilling Program, Scientific Results*, *volume 154,* 451-461. College Station, Texas: Ocean Drilling Program.

FLOWER, B. P., 1999. Data report: Planktonic foraminifers from the subpolar North Atlantic and Nordic Sea: Sites 980-987 and 907. In: Raymo, M. E., Jansen, E., Blum, P. and Herbert, T. D., Eds., *Proceedings of the Ocean Drilling Program, Scientific Results, volume 162,* 19-34. College Station, Texas: Ocean Drilling Program.

FÖLLMI, K. B., BADERTSCHER, C., DE KAENEL, E., STILLE, P., JOHN, C. M., ADATTE, T. and STEINMANN, P., 2005. Phosphogenesis and organic-carbon preservation in the Miocene Monterey Formation at Naples Beach, California – The Monterey hypothesis revisited. *Geological Society America Bulletin*, 117: 589-619.

HALFAR, J. and MUTTI, M., 2005. Global dominance of coralline red-algal facies: a response to Miocene oceanographic events. *Geology*, 33: 481-484.

HALLOCK, P., PREMOLI SILVA, I. and BOERSMA, A. 1991. Similarities between planktonic and larger foraminiferal evolutionary trends through Paleogene paleoceanographic changes. *Palaeogeography, Palaeoclimatology, Palaeoecology*, 83: 49-64.

HANNAH, M.J., 2006. The palynology of ODP Site 1165, Prydz Bay, East Antarctica: a record of Miocene glacial advance and retreat. *Palaeogeography, Palaeclimatology, Palaeoecology,* 231: 120-133.

HARZHAUSER, M., PILLER, W.E. and STEININGER, F.F., 2002. Circum-Mediterranean Oligo-Miocene biogeographic evolution: the gastropods' point of view. *Palaeogeography, Palaeoclimatology, Palaeoecology*, 183: 103-133.

HEMLEBEN, Ch., SPINDLER, M. and ANDERSON, O. R., 1989. *Modern Planktonic Foraminifera*. Springer Verlag, 363 pp.

HOLBOURN, A. E. and HENDERSON, A. S., 2002. Re-illustration and revised taxonomy for selected deep-sea benthic foraminifers: *Palaeontologia Electronica*, v. 4, art. 3, 36 p. http://palaeo-electronica.org/2001_2/foram/issue2_01.htm

HOLBOURN, A., KUHNT, W., SCHULZ, M. and ERLENKEUSER, H., 2005. Impacts of orbital forcing and atmospheric carbon dioxide on Miocene ice-sheet expansion. *Nature,* 438: 483-487.

HUBER, B. T. and BOERSMA, A., 1994. Cretaceous origination of *Zeauvigerina* and its relationship to Paleocene biserial planktonic foraminifera. *Journal of Foraminiferal Research,* 24:268-287.

HUBER, B. T., OLSSON, R. K. and PEARSON, P. N., 2006. Taxonomy, biostratigraphy and phylogeny of Eocene microperforate planktonic foraminifera (*Jenkinsina, Cassigerinelloita, Chiloguembelina, Streptochilus, Zeauvigerina, Tenuitella* and *Cassigerinella*) and problematic (*Dispidripella*). *Cushman Foundation of Foraminiferal Research, Special Publication*, 41: 461-508.

HUENI, C., MONROE, J.A., GEVIRTZ, J. and CASEY, R., 1978. Distribution of living benthonic foraminifera as indicators of oceano-

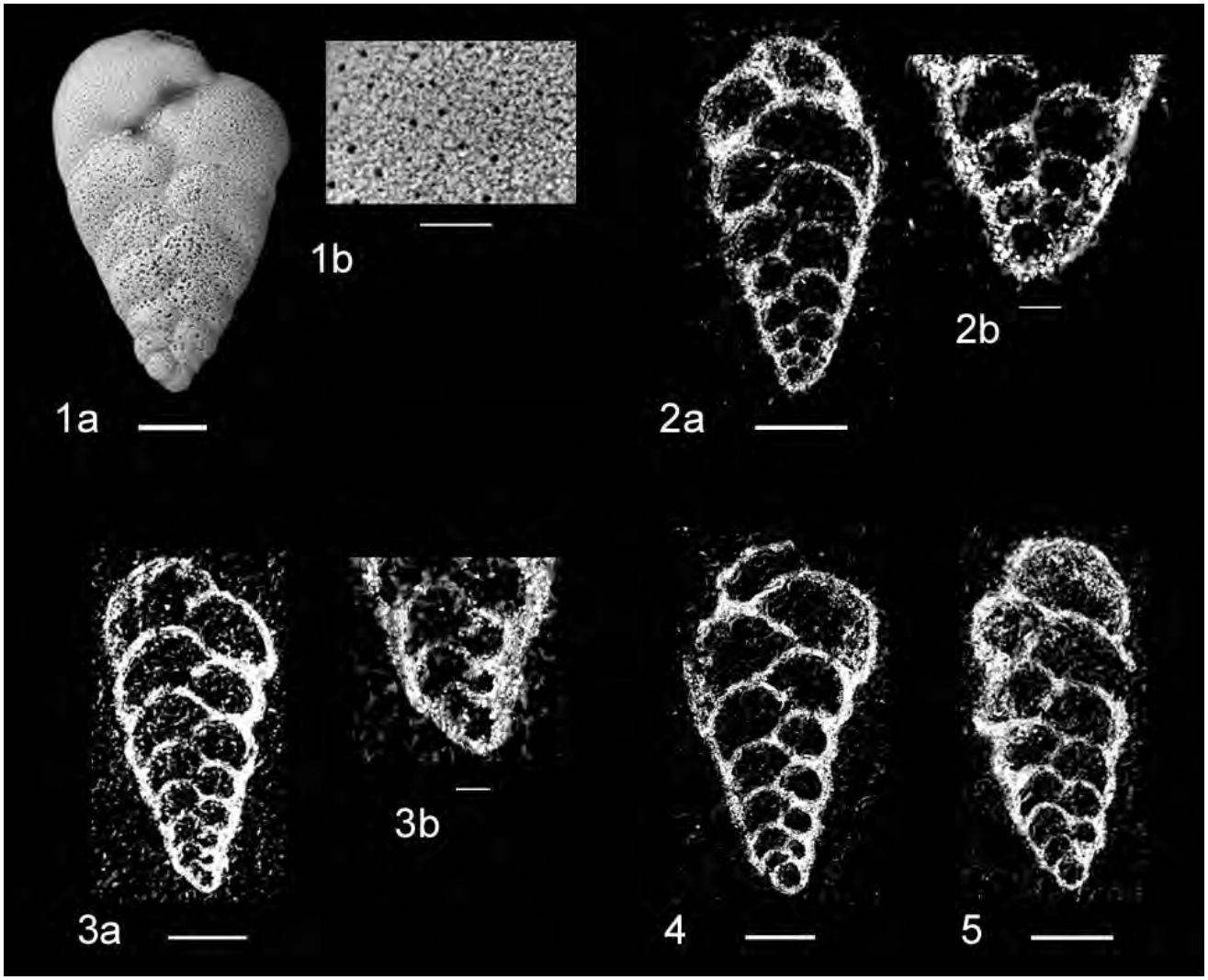

PLATE 9
Scanning electron micrographs of *Streptochilus cetacensis* sp. nov.; paratypes.

1 a, Side view of paratype (reg. no. BM(NH) PF 68090), uncoated, scale bar = 50µm; b, detail of wall showing fine granular texture and small pores, scale bar = 10µm (DSDP 74-529-8-3, 74-76cm, 69.24 mbsf).

2 a, Side view of paratype (reg. no. BM(NH) PF 68224), polished megalospheric specimen, uncoated, scale bar = 50µm; 3b detail of initial part, scale bar = 10µm (ODP 208-1264B-21-1, 78-80cm, 210.60 mcd).

3 a, Side view of paratype (reg. no. BM(NH) PF 68235), polished microspheric specimen, uncoated, scale bar = 50µm; b, detail of initial part, scale bar = 10µm (ODP 208-1264B-21-1, 78-80cm, 210.60 mcd).

4-5 Side views of paratypes (4 reg. no. BM(NH) PF 68227, 5 reg. no. BM(NH) PF 68232), polished megalospheric specimens, uncoated, scale bars = 50µm (ODP 208-1264B-21-1, 78-80cm, 210.60 mcd).

graphic processes on the South Texas outer continental shelf. *Transactions of the Gulf Coast Association of Geological Societies*, 28: 193-200.

JORISSEN, F. J., FONTANIER, C. and THOMAS, E., in press, 2007. Paleoceanographical proxies based on deep-sea benthic foraminiferal assemblage characteristics. In: Hillaire-Marcel, C. and de Vernal, A., Eds., *Proxies in Late Cenozoic Paleoceanography (Pt. 2): Biological tracers and biomarkers.* Amsterdam: Elsevier.

KENNETT, J. P. and SRINIVASAN, M. S., 1983. *Neogene Planktonic Foraminifera: a phylogenetic atlas*. 265 pp.

KROON, D. and GANSSEN, G., 1989, Northern Indian Ocean upwelling cells and the stable isotope composition of living planktonic foraminifera. *Deep-Sea Research,* 36: 1219-1236.

KROON, D. and NEDERBRAGT, A.J., 1990. Ecology and paleoecology of triserial planktic foraminifera. *Marine Micropaleontology*, 16: 25-38.

KROON, D., WILLIAMS, T., PIRMEZ, C., SPEZZAFERRI, S., SATO, T. and WRIGHT, J. D. 2000. Coupled early Pliocene-middle Miocene bio-cyclostratigraphy of Site 1006 reveals orbitally induced cyclicity patterns of Great Bahama Bank carbonate production. In: Swart, P. K., Eberli, G. P., Malone, M. J. and Sarj, J. F., Eds., *Proceedings of the Ocean Drilling Program, Scientific Results*, volume 166:155-166. College Station, Texas: Ocean Drilling Program.

LANKESTER, E. R., 1885. *Protozoa.* In: *Encyclopaedia Britannica,* vol. 19, 9th ed.: 830-866.

LEAR, C.H., ROSENTHAL, Y. and WRIGHT, J.D., 2003. The closing of a seaway: ocean water masses and global climate change. *Earth and Planetary Science Letters*, 210: 425-436.

LEAR, C., ROSENTHAL, Y., COXALL, H.K. and WILSON, P.A., 2004. Late Eocene to early Miocene ice sheet dynamics and the global carbon cycle: *Paleoceanography*, 19, PA4015, doi: 10.1029/2004PA001039.

LEE, J. J.. 1990. Phylum Granuloreticulosa (Foraminifera). In: Margulis, L., Corliss, J.O., Melkonian, M., Chapman, D.J., Eds., *Handbook of Protoctista*, 524-548. Boston: Jones & Bartlett.

LIDZ, B., 1966. Planktonic foraminifera in the water column of the mainland shelf off Newport Beach, California. *Limnology Oceanography*, 11: 257-263.

LOEBLICH, A. R. and TAPPAN, H. 1987. *Foraminiferal genera and their classification.* New York: Van Nostrand Reinhold Company, 2nd vol., 1182 pp.

———, 1992. Present status of foraminiferal classification. In: Takayanagi, Y. and Saito, T., Eds., *Studies in Benthic Foraminifera,* 93-102. Tokyo: Tokai University Press, Japan.

LOURENS, L.J., HILGEN, F.J., LASKAR, J., SHACKLETON, N.J. and WILSON, D., 2004, The Neogene Period, *in* Gradstein, F.M., Ogg, J.G. and Smith, A.G., Eds., *A Geologic Time Scale 2004*, p. 409-440. Cambridge: Cambridge University Press.

MILLER, K. G., WRIGHT, J. D. and BROWNING, J. V., 2005. Visions of ice sheets in a greenhouse world. *Marine Geology*, 217: 215-231.

MURRAY, J. W., 1971. *An Atlas of British Recent Foraminiferids.* London: Heinemann Educational Books.

NAIDU, P. D. and NIITSUMA, N., 2004. Atypical $\delta^{13}C$ signature in *Globigerina bulloides* at the ODP Site 723A (Arabian Sea): implications of environmental changes caused by upwelling. *Marine Micropaleontology*, 53: 1-10.

PLATE 10

Scanning electron micrographs of *Streptochilus cetacensis* sp. nov.; paratypes.
All specimens are from ODP 108-667A-22H-7, 6-8cm, 200.36 mbsf.

1 a, Side view of paratype (reg. no. BM(NH) PF 68122), uncoated, scale bar = 50µm; b, detail of wall showing pores, scale bar = 10µm.

2-7 Side views of paratypes, all uncoated..

2 reg. no. BM(NH) PF 68123, scale bar = 50µm;

3 reg. no. BM(NH) PF 68124, scale bar = 50µm;

4 reg. no. BM(NH) PF 68125, scale bar = 50µm;

5 reg. no. BM(NH) PF 68126, scale bar = 50µm;

6 reg. no. BM(NH) PF 68127, scale bar = 50µm;

7 reg. no. BM(NH) PF 68128, scale bar = 50µm;

8 a, Edge view of paratype (reg. no. BM(NH) PF 68129), uncoated, scale bar = 50µm; b, detail of aperture showing infolded rimmed margin, scale bar = 10µm;

9 a, Oblique view of paratype (reg. no. BM(NH) PF 68130), gold coated, scale bar = 50µm; b, detail of aperture showing rimmed infolded margin, scale bar = 10µm.

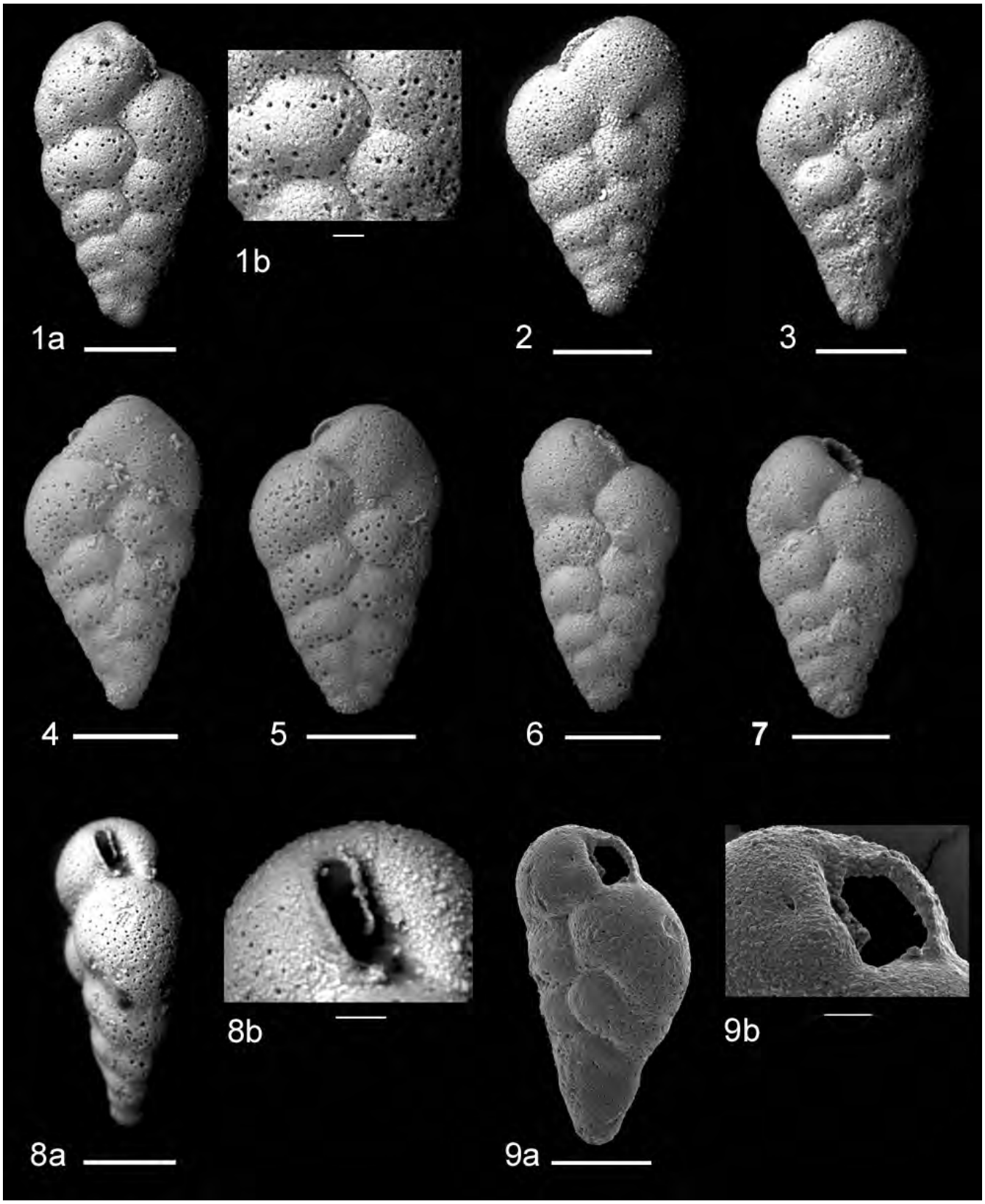
1a
1b
2
3
4
5
6
7
8a
8b
9a
9b

NIKOLAEV, S. D., OSKINA, N. S., BYLUM, N. S. and BUBENSHCHIKOVA, N. V., 1998, Neogene-Quaternary variations in the 'Pole-Equator' temperature gradient of the surface oceanic waters in the North Atlantic and North Pacific. *Global and Planetary Change*, 18: 85-111.

OLAFSSON, G., 1991. Late Oligocene through Late Miocene Calcareous Nannofossil Biostratigraphy and Biochronology. *Meddelanden från Stockholms Universitets Institution för Geologi og Geokemi*, Nr. 283, 157 p.

OLSSON, R. K., HEMLEBEN, C., BERGGREN, W. A. and HUBER, B. T., 1999. *Atlas of Paleocene Planktonic Foraminifera.* Smithsonian Contributions to Paleobiology, 85.

PAGANI, M., ARTHUR, M. A. and FREEMAN, K. H., 1999. The Miocene evolution of atmospheric carbon dioxide. *Paleoceanography*,14: 273-292.

PAGANI, M., ARTHUR, M. A. and FREEMAN, K. H., 2000. Variations in Miocene phytoplankton growth rates in the southwest Atlantic: Evidence for Changes in Ocean Circulation: *Paleoceanography*, 15: 486-496.

PEARSON, P. N. and PALMER, M. R., 2000. Atmospheric carbon dioxide concentrations over the past 60 million years. *Nature*, 406: 695-699.

PEKAR, S. F. and DECONTO, R. M., 2006. High-resolution ice-volume estimates for the early Miocene: evidence for a dynamic ice sheet on Antarctica. *Palaeogeography, Palaeclimatology, Palaeoecology,* 231: 101-109.

POAG, C. W. and LOW, D., 1985. Environmental trends among Neogene benthic foraminifers at DSDP Site 548, Irish continental margin, *in* GRACIANSKY, P. C. de, POAG, C. W. and others, Eds., *Initial Reports of the Deep Sea Drilling Project*, 80: 489-503. Washington, DC: US Government Printing Office.

POORE, H. R., SAMWORTH, R., WHITE, N. J., JONES, S.M. and MCCAVE, I. N., 2006. Neogene overflow of Northern Component water at the Greenland-Scotland Ridge. *Geochemistry, Geophysics, Geosystems*, 7: QO6010, doi: 10.1029/GC001085.

POORE, R. Z. and GOSNELL, L. B., 1985. Apertural features and surface texture of upper Paleogene biserial planktonic foraminifers: links between *Chiloguembelina* and *Streptochilus*. *Journal of Foraminiferal Research*, 15: 1-5.

PREMOLI SILVA, I. and VIOLANTI, D., 1981. Cenozoic planktonic foraminifer biostratigraphy of the Deep Sea Drilling Project Hole 462, Nauru Basin (Western Equatorial Pacific) and distribution of the pelagic components, *in* LARSON, R. L, SCHLANGER, S. O., eds, *Initial Reports of the Deep Sea Drilling Project*, *Volume 61*, p. 397-422. US Government Printing Office, Washington, DC.

RAMSAY, A. T. S., SMART, C. W. and ZACHOS, J. C., 1998. A model of early to middle Miocene deep ocean circulation for the Atlantic and Indian oceans. In: Cramp, A., Macleod, C. J., Lee, S. V. and Jones, E. J. W., Eds., *Geological evolution of ocean basins: results from the Ocean Drilling Program,* 55-70. Geological Society, London, Special Publication No. 131.

REISS, Z., 1963. Reclassification of perforate foraminifera. *State of Israel Geological Survey Bulletin*, 35: 1-111.

RESIG, J., 1989. Stratigraphic distribution of late Neogene species of the planktonic foraminifer *Streptochilus* in the Indo-Pacific. *Micropaleontology*, 35: 49-62.

RESIG, J. and KROOPNICK, P., 1983. Isotopic and distributional evidence of a planktonic habitat for the foraminiferal genus *Streptochilus* Brönnimann and Resig, 1971. *Marine Micropaleontology*, 8: 235-248.

ROYER, D. L., WING, S. L., BEERLING, D. J., JOLLEY, D. W., KOCH, P. L., HICKEY, L. J. and BERNER, R. A. 2001. Palaeo-

---

PLATE 11

Scanning electron micrographs of *Streptochilus cetacensis* sp. nov.; paratypes.
All specimens are from ODP 108-667A-22H-7, 6-8cm, 200.36 mbsf.

1 a, Edge view of paratype (reg. no. PF 68131), dissected specimen, gold coated, scale bar = 50µm; b, detail of aperture, note internal plate connecting with apertural rim, scale bar = 10µm;

2 a, Edge view of paratype (reg. no. PF 68132), dissected specimen, gold coated, scale bar = 50µm; b, detail of aperture, note internal plate connecting with apertural rim, scale bar = 10µm;

3 a, Oblique view of paratype (reg. no. PF 68133), gold coated, scale bar = 50µm; b, detail of wall showing pores, scale bar = 10µm;

4 Side view of paratype (reg. no. PF 68244), polished specimen (probably microspheric), uncoated, scale bar = 50µm;

5-7 Side views of paratypes (5 reg. no. PF 68243, 6 reg. no. PF 68246, 7 reg. no. PF 68248), polished megalospheric specimens, uncoated, scale bars = 50µm.

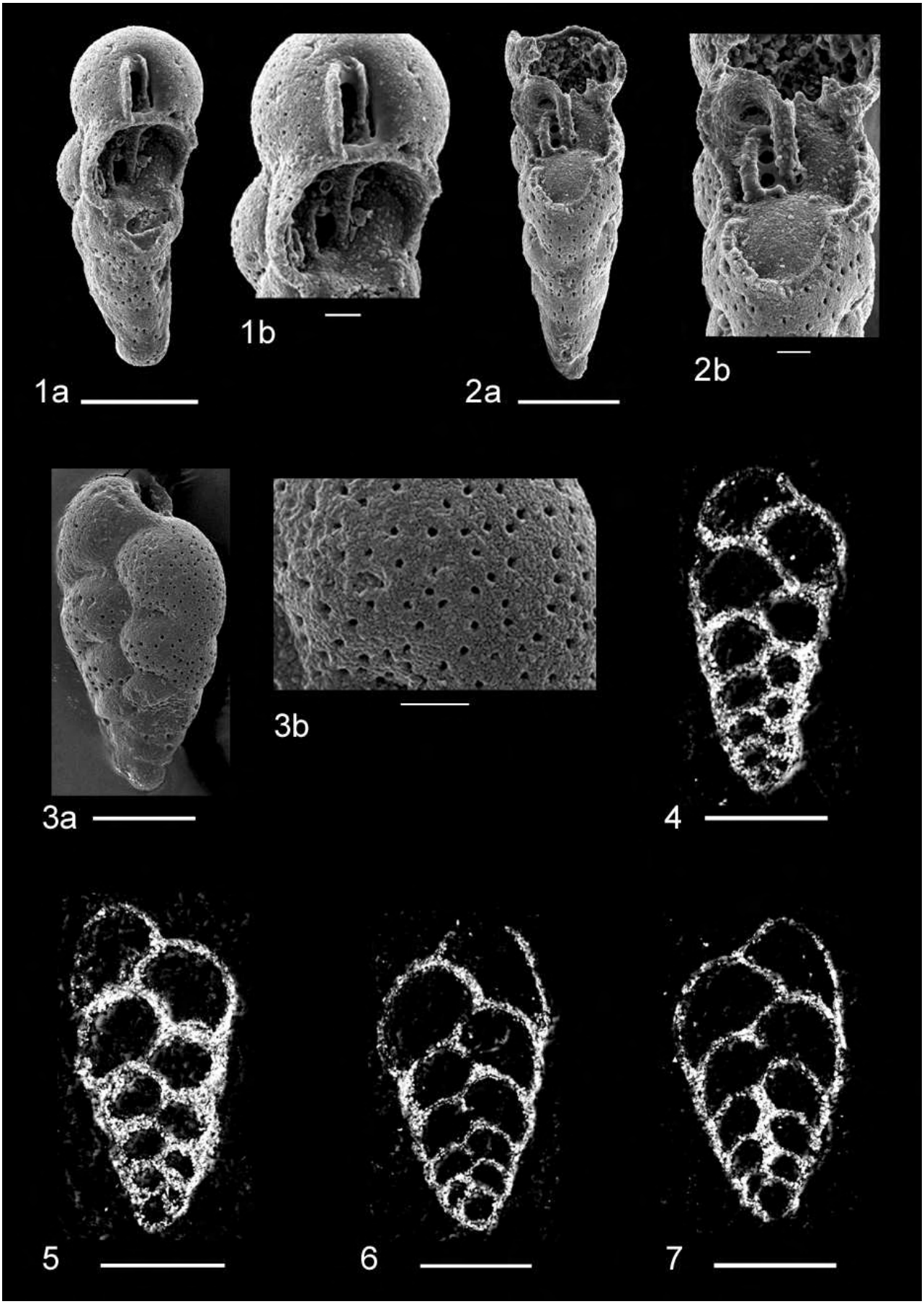
1a
1b
2a
2b
3a
3b
4
5
6
7

botanical evidence for near present-day levels of atmospheric CO_2 during part of the Tertiary. *Nature*, 292: 2310-2313.

SCHMUKER, B. and SCHIEBEL, R., 2002. Planktic foraminifera and hydrography of the eastern and northern Caribbean Sea. *Marine Micropaleontology*, 46: 387-403.

SEXTON, P. E., WILSON, P. A. and PEARSON, P. N., 2006. Palaeoecology of late middle Eocene planktic foraminifera and evolutionary implications. *Marine Micropaleontology*, 60: 1-16.

SIJP, W.P. and ENGLAND, M., 2004. Effect of the Drake Passage Throughflow on global climate. *Journal of Physical Oceanography*, 34: 1254-1266.

SMART, C.W., 1992. Early to middle Miocene benthic foraminiferal faunas from DSDP Sites 518 and 529, South Atlantic: preliminary investigations. In: Takayanagi, Y. and Saito, T., Eds., *Studies in Benthic Foraminifera*, 245-248. Tokyo: Tokai University Press.

———, 2002. Environmental applications of deep-sea benthic foraminifera. In: Haslett, S. K., Ed., *Quaternary Environmental Micropalaeontology*, 14-58. Arnold.

SMART, C.W. and MURRAY, J.W., 1994. An early Miocene Atlantic-wide foraminiferal/ palaeoceanographic event. *Palaeogeography, Palaeoclimatology, Palaeoecology*, 108: 139-148.

SMART, C. W. and RAMSAY, A. T. S., 1995. Benthic foraminiferal evidence for the existence of an early Miocene oxygen-depleted oceanic water mass? *Journal of the Geological Society, London*, 152: 735-738.

SMART, C. W. and THOMAS, E., 2006. The enigma of early Miocene biserial planktic foraminifera. *Geology*. 34: 1041-1044.

SMART, C. W., THOMAS, E. and RAMSAY, A. T. S., 2007. Middle-late Miocene benthic foraminifera in a western equatorial Indian Ocean depth transect: Paleoceanographic implications. *Palaeogeography, Palaeoclimatology, Palaeoecology,* 247: 402-420. doi:10.1016/j.palaeo.2006.11.003

SYKES, T. J. S., RAMSAY, A. T. S. and KIDD, R. B., 1998. *Southern hemisphere Miocene bottom water circulation: a paleobathymetric analysis*, 43-54. In: Cramp, A., MacLeod, C.J., Lee, S.V. and Jones, E.J.W., Eds., Geological Society of London, Special Publication 131.

THOMAS, E., 1985. Late Eocene to Recent deep-sea benthic foraminifera from the central equatorial Pacific Ocean. In: Mayer, L., Theyer, F. and others, Eds., *Initial Reports of the Deep Sea Drilling Project*, *volume 85,* 655-694. Washington, DC: US Government Printing Office.

———, 1986. Early to Middle Miocene benthic foraminiferal faunas from DSDP Sites 608 and 610, North Atlantic. In: Summerhayes, C. P. and Shackleton, N. J., Eds., *North Atlantic Palaeoceanography*, 205-218. Geological Society, London, Special Publication, 21.

———, 1987. Late Oligocene to Recent benthic foraminifers from Deep Sea Drilling Project Sites 608 and 610, northeastern North Atlantic, In: Ruddiman, W. F., Kidd, R. B., Thomas, E. and others, Eds., *Initial Reports of the Deep Sea Drilling Project*, v. 94: 997-1031. Washington, DC: US Government Printing Office.

———, 1990. Late Cretaceous through Neogene deep-sea benthic foraminifers (Maud Rise, Weddell Sea, Antarctica). In: Barker, P.F., Kennett, J.P., et al., Eds., *Proceedings Ocean Drilling Program, Scientific Results*, *volume 113,* 571-594. College Station, Texas: Ocean Drilling Program.

VINCENT, E. and BERGER, W. H., 1985. Carbon dioxide and polar cooling: The Monterey Hypothesis. In: Sundquist, E. T. and Broecker, W. S., Eds., *The carbon cycle and atmospheric CO_2, natural variations Archaean to Present,* 455-468. American Geophysical Union, Monographs, 32.

PLATE 12

Scanning electron micrographs of *Streptochilus mascarenensis* sp. nov.; 1 holotype, 2-8 paratypes.

1 a, Side view of holotype (reg. no. BM(NH) PF 68152), uncoated, scale bar = 50µm; b, detail of wall, scale bar = 10µm; c, greater detail of wall showing granular texture and small pores, scale bar 5µm (DSDP 24-237-18-6, 69-71cm, 166.69 mbsf)

2-5 Side views of paratypes, all uncoated, all scale bars = 50µm; 2 (reg. no. BM(NH) PF 68153), 3 (reg. no. BM(NH) PF 68154), 4 (reg. no. BM(NH) PF 68155), 5 (reg. no. BM(NH) PF 68156) (all from DSDP 24-237-18-6, 69-71cm, 166.69 mbsf).

6 a, Edge view of paratype (reg. no. BM(NH) PF 68157), uncoated, scale bar = 50µm; b, oblique view, scale bar = 50µm; c, detail of aperture showing infolded rimmed margin, scale bar = 10µm (DSDP 24-237-18-6, 69-71cm, 166.69 mbsf).

7 a, Edge view of paratype (reg. no. BM(NH) PF 68158), gold coated, scale bar = 50µm; b, detail of aperture showing infolded rimmed margin, scale bar = 10µm (DSDP 24-237-18-3, 72-74cm, 162.22 mbsf).

8 a, Edge view of paratype (reg. no. BM(NH) PF 68159), gold coated, scale bar = 50µm; b, detail of aperture showing infolded rimmed margin, scale bar = 10µm (DSDP 24-237-18-3, 72-74cm, 162.22 mbsf).

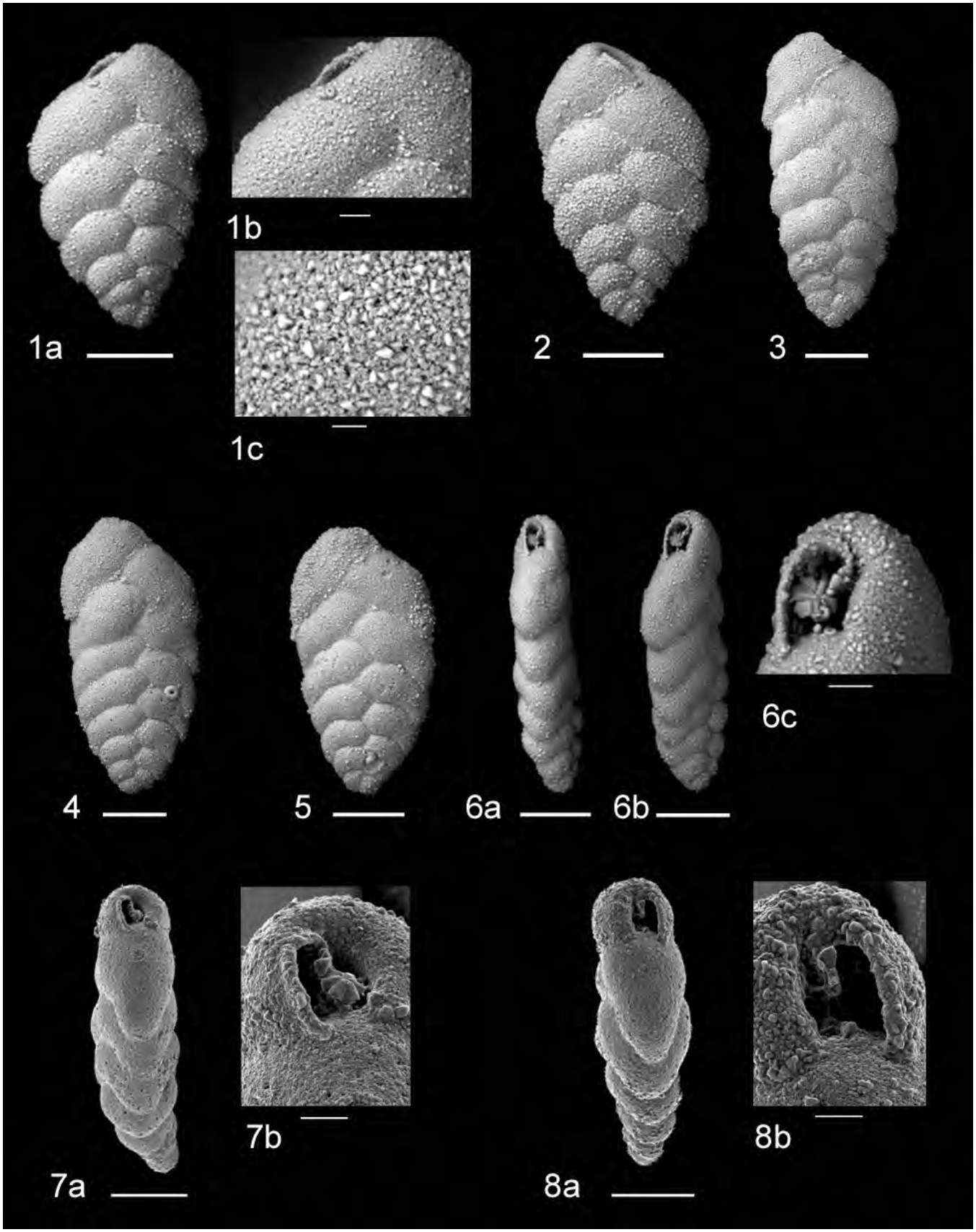
1a
1b
1c
2
3
4
5
6a
6b
6c
7a
7b
8a
8b

VLASTELIC, I., CARPENTIER, M. and LEWIN, E., 2005. Miocene climate change recorded in the chemical and isotopic (Pb, Nd, Hf) signature of Southern Ocean sediments. *Geochemistry, Geophysics, Geosystems*, 6, QO3003, doi: 10.1029/2004GC000819.

WILLIAMSON, W. C., 1858. *On the Recent Foraminifera of Great Britain.* London, England: Ray Society, 1- 107.

WOODRUFF, F. and SAVIN, S.M., 1989. Miocene deepwater oceanography. *Paleoceanography*, 4: 87-140.

WRIGHT, J. D., 1998. Role of the Greenland-Scotland Ridge in Neogene Climate. In: Crowley, T.J. and Burke, K.C., Eds., *Tectonic boundary conditions for climatic reconstructions*, 192-211. Oxford University Press.

WRIGHT, J. D., MILLER, K. G. and FAIRBANKS, R. G., 1992. Early and middle Miocene stable isotopes: implications for deepwater circulation and climate. *Paleoceanography*, 7**:** 357-389.

WRIGHT, J. D. and MILLER, K. G., 1996. Control of North Atlantic deep water circulation by the Greenland-Scotland Ridge. *Paleoceanography,* 11: 157-170.

ZACHOS, J., PAGANI, M., SLOAN, L., THOMAS, E. and BILLUPS, K., 2001. Trends, rhythms and aberrations in global climate: 65 Ma to present. *Science*, 292: 686-693.

ZACHOS, J. C., KROON, D., BLUM, P. et al., 2004. *Proceedings of the Ocean Drilling Program, Initial Reports,* 208 [CD-ROM]. Available from: Ocean Drilling Program, Texas A&M University, College Station TX 77845-9547, USA.

Manuscript received July 28, 2006
Manuscript accepted March 3, 2007

PLATE 13

Scanning electron micrographs of *Streptochilus mascarenensis* sp. nov.; paratypes.

1 a, Edge view of paratype (reg. no. BM(NH) PF 68160), dissected specimen, gold coated, scale bar = 50µm; b, detail of aperture, note internal plate connecting with apertural rim, scale bar = 10µm; greater detail of aperture, scale bar = 10µm (DSDP 24-237-18-3, 72-74cm, 162.22 mbsf).

2 a, Side view of paratype (reg. no. BM(NH) PF 68161), uncoated, scale bar = 50µm; 2b, detail of wall showing fine granular texture and small pores, scale bar = 10µm (DSDP 24-237-18-6, 69-71cm, 166.69 mbsf).

3 a, Side view of paratype (reg. no. BM(NH) PF 68258), polished megalospheric specimen, uncoated, scale bar = 50µm; 3b, detail of initial part, scale bar = 10µm (DSDP 24-237-18-3, 72-74cm, 162.22 mbsf).

4-7 Side views of paratypes (4 reg. no. BM(NH) PF 68260, 5 reg. no. BM(NH) PF 68264, 6 reg. no. BM(NH) PF 68265, 7 reg. no. BM(NH) PF 68271), polished microspheric specimens, uncoated, all scale bars = 50µm; 4 is from DSDP 24-237-18-3, 72-74cm, 162.22 mbsf; 5-7 are from DSDP 24-237-18-6, 69-71cm, 166.69 mbsf.

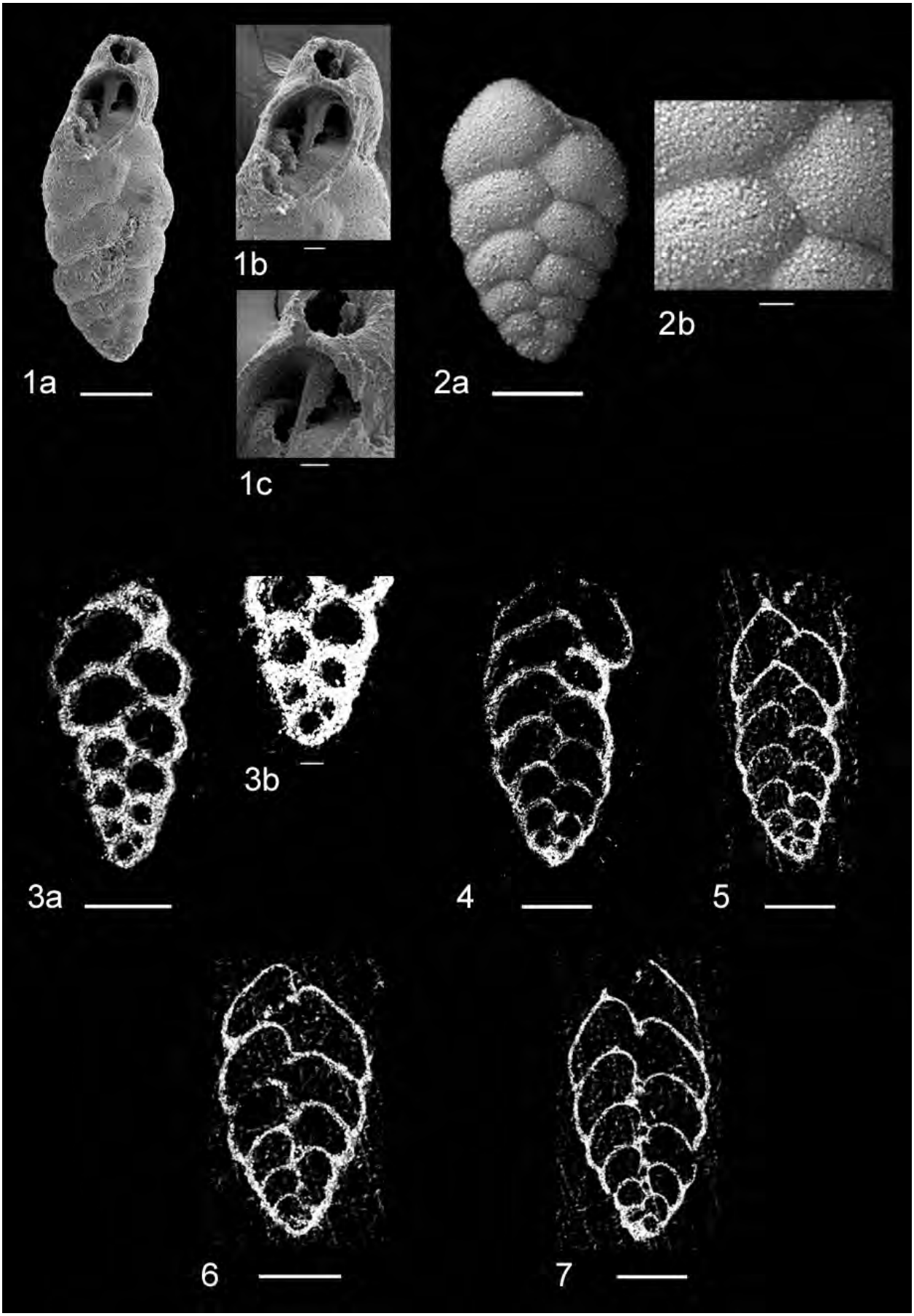
1a
1b
1c
2a
2b
3a
3b
4
5
6
7

TAXONOMIC NOTE

New names for two Triassic radiolarian genera from the Queen Charlotte Islands: *Ellisus* replaces *Harsa* Carter 1991 non Marcus 1951; *Serilla* replaces *Risella* Carter 1993 non Gray 1840 (1847)

Elizabeth S. Carter
Portland State University, Portland, Oregon 97701
mailing address: 17375 Jordan Road, Sisters, Oregon 97759
*e*mail: cartermicro@earthlink.net

It has recently come to my attention that the names of two Triassic genera *Harsa* Carter1991 and *Risella* Carter 1993 are pre-occupied by a free-living flatworm and a gastropod, respectively.

In 1991, I erected the genus *Harsa* for an early Norian radiolarian (Entactinaria) with a large flattened cortical shell and three triradiate spines. Recently, I discovered that Marcus (1951) first gave the name *Harsa* to a flatworm (Platyhelminthes (Turbellaria)). The name *Ellisus* is herein proposed as a replacement (type species *Ellisus siswaiensis* (Carter) 1991) for the preoccupied homonym *Harsa* Carter 1991, non Marcus 1951. *Ellisus* is named after Ellis Point near the type locality on Fredrick Island, Queen Charlotte Islands; masculine gender.

Similarly, Gray (1840 [n.n], 1847) gave the name *Risella* to a mollusk in the collections of the British Museum. Nearly one hundred and fifty years later, I assigned the name *Risella* to a new spumellarian radiolarian genus with a subtriangular shell and three strongly twisted spines that is diagnostic for the late Rhaetian (Carter1993). *Serilla* is now proposed as a replacement name (type species *Serilla tledoensis* (Carter) 1993) for the preoccupied homonym *Risella* Carter 1993 non Gray 1840 (1847). The name *Serilla* is an anagram of *Risella*; feminine gender.

REFERENCES

CARTER, E. S., 1991. Late Triassic radiolarian biostratigraphy of the Kunga Group, Queen Charlotte Islands, British Columbia. In: Evolution and hydrocarbon potential of the Queen Charlotte Basin, British Columbia, G. Woodsworth, Ed., *Geological Survey of Canada Paper* 90-10 p. 195-202.

———, 1993. Biochronology and Paleontology of uppermost Triassic (Rhaetian) radiolarians from the Queen Charlotte Islands, British Columbia, Canada. *Mémoires de Géologie* (Lausanne) 11, 175 p.

GRAY, J. E., 1840. [Mollusca (n.n)], p. 147. In: *Synopsis of the contents of the British Museum [42nd. ed.]*. London: G. Woodfall and Son, 304 p.

———, 1847. A list of the genera of Recent Mollusca, their synonma and types. *Proceedings of the Zoological Society of London*, 15: 195.

MARCUS, E., 1951. Turbellaria brasileiros (9). *Bolitim da Faculdade de Filosofia, Ciências e Letras da Universidade de São Paulo, Sér Zoologia, São Paulo*,16: 5-215.

Mid-Pliocene planktic foraminifer assemblage of the North Atlantic Ocean

Harry J. Dowsett and Marci M. Robinson
US Geological Survey, 926A National Center, Reston, Virginia, 20192
email: hdowsett@usgs.gov

ABSTRACT: The US Geological Survey Pliocene Research, Interpretation and Synoptic Mapping (PRISM) North Atlantic faunal data set provides a unique, temporally constrained perspective to document and evaluate the quantitative geographic distribution of key mid-Pliocene taxa. Planktic foraminifer census data from within the PRISM time slab (3.29 to 2.97 Ma) at thirteen sites in the North Atlantic Ocean have been analyzed. We have compiled Scanning Electron Micrographs for an atlas of mid-Pliocene assemblages from the North Atlantic with descriptions of each taxon to document the taxonomic concepts that accompany the PRISM data. In mid-Pliocene assemblages, the geographic distributions of extant taxa are similar to their present day distributions, although some are extended to the north. We use the distribution of extinct taxa to assess previous assumptions regarding environmental preferences.

INTRODUCTION

Understanding future climate change is fundamentaly important, and identifying and predicting human related changes must take into account natural climate variability and the complex interactions of the different components of the Earth's climate system (National Research Council 2002). One approach to understand such interactions uses analyses of past intervals of global warmth. The mid-Pliocene is the most recent period in Earth's history that was significantly warmer than today; in many respects the mid-Pliocene was as warm as climate models predict for the next century (Intergovernmental Panel on Climate Change [IPCC] 2001). The US Geological Survey Pliocene Research, Interpretation and Synoptic Mapping (PRISM) Project has documented the characteristics of mid-Pliocene climate on a global scale, relying heavily on quantitative analyses of planktic foraminifer assemblages. The PRISM paleoclimate reconstruction is being used to test the ability of climate models to simulate past warmer conditions on Earth and to provide insights into the causes, mechanisms and effects of global warming (e.g., Dowsett et al. 1992, Chandler et al. 1994, Sloan et al. 1996, Haywood et al. 2002, Haywood and Valdes 2004, Dowsett et al. 2005, Jiang et al. 2005, Haywood et al. 2007).

A wealth of foraminiferal species abundance data has been generated by PRISM, and the highest concentration of these data are in the North Atlantic. In this paper we document the North Atlantic planktic foraminifer assemblage from the PRISM time slab, the ~300kyr interval between 3.29 Ma and 2.97 Ma (Dowsett and Robinson 2006). We first document the taxonomic concepts used by PRISM workers in generating species census data in a detailed list of species descriptions and accompanying plates. Secondly, we take advantage of the unique large array of foraminiferal abundance data from a focused stratigraphic interval to establish mid-Pliocene quantitative geographic distributions of key taxa and to compare them to modern distributions. Finally, we evaluate previous taxonomic grouping schemes and associated assumptions utilized by PRISM workers to facilitate application of factor analytic transfer functions and modern analog techniques to Pliocene marine sequences (Dowsett and Poore 1990, Dowsett 1991, Dowsett and Robinson 1998).

DATA AND METHODS

Chronology. The PRISM time slab is a ~300kyr interval lying between the transition of oxygen isotope stages M2/M1 and G19/G18 (Shackleton et al. 1995) in the middle part of the Gauss Normal Polarity Chron (Dowsett et al. 1999, 2005, Dowsett and Robinson 2006) (text-fig. 1). The interval of 3.29 Ma to 2.97 Ma (geomagnetic polarity time scale of Berggren et al. 1995; astronomically tuned timescale of Lourens et al. 1996) ranges from near the bottom of C2An1 (just above Kaena reversed polarity) to within C2An2r (Mammoth reversed polarity). This interval correlates in part to planktic foraminiferal zones PL3 (*Globorotalia margaritae-Sphaeroidinellopsis seminulina* Interval Zone), PL4 (*Sphaeroidinellopsis seminulina-Dentoglobigerina altispira* Interval Zone) and PL5 (*Dentoglobigerina altispira-Globorotalia miocenica* Interval Zone) of Berggren et al. (1995). It falls within calcareous nannofossil zone NN16 of Martini (1971) or CN12a of Bukry (1973, 1975).

Sample Processing. Samples were obtained from the 3.29 to 2.97 Ma interval of DSDP Holes 502A, 541, 546, 548, 552A, 603C, 606, 609B and 610 and ODP Holes 659A, 661A, 667A and 672A (text-fig. 2). Data from Holes 541 and 672A were combined as each covered only a portion of the time slab. Sediment samples used in this study were oven dried at ≤50°C. The dried bulk samples were disaggregated in 250ml of warm tap water with ~2ml of dilute sodium hexametaphosphate (5gm/l water). The samples were agitated for 1 hour at room temperature and then washed over a 63μm sieve using a fine spray hose. The coarse fraction was dried in an oven at ≤50°C. Some samples required an additional wash cycle and a few required 10ml of 10% hydrogen peroxide added to the wash in order to obtain clean specimens. A split of 300-350 planktic foraminifer specimens was obtained from the ≥150μm size fraction using a Carpco™ sample splitter. Specimens were sorted, identified and glued to 60-square micropaleontological slides.

Taxonomy. Planktic foraminifers have been analyzed from the North Atlantic region for over a century, and while classification and higher taxonomic nomenclature are constantly changing, most species concepts are fairly stable. In general we

TABLE 1
Location and water depths of DSDP and ODP Holes examined in this study, availability of paleomagnetic data, average temporal resolution of samples, number of taxa found within the PRISM time slab, and references for the faunal data.

DSDP/ ODP Hole	Latitude	Longitude	Water Depth (m)	Sediment-ation Rate (cm/kyr)	Paleo-magnetic Data	Average temporal resolution (kyr)	No. Taxa in Timeslab	Faunal Data[2]
502A	11.49°	-79.38°	3051	2.71	Yes	13.46	33	2
546	33.80°	-9.60°	3958	1.98	No	50.00	28	3
548	48.50°	-12.00°	1251	4.10	Yes	15.91	18	9
552A	56.04°	-23.23°	2301	1.63	Yes	18.42	22	11
603C	35.49°	-70.03°	4633	10.02	Yes	38.89	35	7
606	37.34°	-35.50°	3007	4.27	Yes	11.67	35	8
609B	49.88°	-24.24°	3883	9.22	Yes	11.67	28	10
610	53.22°	-18.89°	2417	3.64	Yes	12.50	26	10
659A	18.00°	-21.10°	3070	3.48	Yes	20.59	35	5
661A	9.45°	-19.39°	4006	3.37	Yes	12.07	32	6
667A	4.55°	-21.90°	3529	2.07	No	20.59	29	5
672A	15.50°	-58.50	4975	1.89	No	31.82[1]	30	4
541[1]	15.50°	-58.73°	4940	2.68	Yes	31.82[1]	25	3

[1] DSDP 541 and ODP 672A were combined for an average temporal resolution of 31.82kyr.
[2] Reference to original faunal data: (2) Wiggs and Poore 1991, (3) Dowsett and Polanco 1992, (4) Wiggs and Dowsett 1992, (5) Foley and Dowsett 1992, (6) Dowsett and West 1992, (7) Poore 1991, (8) Dowsett et al. 1988, (9) Loubere and Moss 1986, (10) PRISM 1996, (11) Dowsett and Poore 1990.

follow the taxonomy of Parker (1962, 1967) and Blow (1969) with modifications (see annotated species list). The scope of this paper is limited in a temporal sense to the mid-Pliocene PRISM time slab. Therefore, we treat the taxa as distinct and recognizable morphologic units, without consideration to their phylogenetic relationships.

The faunal census data analyzed in this paper were generated by a number of workers, and raw data are available from all cores (Table 1). For this study, we extracted only those samples from each time series that have been attributed to the PRISM time slab, using the stratigraphic framework of Dowsett and Robinson (2006).

Data Analysis. Since the temporal distribution of samples within the PRISM time slab, at each site, is highly variable, we produced multiple values for each taxon across all sites to aid in comparison. First, all counts were transformed to percent data. From the percent data, we determined mean and maximum percent abundance for each taxon at each locality (Table 2).

To aid understanding of the quantitative geographic distribution of the mid-Pliocene assemblage, R-mode and Q-mode Hierarchial Cluster Analyses were performed. We used a similarity metric based upon the Pearson correlation coefficient. The correlation between two vectors (samples) $x = \{x_1, x_2, ..., x_n\}$ and $y = \{y_1, y_2, ..., y_n\}$ is given by:

$$r = \frac{1}{n}\sum_{i=1}^{n}\left(\frac{x_i - \bar{x}}{\sigma_x}\right)\left(\frac{y_i - \bar{y}}{\sigma_y}\right)$$

The coefficient (r) ranges from 1 to -1 and is transformed into distance (0 to 2.0) where 0 equals no distance between vectors, and higher values indicate increasing distance. Clusters are formed using a weighted pair-group method with arithmetic averaging.

RESULTS

Text-figure 3 provides a stratigraphic summary of the cores included in this study and the approximate positions of paleomagnetic reversal boundaries. Using standard techniques, calibrated fossil first and last occurrence data and the magnetobiochronology of Berggren et al. (1995) were used to construct age models for the cores (Dowsett and Robinson 2006). In text-figure 3 the *jagged* band highlights the approximate position of the PRISM time slab. Average temporal resolution ranges from ~50kyr to ~12kyr depending on sample spacing as well as sediment accumulation rates, dissolution, and post-depositional changes (Dowsett and Robinson 2006).

Cluster analysis of the mid-Pliocene planktic foraminifer abundance data reveals a simple three-part division both in terms of core location (Q-mode) and assemblage composition (R-mode) (text-figs. 4 and 5). Three assemblages designated Low Latitude (LL), Mid-Latitude (ML) and High Latitude (HL) are identified in text-figure 4. The LL assemblage is characterized by *Dentoglobigerina altispira, Globigerinoides obliquus, Globigerinoides ruber, Globigerinoides sacculifer, Globorotalia menardii, Globigerina woodi, Pulleniatina obliquiloculata, Neogloboquadrina humerosa, Orbulina universa* and *Sphaeroidinellopsis* spp. DSDP Holes 502A (Caribbean Sea), 541/672A (Western Equatorial Atlantic), ODP Holes 661A and 667A (Eastern Equatorial Atlantic) are all quantitatively dominated by the LL assemblage (text-figs. 2 and 5).

The ML assemblage is distinguished by *Globigerina falconensis*, *Globigerinita glutinata*, *Globigerinella aequilateralis*, *Globorotalia crassafomis*, *Globorotalia scitula* and *Globorotalia hirsuta*. The cluster analysis defines a group of core sites (DSDP Holes 546, 603C, 606 and ODP Hole 659A) geographically intermediate to LL and HL characterized by the taxa listed above (text-figs. 2, 4 and 5).

The HL assemblage is found north of 48° North in the northeastern Atlantic at DSDP Holes 548, 552A, 609B and 610 (text-figs. 2 and 5). *Neogloboquadrina atlantica* (sinistrally and dextrally coiled varieties), *Neogloboquadrina pachyderma* (sinistrally and dextrally coiled varieties), *Neogloboquadrina acostaensis*, *Turborotalita quinqueloba*, *Globigerina bulloides*

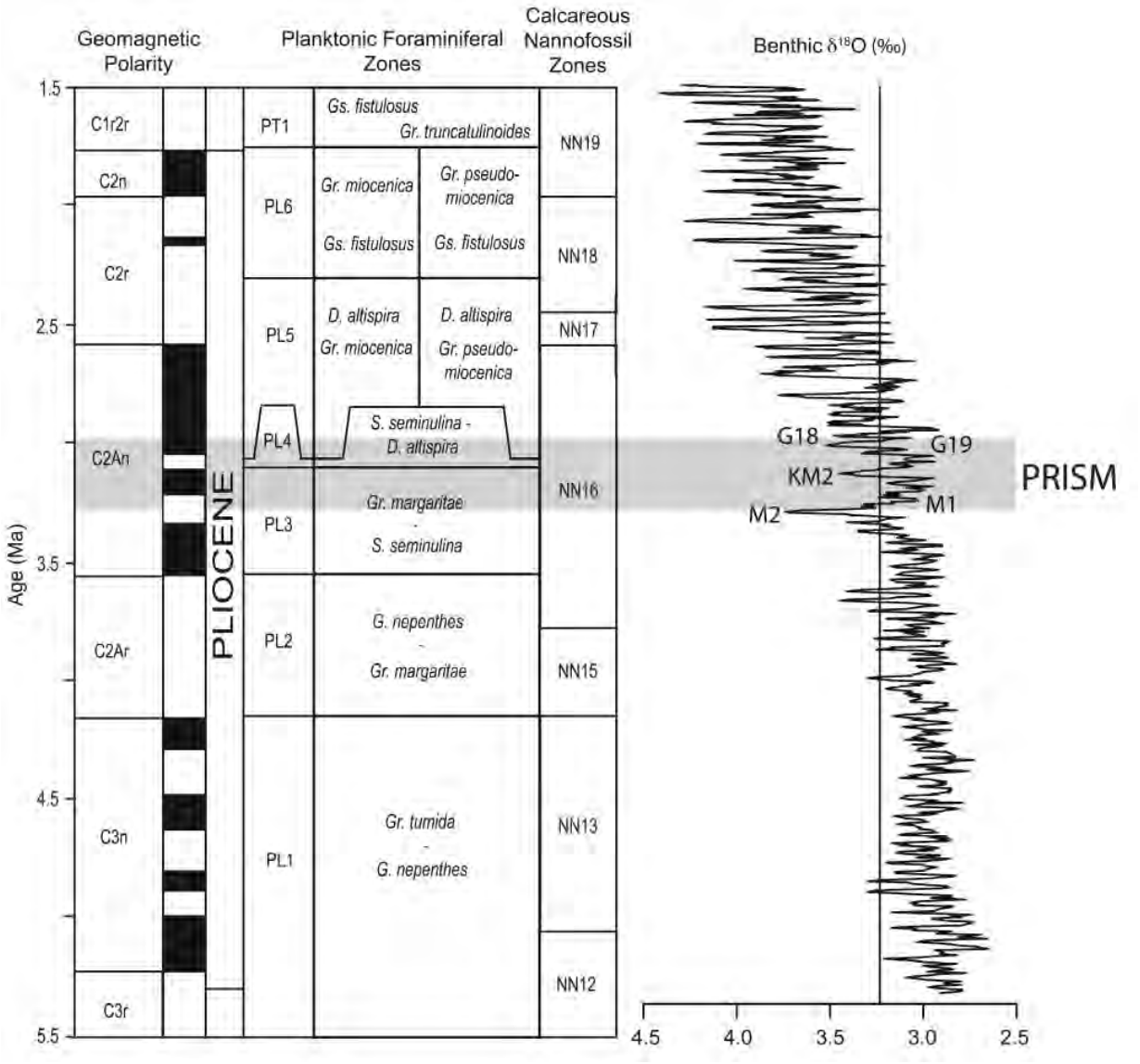

TEXT-FIGURE 1
Pliocene magnetobiostratigraphic framework after Berggren et al. 1995. Gray band approximates the PRISM time slab. Benthic $\delta^{18}O$ record from Lisiecki and Raymo 2005.

and *Globorotalia puncticulata* characterize the HL assemblage (text-fig. 4).

These three assemblages are similar to those defined by the 5-factor models used previously for North Atlantic foraminifer studies. These models are applicable to Pliocene through Recent sediments for the North Atlantic which included tropical, subtropical, subpolar, polar and gyre margin assemblages (Dowsett and Poore 1990, Dowsett 1991). In this study the subtropical and subpolar assemblages of these earlier studies are mixed into a transitional assemblage roughly equivalent to ML. The density and distribution of core sites is insufficient to recognize a gyre margin component (text-fig. 2).

Extant taxa

Extant taxa in this study, present in significant abundances, include: *Neogloboquadrina pachyderma, Globorotalia hirsuta, Globorotalia menardii, Globorotalia crassaformis, Globigerina bulloides, Globigerina falconensis, Globigerinoides ruber, Globigerinoides sacculifer* and *Globigerinita glutinata*. The following discussion relies on both the mean and maximum abundance data sets; however, maximum abundance is often noisy and misrepresentative of the time slab as a whole. Modern sea-floor distribution maps are provided (text-fig. 6 A-J) for extant taxa discussed below except those with rare and patchy occurences at the core top (e.g. *Globorotalia crassaformis*).

Neogloboquadrina pachyderma. Recent molecular data on *Neogloboquadrina pachyderma* (sinistral) from the North Atlantic suggest its present affinity for polar (cold) waters (text-fig. 6A) can be traced back to just over 1.1 Ma (Darling et al. 2004). Molecular evidence exists to consider *N. pachyderma* (dextral) a different species from the sinistral form (Darling et al. 2004). Because mid-Pliocene forms provide

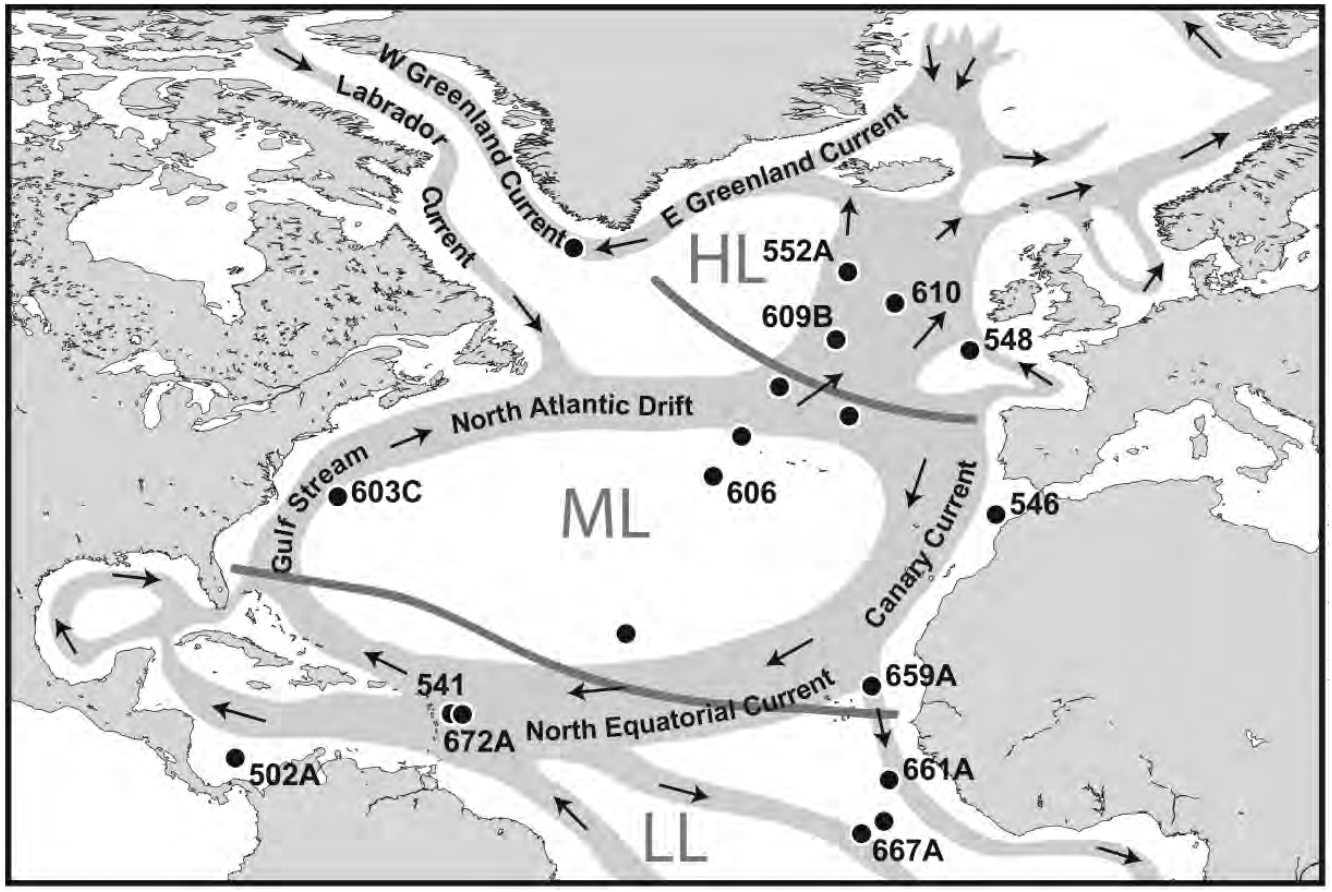

TEXT-FIGURE 2
Location of open ocean core sites discussed in this study (bold). Approximate position of present day currents also shown. LL, ML and HL: Low-Latitude, Mid-Latitude, and High-Latitude assemblage domains, respectively.

only morphologic data, and because *N. pachyderma* (sensu lato) has been documented from subpolar to polar regions since its first appearance in the Miocene, we continue to assign present day cold water preferences to the mid-Pliocene morphospecies (text-figs. 6A and 7A-B). Text-figure 7A shows that, at least in the mid-Pliocene assemblages from the North Atlantic, *N. pachyderma* (sinistral) is rare, although its highest abundance is attained at our most northern site, DSDP 552A. The dextral coiling variety is only slightly more abundant (Table 2, text-fig. 7B) and has a similar maximum in the northeast Atlantic.

In practice PRISM procedure is to combine *Neogloboquadrinids* into two simple groups for transfer function analyses: warm and cool. Both dextral and sinistral *N. pachyderma* are assigned to the cool group along with *N. atlantica*. If in fact mid-Pliocene *N. pachyderma* had a preference for warmer waters, designating it a cool-water signal carrier would drive temperature estimates cooler, resulting in a conservative estimate for surface water warming. The mid-Pliocene warm group contains *N. acostaensis* and *N. humerosa*, both generally recognized throughout the Neogene as warm-water taxa (Hooper and Weaver 1987). The abundance plots of these two latter taxa (text-fig. 7C-D) show similarity in abundance in the LL region, although *N. acostaensis* reaches maximum abundance in the northeastern Atlantic and thus clusters with the HL assemblage (see *N. acostaensis* discussion below).

Globorotalia hirsuta. The distribution of *Globorotalia hirsuta* in the mid-Pliocene is similar to the modern core-top distribution (text-fig. 6B) with maximum abundance in the central part of the gyre. The mid-Pliocene distribution (text-fig. 7E) shows a displacement to the northeast, as do many taxa from this time period. The maximum abundance data set (Table 2) shows a value more than twice the maximum at the core-top (Kipp 1976). Close inspection of the quantitative distribution in a temporal sense shows that this spuriously high value is restricted to the base of the time slab interval at DSDP 606 and is attributed to dissolution which removed many of the more fragile elements of the fauna, thus artificially increasing the abundance of *Gr. hirsuta*.

Globorotalia menardii. The mid-Pliocene distribution of *Globorotalia menardii* (including *Globorotalia tumida*) is essentially identical to the modern core-top distribution (text-fig. 6C). Today, this taxon reaches peak abundance in the southeastern North Atlantic (30%) and generally follows the path of the Gulf Stream. It is present today in low abundance in the central gyre. The maximum abundance of 26% during the PRISM time slab at ODP Hole 667A (text-fig. 7F) and presence at Holes 502A and 603C corroborate a similar geographic distribution during the mid-Pliocene.

Globorotalia crassaformis. The mid-Pliocene distribution of *Globorotalia crassaformis* is shown in text-fig. 7G. It is associ-

TABLE 2
Mid-Pliocene mean (maximum) abundance data for selected North Atlantic sites

HOLE	*Dentoglobigerina altispira*	*Globigerina bulloides*	*Globigerina falconensis*	*Globigerina woodi*	*Globigerinella aequilateralis*	*Globigerinita glutinata*	*Globigerinoides obliquus*	*Globigerinoides ruber*	*Globigerinoides sacculifer*	*Globorotalia crassaformis*	*Globorotalia hirsuta*	*Globorotalia inflata*	*Globorotalia puncticulata*	*Globorotalia scitula*	*Neogloboquadrina acostaensis*	*Neogloboquadrina atlantica (d)*	*Neogloboquadrina atlantica (s)*	*Neogloboquadrina humerosa*	*Neogloboquadrina pachyderma (d)*	*Neogloboquadrina pachyderma (s)*	*Orbulina universa*	*Pulleniatina obliquiloculata*	*Sphaeroidinellopsis spp.*	*Turborotalita quinqueloba*
502A	1(11)	6(12)	0(3)	9(25)	1(2)	7(13)	6(12)	11(20)	11(28)	1(5)	2(8)	8(16)	0(1)	0(1)	8(17)	0(0)	0(0)	12(28)	0(1)	0(0)	2(6)	0(1)	1(7)	0(0)
541	8(14)	0(0)	0(0)	0(1)	0(0)	3(6)	8(17)	10(17)	18(26)	1(2)	0(1)	0(1)	9(16)	1(2)	9(15)	0(0)	0(0)	4(7)	0(1)	1(1)	3(7)	0(1)	15(39)	0(1)
546	1(4)	12(12)	1(3)	8(11)	1(3)	9(19)	3(7)	8(12)	5(9)	13(18)	0(0)	1(4)	15(27)	1(2)	4(6)	0(0)	0(0)	0(1)	1(4)	0(0)	2(6)	1(2)	2(7)	0(0)
548	0(0)	5(13)	3(6)	3(7)	1(3)	7(11)	0(0)	0(0)	0(0)	4(13)	1(12)	0(0)	22(49)	2(4)	25(43)	4(14)	9(40)	0(0)	1(24)	0(1)	2(4)	0(0)	0(0)	3(8)
552A	0(0)	12(17)	1(3)	1(2)	0(2)	7(15)	0(0)	0(0)	0(0)	2(6)	0(3)	0(0)	19(29)	1(2)	8(16)	2(7)	29(45)	0(0)	8(12)	2(5)	0(0)	0(0)	0(0)	2(6)
603C	3(6)	4(6)	10(15)	5(13)	1(2)	11(22)	9(14)	13(24)	10(20)	9(19)	0(0)	3(5)	2(8)	1(2)	2(4)	0(1)	0(2)	1(3)	0(1)	0(1)	3(8)	0(0)	1(7)	0(1)
606	1(11)	10(16)	14(25)	11(18)	2(4)	9(14)	4(9)	5(10)	3(6)	9(24)	3(19)	0(1)	8(26)	1(4)	4(7)	0(1)	0(0)	0(0)	2(5)	0(0)	1(4)	0(0)	0(0)	0(0)
609B	0(1)	5(16)	1(3)	2(6)	0(1)	9(18)	0(1)	0(1)	0(0)	7(21)	0(4)	0(0)	27(53)	1(5)	26(50)	1(4)	10(27)	1(10)	0(2)	1(2)	1(3)	0(0)	0(0)	0(0)
610	0(0)	5(17)	1(4)	1(4)	0(2)	8(17)	0(0)	0(1)	0(0)	6(16)	0(11)	0(0)	22(45)	1(2)	13(26)	17(39)	15(40)	0(2)	0(1)	0(1)	0(1)	0(0)	0(0)	0(0)
659A	3(7)	7(12)	0(1)	12(21)	0(0)	6(11)	4(7)	5(9)	2(5)	1(5)	0(1)	4(6)	22(38)	0(1)	10(20)	0(0)	0(0)	16(44)	0(1)	0(0)	0(1)	0(0)	0(1)	0(0)
661A	7(10)	5(10)	0(5)	3(8)	1(2)	2(5)	7(15)	6(11)	15(22)	3(5)	0(0)	9(18)	3(11)	1(3)	3(21)	0(0)	0(0)	16(26)	0(0)	0(0)	2(5)	0(1)	5(19)	0(3)
667A	12(24)	4(10)	1(2)	2(3)	1(3)	4(7)	12(19)	7(16)	14(18)	1(3)	0(1)	15(26)	2(5)	0(1)	1(3)	0(0)	0(0)	13(25)	0(0)	0(0)	1(2)	0(6)	4(8)	0(0)

ated with the ML assemblage, and the pattern of mean distribution shows extension into the HL region, as do many taxa from this time period. In core-top samples, *Gr. crassaformis* never exceeds 8% abundance, but the distribution is patchy and difficult to map (Kipp 1976). During the PRISM time slab interval, mean abundance is essentially the same (1-13%) as at the core-top. The maximum abundance data set shows several high values, but samples from which these values were derived all exhibit signs of pervasive dissolution (Table 2).

Globigerina bulloides. *Globigerina bulloides* has a basically ubiquitous mid-Pliocene distribution, with slightly higher maximum abundance in the Northeastern Atlantic (17%) (Table 2, text-fig. 7H). While *G. bulloides* is reported to comprise up to 50% of some core-top samples (Kipp 1976), maximum abundances over ~20% are uncommon (Prell et al. 1999) (text-fig. 6D). This taxon is recognized as an important component of the HL assemblage in this study and a sub-polar taxon in modern core-top studies (Kipp 1976, Dowsett 1991).

Globigerina falconensis. The mid-Pliocene distribution of *Globigerina falconensis* (text-fig. 7I), with maximum abundance at sites in the northern part of the central gyre (DSDP 603C and 606), is similar to its coretop distribution (text-fig. 6E). On the seabed today, *G. falconensis* is most abundant in the eastern Atlantic, south of the *G. bulloides* maxima. *G. falconensis* is associated with the mid-Pliocene ML assemblage.

Globigerinita glutinata. This taxon is present at most sites during the mid-Pliocene at abundances ranging from 2-10% with a maximum abundance of ~20% at a few locations (text-fig. 7J, Table 2). The present day seabed distribution of *Globigerinita glutinata* (text-fig. 6F) closely matches the mid-Pliocene distribution. During the mid-Pliocene, *G. glutinata* helps distinguish the ML assemblage but also makes important contributions to the HL assemblage.

Globigerinoides ruber. The low latitude distribution of *Globigerinoides ruber* during the mid-Pliocene (text-fig. 7K) is similar to its core-top abundance pattern (text-fig. 6G). The actual abundances during the PRISM interval are significantly less than what is seen in the distribution of both pink and white varieties of *Gs. ruber* on the seabed today. During the mid-Pliocene, now extinct *Gs. obliquus* (see below) had an almost identical geographic distribution as *Gs. ruber*, and the two taxa together reach abundances similar to the present day core-top distribution of *Gs. ruber.*

Globigerinoides sacculifer. During the mid-Pliocene, *Globigerinoides sacculifer* sensu lato is restricted to the low latitude region and appears to be most abundant in the southern and western limbs of the main gyre (text-fig. 7L). This mid-Pliocene abundance pattern is similar to the present day "gyre-margin" distribution of this low latitude taxon (text-fig. 6H). In the present day ocean, *Gs. sacculifer* is a stenohaline species, usually representing high salinity conditions (Dowsett 1991).

Extinct taxa

Extinct taxa are problematic for understanding paleoclimate records. The mid-Pliocene geographic distribution of now extinct taxa are documented below, and environmental tolerances can be inferred by co-occurrence with extant taxa and assumptions based upon ancestor-decendent pairs. Extinct taxa present in significant quantities and/or taxa considered important in the mid-Pliocene North Atlantic include *Dentoglobigerina altispira, Globigerinoides obliquus, Neogloboquadrina atlantica, Neogloboquadrina acostaensis, Neogloboquadrina humerosa, Globorotalia puncticulata,* and *Globigerina woodi.*

Dentoglobigerina altispira. During the mid-Pliocene this taxon is present at all sites south of 40°N in the North Atlantic (text-fig. 7M). *Dentoglobigerina altispira* is most abundant in low latitudes where its average abundance reaches 4% - 12% (Table 2, text-fig. 7M). *Dentoglobigerina altispira* groups with extant and other extinct taxa in the LL assemblage. Its mid-Pliocene geographic distribution matches closely that of extant *Globigerinoides ruber* (text-fig. 6G) and extinct *Neogloboquadrina humerosa* (text-fig. 7D). This does not imply a relationship with either of these taxa, but suggests that environmental preferences of the three may be similar.

Globigerinoides obliquus. In the mid-Pliocene North Atlantic, the quantitative geographic distribution of *Globigerinoides obliquus* closely matches that of extant *Gs. ruber* (text-fig. 7N). A well-known replacement of *Gs. obliquus* by *Gs. ruber* takes place within the Pliocene. The exact reason for the switch in dominance within the *Globigerinoides* is not clear, but assigning similar evironmental preferences to both groups seems reasonable. The combination of *Gs. ruber* and *Gs. obliquus*, first

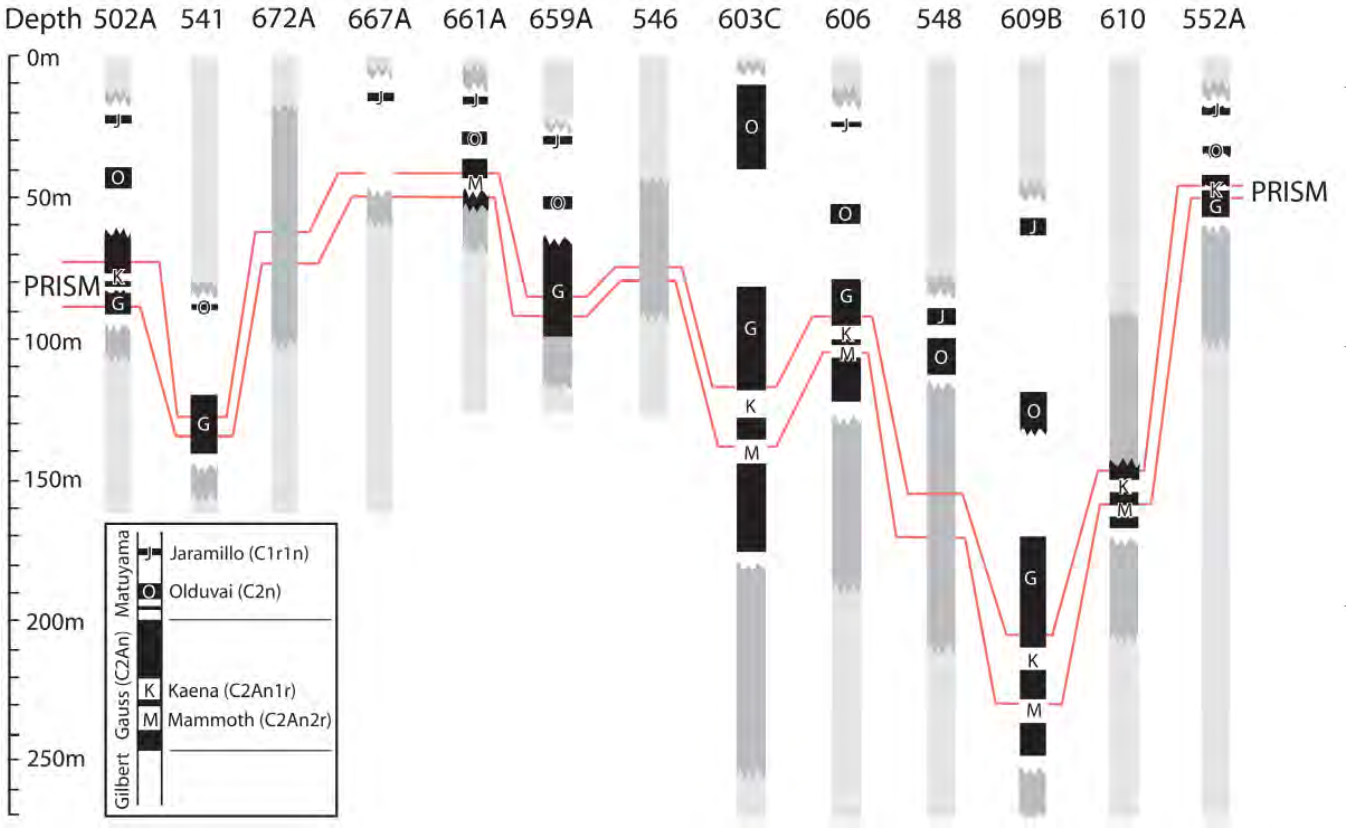

TEXT-FIGURE 3
Magnetobiostratigraphy of North Atlantic DSDP and ODP cores arranged in order of increasing latitude. Section of core analyzed is shown in dark gray. Magnetic polarity shown as normal (black) or reversed (white) with broken lines indicating unknown boundaries. Jagged correlation lines mark approximate limits of PRISM time slab.

suggested by Thunnell (1979a,b) and utilized by Dowsett and Poore (1990) and Dowsett (1991), produces a mid-Pliocene low latitude Atlantic taxon roughly equivalent in terms of quantitave dominance to present day *Gs. ruber*.

Neogloboquadrina atlantica. This taxon is by far the most problematic foraminiferal species of the mid-Pliocene. In terms of distribution, *Neogloboquadrina atlantica* has a maximum abundance at Holes 548, 552A, 609B and 610, the most northern sites addressed in this study (text-fig. 7O-P). Previous work in the North Atlantic (Berggren 1972, Poore 1979, Weaver 1987, Hooper and Weaver 1987, Dowsett and Poore 1990, PRISM 1996) establishes *N. atlantica* as a cold water taxon, and it is present outside the North Atlantic as well (Dowsett and Ishman 1995, Dowsett and Poore 2000). Dowsett and Poore (1990) considered *N. atlantica* to be the cold end member of the genus *Neogloboquadrina* during the mid-Pliocene. In so doing, they consciously placed a cool bias on possible high-latitude SST warming. If *N. atlantica* occupied warmer waters than those occupied by sinistrally coiling *N. pachyderma* in the modern ocean, transfer function results would assign cooler SST estimates to the high latitudes. The division of *Neogloboquadrina* into two groups, warm and cold, further reinforced this planned conservative (with respect to estimates of warming) approach.

G. bulloides and *N. atlantica* can appear very similar under the light microscope. Although the difference in surface texture in pristine specimens is clear, preservational alteration often impedes proper identification. Dowsett and Poore (1990) found the separation of the two taxa at Site 552 so troublesome that they performed sensitivity tests to determine the effect of misidentifying individuals on the estimated SSTs. Those tests showed that misidentification of small amounts of *G. bulloides* as *N. atlantica* had negligable effects on transfer function results (Dowsett and Poore 1990). As before, the assignment of some *G. bulloides* (subpolar in the modern ocean) to *N. atlantica* would result in cooler SST estimates and therefore conservative estimates of mid-Pliocene warming at high latitudes.

Neogloboquadrina humerosa. The mid-Pliocene distribution of *Neogloboquadrina humerosa* shows maxima in the southeastern North Atlantic in the upwelling region off Africa (text-fig. 7D). It is also present in moderate abundances in the Colombia Basin at Hole 502A. This distribution, both in geographic extent and magnitude, is remarkably similar to that of *N. dutertrei* on the modern seabed (text-fig. 6I).

Neogloboquadrina acostaensis. Specimens we identify as *Neogloboquadrina acostaensis* occur at all sites, but the *mean ab*undance data set shows moderate abundance in the southern and eastern part of the North Atlantic similar to the distribution of *N. humerosa*. *N. acostaensis* differs from *N. humerosa* by increasing to maximum abundance in the northeast Atlantic (text-fig. 7C-D). Dowsett and Poore (1990) and Dowsett (1991) divided the present day *Neogloboquadrina* into two groups with

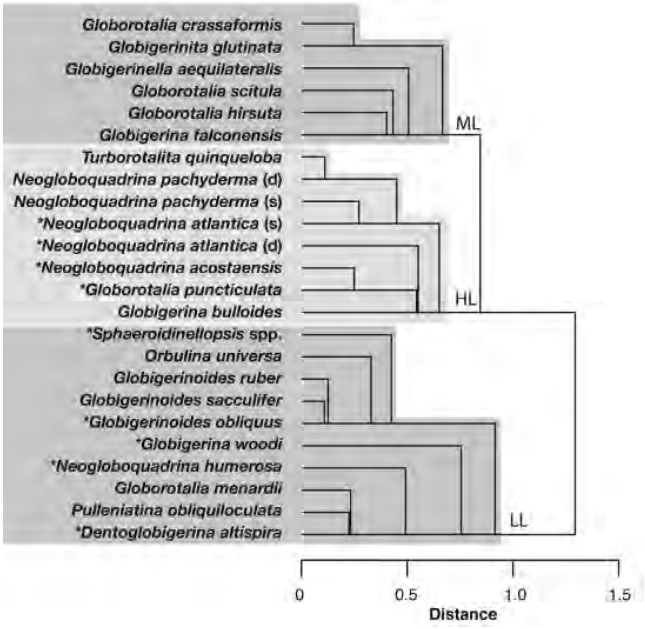

TEXT-FIGURE 4
R-mode cluster analysis showing species groupings within the mid-Pliocene interval of the North Atlantic Ocean (see text for details). Cluster HL = High Latitude, ML = Mid-Latitude and LL = Low Latitude. Extinct taxa preceded by "*."

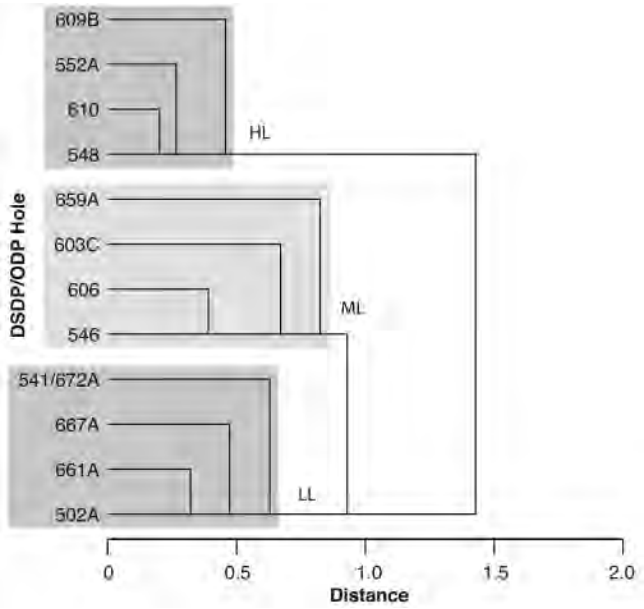

TEXT-FIGURE 5
Q-mode cluster analysis showing sample groupings within the mid-Pliocene interval of the North Atlantic Ocean (see text for details). Cluster HL = High Latitude, ML = Mid-Latitude and LL = Low Latitude.

warm and cool preferences. Present day *N. pachyderma* (dextral and sinistral) represented the cool group while *N. dutertrei* represented the warm group. The artificial "dupac" or *N. dutertrei-N. pachyderma* intergrade of Kipp (1976), a 4 ½ chambered dextrally coiling form of *N. pachyderma* with a similar temperature salinity response (Dowsett, 1991), is included in the warm category.

The *Neogloboquadina acostaensis – N. humerosa – N. dutertrei* lineage began in the late Miocene (N16) and has been restricted to relatively warm water regions throughout its history (Kennett and Srinivasan 1983, Bolli and Saunders 1985, Dowsett 1991). For Pliocene sequences containing extinct taxa, *N. atlantica* (sinistral and dextral) are combined with *N. pachyderma* to form the cool group, while *N. humerosa* is considered analogous in terms of environmental preferences to present day *N. dutertrei*. *N. acostaensis* is also included in the warm category as well as Pliocene representatives of the "aco-pac" taxon of Loubere (1988). The overall grouping of modern taxa in this fashion was intended to produce conservative estimates of warming. However if the *N. acostaensis* observed in the northeast Atlantic from the mid Pliocene was actually a different population from those found in the low latitudes, inclusion in the warm subgroup of *Neogloboquadrina* could result in artificially high estimates of warming. Conversely, if all mid-Pliocene specimens assigned to *N. acostaensis* and *N. humerosa* had similar temperature preferences, then the abundance of *N. acostaensis* in the northeast Atlantic during the mid-Pliocene documents considerable warming. Since *N. humerosa* does not show elevated abundance in the northeast Atlantic during the mid-Pliocene, further work is necessary to refine the environmental tolerance of *N. acostaensis* using muti-species isotopic and Mg/Ca studies.

Globorotalia puncticulata. *Globorotalia puncticulata* is well established as the ancestor to the extant *Gr. inflata* (Kennett and Vella 1975). The distribution of *Gr. puncticulata* within the PRISM time slab shows highest abundances in the east and northeast North Atlantic (text-fig. 7Q). The present-day distribution of *Gr. inflata* (text-fig. 6J) shows highest abundances associated with the northern limb of the subtropical gyre, the North Atlantic Drift. A patch of high abundance of *Gr. inflata* is located south of the core sites that fall in the Pliocene HL assemblage (text-figs. 2 and 6J). Allowing for a northward shift of the Pliocene Gulf Stream Current, relative to today, the mid-Pliocene quantitative distribution of *Gr. puncticulata* closely resembles the modern distribution of *Gr. inflata.*

Globigerina woodi. *Globigerina woodi* reaches highest abundance in the Caribbean (Hole 502A) and off Africa and clusters with the LL assemblage. It does however reach moderate abundance in cores assigned to the ML assemblage. *G. woodi*, including closely related *G. apertura*, is rare in the HL region (text-fig. 7R).

Sphaeroidinellopsis seminulina. In terms of mean abundance, this taxon is most significant in the low latitude regions of the North Atlantic during the mid-Pliocene (text-fig. 7S).

SUMMARY AND CONCLUSIONS

The species concepts used by PRISM researchers to identify mid-Pliocene planktic foraminifers are presented in Plates 1-3 and noted in the species list below. The mid-Pliocene was chosen as a target for paleoclimate reconstruction in part because a large fraction of the taxa found in that interval are extant. Both extant and extinct taxa are common entries in the literature, and the taxonomic concepts presented are consistent with the planktic foraminifer community.

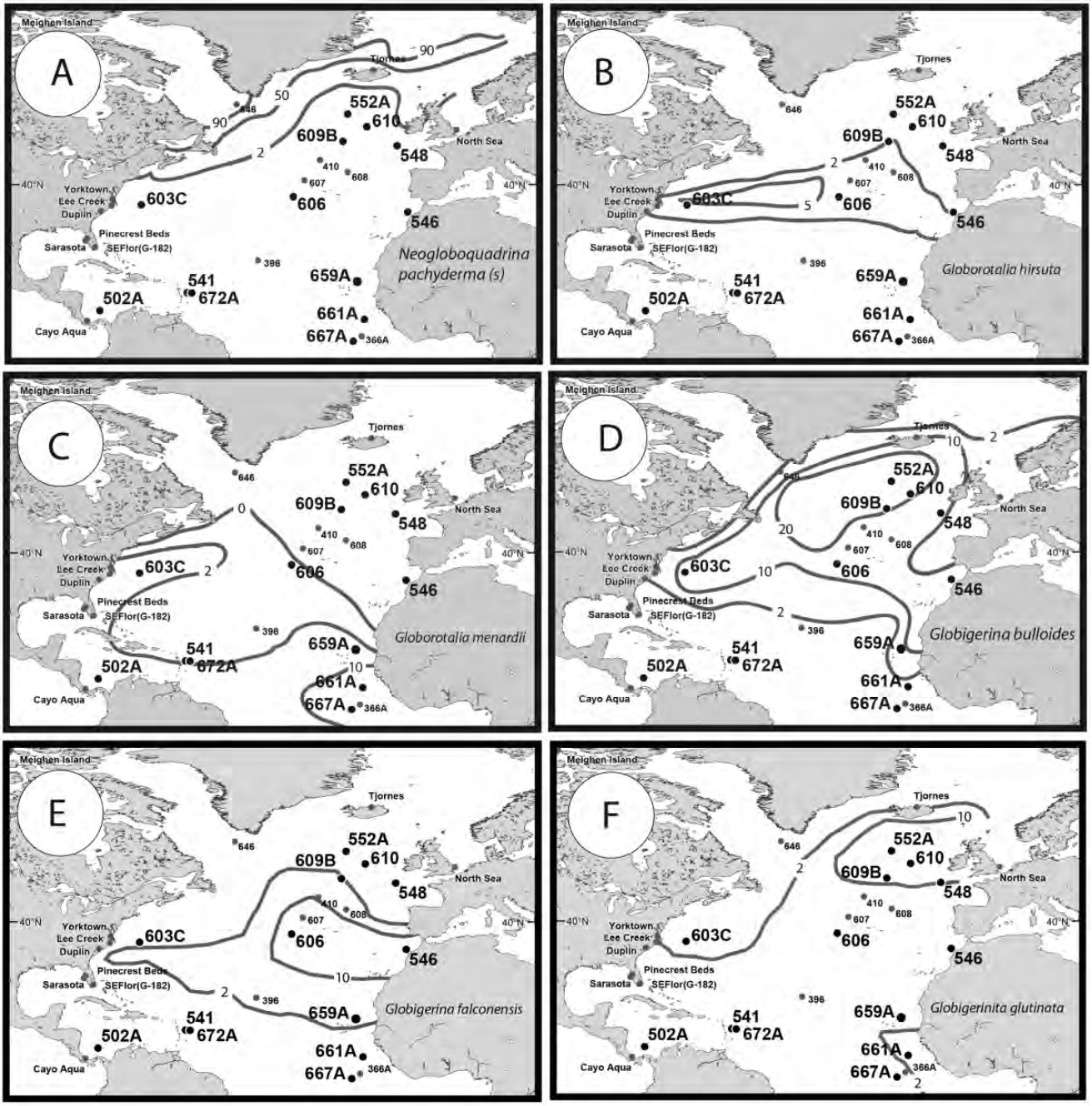

TEXT-FIGURE 6A-F
Sea floor (present) distribution of selected planktic foraminifer species. A = *Neogloboquadrina pachyderma* (s); B = *Globorotalia hirsuta*; C = *Globorotalia menardii;* D = *Globigerina bulloides*; E = *Globigerina falconensis*; F = *Globigerinita glutinata.*

The quantitative distribution of foraminifers in the North Atlantic during the mid-Pliocene is a useful representation of environmental preferences of individual species. The distribution patterns reconstructed from this limited data set suggest species distributions similar to modern, although often shifted northward. PRISM SST reconstructions based on these distributions indicate warming at mid- and high latitudes during the mid-Pliocene. It is important to note that available multi-proxy estimates of surface conditions (pollen spectra, quantitative distribution of shallow water ostracodes, Mg/Ca estimates of SST from *Globigerina bulloides*, and alkenone SST estimates (text-fig. 8)) all indicate warming of the same magnitude suggested by foraminiferal-based faunal estimates, in the northeast Atlantic during the mid-Pliocene (e.g., Cronin 1991a,b, Willard 1994, Dowsett et al. 1994). Thus, we feel that assigning modern environmental preferences to mid-Pliocene taxa is justified for most taxa at most sites. The next step in verifying previously reported high latitude warming in the North Atlantic must await results of experiments in progress utilizing multiproxy approaches at multiple sites.

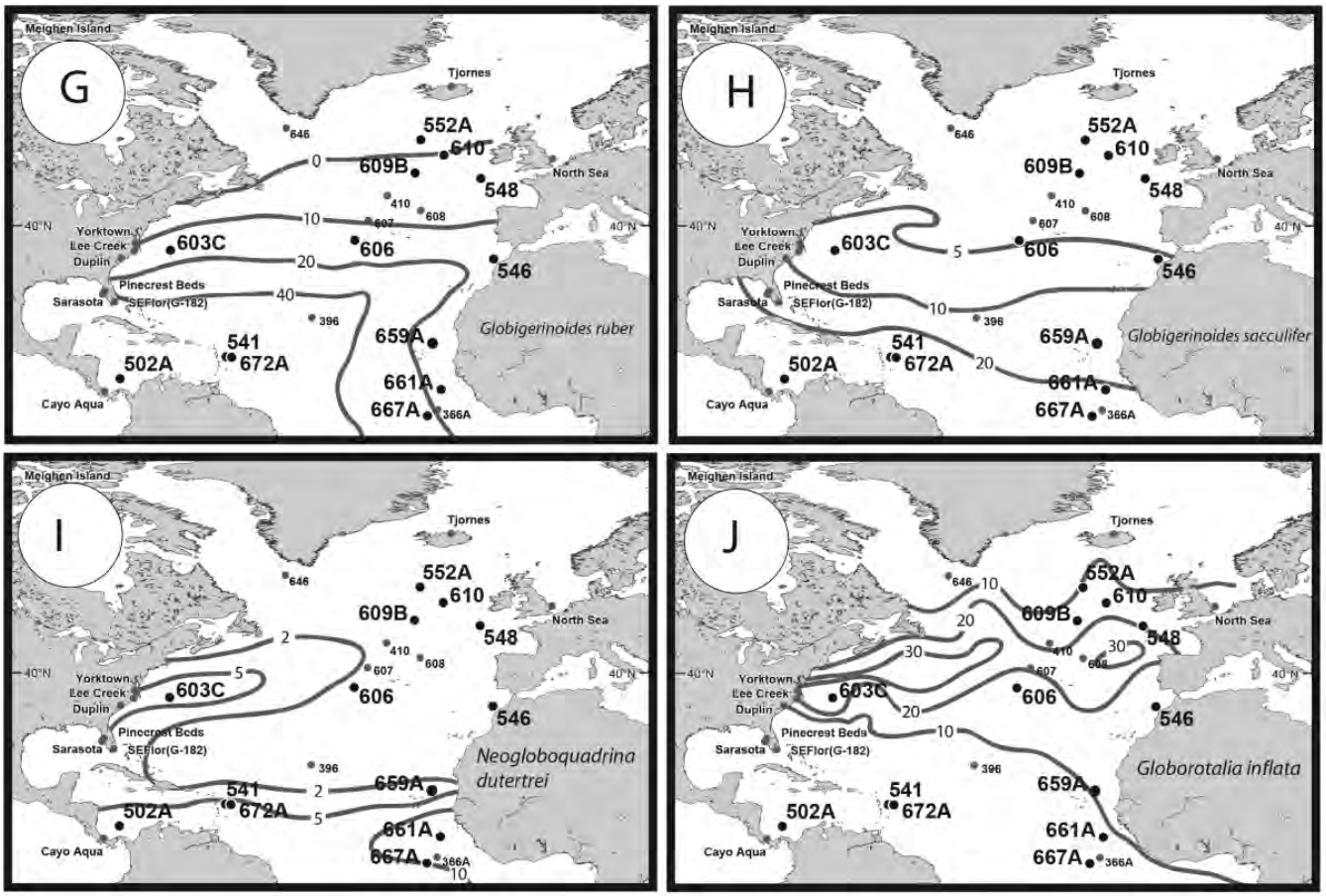

TEXT-FIGURE 6G-J
Sea floor (present) distribution of selected planktic foraminifer species. G = *Globigerinoides ruber*; H = *Globigerinoides sacculifer;* I = *Neogloboquadrina dutertrei*; J = *Globorotalia inflata.*

The high abundances of *Globorotalia puncticulata* and *Neogloboquadrina acostensis* in the northeastern Atlantic region are puzzling. These taxa may be present in high abundances in this region because they had the same preferences as present day *Globorotalia inflata* and *Neogloboquadrina dutertrei*, respectively. This would demonstrate significant warming in the northeastern Atlantic during the mid-Pliocene in agreement with other fossil and geochemical indicators. Alternatively, mid-Pliocene SST could have been unchanged relative to today, implying these taxa had broader temperature preferences than the modern taxa we associate with them. Stated differently, assignment of ecological preferences based upon ancestor-decendent relationships could be incorrect. In the case of *N. acostaensis*, it is possible that combining it with *N. humerosa* to represent a "warm end member" of the genus *Neogloboquadrina*, is inapropriate, and the high abundances of *N. acostaensis* in the northeast Atlantic drive the transfer function equations to produce anomalously high SSTs. Since both taxa are commonly thought to be subsurface dwellers, it may be important to decouple them from surface temperature estimates. They may be monitoring a unique and possibly non-analogous oceanographic situation where surface temperatures were elevated and not necessarily related to subsurface productivity.

SPECIES LIST

Candeina nitida
Plate 1, figure 1

Candeina nitida D'ORBIGNY 1839, p. 107, pl. 2, figs. 27-28

Description: Test high trochospire; 3 globular chambers in final whorl, increasing regularly in size; primary aperture not visible; multiple round supplementary apertures bordered by lips completely surrounding final few chambers; sutures depressed, radial; test surface smooth.

Dentoglobigerina altispira (Cushman and Jarvis)
Plate 1, figure 2

Globigerina altispira CUSHMAN and JARVIS 1936, p. 5, pl. 1, figs. 13a-c

Description: Test high trochospire, early chambers sub spherical, 4-5 compressed and elongated chambers in final whorl increasing regularly in size; aperture umbilical; umbilicus wide and open with projecting teeth; sutures depressed, radial to slightly curved, equatorial periphery lobate; surface cancellate.

Globigerina bulloides d'Orbigny
Plate 1, figures 3-5

Globigerina bulloides D'ORBIGNY 1826, p. 3, pl. 1, figs. 1-4

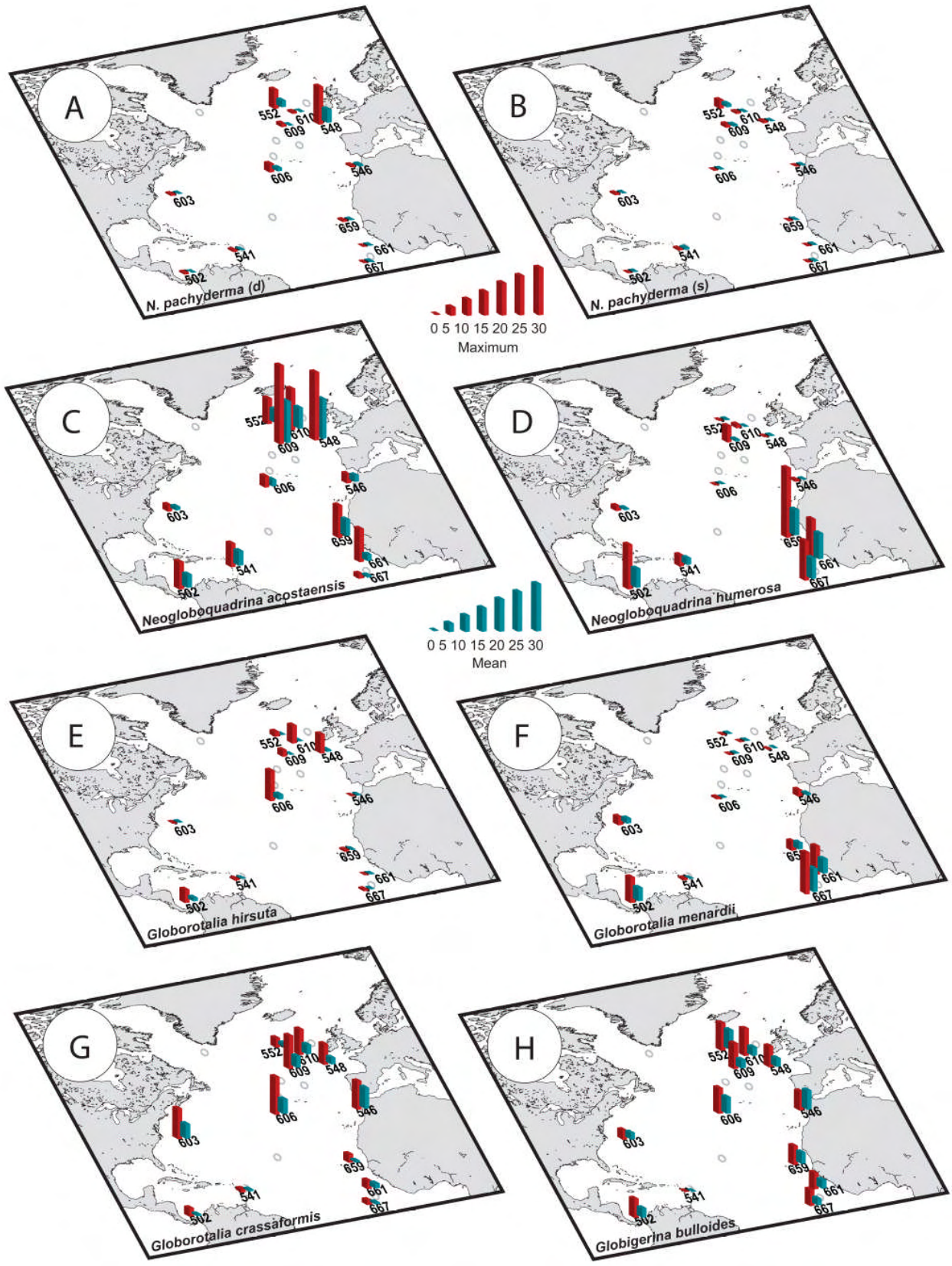

TEXT-FIGURE 7A-H
Mean and maximum (Pliocene) abundance of selected taxa within the PRISM time slab. A= *Neogloboquarina pachyderma* (d); B = *Neogloboquadrina pachyderma* (s); C = *Neogloboquadrina acostaensis;* D = *Neogloboquadrina humerosa;* E = *Globorotalia hirsuta*; F = *Globorotalia menardii*; G = *Globorotalia crassaformis;* H = *Globigerina bulloides.*

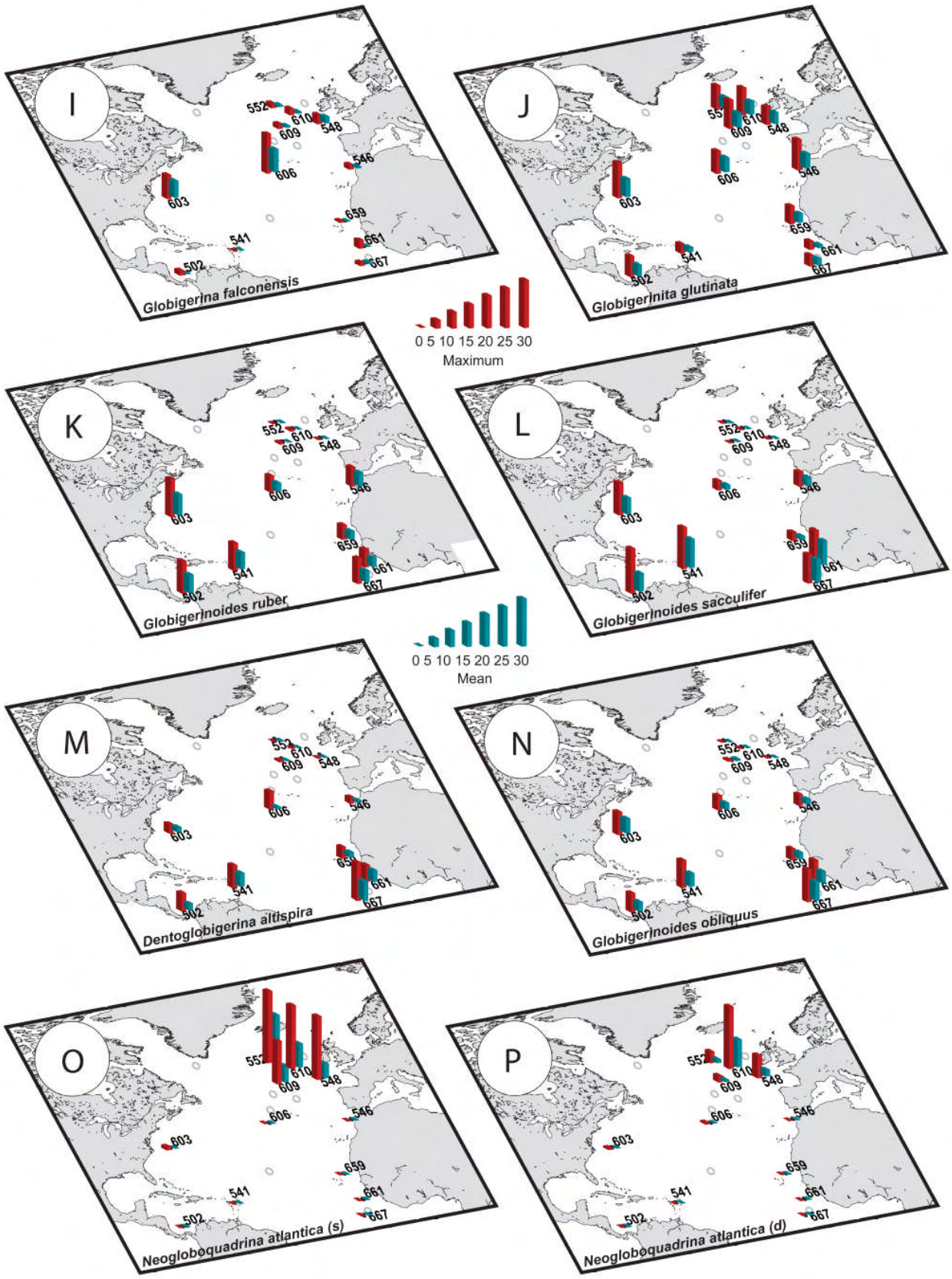

TEXT-FIGURE 7I-P
Mean and maximum (Pliocene) abundance of selected taxa within the PRISM time slab. I = *Globigerina falconensis*; J = *Globigerinita glutinata*; K= *Globigerinoides ruber*; L = *Globigerinoides sacculifer*; M = *Dentoglobigerina altispira*; N = *Globigerinoides obliquus*; O = *Neogloboquadrina atlantica* (s); P = *Neogloboquadrina atlantica* (d).

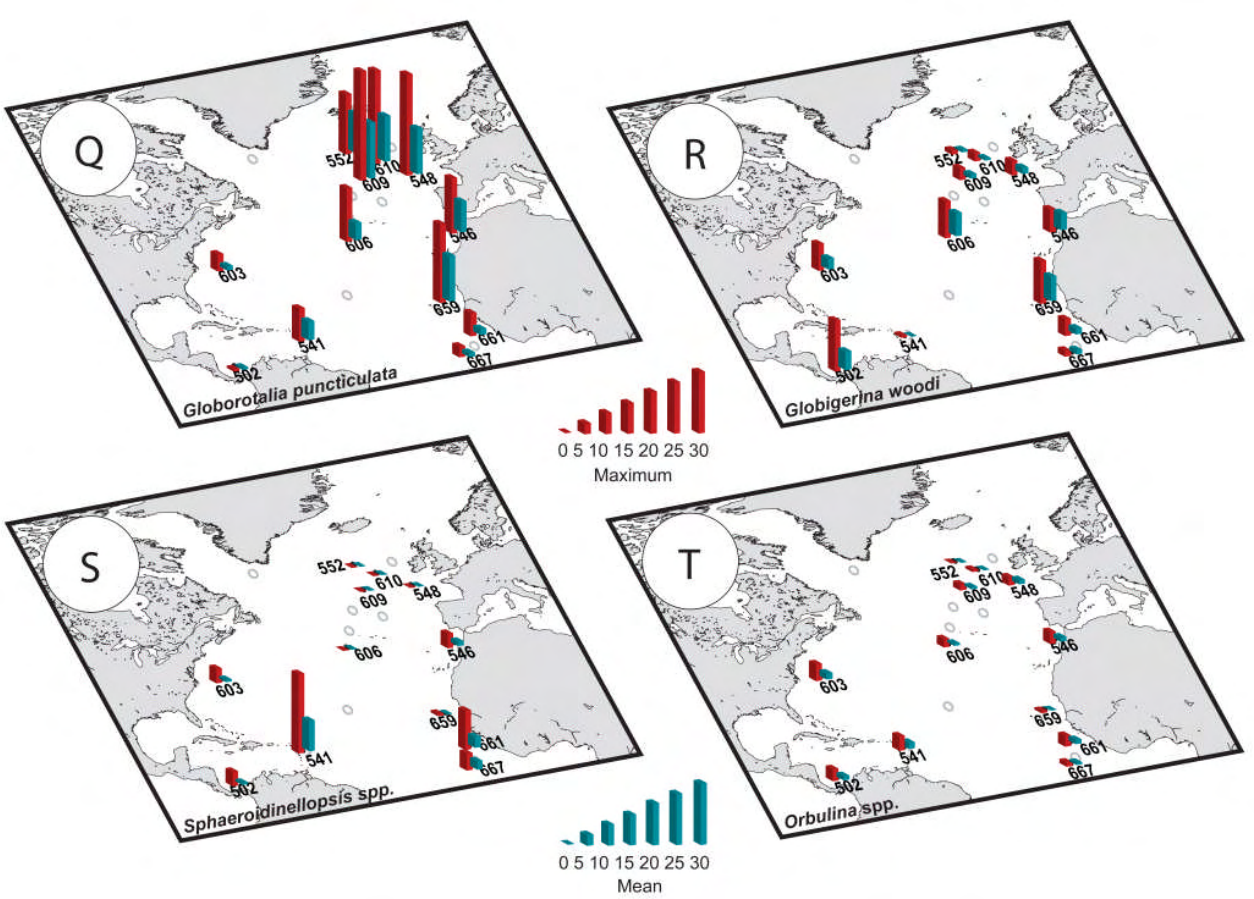

TEXT-FIGURE 7Q-T
Mean and maximum (Pliocene) abundance of selected taxa within the PRISM time slab. Q = *Globorotalia puncticulata*; R = *Globigerina woodi*; S = *Sphaeroidinellopsis* spp.; T = *Orbulina* spp.

Description: Test low-trochospire; 4 spherical to sub spherical chambers in final whorl, increasing regularly in size; aperture interiomarginal, umbilical, a high arch; sutures depressed; test surface densely perforate and pustulate (spine bases).

Remarks: See *Neogloboquadrina atlantica* below for note concerning recalcification of typical *G. bulloides* pore-pitted surface with pustules (see also Dowsett and Ishman, 1995).

Globigerina decoraperta Takayanagi and Saito
Plate 1, figure 6

Globigerina druryi Akers *decoraperta* TAKAYANAGI and SAITO, 1962, p. 85, pl. 28, figs 10a-c.

Description: Test medium-to-high trochospire; 4 spherical to sub spherical chambers in final whorl, increasing regularly in size; aperture interiomarginal, umbilical, semicircular arch bordered by a rim; sutures radial, depressed; equatorial periphery lobate; test surface cancellate.

Globigerina falconensis Blow
Plate 1, figure 7

Globigerina falconensis BLOW 1969, p.177, pl. 9, figs. 40a-c, 41

*Description: T*est low trochospire; 4 spherical chambers in final whorl increasing gradually in size; last chamber often smaller than penultimate chamber; aperture interiomarginal, umbilical, bordered by a low broad lip; sutures depressed, radial; equatorial periphery lobate, test surface perforate and pustulate (spine bases).

Remarks: Globigerina falconensis is distinguished from *G. bulloides* by its ultimate chamber with distinctive lip.

Globigerina incisa (Bronnimann and Resig)
Plate 1, figure 8

Globorotalia incisa BRONNIMANN and RESIG 1971, p. 1278-1279, pl. 45, figs. 5,7, pl. 46, figs. 1-8.

Description: Test low-trochospire; 3 ½ -5 chambers in the final whorl, increasing rapidly in size; aperture extraumbilical-umbilical low arch bordered by a rim; sutures radial and deeply depressed; equatorial periphery sub-lobate; test surface dense with pustules surrounding pores.

Globigerina nepenthes Todd
Plate 1, figure 9

Globigerina nepenthes TODD 1957, p. 3-1, figs. 7a-7b.

Description: Test low-medium trochospire; 4 sub spherical compressed chambers in the final whorl, increasing gradually in size; ultimate chamber distinctly hood shaped; aperture umbili-

cal low arch bordered by a thickened rim; sutures radial to curved, depressed; test surface cancellate.

Remarks: Globigerina nepenthes has a last appearance prior to the PRISM time slab but is included because it is an important element of the Early Pliocene fauna.

Globigerina praedigitata Parker
Plate 1, figure 10

Globigerina praedigitata PARKER 1967, p. 151, pl. 19, figs. 5–8.

Description: Test low-medium trochospire; 4-5 subspherical becoming ovate chambers in the final whorl, increasing rapidly in size; aperture interiomarginal, umbilical, low arch bordered by a distinct lip; sutures depressed; equatorial periphery lobate; test surface smooth, dense with pores and irregularly spaced spine bases.

Globigerina woodi Jenkins
Plate 1, figure 11

Globigerina woodi JENKINS 1960, p. 352, pl. 2, figs. 2a-2c.

Description: Test low trochospire; 4 spherical to sub spherical chambers in the final whorl increasing regularly in size; aperture interiomarginal, umbilical, high circular arch bordered by a thickened rim; sutures radial, depressed; equatorial periphery quadrate; test surface cancellate with regularly spaced pores in the center of pore pits.

Remarks: Globigerina apertura Cushman is similar in all respects to *G. woodi* but is distinguished by a larger aperture. We identify both taxa in North Atlantic samples but consider them as one group for paleoclimate applications.

Globigerinella aequilateralis (Brady)
Plate 1, figures 12-13

Globigerina aequilateralis BRADY 1879, p. 285 (figs. in Brady 1884, pl. 80, figs. 18-21).

Description: Test low trochospire becoming planispiral in last few chambers; 5-6 globular chambers in final whorl, increasing rapidly in size; aperture interiomarginal, equatorial, low arch; sutures radial, depressed; equatorial periphery lobate; test surface hispid with regularly spaced pores.

Globigerinella pseudobesa (Salvatorini)
Plate 1, figure 14

Turborotalita pseudobesa SALVATORINI 1966, p.10, pl. 2, figs. 6a-15.

Description: Test low trochospire; 4 spherical chambers in final whorl, increasing rapidly in size; aperture interiomarginal, extraumbilical-umbilical, low arch; sutures depressed, radial (sometimes slightly curved on umbilical side); equatorial periphery lobate; test surface densely perforate with spine bases.

Globigerinita glutinata (Egger)
Plate 1, figures 15-16

Globigerina glutinata EGGER 1893, p. 371, pl. 13, figs. 19-21

Description: Test low trochospire; 3-4 spherical chambers in final whorl, increasing rapidly in size; aperture interiomarginal, umbilical, low arch bordered by lip; umbilicus sometimes covered by bulla with peripheral supplementary apertures; sutures depressed, radial; equatorial periphery lobate; test surface microperforate and covered with pustules.

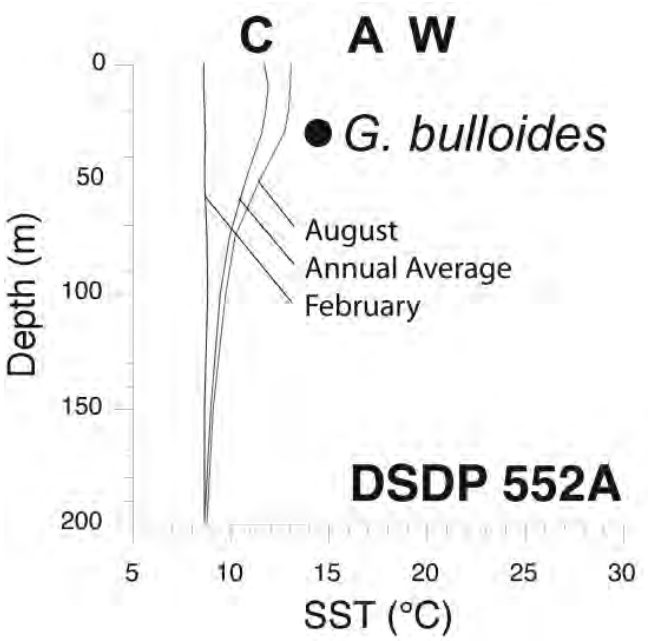

TEXT-FIGURE 8
Multiple proxy mid-Pliocene SST estimates plotted on modern temperature vs. depth curves. C = faunal-based cold season SST estimate. W = faunal-based warm season SST estimate. A = alkenone-derived SST estimate. Dot indicates Mg/Ca-derived SST estimate from *G. bulloides* plotted at this species' preferred habitat. SST estimates are corrected for calibration differences between proxies and plotted as anomalies from modern. August, annual average and February temperatures at depth are from Levitus and Boyer (1994).

Globigerinoides conglobatus Brady
Plate 2, figure 1

Globigerinoides conglobatus BRADY 1879, p. 28b.

Description: Test medium trochospire; 3-3 ½ sub globular chambers in final whorl, increasing gradually in size, ultimate chamber compressed; primary aperture interiomarginal, umbilical, low arch bordered by a rim; sutural supplementary apertures on spiral side; sutures depressed, radial; equatorial periphery rounded; test surface coarsely perforated and covered with spine bases.

Globigerinoides extremus Bolli and Bermudez
Plate 2, figure 2

Globigerinoides obliquus extremus BOLLI and BERMUDEZ 1965, p. 139, pl. 1, figs. 10-12

Description: Test medium to high trochospire; 4 compressed chambers in the final whorl, increasing regularly in size, ultimate chamber often flattened and smaller than penultimate chamber; primary aperture interiomarginal, umbilical, medium arch; supplementary aperture opposite primary aperture on chambers of the final whorl; sutures depressed, radial to slightly curved; test surface pitted.

Remarks: This taxon differs from *Globigerinoides obliquus* by possessing a higher spire and laterally compressed and flattened final chamber.

Globigerinoides fistulosus (Schubert)
Plate 2, figure 3

Globigerina fistulosa SCHUBERT 1910, p. 323, text fig. 1.

Description: Test low trochospire; 3-4 spherical chambers in the final whorl, increasing regularly in size; ultimate and penultimate chambers elongated with fistular extensions; primary aperture interiomarginal, umbilical, broad arch; supplementary apertures over sutures of earlier chambers; sutures depressed, radial to slightly curved; test surface densely perforated.

Globigerinoides obliquus Bolli
Plate 2, figure 4

Globigerinoides obliquus BOLLI 1957, p. 113, pl. 25, figs. 10a-c

Description: Test low trochospire; 3-4 spherical chambers in final whorl, increasing rapidly in size, final chamber compressed; primary aperture interiomarginal, umbilical, high arch; supplementary apertures opposite primary aperture on chambers of the final whorl; sutures depressed, radial; test surface pitted and perforated.

Remarks: *Globigerinoides extremus* differs from this taxon by possessing a higher spire and laterally compressed and flattened final chamber.

Globigerinoides ruber (d'Orbigny)
Plate 2, figure 5

Globigerina rubra D'ORBIGNY 1839, p. 82, pl. 4, figs. 12-14

Description: Test low to high trochospire; 3 sub spherical chambers in final whorl, increasing regularly in size; primary aperture interiomarginal, umbilical, wide arch bordered by a rim; supplementary sutural apertures opposite sutures of earlier chambers; sutures depressed, radial; test surface densely perforated with honeycomb appearance.

Remarks: Globigerinoides ruber is differentiated from *Gs. obliquus* by its primary aperture being centered over the suture between the antepenultimate and penultimate chambers. *Globigerinoides obliquus* has the primary aperture centered over antepenultimate chamber.

Globigerinoides sacculifer (Brady)
Plate 2, figure 6

Globigerina sacculifera BRADY 1877, p. 164, pl. 9, figs. 7–10.

Description: Test low trochospire; 3½ - 4 spherical chambers in final whorl, increasing gradually in size; ultimate chamber often elongated and sack-like; primary aperture interiomarginal, umbilical, low to medium arch bordered by rim; sutures slightly curved and depressed.

Remarks: We include specimens assignable to *Globigerina quadrilobatus* (d'Orbigny) and *Globigerina trilobus* (Reuss). Thus the equatorial periphery ranges from triangular to subquadrate to lobate.

Globorotalia crassaformis (Galloway and Wissler)
Plate 2, figures 7-10

Globigerina crassaformis GALLOWAY and WISSLER 1927, p. 41, pl. 7, fig. 12.

Description: Test low trochospire; 4 compressed chambers in final whorl, increasing rapidly in size, flat on spiral side convex on umbilical side; aperture interiomarginal, extraumbilical-umbilical, low slit arch bordered by lip; sutures depressed, curved on spiral side, radial on umbilical side; equatorial periphery lobate to subquadrate; axial periphery planoconvex-hemispherical; test surface finely perforated and pustulate.

Remarks: We include specimens referable to *Globorotalia ronda* Blow, *Globorotalia oceanica* Cushman and Bermudez and *Globorotalia crassaformis viola* Blow in our concept of this taxon. Specimens of "keeled" *Gr. crassaformis* (Plate 2 figure 10), similar to *Gr. crassaformis viola* are tallied separately from the other morphotypes in our quantitative data.

Globorotalia hirsuta (d'Orbigny)
Plate 2, figure 11

PLATE 1

Scale bars = 100µm

1 *Candeina nitida*, ODP 667A, 6-6, 13cm;

2 *Dentoglobigerina altispira*, DSDP 502A, 19-3, 49.5cm;

3 *Globigerina bulloides*, DSDP 552A, 10-3, 93cm;

4 *Globigerina bulloides*, DSDP 606, 12-1, 132cm;

5 *Globigerina bulloides*, DSDP 552A, 10-2, 90-92cm;

6 *Globigerina decoraperta*, DSDP 607, 14-5, 126cm;

7 *Globigerina falconensis*, DSDP 606, 12-1, 132cm;

8 *Globigerina incisa*, DSDP 610A, 17-2, 42cm;

9 *Globigerina nepenthes*, DSDP 502A, 34-1, 49.5cm;

10 *Globigerina praedigitata*, DSDP 606, 11-6, 56cm;

11 *Globigerina woodi*, DSDP 609B, 24-3, 135cm;

12 *Globigerinella aequilateralis*, DSDP 607, 14-6, 84cm;

13 *Globigerinella aequilateralis*, DSDP 607, 14-6, 24cm;

14 *Globigerinella psuedobesa*, DSDP 606, 11-2, 98cm;

15 *Globigerinita glutinata*, DSDP 502A, 20-1, 50.5cm;

16 *Globigerinita glutinata*, DSDP 502A, 20-1, 50.5cm.

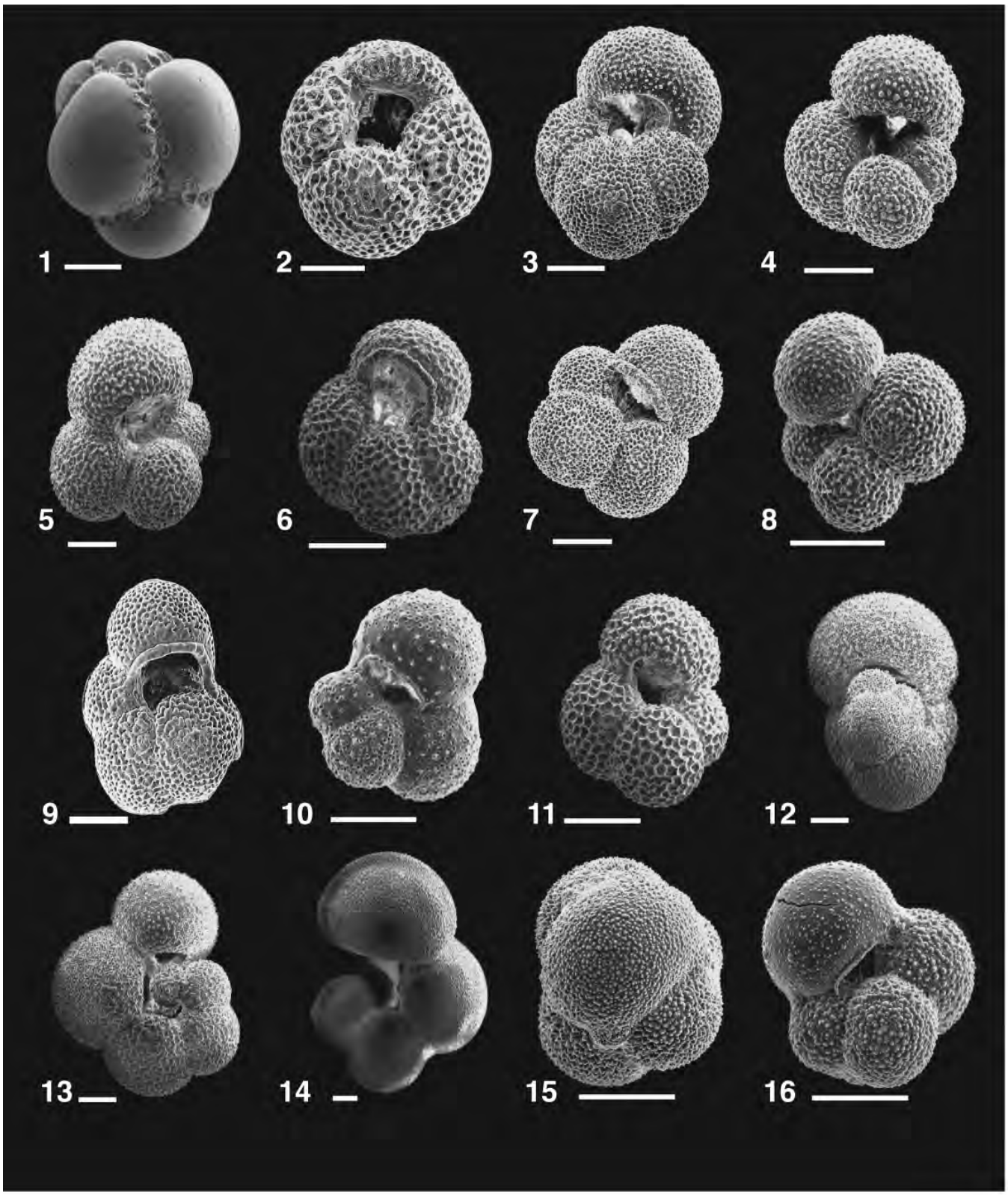
1
2
3
4
5
6
7
8
9
10
11
12
13
14
15
16

Rotalina hirsuta D'ORBIGNY 1839, p. 131, pl. 1, figs. 34–36.

Description: Test high trochospire; 4 chambers in final whorl increasing rapidly in size; aperture interiomarginal, extraumbilical-umbilical, low slit bordered by a weak lip; sutures depressed, curved on spiral side and sinuous on umbilical side; equatorial periphery ovate; axial periphery concavo-convex to weakly biconvex; test surface finely perforated and pustulate.

Globorotalia margaritae Bolli and Bermudez
Plate 2, figure 12

Globorotalia margaritae BOLLI and BERMUDEZ, 1965, p. 138, pl. 1, figs. 1-9.

Description: Test low trochospire; umbilical side slightly concave, spiral side convex; 5 compressed chambers in the final whorl, increasing rapidly in size; aperture interiomarginal, extraumbilical-umbilical, low slit bordered by a lip; sutures on spiral side curved, limbate, raised; sutures on umbilical side depressed and curved; equatorial periphery slightly ovate; axial periphery acute, keeled; test surface densely perforated, early chambers pustulose.

Remarks: Globorotalia margaritae has a last appearance prior to the PRISM time slab but is included because it is an important element of the Early Pliocene fauna.

Globorotalia menardii (Parker, Jones, and Brady)
Plate 2, figure 13, 14

Rotalia menardii PARKER, JONES, and BRADY 1865, p. 20, pl. 3, fig. 81

Description: Test low trochospire; 5-6 wedge shaped chambers in the final whorl, increasing regularly in size; aperture interioriomarginal, extraumbilical-umbilical, low arch bordered by a lip; spiral side sutures raised, strongly curved, umbilical side sutures radial to slightly curved, depressed; equatorial periphery lobate; axial periphery acute, keeled; test surface smooth, densely perforated.

Globorotalia puncticulata (Deshayes)
Plate 2, figure 15, Plate 3, figure 1

Globigerina puncticulata DESHAYES 1832, p. 170 (figs. in Fornasini, 1899, fig. 5)

Description: Test low trochospire; spiral side flat, umbilical side high and vaulted; 4 conical chambers in the final whorl, increasing gradually in size; aperture interiomarginal, extraumbilical-umbilical, high arch bordered by a rim; spiral side sutures depressed, curved; umbilical side sutures sinuous and depressed; equatorial periphery weakly quadrate; axial periphery rounded; test surface finely perforate.

Globorotalia scitula (Brady)
Plate 3, figure 2

Pulvinulina scitula BRADY 1882, p. 27, pl. 5, fig. 5

Description: Test low-medium trochospire; biconvex; 4-5 crescent shaped chambers in final whorl, increasing regularly in size; aperture interiomarginal, extraumbilical-umbilical, low slit bordered by a lip; spiral side sutures raised and curved; umbilical side sutures radial to slightly curved and depressed; equatorial periphery lobate; axial periphery angular with a rim; test surface densely perforated.

Globorotalia tumida (Brady)
Plate 3, figure 3

Pulvinulina menardii (d'Orbigny) var. *tumida* BRADY 1877, pl. 103, figs. 4-6.

Description: Test low trochospire; biconvex; 5-6 wedge shaped chambers in final whorl, increasing gradually in size; aperture interiomarginal, extraumbilical-umbilical, low arch bordered by flat lip; spiral side sutures raised, limbate and curved; umbilical side sutures radial and depressed; equatorial periphery ovate; axial periphery acute with thick keel; test surface densely perforated.

Globorotaloides hexagona (Natland)
Plate 3, figure 4-5

PLATE 2
Scale bars = 100µm

1 *Globigerinoides conglobatus*, ODP 667A, 6-6, 44cm;

2 *Globigerinoides extremus*, DSDP 502A, 21-1, 65.5cm;

3 *Globigerinoides fistulosus*, DSDP 502A, 20-1, 140cm;

4 *Globigerinoides obliquus*, DSDP 502A, 20-1, 50.5cm;

5 *Globigerinoides ruber*, DSDP 502A, 20-1, 50.5cm;

6 *Globigerinoides sacculifer*, DSDP 502A, 20-1, 50.5cm;

7 *Globorotalia crassaformis*, DSDP 606, 11-6, 21cm;

8 *Globorotalia crassaformis*, DSDP 609B, 24-2, 26cm;

9 *Globorotalia crassaformis*, DSDP 609B, 24-2, 26cm;

10 *Globorotalia crassaformis*, DSDP 606, 11-6, 21cm;

11 *Globorotalia hirsuta*, DSDP 606, 12-4, 119cm;

12 *Globorotalia margaritae*, DSDP 502A, 26-1, 95.5cm;

13 *Globorotalia menardii*, ODP 661A, 7-1, 83cm;

14 *Globorotalia menardii*, ODP 661A, 7-1, 83cm;

15 *Globorotalia puncticulata*, DSDP 609B, 24-2, 26cm.

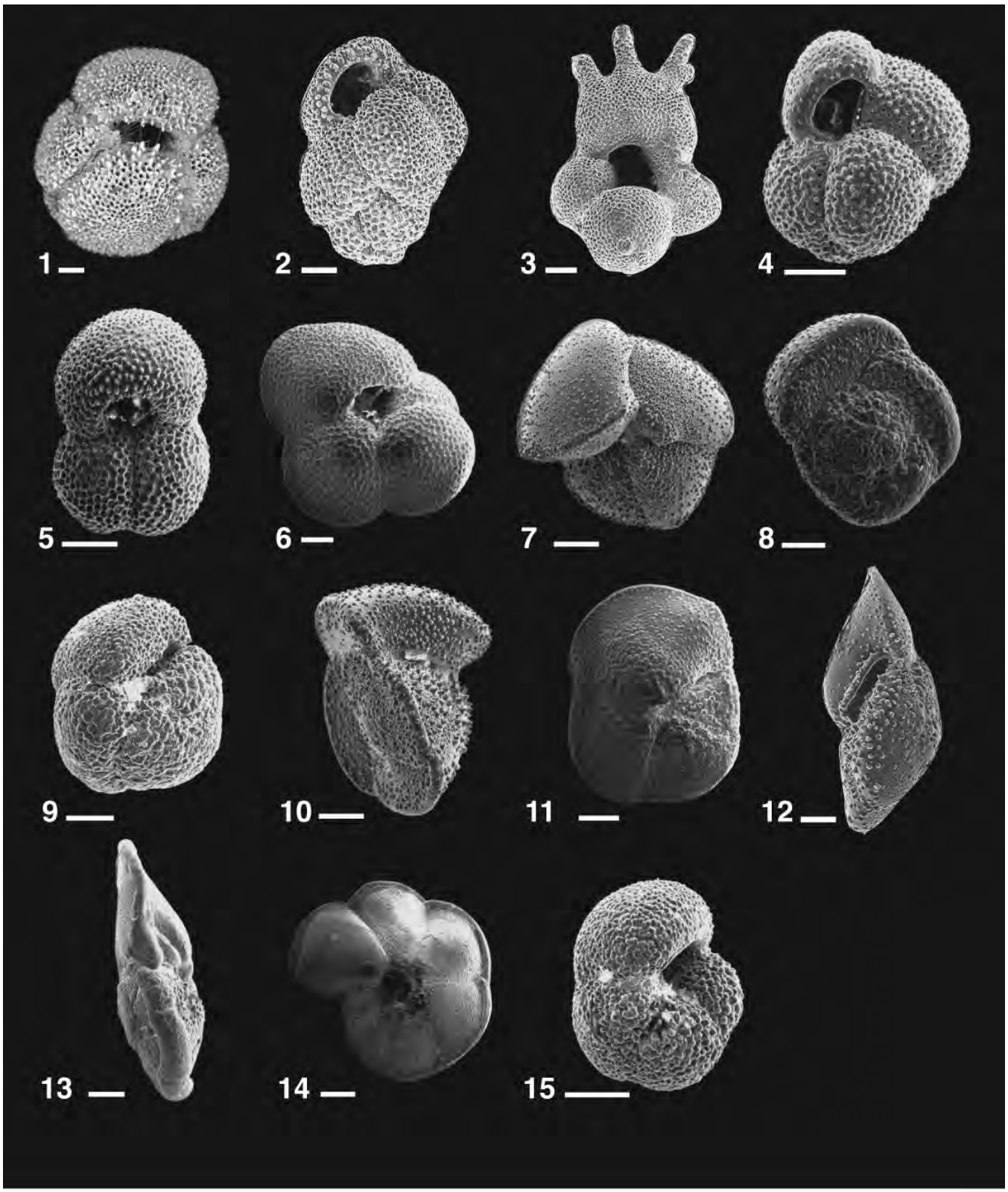
1
2
3
4
5
6
7
8
9
10
11
12
13
14
15

Globigerina hexagona NATLAND 1938, p. 149, pl. 7, figs. 1a-c

Description: Test low trochospire; 5 spherical chambers in final whorl increasing rapidly in size; aperture interiomarginal, extraumbilical-umbilical, low arch bordered by plate; sutures depressed and curved; equatorial periphery lobate; axial periphery rounded; test surface cancellate with pores in hexagonal pore pits.

Neogloboquadrina acostaensis (Blow)
Plate 3, figure 6

Globorotalia acostaensis BLOW 1959, p. 208, pl. 17, figs. 106a-106c.

Description: Test low trochospire; 5-5 ½ spherical chambers in final whorl, increasing gradually in size; aperture interiomarginal, extraumbilical-umbilical, low arch bordered by rim or plate; sutures depressed, radial; equatorial periphery lobate; axial periphery rounded; test surface cancellate with pores and pore pits.

Remarks: We include 4 ½ chambered dextral coiled forms transitional between *N. acostaensis* and *N. pachyderma*. These transitional forms have a distribution similar to the artificial "dupac" taxon of Kipp (1976). See also *N. pachyderma*.

Neogloboquadrina atlantica Berggren
Plate 3, figures 7-8

Neogloboquadrina atlantica BERGGREN 1972, pl. 1, figs. 7-9.

Description: Test low to medium trochospire; 4-5 sub spherical chambers in final whorl, increasing gradually in size; ultimate chamber sometimes kummerform; aperture interiomarginal, extraumbilical-umbilical, low arch bordered by a rim; sutures depressed and radial; equatorial periphery ovate; test surface primarily cancellate.

Remarks: This is a highly variable taxon (see Poore and Berggren 1975). When preservation conditions are less than excellent and using light microscopy, the gross chamber arrangement of *Neogloboquadrina atlantica* and *Globigerina bulloides* can be quite similar in the sub-polar North Atlantic. Care must be taken to distinguish true reticulate-microcrystalline test surface ultrastructure from recalcified globigerine test surface ultrastructure of *Globigerina bulloides* (see also Dowsett and Ishman 1995).

Neogloboquadrina humerosa (Takayanagi and Saito)
Plate 3, figures 9-10

Globorotalia humerosa TAKAYANAGI and SAITO 1962, p. 78, pl. 28, figs. 1a-2b.

Description: Test low trochospire; 6-7 ovate chambers in final whorl, increasing gradually in size; aperture interiomarginal, extraumbilical-umbilical, low arch bordered by a rim; sutures depressed, radial; equatorial periphery lobate, axial periphery rounded; test surface cancellate.

Neogloboquadrina pachyderma (Ehrenberg)
Plate 3, figure 11

Aristopira pachyderma EHRENBERG 1861, p. 276-277, 303.

Description: Test low trochospire; 4-4 ½ sub spherical chambers increasing rapidly in size; ultimate chamber sometimes kummerform; aperture innteriomarginal, extraumbilical-umbilical, low arch bordered by a rim; sutures radial, depressed; equatorial periphery sub quadrate to lobate; test surface cancellate.

Remarks: We recognize dextral and sinistral morphologies in the mid-Pliocene as follows: sinistral are relatively small, compact *Neogloboquadrina* with 4-5 chambers in the ultimate whorl, kummerform ultimate chamber, and a slightly-to-distinct oval equatorial outline. Separating small sinistral *Neogloboquadrina atlantica* from large sinistral *Neogloboquadrina pachyderma* is arbitrary in many high-latitude North Atlantic sites. The dextral coiling morphology is restricted to specimens with four chambers in the ultimate whorl. Dextral forms with more than four chambers in the ultimate whorl have a distinct distribution during the mid-Pliocene, similar to the artificial

---

PLATE 3

Scale bars = 100µm

1 *Globorotalia puncticulata*, DSDP 502A, 21-2, 20cm;

2 *Globorotalia scitula*, ODP 661A, 7-2, 120cm;

3 *Globorotalia tumida*, ODP 661A, 6-6, 119cm;

4 *Globorotaloides hexagona*, ODP 659A, 10-4, 119cm;

5 *Globorotaloides hexagona*, ODP 659A, 10-4, 119cm;

6 *Neogloboquadrina acostaensis*, DSDP 606, 11-3, 58cm;

7 *Neogloboquadrina atlantica*, DSDP 606, 11-4, 79cm;

8 *Neogloboquadrina atlantica*, DSDP 552A, 10-2, 91cm;

9 *Neogloboquadrina humerosa*, ODP 661A, 7-1, 83cm;

10 *Neogloboquadrina humerosa*, ODP 661A, 7-1, 83cm;

11 *Neogloboquadrina pachyderma*, DSDP 552A, 10-3, 93cm;

12 *Orbulina universa*, DSDP 609B, 24-3, 135cm;

13 *Pulleniatina obliquiloculata*, DSDP 502B, 11-2, 131cm;

14 *Sphaeroidinellopsis seminulina*, ODP 661A, 7-1, 83cm;

15 *Turborotalita quinqueloba*, DSDP 552A, 10-3, 93cm.

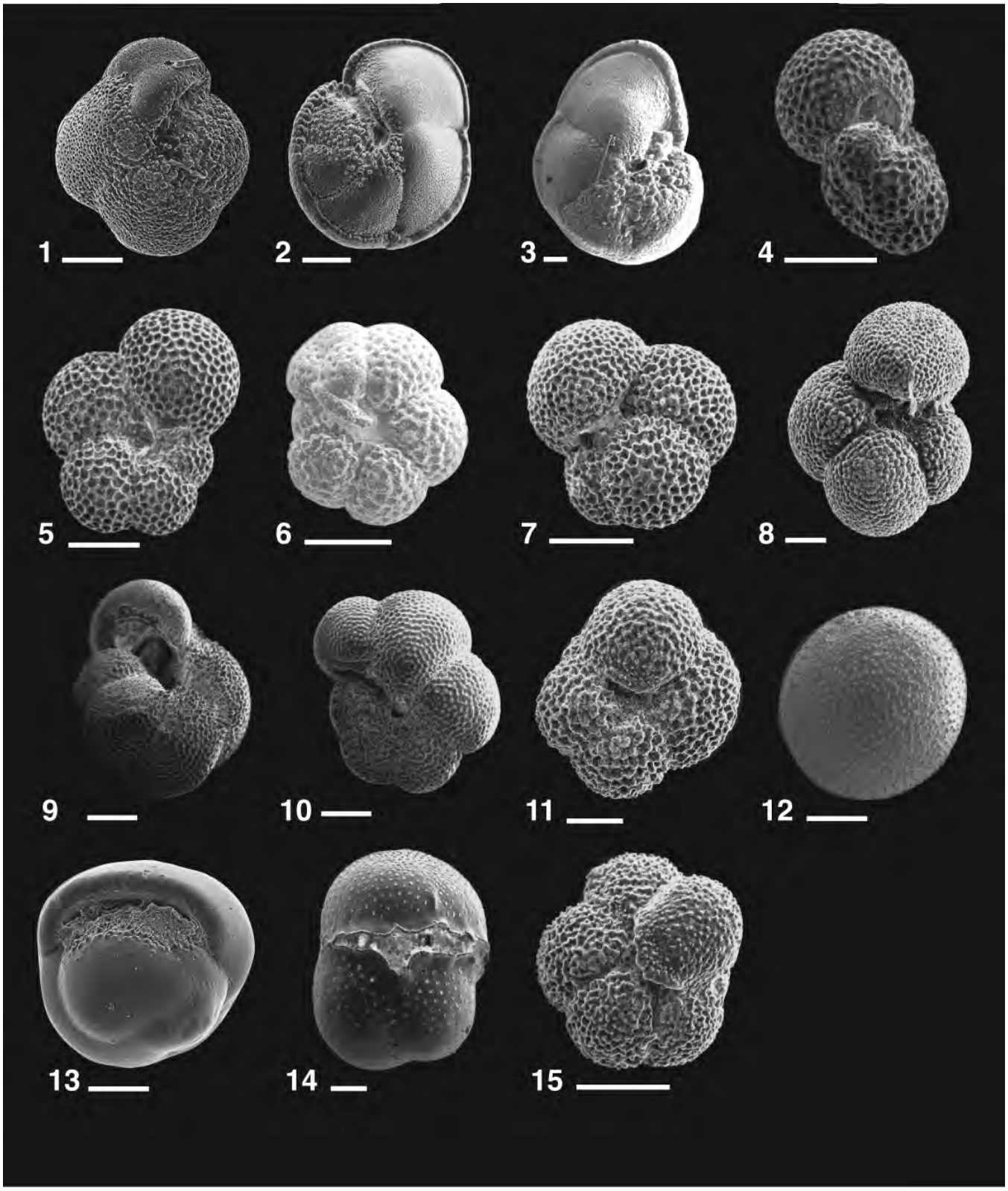
1
2
3
4
5
6
7
8
9
10
11
12
13
14
15

"du-pac" or *N. pachyderma – N. dutertrei* intergrade category used in many Pleistocene studies. See also *N. acostaensis.*

Orbulina universa d'Orbigny
Plate 3, figure 12

Orbulina universa D'ORBIGNY 1839, p. 3, pl. 1, fig. 1

Description: Spherical ultimate chamber completely enveloping earlier whorls; test surface densely perforated with apertural pores scattered across ultimate chamber.

Pulleniatina obliquiloculata (d'Orbigny)
Plate 3, figure 13

Pullenia sphaeroides (d'Orbigny) var. *obliquiloculata* PARKER and JONES 1865, p. 368, pl. 19, figs. 4a–b.

Description: Test streptospiral; 4-5 rounded chambers in final whorl; aperture spiro-umbilical, low arch; sutures indistinct; axial periphery rounded; test surface smooth.

Sphaeroidinellopsis seminulina (Schwager)
Plate 3, figure 14

Globigerina seminulina SCHWAGER 1866, p. 256, pl. 7, fig. 112.

Description: Test low trochospire; 3 sub globular chambers in final whorl; aperture elongate umbilical opening through cortex; sutures hidden by cortex; equatorial periphery ovate to triangular; test surface covered by perforated secondary cortex.

Turborotalita quinqueloba (Natland)
Plate 3, figure 15

Globigerina quinqueloba NATLAND 1938, p. 149, pl. 6, figs. 7a-c.

Description: Test low trochospire; 5 sub globular chambers in final whorl, increasing rapidly in size; ultimate chamber elongated, ovate with flap extending over umbilicus; aperture umbilical, low slit bordered by umbilical flap extending from ultimate chamber; sutures depressed, radial; equatorial periphery slightly lobate; test surface spinose.

ACKNOWLEDGMENTS

This paper benefited from reviews by Thomas Cronin, Debra Willard, Robert Fleisher and an anonymous reviewer. We thank Rocío Caballero for help with various aspects of data reduction. This work is a product of the U.S. Geological Survey Earth Surface Dynamics Program.

REFERENCES

BERGGREN, W. A., 1972. Cenozoic biostratigraphy and paleobiogeography of the North Atlantic. In: Laughton, A.S. et al., *Initial Reports of the Deep Sea Drilling Project, volume 12*, 965-1000. Washington, DC: US Government Printing Office.

BERGGREN, W. A., KENT, D. V., SWISHER, C. C. and AUBRY, M.-P., 1995. A revised Cenozoic geochronology and chronostratigraphy. In: Berggren, W. A., Kent, Aubry, M.-P. and Hardenbol, J., Eds., *Geochronology, time scales and global stratigraphic correlation*, 129-212. Tulsa, Society for Sedimentary Geology Special Publication 54.

BLOW, W. H., 1959. Age, correlation, and biostratigraphy of the Upper Tocuyo (San Lorenzo) and Pozon Formations, Eastern Falcon, Venezuela. *Bulletins of American Paleontology*, 39(178): 1-105.

———, 1969. Late middle Eocene to Recent planktonic foraminiferal biostratigraphy. In: Bronnimann, P., and Renz, H. H., Eds., *Proceedings of First International Conference on Planktonic Microfossils, Geneva, 1967,* 199-422. Leiden: E. J. Brill.

BOLLI, H. M., 1957. Planktonic foraminifera from the Oligocene-Miocene Cipero and Lengua Formations of Trinidad, B.W.I. *Bulletins of the U.S. National Museum*, 215: 97-123.

BOLLI, H. M., and BERMUDEZ, P. J., 1965. Zonation based on planktonic foraminifers of Middle Miocene to Pliocene warm-water sediments. *Asociación Venezolana de Geologia, Mineralogia y Petroleo, Boletin Informativo*, 8:119-149.

BOLLI, H. M., and SAUNDERS, J. B., 1985. Oligocene to Holocene low latitude planktic foraminifera. In: Bolli, H. M., Saunders, J. B., and Perch-Nielsen, K., Eds., *Plankton Stratigraphy*, 155-262. Cambridge: Cambridge University Press.

BRADY, H. B., 1877. Supplementary note on the foraminifers of the Chalk (?) of the New Britain Group. *Geological Magazine*, 4:534–546.

———, 1879. Notes on some of the reticularean Rhizopoda of the Challenger Expedition, Part II. Additions to the knowledge of the porcellanous and hyaline types. *Quarterly Journal of the Microscopical Society*, 19:261–299.

———,1882. Report on the Foraminifers. In Tizard, L., and Murray, J., Eds., Exploration of the Faroe Channel during the summer of 1880, in Her Majesty's Ship *Knight Errant*, with subsidiary reports. *Proceedings of the Royal Society, Edinburgh*, 11:708–717.

———,1884. Report on the Foraminifera dredged by *H.M.S. Challenger,* during the years 1873–1876. *Reports of the Scientific Results of the Challenger Expedition, Zoology,* 9:1–814.

BRONNIMANN, P. and RESIG, J., 1971. A Neogene Globigerinacean biochronologic time-scale of the southwestern Pacific. In: Winterer, E.L. et al., *Initial Reports of the Deep Sea Drilling Project, Volume 7*, 1235-1469. Washington, DC: US Government Printing Office.

BUKRY, D., 1973. Low-latitude coccolith biostratigraphic zonation. *Initial Reports of the Deep Sea Drilling Project, Volume 15,* 685-703. Washington, DC: US Government Printing Office.

———, 1975. Coccolith and Silicoflagellate Stratigraphy, Northwestern Pacific Ocean, Deep Sea Drilling Project Leg 32. *Initial Reports of the Deep Sea Drilling Project Volume 32,* 677-701. Washington, DC: US Government Printing Office.

CHANDLER, M., RIND, D. and THOMPSON, R. 1994. Joint investigations of the middle Pliocene climate II: GISS GCM Northern Hemisphere results. *Global and Planetary Change*, 9:197-219.

CRONIN, T. M. 1991a. Late Neogene marine ostracoda from Tjörnes, Iceland. *Journal of Paleontology*, 65: 767-794.

———, 1991b. Pliocene shallow water paleoceanography of the North Atlantic Ocean based on marine ostracodes. *Quaternary Science Reviews*, 10:175-188.

CUSHMAN, J. A. and JARVIS, P. W., 1936. Three new Foraminifera from the Miocene Bowden Marl, of Jamaica. *Cushman Laboratory for Foraminiferal Research Contributions*, 12: 3-5.

DARLING K. F., M. KUCERA, C. J. PUDSEY, C. M. WADE., 2004. Molecular evidence links cryptic diversification in polar planktonic protists to Quaternary climate dynamics. *Proceedings of the National Academy of Science,* 101:7657–7662.

DESHAYES, G. P., 1832. *Encyclopedie methodique; Histoire naturelle des vers*, Mme. V. Agasse, vol. 2, pp. 1-594; vol. 3, pp. 595-1152.

d'ORBIGNY, A. D., 1839. Foraminifères. In de la Sagra, R., Ed., *Histoire Physique, Politique et Naturelle de L'isle de Cuba*: Paris: Arthus Bertrand, 8:1–224.

———, 1826. Tableau meìthodique de la classe des ceìphalopodes. *Annals des Sciences Naturelle, Paris*, Ser. 1, 7:96–314.

DOWSETT, H. J., in press. The PRISM Palaeoclimate Reconstruction and Pliocene Sea-Surface Temperature. In: Williams, M., Haywood, A., Gregory, J. and Schmidt, D., Eds., *Deep Time Perspectives on Climate Change: Marrying biological proxies and Climate Models.* London: Micropalaeontological Society & the Geological Society.

———, 1991. The development of a long-range foraminifer transfer function and application to Late Pleistocene North Atlantic climatic extremes. *Paleoceanography* 6: 259-273.

DOWSETT, H. J., BARRON, J.A, POORE, R.Z., THOMPSON, R.S., CRONIN, T.M., ISHMAN, S.E. and WILLARD, D.A., 1999. *Middle Pliocene Paleoenvironmental Reconstruction: PRISM2.* U.S. Geological Survey Open File Report 99-535, 236 pp. http://pubs.usgs.gov/openfile/of99-535/.

DOWSETT, H.J., CHANDLER, M.A., CRONIN, T.M. and DWYER, G.S. 2005. Middle Pliocene sea surface temperature variability. *Paleoceanography* 20, PA2014, doi:10.1029/2005PA001133.

DOWSETT, H. J., CRONIN, T. M., POORE, R. Z., THOMPSON, R. S., WHATLEY, R. C. and WOOD, A. M. 1992. Micropaleontological evidence for increased meridional heat transport in the North Atlantic Ocean during the Pliocene. *Science*, 258:1133-1135.

DOWSETT, H. J., GOSNELL, L. B. and POORE, R. Z., 1988. *Pliocene planktic foraminifer census data from Deep Sea Drilling Project Holes 366A, 410, 606, and 646B.* U.S. Geological Survey Open File Report 88-654: 14p.

DOWSETT, H. J. and ISHMAN, S. E., 1995. Middle Pliocene planktonic and benthic foraminifers from the subarctic North Pacific: Sites 883 and 887. *Proceedings of the Ocean Drilling Program, Scientific Results*, 145: 141-156.

DOWSETT, H. J. and POLANCO, E. F., 1992. *Pliocene planktic foraminifer census data from Deep Sea Drilling Project Holes 541 and 546:* U.S. Geological Survey Open File Report 92-418, 4p.

DOWSETT, H. J. and POORE, R. Z., 1990. A new planktic foraminifer transfer function for estimating Pliocene through Holocene Sea Surface temperatures. *Marine Micropaleontology* 16: 1-23.

———, 2000. Data Report: Pliocene planktonic foraminifers from the California margin: Site 1021. In: Lyle, M., Koizumi, I., Richter, C., and Moore, T. C., Jr., Eds., *Proceedings of the Ocean Drilling Program, Scientific Results,* 167: 115-117.

DOWSETT, H. and ROBINSON, M., 1998. Application of the modern analog technique (MAT) of sea surface temperature estimation to middle Pliocene North Pacific planktic foraminifer assemblages. *Paleontologia Electronica*, 1. http://www.odp.tamu.edu/paleo/1998_1/dowsett/issue1.htm

———, 2006. Stratigraphic framework for Pliocene paleoclimate reconstruction: the correlation conundrum. *Stratigraphy*, 3:53-64.

DOWSETT, H. J., THOMPSON, R. S., BARRON, J. A., CRONIN, T. M., FLEMING, R. F., ISHMAN, S. E., POORE, R. Z., WILLARD, D. A. and HOLTZ, Jr., T. R., 1994. Paleoclimatic reconstruction of a warmer earth: PRISM Middle Pliocene Northern Hemisphere synthesis. *Global and Planetary Change*, 9: 169-195.

DOWSETT, H. J. and WEST, S. M. 1992. Pliocene planktic foraminifer census data from Deep Sea Drilling Project Hole 607 and Ocean Drilling Program Hole 661A: *U.S. Geological Survey Open File Report* 92-413, 4p.

EGGER, J. G., 1893. Foraminiferen aus Meeresgrundproben gelothet von 1874 bis 1876 von S. M. Sch. "Gazelle." *Abhandlungen Bayerische Akademie Wissenschaftliche, Mathematik Physik. Kl.*, 18:193–458.

EHRENBERG, C.G., 1861. Elemente des tiefen Meeresgrundes in Mexikanischen Golfstrome bei Florida; Ueber die Tiefgrund-Verhaltnisse des Oceans am Eingang der Davisstrasse und bei Island. *Konigliche Preussischen Akademie der Wissenschaftliche Berlin, Monatsberichte,* 276–277.

FOLEY, K.M. and DOWSETT, H.J., 1992. *Pliocene planktic foraminifer census data from Ocean Drilling Program Holes 667 and 659A.* U.S. Geological Survey Open File Report 92-434, 8p.

FORNASINI, C., 1899. Le Globigerine fossili d'Italia. *Paleontographia Italia,* 4, 203-216.

GALLOWAY, J.J., and WISSLER, S.G., 1927. Pleistocene foraminifers from the Lomita Quarry, Palos Verdes Hills, California. *Journal of Paleontology*, 1:35–87.

HAYWOOD, A.M., VALDES, P.J., FRANCIS, J.E . and SELLWOOD, B.W., 2002. Global middle Pliocene biome reconstruction: A data/model synthesis. *Geochemistry, Geophysics, Geosystems*, 3:1072, doi:10.1029/2002GC000358.

HAYWOOD, A.M. and VALDES, P.J. 2004. Modeling Pliocene warmth: contributions of atmosphere, oceans and cryosphere. *Earth and Planetary Science Letters*, 218: 363-377.

HAYWOOD, A. M., VALDES, P.J., AND PECK, V.L., 2007. A permanent El Nino–like state during the Pliocene?, *Paleoceanography*, 22, doi:10.1029/2006PA001323.

HOOPER, P. W. P., and WEAVER, P. P. E., 1987. Late Neogene species of the genus Neogloboquadrina Bandy, Frerichs and Vincent in the North Atlantic: a biostratigraphic, paleoceanographic and phylogenetic review. In: Hart, M. B., Ed., *Micropaleontology of carbonate environments*, 21-43. Chichester, U.K.: Ellis Horwood Limited.

IPCC, 2001. *Climate Change 2001: Synthesis Report. A contribution of Working Groups I, II, and III to the Third Assessment Report of the Integovernmental Panel on Climate Change.* Watson, R.T. and the Core Writing Team, Eds. Cambridge and New York: Cambridge University Press, 398 pp.

JENKINS, D.G., 1960. Planktonic foraminifers from the Lakes Entrance oil shaft, Victoria, Australia. *Micropaleontology*, 6:345–371.

JIANG, D., WANG, H., DING, Z., LANG, X. and DRANGE, H., 2005. Modeling the middle Pliocene climate with a global atmospheric general circulation model. *Journal of Geophysical Research*, 110, D14107, doi:10.1029/2004JD005639.

KENNETT, J. P. and P. VELLA, 1975. Late Cenozoic planktonic foraminifera and paleoceanography at DSDP Site 284 in the cool subtropical South Pacific. *Initial Reports of the Deep Sea Drilling Project, volume 29,* 769-799. Washington, DC: US Government Printing Office.

KENNETT, J. P. and M. S. SRINIVASAN, 1983. *Neogene Planktonic Foraminifera: A Phylogenetic Atlas.* Stroudsburg, Pennsylvania:Hutchinson Ross, 230 pages.

KIPP, N.G., 1976. New transfer function for estimating past sea-surface conditions from sea-bed distribution of planktonic foraminiferal assemblages in the North Atlantic. In: Cline, R. M. and Hays, J. D.,

Eds., *Investigations of late Quaternary Paleoceanography and Paleoclimatology,* 3-41. Geological Society of America Memoir, 145.

LEVITUS, S. and BOYER, T., 1994. *World Ocean Atlas Volume 4: Temperature.* NOAA Atlas NESDIS 4. Washington, DC: US Government Printing Office.

LOUBERE, P. and MOSS, K., 1986. Late Pliocene climatic change and the onset of Northern Hemisphere glaciation as recorded in the northeast Atlantic Ocean. *Geological Society of America Bulletin*, 97: 818-828.

LOUBERE, P., 1988. Gradual late Pliocene onset of glaciation: a deep-sea record from the northeast Atlantic. *Palaeoclimatology, Palaeogeography, Palaeobiology,* 63:327-334.

LISIECKI, L.E. and RAYMO, M.E., 2005. A Plio-Pleistocene stack of 57 globally distributed benthic $\delta^{18}O$ records, *Paleoceanography* 20, PA1003, doi:10.1029/2004PA001071.

LOURENS, L. J., ANTONARAKOU, A., HILGEN, F. J., VAN HOOF A. A. M., VERGNAUD-GRAZZINI, C. and ZACHARIASSE, W. J. 1996. Evaluation of the Plio-Pleistocene astronomical timescale. *Paleoceanography*, 11: 391-413.

MARTINI, E., 1971. Standard Tertiary and Quaternary calcareous nannoplankton zonation. In: Ferinacci, A., Ed., *Proceedings of the Second International Planktonic Conference, Roma, 1970, Vol. 2*, 739-785. Rome: Tecnoscienza.

NATLAND, M. L., 1938. New species of Foraminifers from off the West Coast of North America and from the later Tertiary of the Los Angeles basin. *Scripps Institution of Oceanography Bulletin, Technical Series,* 4:137–152.

NATIONAL RESEARCH COUNCIL, Committee on Abrupt Climate Change 2002. *Abrupt Climate Change: Inevitable Surprises*. Washington, DC: National Academies Press, 244p.

PARKER, F. L., 1962. Planktonic foraminiferal species in Pacific sediments. *Micropaleontology*, 8: 219-254.

———, 1967. Late Tertiary biostratigraphy (Planktonic Foraminifera) of tropical Indo-Pacific deep-sea cores. *Bulletins of American Paleontology*, 52: 115-208.

PARKER, W. K., and JONES, T. R., 1865. On some foraminifers from the North Atlantic and Arctic Oceans, including Davis Straits and Baffin's Bay. *Philosophical Transactions of the Royal Society of London*, 155:325–441.

PARKER, W. K., JONES, T. R., and BRADY, H. B., 1865. On the nomenclature of the foraminifers, Part XII. The species enumerated by d'Orbigny in the "Annales des Sciences Naturelles, vol. 7, 1826." *Annals and Magazine of Natural History, Ser. 3, 16:15–41.*

POORE, R. Z., 1979. Oligocene through Quaternary planktonic foraminiferal biostratigraphy of the North Atlantic: DSDP Leg 49. *In* Luydendyk, B. P., Cann, J. R., et al., *Initial Reports of the Deep Sea Drilling Project Volume 49*, 447-517. Washington, DC: US Government Printing Office.

_____, 1991. *Pliocene planktic foraminifer census data from Deep Sea Drilling Project Hole 603C.* U.S. Geological Survey Open File Report 91-309, 7p.

POORE, R. Z., and BERGGREN, W. A., 1975, The morphology and classification of *Neogloboquadrina atlantica* (Berggren). *Journal of Foraminiferal Research,* 5: 77-84.

PRELL, W., MARTIN, A., CULLEN, J. and TREND, M., 1999. *The Brown University Foraminiferal Data Base*, IGBP PAGES/World Data Center-A for Paleoclimatology, Data Contribution Series #1999-027. Boulder CO: NOAA/NGDC Paleoclimatology Program, USA.

PRISM Project Members, 1996. Pliocene Planktic Foraminiferal Census Data from 19 Core Sites in the North Atlantic Region. *U.S. Geological Survey Open-File Report* 96-669.

SALVATORINI, G., 1966. Alcuni nuova specie di foraminiferi del Miocene superiori della Toscana Marittima. *Atti della Societa Toscana di Scienze Naturali Residente in Pisa Memorie Serie A*, 73

SCHUBERT, R. J., 1910. Ueber Foraminiferen und einen Fischotolithen aus dem fossilen Globigerinenschlamm von Neu-Guinea. *Verhandlungen der Geologisches Reichs-anstalt,* Wien, 318–328.

SCHWAGER, C., 1866. Fossile Foraminiferen von Kar Nikobar. Novara Expedition, 1857–1859, *Wien, Geologische Theil*, 2: 187–268.

SHACKLETON, N. J., HALL, M. A. and PATE, D. 1995. Pliocene stable isotope stratigraphy of Site 846. In: Pisias, N. G., Mayer, L. A., Janecsek, T.R., et al., *Proceedings of the Ocean Drilling Program, Scientific Results volume 138,* 337-355. College Station, TX: Ocean Drilling Program.

SLOAN, L.C., CROWLEY, T.J. and POLLARD, D. 1996. Modeling of middle Pliocene climate with the NCAR GENESIS general circulation model. *Marine Micropaleontology*, 27: 51-61.

TAKAYANAGI, Y. and SAITO, T., 1962. Planktonic Foraminifera from the Nobori Formation, Shikoku, Japan. *Science Reports, Tohoku University*, *special volume 5 (ser.2 [Geology]),* 67-106.

THUNELL, R.C. 1979a. Climatic evolution of the Mediterranean Sea during the last 5.0 million years. *Sedimentary Geology*, 23: 67-79.

———, 1979b. Pliocene-Pleistocene paleotemperature and paleosalinity history of the Mediterranean Sea: Results from DSDP Sites 125 and 132. *Marine Micropaleontology*, 4: 173-187.

TODD, R., 1957. Smaller foraminifers. In: *Geology of Saipan, Mariana Islands (Pt. 3), Paleontology*, 265–320. U.S. Geological Survey Professional Paper 280-H.

WEAVER, P. P. E., 1987. Late Miocene to Recent planktonic foraminifers from the North Atlantic: Deep Sea Drilling Project Leg 94. In: Ruddiman, W. R, Kidd, R. B., Thomas, E., et al., *Initial Reports of the Deep Sea Drilling Project, Volume 94, Pt. 2,* 703-727. Washington, DC: US Government Printing Office.

WIGGS, L. B. and POORE, R. Z., 1991. *Pliocene planktic foraminifer census data from Deep Sea Drilling Project Holes 502A, B, C.* U.S. Geological Survey Open File Report, 91-325.

WIGGS, L. B. and DOWSETT, H. J., 1992. *Pliocene planktic foraminifer census data from Deep Sea Drilling Project Hole 396 and Ocean Drilling Program Hole 672.* U.S. Geological Survey Open File Report, 92-414.

WILLARD, D. A. 1994, Palynological record from the North Atlantic region at 3 Ma: vegetational distribution during a period of global warmth. *Review of Palaeobotany and Palynology,* 83: 275-297.

Manuscript received November 13, 2006
Revised manuscript accepted April 17, 2007

Nannofossil biostratigraphy of the Paleocene-lower Eocene succession in the Thamad area, east central Sinai, Egypt

Mahmoud Faris[1] and Aziz Mahmoud Abu Shama[2]

[1]*Geology Department, Faculty of Science, Tanta University, Egypt*
email: mhmfaris@yahoo.com

[2]*Biological and Geological Sciences Department, Faculty of Education Kafr El Sheikh University, Egypt*
email: mabushama2002@yahoo.com

ABSTRACT: In the Thamad area, east central Sinai, two stratigraphic sections are measured and sampled; Gebel El Mishiti and G. El Keeh, in order to determine the nannofossil biostratigrapy of the Paleocene-lower Eocene rocks. Gebel El Mishiti section is considered one of the most complete sections across the K/P boundary in Egypt where all the exposed rocks at G. El Keeh belong to the lower Eocene Egma Formation.

A nearly complete sucession of Paleocene nannofossil biozones is recorded from the Esna Formation at G. El Mishiti. They are arranged from base to top as follows: *Markalius inversus* (NP1), *Cruciplacolithus tenuis* (NP2), *Chiasmolithus danicus* (NP3), *Ellipsolithus macellus* (NP4), *Fasciculithus tympaniformis* (NP5), *Heliolithus kleinpellii* (NP6), *Discoaster mohleri* (NP7/8) and *Discoaster multiradiatus* (NP9) zones.

The Danian/Selandian boundary is located at the base of Zone NP5 at the level of the first appearance of *Fasciculithus* taxa. The Selandian/Thanetian boundary can be traced tentatively at the base of the *Discoaster mohleri* Zone (NP7/8). The Paleocene/Eocene boundary is traced between the NP9a/NP9b subzonal boundary which is marked by the first appearances of *Discoaster araneus*, *Rhomboaster calcitrapa, R. bitrifida* and *R.cuspis*. The Paleocene /Eocene boundary lies within the upper part of the Esna Formation.

A very thin layer of conglomeratic chalk with no paleontological break is located between Zone NP9 and NP10. However, a very short nannofossil break is noted within Zone NP10 (subzones NP10b and NP10c are missing) which is overlain by Zone NP11. The lower part of the latter covers the topmost part of the Esna Formation where its upper part lies within the base of the Egma Formation; therefore, a conformable relationship between the two formations is suggested.

At Gebel El Mishiti, the lower Eocene nannofossil biozones NP11, NP12, NP13 and lower/middle Eocene Zone NP14 are recorded. On the other hand, Gebel El Keeh section, which is about 95m thick is only represented by the *Discoaster sublodoensis* Zone (NP14).

INTRODUCTION

The Thamad (Themed) area is located in east central Sinai between latitude 29º32'-29º52'N and longitudes 34º8-34º40' E. The material for the present study was collected from the Paleocene and lower Eocene secession in this area. Two lithostratigraphic sections were measured, described and sampled in detail. These were Gebel El Mishiti and Gebewl El Keeh (text-fig. 1).

The Paleocene-lower Eocene succession in the studied area comprises two mappable rock units with the Esna Formation (shale facies) underlying the Egma Formation (limestone facies). The Esna Formation consists of calcareous and argillaceous marl intercalated by carbonate ledges. The Egma Formation rests conformably on the Esna Formation and is composed of massive to poorly bedded chalky limestone with several chert bands (text-fig. 2).

This study describes the nannofossil biozones of the Paleocene-Eocene interval and discusses the most critical nannofossil evidences for the location of the Danian/Selandian, Selandian/Thanetian, Paleocene/Eocene and lower Eocene/middle Eocene boundaries in the Thamad area, east central Sinai, Egypt. Examination of the calcareous nannofossils was carried out in the present study with the help of the polarizing microscope (Olympus BH) using 1250X magnification. Smear slides of each sample were prepared using the techniques used by Perch-Nielsen (1985). Geochemical analyses were carried out at the Central Laboratories Sector of the Egyptian Geological Survey.

NANNOFOSSIL BIOSTRATIGRAPHY

The lower Paleogene standard zonation proposed by Martini (1971) is adopted here. The nannofossil events in the Paleocene-Eocene interval in the studied sections are shown on text-figure 3. The distribution of the biozones and the stratigraphic ranges of the nannofossil species are presented in text-figures 4-5. Selected nannofossil taxa are illustrated on plates 1-3.

PALEOCENE BIOZONES

At Gebel El Mishiti, all the Paleocene biozones of Martini (1971) are recognized and they conformably overlie the uppermost Maastrichtian *Micula prinsii* Zone. This section is regarded as one of the most complete Cretaceous/Paleocene boundary interval in Egypt (Faris and Abu Shama 2003). The Paleocene biozones at Gebel El Mishiti and their characteristics are discussed below:

Markalius inversus Zone (NP1)

This zone includes the interval from the increased frequency of *Thoracosphaera operculata* to the lowest occurrence (LO) of the *Cruciplacolithus tenuis.* The calcareous nannoplankton taxa in Zone NP1 are the same as the *Micula prinsii* Zone, in addition to the increased frequency of *Thoracosphaera operculata* and *T. saxea* and the presence of rare *Biantholithus sparsus* and

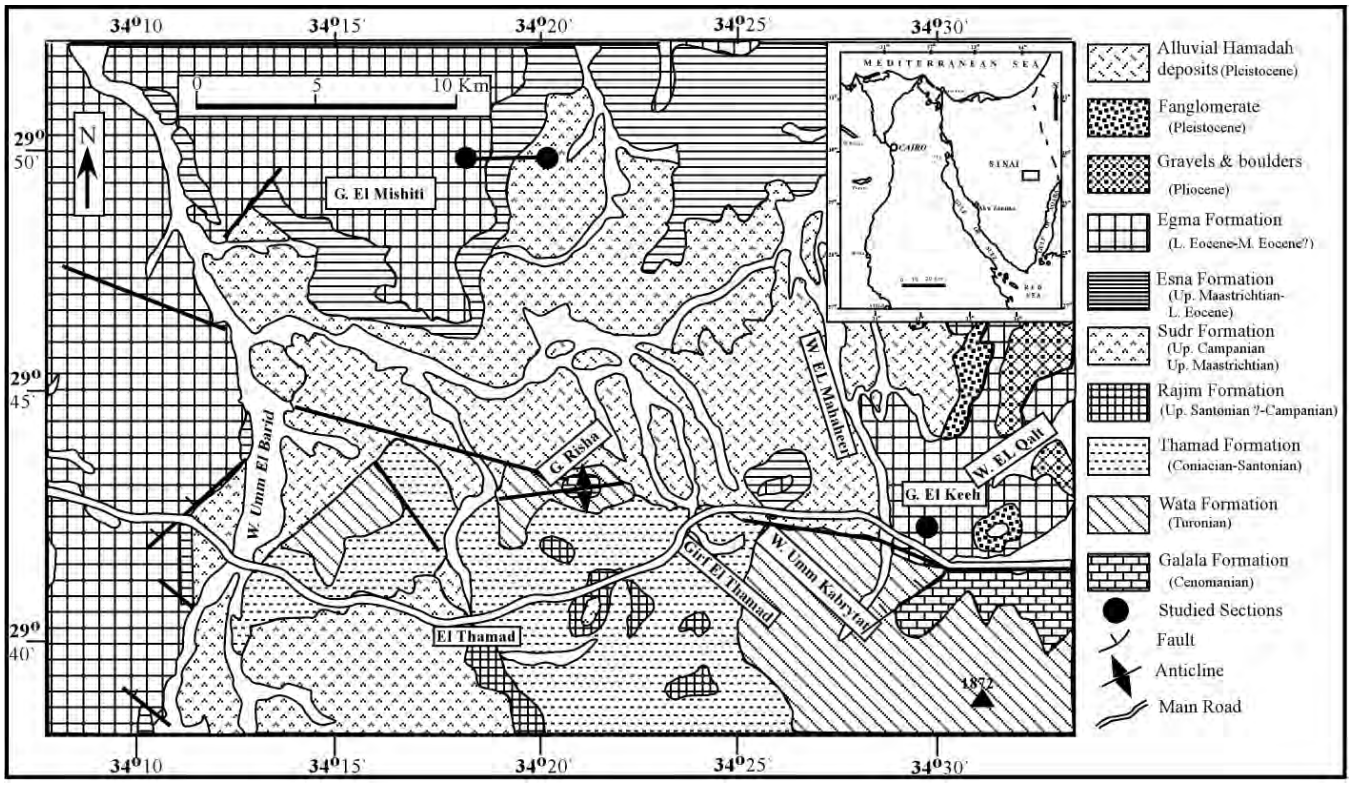

TEXT-FIGURE 1
Geological map of the Thamad area, east central Sinai (modified from Geological Map of Sinai, 1994).

Biscutum constans. The abundance of *Placozygus sigmoides* varies from rare to few. However, abrupt decrease of Cretaceous taxa is recorded in this zone. Rare specimens of *Cruciplacolithus primus* (small) are present at the lower part of this zone, but rare *C. primus* of large sizes are recorded at the top of the zone.

***Cruciplacolithus tenuis* Zone (NP2)**

The *Cruciplacolithus tenuis* Zone is the interval from the LO of *C. tenuis* to the LO of *Chiasmolithus danicus*. This zone reaches about one meter in thickness, and it consists of dark grey argillaceous marl. It is represented by Sample M46 and M47 where the nannofossils are very abundant and well preserved. Although Cretaceous taxa are still present, their abundance is greatly reduced. Survivors such as *Thoracosphaera operculata*, *T. saxea, Cyclagelosphaera reinhardtii, Chiastozygus ultimus* and *Placozygus sigmoides* are still abundant. However, *Zygolithus crux* does not occur in this zone. In addition, the total abundance of survivors has decreased in Zone NP2.

***Chiasmolithus danicus* Zone (NP3)**

This zone is defined as the interval from the LO of *Chiasmolithus danicus* to the LO of *Ellipsolithus macellus.* Its thickness reaches about 21m; it consists of dark grey argillaceous marl and dark grey calcareous marl, represented by Samples M48-M69. Except for Samples M55, M60 and M61 that contain moderately preserved calcareous nannofossils, all samples yielded well-preserved taxa. The LOs of the two zonal markers *Chiasmolithus danicus* and *Cruciplacolithus edwardsii* are found together in Sample M48. At the top of this zone only two vanishing Cretaceous species, *Micula decussata* and *Watznaueria barnesae*, are recorded. These are dissolution resistant forms. The incoming early Paleocene species become more common and diversified at the top of Zone NP3.

A count of tentatively interpreted warm-water and cool-water taxa in our sections reveals the prevalence of cool-water taxa at the end of Danian. Similarly, Bassiouni et al. (1991) recorded decreased values of the ratio between warm-water/cool-water taxa in the Ain Dabadib section, Kharga Oasis, suggesting a slight cooling in the surface waters at the end of the Danian. It is worth mentioning here that the mid Zone NP3 (Samples M55 and M56) contains none of the incoming Paleocene species but the abundance of the vanishing Cretaceous and survivors increases. At the base of this zone, the size of *Placozygus sigmoides* increases to about 10µm while the size of *Eiffellithus turriseffelii* is decreased.

***Ellipsolithus macellus* Zone (NP4)**

It is defined as the interval from the LO of *Ellipsolithus macellus* to the LO of *Fasciculithus tympaniformis*. Noticeable lithologic changes took place from yellowish grey, nodular calcareous marl at the top of NP3 to dark grey, fissile calcareous marl at the base of Zone NP4. This zone is about 5.5m thick, and represented by Samples M70 and M71. The calcareous nannofossil assemblages which are very abundant at the base of the zone, becoming abundant at its top and most assemblages are well preserved. Except for the occurrence of the delicate form *Ellipsolithus macellus*, all the nannofossil taxa are the same as in the top of Zone NP3.

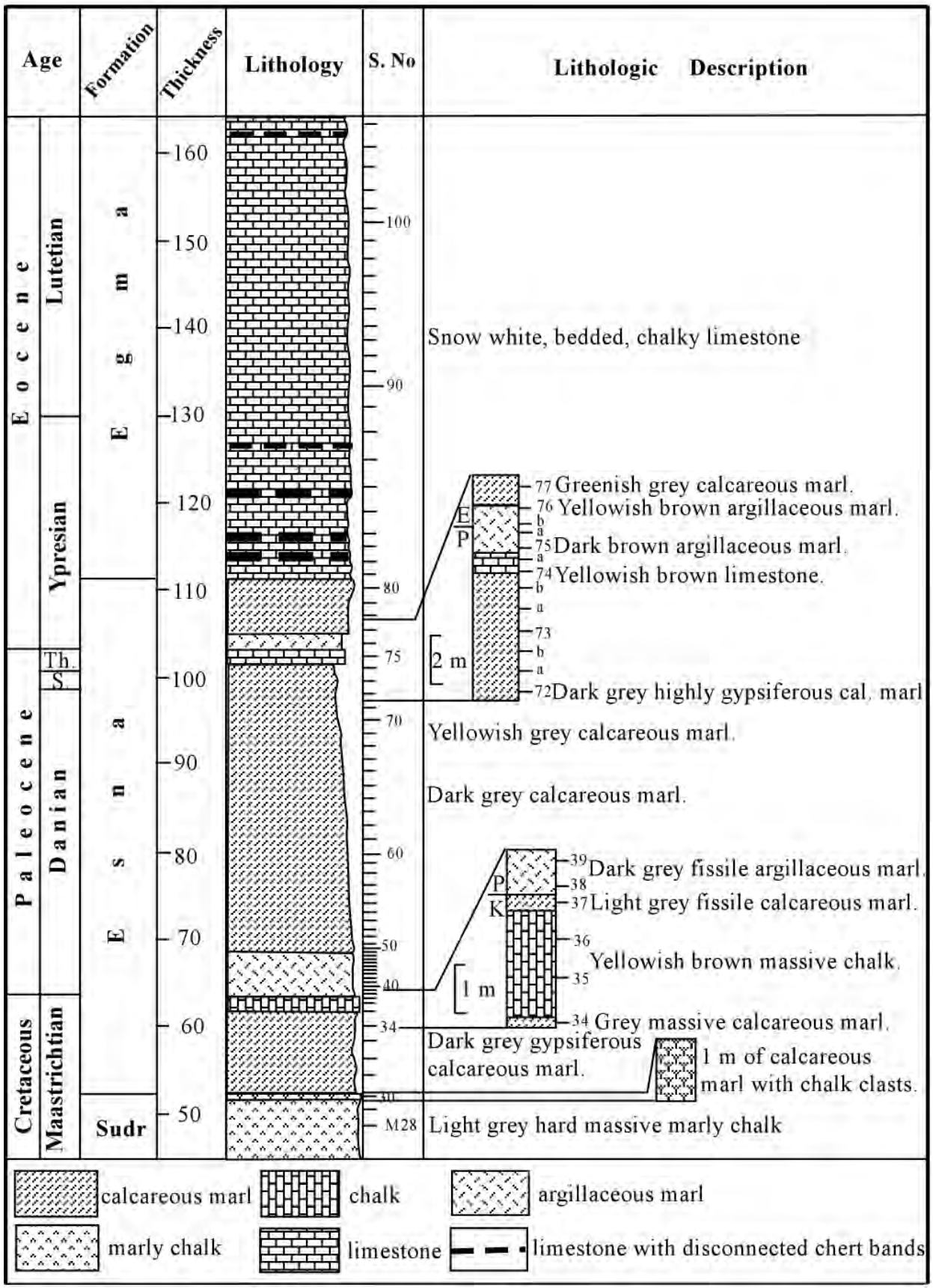

TEXT-FIGURE 2
Litholological description of the Upper Maastrichtian -Lower Eocene succession at Gebel El-Mishiti. (S: Selandian; Th: Thanetian ages)

***Fasciculithus tympaniformis* Zone (NP5)**

This is the interval from the LO of *Fasciculithus tympaniformis* to the LO of *Heliolithus kleinpellii*. It consists of about 2.5m of dark grey, fissile calcareous marl that is intercalated with gypsum bands in its upper part. It is represented by Samples M72, M72a and M72b in which all the calcareous nannoplankton are very abundant and well preserved.

At the base of Zone NP5, *Fasiculithus* taxa are easily recognized and thus their lowest occurrence readily mark the NP4/NP5 zonal boundary. A number of new nannofossil taxa characteristic of the Paleocene are recorded in this zone such as rare *Bomolithus elegans, Fasciculithus pileatus* and few to rare *Chiasmolithus consuetus (=Sullivania consueta), Fasciculithus billii, F. ulii,* few *Sphenolithus primus* in addition to the marker species *Fasciculithus tympaniformis*. According to Romein (1979) and Perch-Nielsen (1981), several new species of *Fasciculithus* and related genera such as *Heliolithus* and *Bomolithus* evolved prior to *Heliolithus kleinpellii.* A noticeable increase in abundance of *Ericsonia subpertusa* and *E. robusta* and a decrease in *E. cava/eoplagica* occurs in this zone. The warm-water species, such as *Ericsonia subpertusa, Fasciculithus* spp., *Sphenolithus* spp. are more abundant than the cool-water forms, *Ericsonia cava/eoplagica* and *Chiasmolithus* spp. Bassiouni et al. (1991) suggested a warm surface water paleotemperature for the middle part of *Ellipsolithus macellus* Zone in Dabadib, Kharga Oasis.

***Heliolithus kleinpellii* Zone (NP6)**

This zone comprises the interval from the LO of *Heliolithus kleinpellii* to the LO of *Discoaster mohleri.* It is about 2m thick, of the same lithology as the underlying Zone NP5 (gypsiferous, dark grey calcareous marl), and is represented by Samples M73 and M73a. The calcareous nannofossil species are well preserved and are very abundant in Sample M73 and abundant in Sample M73a.

Bomolithus conicus, Heliolithus cantabriae, Chiasmolithus bidens, Toweius pertusus, Neochiastozygus denticulatus and *Neochiastozygus digitosus* have their LO in this zone, in addtioon to the marker species *Heliolithus kleinpellii.* It is noted that *Fasciculithus pileatus*, *F. billii, F. ulii* occur from Zone NP5 through the base of Zone NP6. Although Perch-Nielsen (1985) mentioned that these Fasciculithus taxa became extinct Biochron NP6, Aubry (1989) recognized that *F. pileatus* ranges from NP5 through NP9.

***Discoaster mohleri* Zone (NP7/8)**

This (combined) zonal entry is defined here following Romein (1979) as the interval from the LO of *Discoaster mohleri* to the LO of *Discoaster multiradiatus* due to the absence of the marker species for the top of Zone NP7 (*Heliolithus riedellii*). It is represented by Samples M73b, M74 and M74a. The first sample is a gypsiferous, dark grey calcareous marl (about 0.5m thick), whereas the other two samples (about 1m) form a hard yellowish brown limestone intercalation. The calcareous nannofossil assemblages are well preserved in all samples; they are abundant in the calcareous marl and very abundant in the limestone. The calcareous nannofossil assemblages are of generally similar composition as those of the underlying Zone NP6. Incoming species are *Discoaster mohleri, Rhabdosphaera pinguis* and *Neochiastozygus junctus.*

***Discoaster multiradiatus* Zone (NP9)**

This zone is defined as the interval from the LO of *Discoaster multiradiatus* to the LO of *Tribrachiatus bramlettei.* It is represented by Samples M75, 75a and 75b. It consists of about 90cm of dark brown calcareous marl which overlies the hard yellowish brown limestone of Zone NP7/8. The calcareous nannofossils are very abundant and well preserved in Sample M75 while in Samples M75a and M75b they are abundant and moderately preserved.

The *Discoaster multiradiatus* Zone (NP9) is considered the last nannofossil zone in the Paleocene (Martini 1971, Romein 1979, Perch-Nielsen 1981, 1985 and others). In Egypt, the NP9 Zone is well represented in G. Owaina, G. Um el Ghanayem (Sadek and Teleb 1978); and Taramsa (Faris et al. 1985); as well as in NE Sinai (Faris 1988); Safaga area (Hewaidy and Faris 1989); Gurnah, Luxor (Faris 1991) and many other localities in Egypt (see Faris 1997; Ouda and Aubry 2003).

In this zone we record 13 incoming species characteristic of the Paleocene. Seven of these species have their LO at the base of the zone: *Discoaster multiradiatus, D. lenticularis, D. nobilis, Fasciculithus alanii, F. lillianae*, *F. bobii* and *Rhomboaster intermedia.* Six species have their LO in the middle part of the zone: *Fasciculithus involutus, Rhomboaster cuspis, R. calcitrapa, R. bitrifida, Discoaster mahmoudii* and *D. araneus.* The incoming taxa of zone NP7/8 also occur through this zone. In fact most taxa of Zone NP9 had their LO in older zones. This agrees well with the statement of Perch-Nielsen (1985) that Paleocene diversity reached a maximum in Zone NP9.

The NP9a/NP9b subzonal boundary occurs between samples M75 and 75a owing to the FOs of *Rhomboaster calcitrapa, R. cuspis, R. bitrifida* and *Discoaster araneus* in Sample M75a. The highest occurrence (HO) of *Fasciculithus alanii* is slightly above the NP9a/NP9b subzonal boundary as previously recorded by Aubry et al. (1999) in the Dababiya section, Nile Valley. We note also that all *Fasciculithus* spp. are absent in the upper part of Subzone NP9b except for *Fasciculithus tympaniformis* whose HO coincides with the NP9/NP10 zonal boundary.

EOCENE BIOZONES

Four calcareous nannofossil biozones (NP10-NP13) are recorded from the lower Eocene at Gebel El Mishiti section. The lower middle Eocene Zone NP14 is recorded in the upper part of the Gebel El Mishiti section and from Gebel El Keeh section which is restricted mainly by this zone. The distribution of Eocene calcareous nannofossils at Gebel El Mishiti is given in text-figure 4; their distribution in the lower middle Eocene at Gebel El Keeh is given in text-figure 5. The identified biozones and their characteristics are discussed below.

***Tribrachiatus contortus* Zone (NP10)**

This biostratigraphic interval is defined by the LO of *Tribrachiatus bramlettei* or *Discoaster diastypus* and its base, and the HO of *Tribrachiatus contortus* at its top. It occupies about 4.5m of yellowish to greenish grey calcareous marl at the upper most part of the Esna Formation. It is represented by Samples M76-M79. Most of the calcareous nannofossil taxa are very abundant and well-preserved except in Sample M77, in which they are abundant and moderately preserved.

Aubry (1996) has subdivided the Zone NP10 into four subzones based on the sequential occurrnece of the different

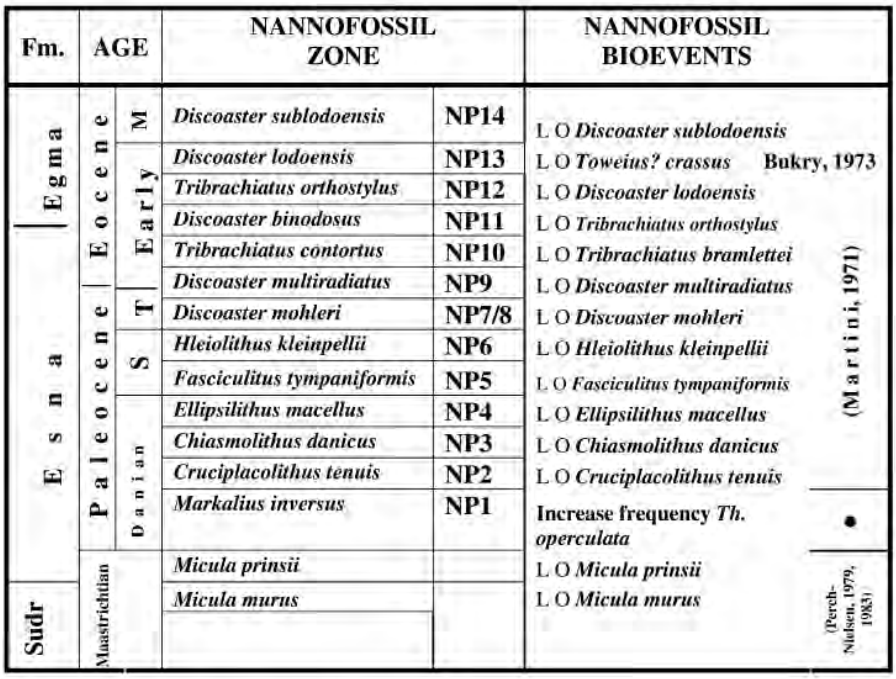

TEXT-FIGURE 3
Proposed calcareous nannoplankton zonal scheme in the studied area. (S: Selandian; T: Thanetian ages)

species of *Tribrachiatus*: 1) Subzone NP10a (*Tribrachiatus bramlettei-Tribrachiatus digitalis* Interval Range Subzone) is defined as the interval between the LO of *T. bramlettei* and the LO of *T. digitalis*; 2) Subzone NP10b (*T. digitalis* Total Range Subzone) is defined by the total range of the nominate taxon; 3) Subzone NP10c (*T. digitalis-T. contortus* Interval Subzone) is the interval between the HO of *T. digitalis* and the LO of *T. contortus*; 4) Subzone NP10d (*T. contortus* Total Range Subzone) is defined by the total range of the nominate taxon. In Egypt, Faris and Strougo (1998) have recorded the four subzones (NP10a through NP10c) in G. Gurnah section, Nile Valley.

In this study the base of Zone NP10 is delineated by the LO of *T. bramlettei, Discoaster binodosus*, and *D. diastypus,* recorded in the upper part of the Esna Formation. Other incoming taxa are *Discoaster falcatus, Pontosphera* sp., *P. multipora, Campylosphaera dela* and *Tribrachiatus contortus.* In the Gebel Mishiti section, only subzones NP10a and NP10d are recorded, subzones NP10b and NP10c are missing. A minor gap is suggested to have formed in the Gebel El Mishti section slightly after the beginning of the early Eocene.

***Discoaster binodosus* Zone (NP11)**

Zone NP11 is the interval from the HO of *Tribrachiatus contortus* to the LO of *Discoaster lodoensis.* This zone is represented by Sample M80 from the upper 70cm of the geeenish grey calcareous marl on the top of the Esna Formation and Sample M81 from the lowest 80cm of the base of the Egma Formation. The calcareous nannofossil assemblages are very abundant and well preserved in Sample M80 (Esna Formation) and become abundant and moderately preserved in Sample M81 (Egma Formation).

An exceptional abundance of *Tribrachiatus contortus* is recorded (< 1 specimen/field of view) in Sample M79. The overlying sample M80 yielded few specimens (1-3 specimens/field of view) of *Tribrachiatus orthostylus* and *Sphenollithus radians* and no *T. contortus.* The LO of *T. orthostylus* usually occurs in the uppermost part of Zone NP10, whereas the LO of *Sphenollithus radians* is recorded in the lower part of Zone NP11 in many areas in the world. The co-occurrence of *Tribrachiatus orthostylus* and *Sphenolithus radians* in Sample M80 may suggest a minor hiatus between Subzone NP10d and Zone NP11 within the uppermost part of the Esna Formation, although no lithologic changes are observed. However, this may be due to sampling gaps rather than non deposition. Zone NP11 extends from the uppermost part of the Esna Formation to the basal part of the Egma Formation. Therefore, the Egma Formation is conformably overlying the Esna Formation. It is noted that nearly all the recorded specimens of *T. orthostylus* in this zone have three arms with slight bifurcation.

***Tribrachiatus orthostylus* Zone (NP12)**

This zone is defined as the interval from the LO of *Discoaster lodoensis* to the HO of *Tribrachiatus orthostylus* or the LO of *Toweius* (?) *crassus.* It occupies about 4.5m of the basal part of the Egma Limestone and is represented by Samples M82-M84. All calcareous nannofossil species are abundant and moderately preserved in this zone except at its top, where they are very abundant. As a rule, the lowest few meters of the Egma Formation yielded abundant and moderately preserved calcareous nannofossil assemblages.

All the calcareous nannofossil taxa in Zone NP11 are observed in this zone. Additional seven genera represented by 14 species are introduced into the calcareous nannofossil assemblages of

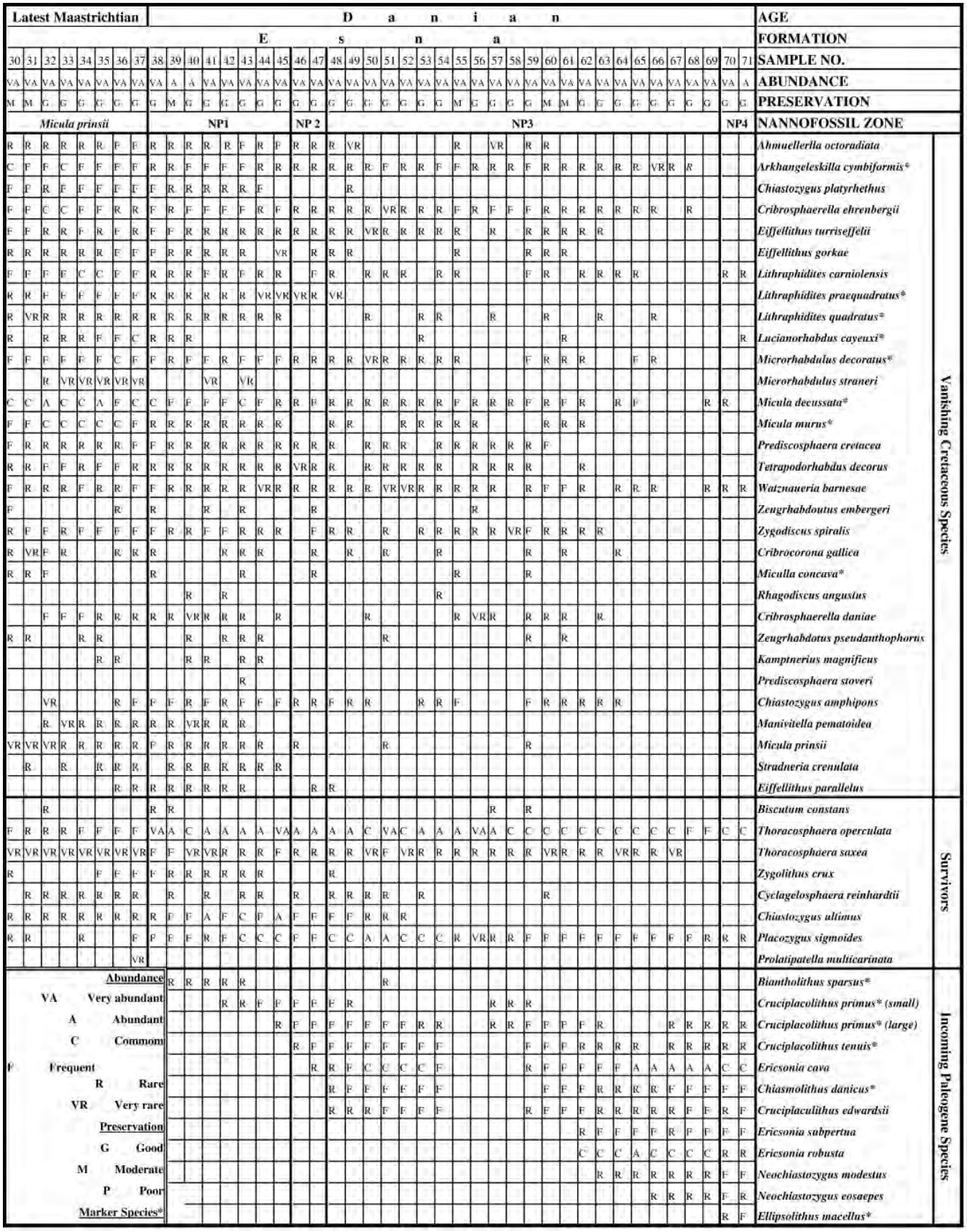

TEXT-FIGURE 4
Distribution of calcareous nannofossil species in Gebel El-Mishiti section (M) northwest El Thamad Village.

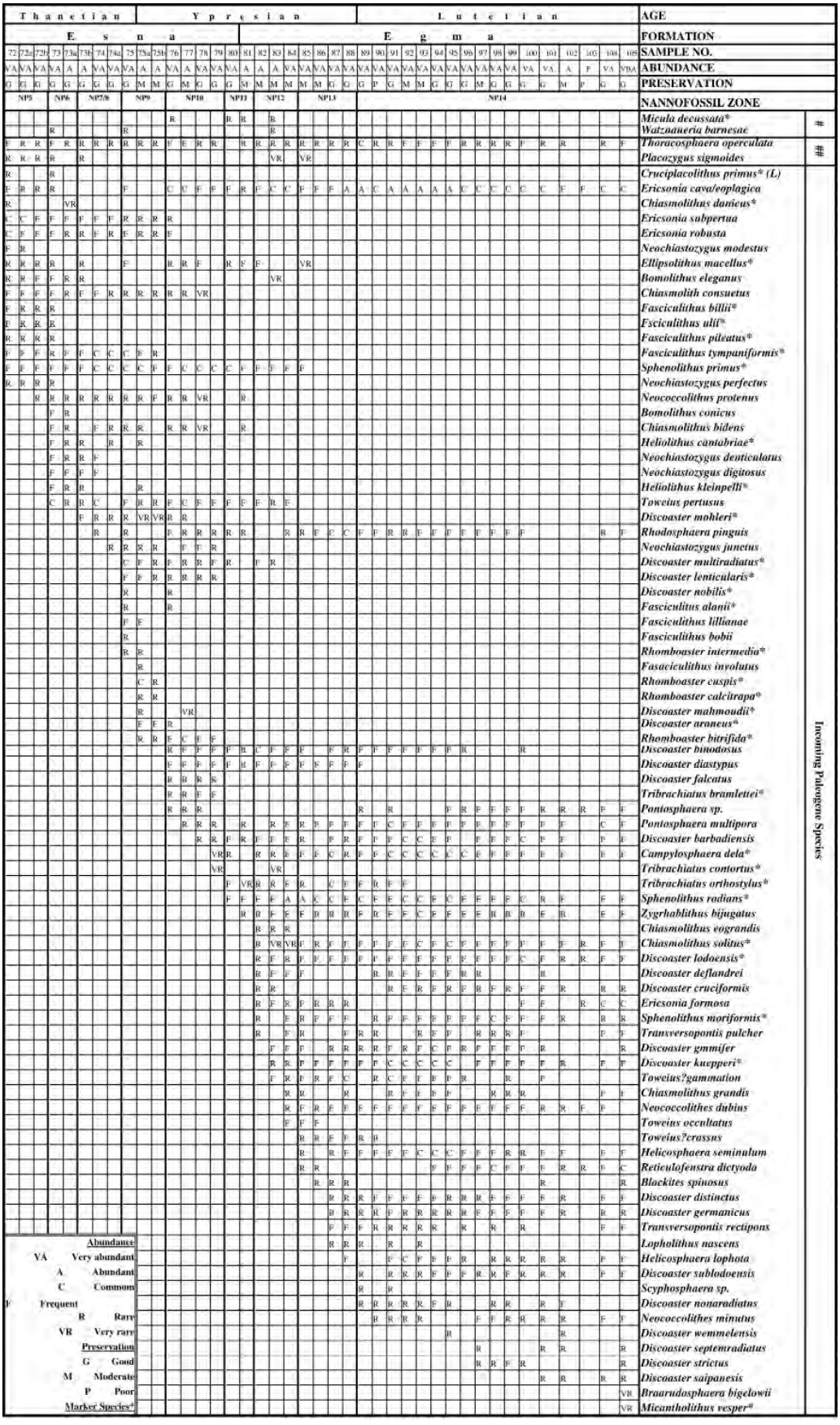

TEXT-FIGURE 4
continued.

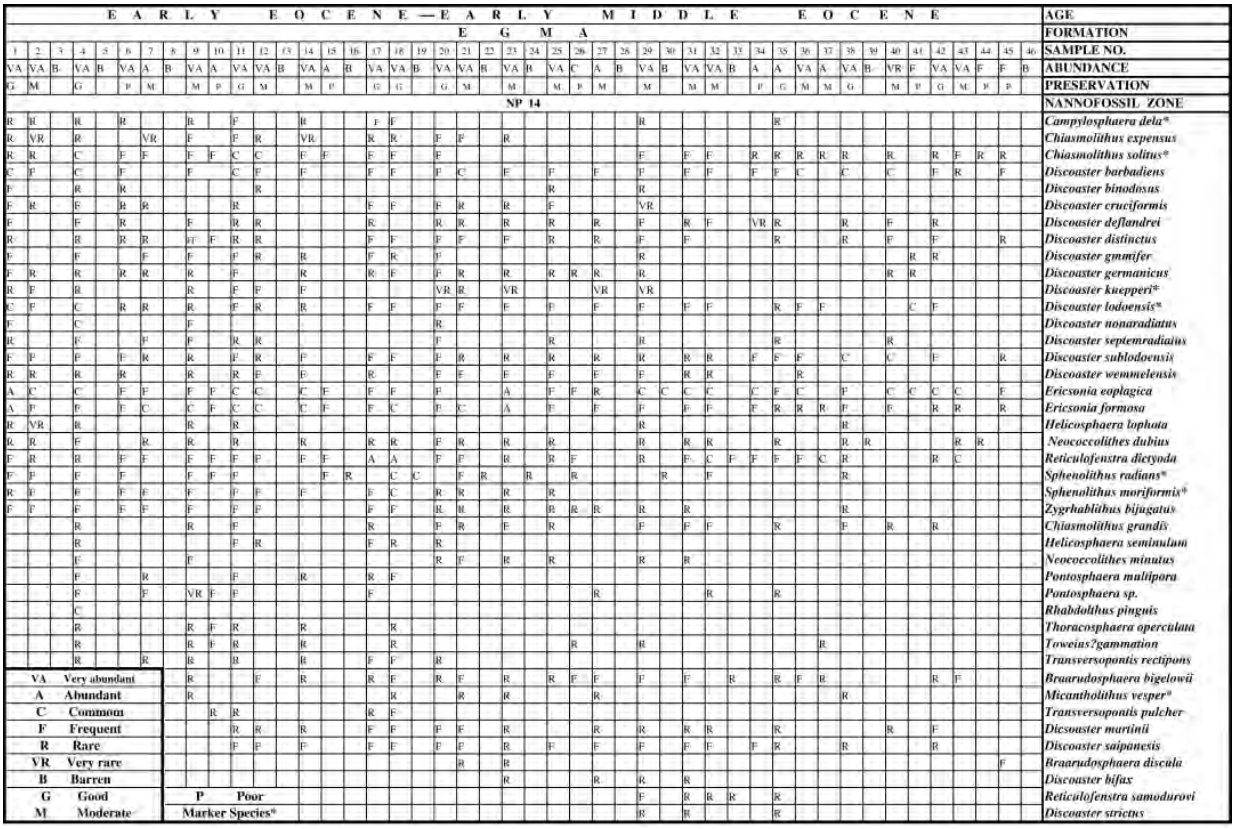

TEXT-FIGURE 5
Distribution of calcareous nannofossil species in Gebel El Keeh section, east El Thamad Village.

the early Eocene in this zone. These are *Chiasmolithus eograndis, Ch. solitus, Ch. grandis, Discoaster lodoensis, D. deflandrei, D. cruciformis, D. gemmifer, D. kuepperi, Ericsonia formosa, Neococcolithus dubius, Sphenolithus moriformis, Transversopontis puchler, Toweius? gamation* and *T. occulatus***.** Some of reworked vanishing Cretaceous taxa are recorded in Sample M83 such as rare *Micula decussata* and *Watznaueria barnesae* and specimens of *Arkhangelskiella cymbiformis*, *Lithraphidites carniolensis, Microrhabdulus decoratus* and *Tetrapodorhabdus decorus*. The presence of the above Cretaceous taxa in the Eocene sediments may pose some problems and needs explanation.

Tribrachiatus orthostylus is common in many early Eocene (uppermost of Zone NP10 to the top of Zone NP12) sections in the world but it is more abundant at mid and high latitudes. The last occurrence of *T. orthostylus* is usually used to define the base of Zone NP13 (Martini 1971). Although the Zone NP12 has generally been distinguished by the overlap of the *Tribrachiatus orthostylus* and *Discoaster lodoensis,* the last occurrence of *T. orthostylus* may range higher than previously indicated. In Arroyo El Bulito section, California, Bukry (1973b) mentioned that the stratigraphic range of *T. orthostylus* is high as the middle Eocene *Nannotetrina quadrata (= N. fulgens)* Zone as several zones present above its presumed level of disappearance. He defined the top of NP12 Zone by the LO of *Coccolithus crassus* (= *Toweius crassus*). From the ODP Hole 690B, Aubry et al. (1996) also recorded *T. orthostylus* in Zone NP14, but they considered these forms as reworked species. Perch-Nielsen (1985) dashed the range of *T. orthostylus* up to CP13 (= NP15). The sporadic occurrence of this taxon above the NP12/NP13 boundary could be attributed to ecological factors or to reworking. Because of reworking of *T. orthostylus*, Hazel et al. (1984) have proposed substituting the first (temporal; evolutionary) appearance datum (FAD) of *Helicosphaera lophota* for the last (temporal; extinction) appearance datum (LAD) of *T. orthostylus* to define the base of NP13. In this study *T. orthostylus* is recorded in the same samples with *Discoaster sublodoensis*, the maker species of NP14. Therefore, the top of NP12 Zone is defined by the LO of *Toweius crassus* following Bukry (1973b) due to the high range of *T. orthostylus*. Two morphotypes of *T. orthostylus* were recognized, however the common one is Type B with no bifurcation in contrast to Zone NP11 where Type A with a slight bifurcation of *T. orthostylus* was the common form.

***Discoaster lodoensis* Zone (NP13)**

This zone includes the interval from the LO of *Tribrachiatus orthostylus* or LO of *Toweius? crassus* to the LO of *Discoaster sublodoensis.* It is represented by Samples M85-M88 and occupies about 9.5m of yellowish chalky limestone intercalated by few thin disconnected cherty bands and disseminated chert nodules. Generally, the recorded calcareous nannofossils are very abundant, moderately preserved in Samples M85 and M86 and good preserved in Samples M87-M88.

Except for *Chiasmolithus eograndis* and *Discoaster cruciformis*, all the calcareous nannofossils recorded in Zone NP12 are still observed in this zone. Rare of *Toweius? crassus*, *Helicosphaera seminulum*, *Reticulofenestra dictyoda*, *Blackites*

TABLE 1
Mineralological and geochemical data in some samples around the P/E boundary at Gebel El Mishiti section.

S. No.	Zone	$CaCO_3$	Organic matter %	P_2O_5%	Clay Minerals		
					Kaolinite	Illite	Smectite
79	NP10d	68.7	0.7	n.d	0.9	6.3	92.9
77	NP10a	63.3	0.76	n.d	0.0	3.80	96.2
76		47.4	0.76	0.87	0.0	3.85	96.15
75a	NP9b	49.2	0.86	1.7	0.5	3.2	96.3
75	NP9a	59.27	0.8	1.71	2.2	6.3	91.5
74	NP7/8	95.84	0.3	0.78	2.5	14.8	82.64
73	NP6	84.5	0.3	n.d	1.7	16.2	82.1

n.d: not determined

spinosus, *Discoaster distinctus*, *D. germanicus* and *Lophodolithus nascens*, few *Transversopontis rectipons* and *Helicosphaera lophota* are observed. *Tribrachiatus orthostylus* ranges above its presumed level of disappearance and having sizes smaller than its sizes in the lower zones (NP11 and NP12). Therefore, ecological factors may be responsible for this sporadic occurrence rather than reworking.

***Discoaster sublodoensis* Zone (NP14)**

This zone is defined as the interval from the LO of *Discoaster sublodoensis* to the LO of *Nannotetrina fulgens* and/or LO of *Rhabdosphaera inflata*. It is represented by Samples M89-M105 at Gebel El Mishiti, is about 40m thick, and consists of white yellowish chalky limestone intercalated with the discontinuous chert bands of the Egma Formation. The exposure of Gebel El Keeh, which consists of about 95m of the Egma Limestone belongs mainly to this zone.

At Gebel El Mishiti the calcareous nannofossil assemblages in this zone are very abundant except in Sample M103 of partially solidified chalk. The assemblages are poorly preserved in two samples, moderately in four samples and well preserved in eleven samples. At Gebel El Keeh, most of the samples are fossiliferous with very poorly preserved calcareous nannofossils. From a total of 46 samples, 8 are poorly preserved, 16 are moderately preserved, 9 samples are well preserved, and 13 samples are barren (text-fig. 5).

The base of the *D. sublodoensis* Zone is defined by the LO of the nominative taxon in Sample M89 at Gebel El Mishiti. Except for the disappearance of *Toweius occultatus*, all the calcareous nannofossil taxa of Zone NP13 occur in Zone NP14 at Gebel El Mishiti. Additional taxa include rare *D. wemmelensis,* rare to few *Neococcolithus minutus*, *D. nonaradiatus* and *Scyphosphaera* sp. The latter taxon is recorded for the first time in Egyptian Eocene sedimentary rocks. Rare *D. septemradiatus, D. strictus, D. saipanensis* and very rare *Braarudosphaera bigelowii,* and *Micrantholithus vesper* also occur in the upper part of the section.

At Gebel El Keeh, *D. sublodoensis* is recorded in Sample K1 through Sample K45. *Discoaster lodoensis* is recorded from sample K1 through sample K42, being completely absent above this sample. *Discoaster kuepperi* is sporadic above sample L14, very rare up to Sample K29. It is absenet above Sample K29. The LO of *D. kuepperi* defines the top of CP12a (Okada and Bukry 1980). An overlap between *D. sublodoensis, D. lodoensis* and *D. Kuepperi* is observed from Sample K1 up to Sample K29. The co-occurrence of these three taxa characterizes Subzone NP14a (see Aubry 1991).

TABLE 2
Geochemical data of some trace and rare earth elements in some selected samples at Gebel El Mishiti section

S. No.	Cr ppm	Ni ppm	V ppm	Nb ppm	Y ppm	La ppm	Ba ppm	Cu ppm
76	61.9	272.6	52.8	4.8	39.4	19.9	2000	104.6
75a	115.5	283.6	135.0	12.5	81.4	56.8	2000	133.2
70	82.9	88.8	81.9	3.0	28.4	23.1	972	99

At Gebel El Keeh, the LOs of *D. saipanensis* and *D. martini* are located in Sample K11. Perch-Nielsen (1985) tentatively extended the occurrence of *D. saipanensis* throughout Zone NP15, its range being confidently established from Zone NP16 through the top of Zone NP20. However, Aubry (1986) noted the first appearance of *D. saipanensis* in upper Zone NP14. While Prins (1971) showed a distribution of *D. martini* from Zone NP13 through Zone NP16, Aubry (1983) used its presence to indicate Zone NP15 and the basal part of Zone NP16 only. In this study, the first occurrence of *D. bifax* is observed in Sample K23. According to Okada and Bukry (1980) its presence defines Zone CP14a (= NP16). However, Aubry (1983, 1986) found *D. bifax* ranging down into NP14 in the hemipelagic or neritic sediments of the Paris and London Basins. Therefore, it is difficult to establish the zonal age of the interval above Subzone NP14a (above Sample K9) in this study. It is surprising that *D. lodoensis* overlaps with *D. sublodoensis* through 85m of the Egma Formation in Zone NP14 at Gebel El Keeh. In the literatures, difficulties related to calcareous nannofossil biostratigraphy of epicontinental deposits are mostly restricted to reworking (Hay and Mohler 1967; Hay et al. 1967) and diagenetic processes, in particular, secondary silicification (Aubry 1986).

STAGE BOUNDARIES

Cretaceous /Paleogene Boundary

The K/P boundary in Gebel El Mishiti section has been delineated between samples M37 and M38 based on the increased frequency of *Thoracosphaera operculata* in sample M38 (Faris and Abu Shama 2003). They mentioned also that the first occurrence of *Biantholithus sparsus* was in Sample M39 (about 0.5m above the boundary). The next taxon to appear in the early Paleocene is *Cruciplacolithus primus* (small), followed by *C. tenuis, Ericsonia cava*, and *C. edwardsii*. This plus the presence of *Micula prinsii* suggested a complete succession from uppermost Maastrichtian through lower Paleocene (Danian).

Danian/Selandian Boundary

The total thickness of rocks of Danian age is about 30m in Gebel El Mishiti section. The base of the Selandian stage was placed by Berggren et al. (1995) in the upper part of ZoneNP4 . The most profound evolutionary changes in the Paleocene calcareous nannoplankton occurred during the later part of Biochron NP4 (Aubry 1998) and the most characteristic genera of the Paleocene originated during this time. The closely related genera *Sphenolithus* and *Fasciculithus* evolved during the Biochron NP4, subsequently giving rise to *Heliolithus* and *Discoaster*. At Gebel El Mishiti, the Danian/Selandian boundary is tentatively placed at the base of Zone NP5 (LO of *Fasciculithus* taxa).

In this study, as mentioned earlier, the base of Zone NP5 is defined by the LO of *Fasciculithus tympaniformis* as well as the LO of *Sphenolithus*. The latter is generally found in Zone NP4 and shortly before the LO of *Fasciculithus tympaniformis*.

However, at Gebel El Mishiti, the LO of *S. primus* coincides with the LO of *Fasciculithus tympaniformis*. Thus either the LO of *S. primus* reprensented a delayed first occurrence, and Zone NP5 overlies Zone NP4 conformably or the stratigraphy juxtaposition reflects a short hiatus without visible lithologic changes. The Danian age was a time of particulary pronounced global highstand of sea level followed by regression at its end (Vail et al. 1977). However, based on the calcareous nannofossils complete sequences across the Paleocene interval recorded in localities in Egypt (Faris 1988; Faris et al. 1999; El Dawoody 1990; Marzouk and Luning 1998) as in this study.

Selandian/Thanethian Boundary

On the bases of calcareous nannofossil bioevents, the Selandian/Thanetian is tentatively placed at the uppermost part of Zone NP6 or the lowermost part of Zone NP7/8 (Berggren et al. 1995). In the current study the first appearance of *D. mohleri* (marker taxon of Zone NP7/8) is used to delineate the boundary. A marked lithologic change from gypsiferous, dark grey calcareous marl to yellowish brown limestone is noted from the upper part of Zone NP6 to Zone NP7/8.

The Paleocene/Eocene (P/E) Boundary

The latest Paleocene-earliest Eocene boundary now clearly appears as a critical interval in earth history. Many events took place in this interval such as global warming (Stott and Kennett 1990; Kennett and Stott 1991), reduction in atmospheric circulation (Rea et al. 1990) and changes in oceanic circulation associated with brief production of deep water at low latitude (Miller et al. 1987; Kennett and Stott 1991; Thomas 1990a, b, 1993). These events were concomitant with major turnovers in the bathyal and abyssal benthic foraminifera (Tjalsma and Lohmann, 1983; Thomas 1990a, b) and the terrestrial mammals (see review in Hooker 1991). Isotopic ($\delta_{13}C$ and $\delta_{18}O$ excursion) and mineralogical (kaolinite peak) evidence suggest that these evolutionary turnovers were related to deep water warming associated with climatic change. Although the proximate cause of the carbon isotope excursion (CIE) may be the massive dissociation of carbon hydrates, the ultimate cause for global warming has not been well identified.

The P/E boundary has traditionally been correlated on the basis of the NP9/NP10 zonal boundary which is defined by the LO of *Tribrachiatus bramlettei* (Martini 1971). The LO of *Discoaster diastypus* was used by Okada and Bukry (1980) to recognize this boudary. Romein (1979) has shown how *T. bramlettei* evolved into *T. contortus* which itself evolved into *T. orthostylus* in the later part of Biochron NP10. *Tribrachiatus contortus* seems to be less restricted in occurrence than *T. bramlettei*. In the absence of *T. bramlettei*, the LO of *Fasciculithus tympaniformis* (or *Fasciculithus* spp.) is used to approximate the NP9/NP10 zonal boundary (Shackleton et al. 1984). Although the three species of *Tribrachiatus* clearly constitute a

---

PLATE 1

All Figures ×2000, from Gebel El Mishiti

1 *Cruciplacolithus tenuis* (Stradner 1961) Hay and Mohler in Hay et al. 1967. Sample No. 49, *Chiasmolithus danicus* Zone.

2 *Chiasmolithus danicus* (Brotzen 1959) Hay and Mohler 1967. Sample No. 54, *Discoaster lodoensis* Zone.

3 *Sphenolithus radians* Deflandre in Grasse 1952. Sample No.80, *Discoaster binodosus* Zone.

4,5 *Ellipsolithus macellus* (Bramlette and Sullivan 1961) Sullivan 1964; 4, Sample No.70; 5, Sample No.71, *Ellipsolithus macellus* Zone.

6 *Discoaster cruciformis* Martini 1958. Sample No.83, *Tribrachiatus orthostylus* Zone.

7 *Discoaster binodosus* Martini 1958. Sample No. 83, *Tribrachiatus orthostylus* Zone.

8,9 *Toweius ? gammation* (Bramlette and Sullivan 1961) Romein (1979). Sample No. 8; 8, *Discoaster lodoensis* Zone.

10 *Toweius ?crassus* (Bramlette and Sullivan 1961) Perch-Nielsen (1984). Sample No. 88, *Discoaster lodoensis* Zone.

11 *Micula prinsii* Perch-Nielsen 1979. Sample No.39, *Markalius inversus* Zone.

12 *Heliolithus kleinpellii* Sullivan 1964. Sample No.73, *Heliolithus kleinpellii* Zone.

13,14 *Tribrachiatus bramlettei* (Bronnimann and Stradner 1960) Proto Decima et al. 1975. Sample No.79, *Tribrachiatus contortus* Zone.

15 *Discoaster multiradiatus* (Bramlette and Riedel 1954). Sample No. 83, *Tribrachiatus orthostylus* Zone.

16,20 *Fasculithus tympaniformis* Hay and Mohler in Hay et al. 1967. Sample No. 72, *Fasculithus tympaniformis* Zone.

17 *Discoaster gemmifer* Stradner 1961. Sample No.83, *Tribrachiatus orthostylus* Zone.

18 *Discoaster barbadiensis* Tan 1927. Sample No.83, *Tribrachiatus orthostylus* Zone.

19 *Discoaster araneus* Bukry 1971. Sample No.75b, *Discoaster multiradiatus* Zone.

21 *Tribrachiatus contortus* (Stradner 1958) Bukry 1972. Sample No.83, *Tribrachiatus orthostylus* Zone.

22-25 *Tribrachiatus orthostylus* Shamrai 1963. 22, sample No. 87, *Discoaster lodoensis* Zone; 23, 24, sample No. 80, *Discoaster binodosus* Zone; 25, sample No. 83, *Tribrachiatus orthostylus* Zone.

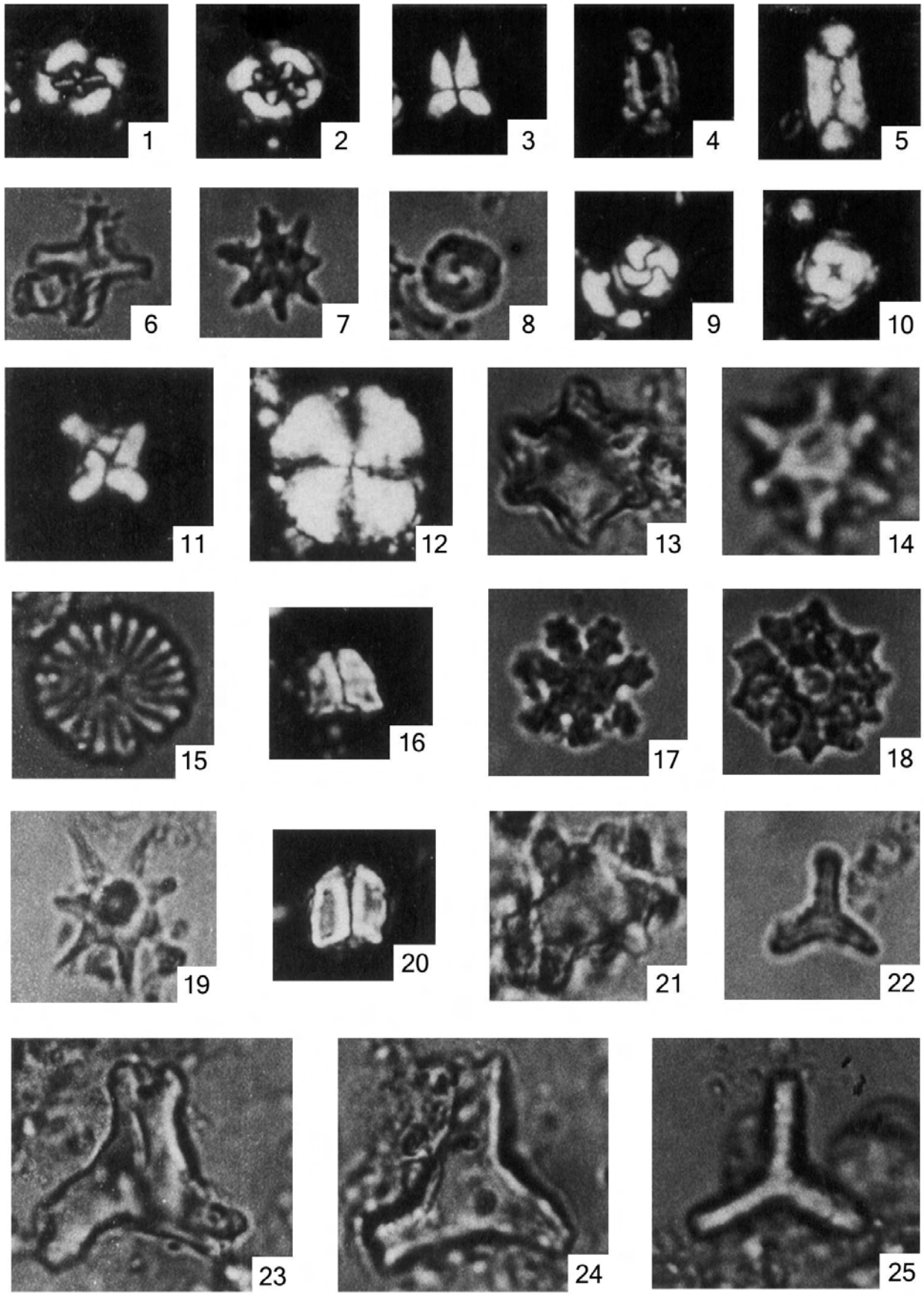
1
2
3
4
5
6
7
8
9
10
11
12
13
14
15
16
17
18
19
20
21
22
23
24
25

lineage, their stratigraphic relationships remain somewhat unclear (see Aubry et al. 1996 for detailed discussion).

In Egypt, the calcareous nannofossil events at the standard P/E boundary were studied by El-Dawoody (1992, 1994), Faris (1991, 1993a), Strougo and Faris (1993), Aubry et al. (1999, 2000), Faris et al. (1999), Dupuis et al. (2003) and Knox et al. (2003). Faris (1993a) used the LO of *T. bramlettei, Discoaster diastypus* and *D. binodosus* to delineate the base of the Eocene in several Egyptian sections. The HO of *Fasciculithus* spp. may have taken place below or slightly above the P/E boundary in different sections in Egypt (see Faris et al. 1999). The boundary lies in the upper part of the Esna Formation and can be traced between the nannofossil zones NP9 and NP10 in some sections and in the uppermost part of Zone NP9 in other sections (Faris et al. 1999). The boundary is marked by a lithologic change in some sections (Strougo and Faris 1993) while no lithologic variations were observed in others (Faris 1991). In West Central Sinai, El-Dawoody (1992) placed the P/E boundary at the contact between the Esna and Thebes Formations which corresponds to the *Discoaster multiradiatus/Tribrachiatus contortus* zonal boundary.

The P/E boundary GSSP is located between Subzones NP9a and NP9b in the Dababiya Quarry section (Dupuis et al. 2003). The NP9a/NP9b subzonal boundary is characterized by the LOs of *Discoaster anartios, D. araneus* and *Rhomboaster* spp. In the present study, the P/E boundary is located between Subzones NP9a and NP9b at Gebel El Mishiti based on the LOs of *Rhomboaster calcitrapa, R. cuspis, R. bitrifida* and *Discoaster araneus* in Sample M75a.

A sedimentological discontinuity between NP9 and NP10a is noted by the presence of intraclasts of calcareous marl of the underlying strata, normally 1-2mm in diameter, forming a few centimeters of intraformational conglomeratic bed. However, this discontinuity can not be detected by the means of calcareous nannofossils. Moreover, the Subzones NP10b and NP10c are absent in Gebel Mishiti section. Therefore, the Zone NP9 is conformably overlain by Subzone NP10a which is uncomfortably overlain by Subzone NP10d. This suggests that Subzones NP10b and NP10c have been eroded slightly after the beginning of the early Eocene.

Smectite reaches about 91.5% (Table 1) in the uppermost Paleocene and its maximum value (96.3%) is just above the Paleocene/Eocene boundary. It is surprising to find that kaolinite completely disappeared at the beginning of the Eocene and instead smectite reaches its maximum value. Very small peak of kaolinite representing about 0.9% of the total clay fraction occur at about 5 meters above the P/E boundary. This contrasts with the observations by many authors such as Egger et al. (1999) who suggested that an increase of kaolinite input took place near the end of Paleocene as a result of climatic change toward more humid conditions.

In Gebel El Mishiti section, the $CaCO_3$ content reach about 95.84% (Table 1) at the top of Zone NP7/8 and decreased to about 54.3% (avg.) through Zone NP9. P_2O_5 is relatively higher at the P/E boundary (Table 2). An increase of total organic matter around the P/E boundary is detected at Gebel El Mishiti section (Table 1). A strong positive correlation between the organic carbon and phosphorous was recorded through the Esna Formation at this section (Abu Shama 2002). Geological system that enriched by organic carbon are also enriched in their phosphorous content.

The study of some trace elements (Table 2) reveals anomalous values at the P/E boundary in Gebel El Mishiti section. These anomalous values of Cr, Ni and V at this boundary may be due to scavenging of the trace elements at the sea floor over years to prevailing reducing conditions, or to as-yet-unidentified events. The anomalous values of Nb, Y and La in the current study may be associated with one or more phosphate minerals as previously shown in pelagic sediments by Arthur et al. (1989). Abnormal values of Barium are also recorded around the P/E boundary. Schmitz (1987) suggested that barium concentration is high in the sediments of high biological productivity. The high anomolies of Ba, Cr, Ni, V and Rees around the P/E Boundary at Gebel el-Qreiya suggest their incorporation in phosphatic components as well as organic matter (Solimann 2003)

PLATE 2

All Figures ×2000, from Gebel El Mishiti section, *Discoaster sublodoensis* Zone.)

1 *Discoaster lodoensis* Bramlette and Reidel 1954. Sample No. 95.

2 *Neococcolithus dubius* (Deflandre 1954) Black (1967). Sample No. 95.

3 *Discoaster wemmelensis* Achuthan and Stradner 1969. Sample No. 95.

4,5 *Pontosphaera multipora* (Kamptner 1948) Roth (1970). Sample No. 91.

6,11 *Discoaster distinctus* Martini 1958. 6, sample No. 95; 11, Sample No. 94.

7,8 *Discoaster germanicus* Stradner 1959. 7, Sample No. 94. 8, Sample No. 91.

9,10 *Campylosphaera dela* (Bramlette and Sullivan 1961) Hay and Mohler (1967)

12 *Discoaster sublodoensis* Bramlette and Sullivan 1961, Sample No. 93.

13,14 *Helicosphaera seminulum* Bramlette and Sullivan 1961, Sample No. 95

15-17 *Scyphosphaera sp.* Lohmann 1902. 15, 16, Sample No. 91; 17, Sample No. 89.

18,19 *Chiasmolithus grandis* (Bramlette and Riedel 1954) Radomski (1968). Sample No. 95.

20 *Discoaster nonaradiatus* Klumpp 1953. Sample No. 92.

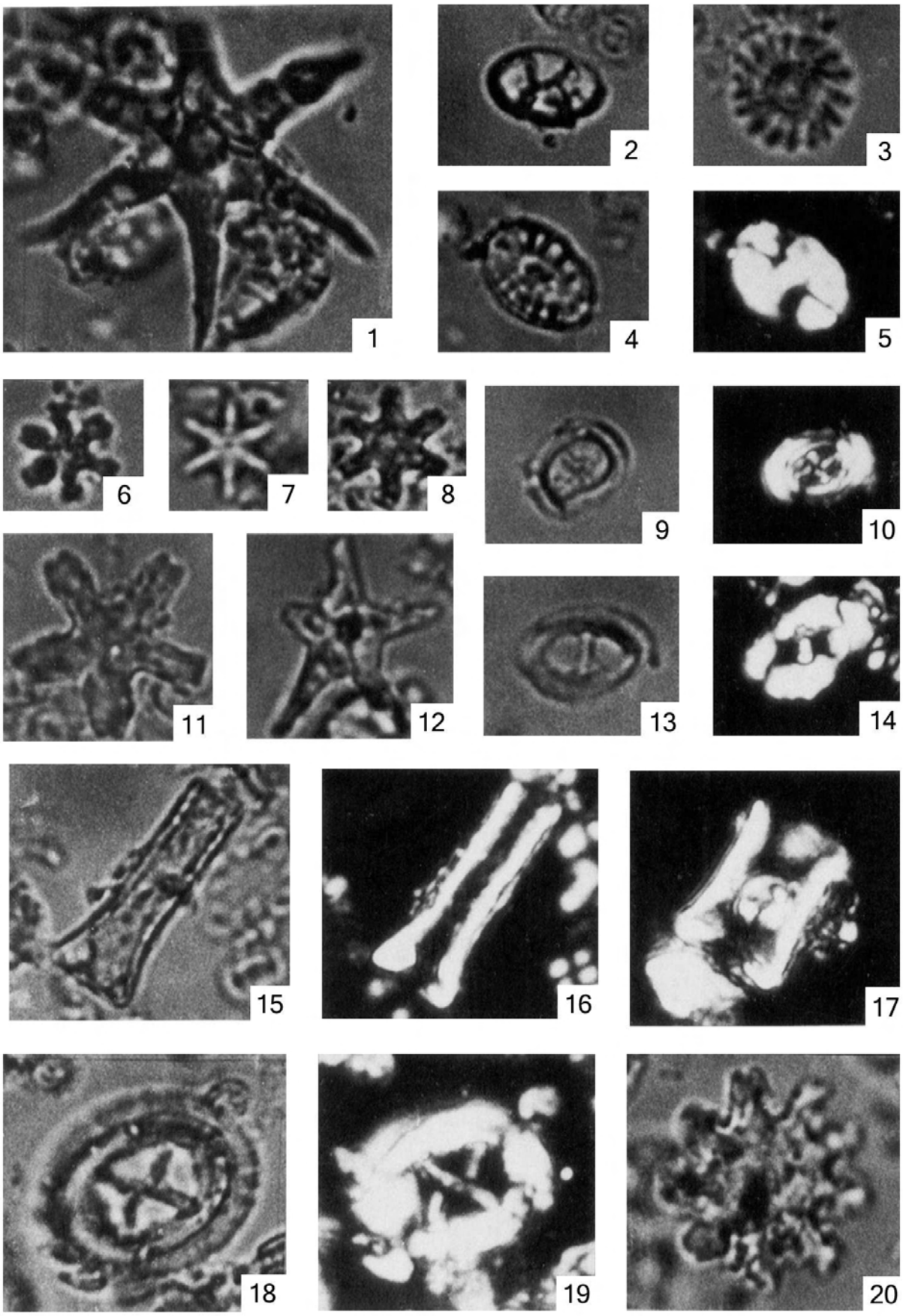
1
2
3
4
5
6
7
8
9
10
11
12
13
14
15
16
17
18
19
20

The lower Eocene/middle Eocene Boundary

The location of lower Eocene/middle Eocene boundary (Ypresian/Lutetian) is correlated with the NP13/NP14 zonal boundary (Martini 1971; Hazel et al. 1984; Perch-Nielsen 1985; Martini and Muller 1986). However, the base of the middle Eocene (Lutetian) is slightly younger (passes within the base NP14) according to some authors (Aubry 1983; Bolli et al. 1985; Berggren et al. 1985, Cavelier and Pomerol 1986). Calcareous nannofossil studies by Steurbaut (1988) and Steurbaut and Nolf (1986) on the Paris and Belgian Basins placed this boundary in the lower part of the NP14.

In Egypt, Strougo and Faris (1993) suggested that the lower Eocene/middle Eocene boundary, if present at Wadi El Dakhl, should lie in the terminal part of the section, at least as high as the NP13/NP14 zonal boundary. In the neritic sequences of the Nile Valley where planktonic species are rare and poorly preserved, Janin et al. (1993) placed this boundary near the Minia/Samalut Formation boundary depending on the abundance variation of 5-rayed discoasters. At Gebel El Mishiti, the NP13/NP14 zonal boundary is located between Sample M88 and Sample 89 (about 17m above the base of Egma Formation). The total thickness of Gebel El Keeh reaches about 95m, and there are no lithologic changes except in the upper 10m; all the section belongs to Zone NP14. Although, the marker species *Discoaster sublodoensis* and other taxa of the younger zones such as *Discoaster bifax* and *D. saipanesis* occur in the uniform Egma Formation, both *Rhabdosphaera inflata* (marker of Subzone NP14b) and *Nannotetrina fulgens* (marker of the Zone NP15) are absent.

Both the Braarudospherids and *Micrantholithus* of the family Braarudosphaeraceae occur in the last sample in Gebel El Mishiti and in most samples of Gebel El Keeh sections. This group is usually common in near-shore and hemi-pelagic deposits (Haq and Lohmann 1976), of the Paleogene where they bloomed repeatedly especially shortly after the Cretaceous/Paleogene (K/P) boundary events and during the middle Eocene (Bybell and Gartner 1972; Perch Nielsen 1985). This group is known to be a marine hypohaline indicator (Gran and Braarud 1935; Bukry 1974). Martini (1965, 1970) and Bukry 1971) considered that *Braarudsphaera* and *Micrantholithus* are characteristic of near shore deposits and considered as warm water indicators by Bukry (1973a).

In Egypt, *Braarudsphaera discula* was reported from the middle Eocene of Wadi Nukhul (El-Dawoody and Morsi 1983). A high percentage of Braarudosphaeraceae was recorded in the middle Eocene of Wadi Daqer, Nile Valley (Janin et al. 1993). The stratigraphic occurrences and geographic distributions of the Early Paleogene pentalith forms in Egyptian localities were discussed by Faris (1993b). He suggested that the presence of some pentalith taxa may be useful as alternative indicators of stratigraphic age in the absence of convential index species of the middle and late Eocene. *Braarudsphaera* and *Micrantholithus* are absent in the Maastrichtian and Paleocene of the studied area, but they occur in the lower middle Eocene. This means at least that changes in the environment of deposition from deep shelf in the Maastrichtian to neritic environment took place in the early middle Eocene. This might be due to tectonic uplifting of the sea floor or falling in the sea level at this time.

At Gebel El Mishiti, the warm-water taxa in Subzone NP14a such as *Thoracosphaera operculata, Sphenolithus* spp., *Discoaster* spp., *Zygrhablithus bijugatus, Pontosphaera* spp., *Ericsonia formosa, Braarudosphaera* spp. and *Micrantholithus vesper* dominate over the cool-water taxa (such as *Ericsonia cava/eoplagica, Chiasmolithus* spp., *Neococcolithus dubius* and *Blackites* spp.) At Gebel El Keeh, the cool-water taxa dominate the assemblages above Sample K39.

SUMMARY AND CONCLUSIONS

In east central Sinai (Gebel El Mishiti and G. El Keeh sections), the Paleocene-lower Eocene sediments are divided into the following nannofossil biozones; *Markalius invesus* (NP1), *Cruciplacolithus tenuis* (NP2), *Chiasmolithus danicus* (NP3),

---

PLATE 3

All figures ×2000, from Gebel El Keeh section, *Discoaster sublodoensis* Zone

1, 2 *Braarudosphaera bigelowii* (Gran and Braarud 1935) Deflandre 1947. Sample No. 18.

3, 4 *Micrantholithus vesper* Deflandre 1954. Sample No. 23.

5 *Discoaster binodosus* Martini 1958. Sample No. 1.

6,7 *Discoaster sublodoensis* Bramlette and Sullivan 1961. 6, Sample No.1. 7, Sample No. 38.

8 *Discoaster barbadiensis* Tan 1927. Sample No. 21.

9, 15 *Discoaster distinctus* Martini 1958. 9, Sample No. 29. 15, Sample No. 9.

10, 16 *Discoaster martinii* Strander 1959. 10, Sample No. 23; 16, Sample No.35.

11, 12 *Discoaster saipanensis* Bramlette and Riedel 1954. 11, Sample No. 11; 12, Sample No.31.

13 *Discoaster lodoensis* Bramlette and Riedel 1954. Sample No. 4.

14 *Discoaster septemradiatus* (Klump 1953) Martini 1958. Sample No. 29.

17, 18 *Reticulofenestra dictyoda* (Deflandrei in Deflandrei and Fert 1954) Strander in Strander and Edwards 1968; 17, Sample No. 9. 18, sample no.35.

19 *Reticulofenestra samodurovii* (Hay, Mohler and Wade 1966) Roth 1970. Sample No. 29.

20-22 *Braarudosphaera discula* Bramlette and Riedel 1954. 20, Sample No. 23; 21-22, Sample No.21.

23 *Neococcolithus minutus* Perch-Nielsen 1967, Perch-Nielsen 1971. Sample No. 21.

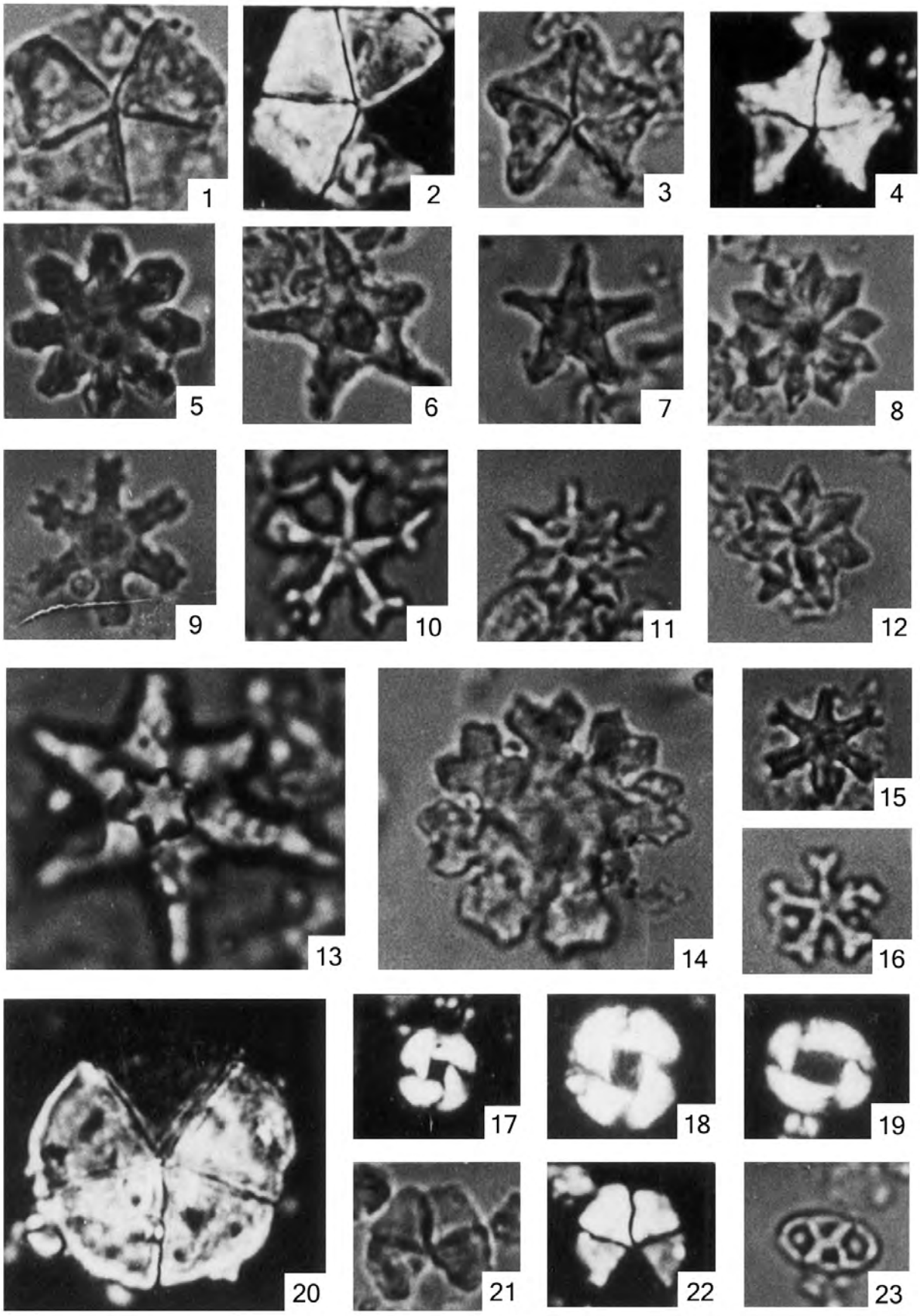
1
2
3
4
5
6
7
8
9
10
11
12
13
14
15
16
17
18
19
20
21
22
23

Ellipsolithus macellus (NP4), *Fasciculithus tympaniformis* (NP5), *Heliolithus kleinpellii* (NP6), *Discoaster mohleri* (NP7/8), *Discoaster multiradiatus* (NP9), *Tribrachiatus contortus* (NP10), *Discoaster binodosus* (NP11), *Tribrachiatus orthostylus* (NP12), *Discoaster lodoensis* (NP13) and *Discoaster sublodoensis* (NP14).

At Gebel El Mishiti section, the Danian/Selandian boundary is placed at the base of Zone NP5 delineated by the LO of *Fasculithus* taxa. The Selandian/Thanetian boundary is tentatively placed at the base of Zone NP7/8 (FO of *Discoaster mohleri*).

Zone NP9 (*Discoaster multiradiatus*) in the present study is subdivided into two subzones (NP9a and NP9b) delineated on the basis of LO of *Rhomboaster calcitrapa*, *R. cuspis, R. bitrifida* and *Discoaster araneus.* The Paleocene/Eocene (P/E) boundary interval at Gebel El Mishiti section is located between these subzones. The disappearance of most *Fasciculithus* taxa occurs in the upper part of Subzone NP9b (Sample M75b). The entry of *Tribrachiatus bramlettei*, *Discoaster binodosus* and *D. diastypus* in Sample M76 indicates the base of Zone NP10. A sedimentological discontinuity between Zone NP9 and Subzone NP10a indicates the presence of intraclasts of calcareous marls of the underlying strata, forming a few centimeters of intraformational conglomeratic bed.

Some mineralogical and geochemical changes are recorded at the P/E boundary in the Gebel El Mishiti section. It is surprising to find that kaolinite completely disappears in the base of the Eocene, and instead smectite reaches a maximum value. Again, a small peak of kaolinite occurs about 5 meters above the P/E boundary. $CaCO_3$ content decreased through Zone NP9, where P_2O_5 and organic matter are relatively increased at this boundary in such section. Around this boundary, anomalous values of Cr, Ni, V, Nb, Y, La and Ba are also recorded.

The subdivisions of Zone NP10 into NP10a, b, c, d as suggested by Aubry (1996) are applied in this study. However, at Gebel Mishiti section, the only two subzones NP10a and NP10d are recorded while other subzones NP10b and NP10c are absent. So a minor hiatus is suggested slightly after the beginning of the early Eocene in the uppermost part of the Esna Formation in this section.

Although, the LAD of *Tribrachiatus orthostylus* lines the top of Zone NP12 (*Discoaster lodoensis* Zone), it is recorded here together with *Discoaster sublodoensis* (marker taxon of Zone NP14). Therefore, the top of Zone NP12 located here at the LO of *Towieus crasus*. In the Gebel Mishiti section, the NP13/NP14 zonal boundary is located at about 17m above the base of the Egma Formation. The early Eocene/middle Eocene boundary is tentatively placed at this level and more detailed works are necessary to precisely determine this boundary. Although, the Gebel El Keeh section is represented by about 95m of the Egma Limestone, it belongs to a single nannofossilzone, Zone NP14. Moreover, it is difficult to subdivide this zone into two subzones NP14a and NP14b because both *Rhabdosphera inflata* (marker of Subzone NP14b) and *Nannotetrina fulgens* (marker taxon of Zone NP15) are absent.

The near shore and hemipelagic Braarudospherids and *Micrantholithus* of the family Braarudosphaeraceae occur in the younger samples of Gebel El Mishiti and in most samples of Gebel El Keeh. These taxa may indicate warm water conditions in the early Middle Eocene.

ACKNOWLEDGMENTS

The authors appreciate the efforts of Professor John van Couvering, editor of Micropaleontology for his encouragement and reading of the manuscript. The authors are also grateful to Professor Marie-Pierre Aubry for her stimulating review.

REFERENCES

ABU SHAMA, A. M., 2002. "Sedimentological and Palaeontological studies on the Thamad area, East Central Sinai, Egypt." Unpubl. Ph. D., Thesis, Faculty of Science, Tanta University, 393 pp, 42 plates.

ARTHUR, M. A., DEAN, W. E., ZACHOS, J. C., KAMINSKI, M., HAGERTY RIEG, S., and ELMSTROM, K., 1989. Geochemical expression of early diagenesis in Middle Eocene-Lower Oligocene pelagic sediments in the southern Labrador sea, site 647, ODP LEG 105. In: Srivastava, S. P., Arthur, M., Clement, B., et al., Eds., *Proceedings of the Ocean Drilling Program, Scientific Results, Volume 105*, 111-135. College Station, TX: Ocean Drilling Program.

AUBRY, M.-P., 1983. "Corrélations biostratigraphiques entre les formations Paléognes épicontinentales de I'Europe du Nord-Ouest, basées sur la nannoplancton calcaire." These Université Pierre et Marie, Paris 6, 83-08, 208 pp.

———, 1986. Paleogene calcareous nannoplankton biostratigraphy of northwest Europe. *Palaeogeography, Palaeoclimatology, Palaeoecology*, 55: 267-334.

———, 1989. *Handbook of Cenozoic Calcareous Nannoplankton, Book 3 (Ortholithae and Hilliolithae),* 279pp. New York: Micropaleontology Press.

———, 1991. Sequence stratigraphy: Eustasy or tectonic imprint? *Journal of Geophysical Research*, 96 (B4): 6641-6679.

———, 1993. Calcareous nannoplankton evolution: dominance, diversification and success. *Geological Society of America, Annual Meeting, Abstracts with programs,* 25 (6): A358.

———, 1996. Towards an upper Paleocene-lower Eocene high resolution stratigraphy based on calcareous nannofossil stratigraphy. *Israel Journal of Earth-Sciences,* 44: 239-253.

AUBRY, M-P., BERGGREN, W. A., CRAMER, B., DUPUIS, C., KENT, D. V., OUDA, K., SCHMITZ, B. and STEURBAUT, E., 1999. Paleocene/Eocene boundary sections in Egypt. *International Symposium on late Paleocene-early Eocene events from North Africa to the Middle East in connection with the 1st International Congress on the Geology of Africa,* 1-11. Assiut, Egypt,

AUBRY, M-P., BERGGREN, W. A., STOTT, L. and SINHA, A., 1996. The upper Paleocene-lower Eocene stratigraphic record and the Paleocene-Eocene boundary carbon isotope excursion: implication for geochronology. In: Knox, R. W. O'B., Corfield, R. M. and Dunay, R. E., Eds., *Correlation of the early Paleogene in Northwest Europe*, 353-380. Geological Society of America Special Publication 101.

AUBRY, M-P., CRAMER, B. S., MILLER, K. G., WRIGHT, J. D., KENT, D. V. and OLSSON, R. K., 2000. Late Paleocene event chronology: unconformities, not diachrony. *Bulletin, Societé Géologique de France,* t. 171, 3:367-378.

BASSIOUNI, M. A., FARIS, M. and SHARABY, S., 1991. Late Maastrichtian and Paleocene calcareous nannofossils from Ain Dabadib section, NW Kharga Oasis. *Qatar University of Science Bulletin,* 11: 357-375.

BERGGREN, W. A., KENT, D. V. and FLYNN, J. J., 1985. Paleogene geochronology and chronostratigraphy. *Geological Society of London*, 10: 141-195.

BERGGREN, W. A., KENT, D. V., SWISHER III, C. C. and AUBRY, M-P., 1995. A revised Cenozoic geochronology and chronostratigraphy. In: Berggren, W. A., Kent, D. V., Aubry, M.-P. and Hardenbol, J., Eds., *Geochronology, Time Scale and Global Stratigraphic Correlation,* 129-212. Society for Economic Paleontology and Mineraology, Special Publication, 54.

BOLLI, H. M., SAUNDERS, J. B. and PERCH-NIELSEN, K., 1985. Comparison of zonal schemes for different fossil groups. In: Bolli, H. M., Saunders, J. B., Perch-Nielsen, K., Eds., *Plankton stratigraphy,* 3-10. Cambridge: Cambridge University Press.

BUKRY, D., 1971. Cenozoic calcareous nannofossils from the Pacific Ocean. *Transactions of the San Diego Society Natural History,* 16: 303-327.

———, 1973a. Coccoliths stratigraphy, Leg 10-Deep Sea Drilling Project. *Initial Reports of the Deep Sea Drilling Project, Volume 10, 385-604. Washington, DC: US Government Printing Office.*

———, 1973b. Low latitude coccoliths biostratigraphic zonation. *Initial Reports of the Deep Sea Drilling Project, Volume, 15,* 685-703. Washington, DC: US Government Printing Office.

———, 1974. Coccoliths as paleosalinity indicators; evidence from the Black Sea. *Bulletin of the American Association of Petroleum Geologists,* 20: 353-363.

BYBELL, L. M. and GARTNER, S., 1972. Provincialism among mid-Eocene calcareous nannofossils. *Micropaleontology* 18(3): 319-336.

CAVELIER, C. and POMEROL, C., 1986. Stratigraphy of the Paleogene. *Bulletin Societé Géologique de France,* 8 (II, 2): 255-265.

DUPUIS, CH., AUBRY, M-P., STEURBAUT, E., BERGGREN, W., OUDA, KH., MAGIONCALDA R., CRAMER, B. S., KENT, D. V., SPEIJER, R. P. and HEILMANN-CLAUSEN, C., 2003. The Dababiya Quarry Section: Lithostratigraphy, clay mineralogy, geochemistry and paleontology. *Micropaleontology*, 49, supplement, 1, 41:59.

EGGER, H., HOMAYOUN, M., KLEIN, P. and ROEG, F., 1999. The Paleocene/Eocene Transition in an abyssal section of the Western Tethyan Realm (Eastern Alps, Austria). *International Symposium on late Paleocene-early Eocene events from North Africa to the Middle East in connection with the 1st International Conference on the Geology of Africa, Assiut, Egypt*, p. 16.

EL-DAWOODY, A. S., 1990. Nannobiostratigraphy of the late Cretaceous-Paleocene succession in Esh-el-Mallaha range, Eastern Desert, Egypt. *Bulletin of the Faculty of Science, Qatar University,* 10: 315-337.

———, 1992. Review on the biostratigraphy of the late Paleocene/ Eocene succession in Egypt. In: Sadek, A., Ed., *Geology of The Arab World II,* 407-432. Cairo: Cairo University.

———, 1994. Early Tertiary calcareous nannoplankton biostratigraphy of North Africa and the Middle East. *2nd International Conference on Geology of the Arab World, Cairo University,* 429-461.

———, Morsi, S. M., 1983. Braarudosphaeres from some Paleogene rocks in the Gulf of Suez area, Egypt. *Abstracts, Geocome II,* Baghdad.

FARIS, M., 1988. Late Cretaceous/early Tertiary calcareous nannofossils from El Qusaima area, NE Sinai, Egypt. *Bulletin of the Faculty of Science, Qena, Assiut University,* 2(1): 263-275.

———, 1991. Remarks on Late Paleocene-early Eocene calcareous nannofossils from Gebel Gurnah section, Luxor, Nile Valley, Egypt. *Delta Journal of Science,* 15 (2): 182-211.

———, 1993a. Calcareous nannofossil events at the Paleocene-Eocene boundary in Egypt. *Bulletin of the Faculty of Science, Qena, Assiut University,* 1(2): 89-99.

———, 1993b. Early Tertiary Pentaliths from Egypt. *Delta Journal of Science* 17 (2): 154-183.

———, 1997. Biostratigraphy of calcareous nannofossils across the K/T boundary in Egypt. *Neues Jahrbuch für Geology und Palaöntology*, Mh., 8: 447-464.

———, 1999. Calcareous nannofossil events at the K/T boundary in Egypt. *Annals of the Geological Survey of Egypt,* 220: 167-180.

FARIS, M. and ABU SHAMA, A. M., 2003. Calcareous nannofossil biostratigraphy of the Upper Cretaceous-Lower Paleocene succession in the Thamad area, eastcentral Sinai,Egypt. *The Third International Conference on the Geology of Africa*, 1B: 707-732.

FARIS, M. and STROUGO, A., 1998. The lower Libyan in Farafra (Western Desert) and Luxor (Nile Valley): Correlation by calcareous nannofossils. M.E.R.C. *Ain Shams University, Earth Science Series,* 12: 137-156.

FARIS, M., ABD EL-HAMEED, A. T., MARZOUK, A. M. and GHANDOUR, I. M., 1999. Early Paleogene calcareous nannofossil and planktonic foraminiferal biostratigraphy in Central Egypt. *Neues Jahrbuch für Geology und Palaöntology*, 213(2): 261-288.

FARIS, M., ALLAM, A. and MARZOUK, A. M., 1985. Biostratigraphy of the Late Cretaceous/Early Tertiary rocks in the Nile Valley (Qena Region), Egypt. *Annals of the Geological Survey of Egypt,* 15: 287-300, Cairo, 1989.

GRAN, H. H. and BRAARUD T. 1935. A quantitive study of the phytoplankton in the Bay of Fundy and the Gulf of Maine. *Journal of the Biology Board*, Canada, 1: 279-267.

HAQ, B. U. and LOHMAN, G. P., 1976. Early Cenozoic calcareous nannoplankton biogeography of the Atlantic Ocean. *Marine Micropaleontology*, 7: 119-194.

HAY, W. W. and MOHLER, H. P., 1967. Calcareous nannoplankton from early Tertiay rocks at Pont Labau, France, and Paleocene-Eocene correlation. *Journal of Paleontology,* 41: 1505-41.

HAY, W. W. MOHLER, H. P., ROTH, P. H. SCHMIDT, R. R. and BOUNDREAUX, J. E., 1967. Calcareous nannoplankton zonation of the Cenozoic of the Coast and Caribbean-Antillean area and transoceanic correlation. *Transactions of the Gulf Coast Association of Geologists*, 17: 428-80.

HAZEL, J. E. EDWARDS, L. E. and BYBELL, L. M., 1984. Significant unconformities and the hiatuses represented them in the Paleogene of the Atlantic and Gulf coastal province. In: Schlee, J., Ed., *Interregional unconformities and Hydrocarbon Accumulations,* 59-66. American Association of Petroleum Geologists, Memoir 36.

HEWAIDY, A. and FARIS, M., 1989. Biostratigraphy and paleoecology of the Late Cretaceous/Early Tertiary sequence in Wasif area, Safaga district, Eastern Desert, Egypt. *Delta Journal of Science*, 13 (4): 1953- 1975.

HOOKER, J. J., 1991. The sequence of mammals in the Thanetian and Ypresian of the London and Belgium basins Location of the Paleocene-Eocene boundary. *Newsletters on Stratigraphy,* 25 (2): 75-90.

JANIN, M. C., BIGNOT G., STROUGO, A. and TOUMAKINE M., 1993. Worldwide discoaster ray number variability at the Early/Middle Eocene boundary Implications for the neritic sequeneces of the Nile Valley, Egypt. *Newsletters on Stratigraphy,* 28 (2,3): 157-169.

KNOX, R. W., AUBRY, M-P., BERGGREN, W. A., DUPUIS, CH., OUDA, KH., MAGIONCLADA, R. and SOLIMAN, M., 2003. The Qreiya Section at Gebel Abu Had: Lithostratigraphy, clay mineralogy, geochemistry and biostratigraphy. *Micropaleontology*, 49, supplement, 1: 93-104.

KENNETT, J. P. and STOTT, L. D., 1991. Abrupt deep-sea warming, Paleoceanographic changes and benthic extinction at the end of the Paleocene. *Nature*, 353: 225-229.

MARTINI, E., 1965. Mid-Tertiary calcareous nannoplankton from Pacific deep-sea cores. In: Whittard, W. F. and Bradshaw, R. B., Eds., *Submarine Geology and Geophysics,* 393-411. Proceedings, 17th Symposium, Colston Research Society, London.

MARTINI, E., 1970. Standard Paleogene calcareous nannoplankton zonation. *Nature*, 226: 560-561.

———, 1971. Standard Tertiary and Quaternary calcareous nannoplankton zonation. In: Farinacci, A., Ed., *Proceedings, II Planktonic Conf. Roma, 2,* 739-785. Rome: Tecnoscienza.

MARTINI, E. and MULLER, C., 1986. Current Tertiary and Quaternary calcareous nannoplankton stratigraphy and correlaions. *Newsletters on Stratigraphy,* 16 (2): 99-112.

MARZOUK, A. M. and LUNING, S., 1998. Comparative biostratigraphy of calcareous nannofossils and planktonic foraminifera in the Paleocene of the Eastern Sinai, Egypt. *Neues Jahrbuch fur Geologie und Paleontologie, Abhandlungen,* 207 (1): 77-105.

MILLER, K. G., JANECEK, T. R., KATZ, M. E. and KEIL, D. J., 1987. Abyssal circulation and benthic foraminiferal changes near the Paleocene/Eocene boundary. *Paleoceanography*, 2: 741-761.

OKADA, H. and BUKRY, D., 1980. Supplementary modification and introduction of code numbers to the low latitude coccolith biostratigraphic zonation (Bukry 1973, 1975). *Marine Micropaleontology*, 5: 321-325.

OUDA, Kh. and AUBRY, M-P., 2003. The upper-Paleocene-lower Eocene of the Upper Nile Valley Part 1, Stratigraphy. *Micropaleontology* 49, Supplement 1, 1-212.

PERCH-NIELSEN, K., 1971. Neue Coccolithen aus dem Paläozän von Dänemark, der Bucht von Biskaya und dem Eozän der Labrador See. *Bulletin of the Geological Society of Denmark,* 21: 51-66.

———, 1979. Calcareous nannofossils in Cretaceous/Tertiary boundary sections in Denmark. *Proceedings, Cretaceous-Tertiary Boundary Events Symposium, Copenhagen, 2*, 120-126.

———, 1981. Les coccolithes du Paleocene de El-Kef, Tunisie et leurs ancetres. *Cahiers du Micropaleontologie,* 3: 7-23.

———, 1983. Recognition of Cretaceous stage boundaries by means of calcareous nannofossils. In: Birkelund, T., et al., Eds., *Abstracts, Symposium on Cretaceous Stage Boundaries, Copenhagen,* 152-156.

———, 1985. Cenozoic calcareous nannofossils. In: Bolli, H. M., Saunders, J. B. and Perch-Nielsen, K., Eds., *Plankton Stratigraphy*, 427-554. Cambridge: Cambridge University Press.

PRINS, B., 1971. Speculations on relation evolution and stratigaphic distribution of discoasters. In: Farinacci, Ed., *Proccedings II Planktonic Conference, Roma, 1970,* 1017- 1037. Rome: Tecnoscienza.

REA, D. K., ZACHOS, J. C., OWEN. R. M. and GINGERICH, P. D., 1990. Global change at the Paleocene-Eocene boundary: climatic and evolutionary consequences of tectonic events. *Paleogeography, Paleoclimatology, Paleoecology*, 79: 117-128.

ROMEIN, A. J. T., 1979. Lineages in Early Paleogene calcareous nannoplankton. *Utrecht Micropaleontological Bulletin,* 22: 1-231.

SADEK, A. and TELEB, F., 1978. Standard nannofossil zones of Egypt. part II (Paleocene). *Revista Español Micropaleontologia*, 10 (3): 443-452.

SCHMITZ, B., 1987. Barium, equatorial high productivity and the northwards wandering of the Indian Continent. *Paleoceanography*, 2: 63-77.

SHACKLETON, N. J., HALL, M. A. and BOERSMA, A., 1984. Oxygen and carbon isotope data from Leg 47 foraminifers. *Initial Reports of the Deep Sea Drilling Project, Volume 74,* 599-612. Washinton, DC: US Government Printing Office.

STEURBAUT, E., 1988. New Early and Middle Eocene calcareous-nonnoplankton events and correlations in middle to high latitudes of the northern hemisphere. *Newsletters on Stratigraphy*, 18 (2): 99-115.

STEURBAUT, E. and NOLF, D., 1986. Revision of Ypresian stratigraphy of Belgium and northwestern France. *Mededelingen van der Werkgruppe Tertiare en Kwarterniare Geologie,* 23 (4): 115-172.

STOTT, L. D. and KENNETT, J. P., 1990. Antarctic Paleogene Planktonic foraminifer biostratigraphy: ODP Leg 113, Sites 689 and 690. In: Barker P. F., Kennett, J. P., et al., *Proceedings of the Ocean Drilling Project, Scientific Reports, Volume 113,* 549-569. College Station, TX: Ocean Drilling Program.

STROUGO, A. and FARIS M., 1993. Paleocene-Eocene stratigraphy of Wadi El-Dakhl southern Galala Plateau. M.E.R.C. *Ain Shams Univ, Earth Science Series,* 7: 49-62.

THOMAS, E., 1990a. Late Cretaceous-early Eocene mass extinctions in the deep sea. In: Sharpton, V. L. and Ward, P. D., Eds., *Global catastrophes in earth histor*y, 481-495. Geological Society of America Special Paper, 247.

———, 1990b. Late Cretaceous through Neogene deep-sea benthic foraminifers (Maud Rise, Weddell Sea Antarctica). In: Barker, P. F., Kennet, J. P., et al., *Proceedings of the Ocean Drilling Program, Scientific Research, Volume 113*, 571-594. College Station TX: Ocean Drilling Program.

———, 1993. Cenozoic deep sea circulation evidence from deep sea benthic foraminifera. In: Kennett, J. P. and Warnke, D., Eds., *The Antarctic paleoenvironment: A perspective on global change,* 141-165. American Geophysical Union Antarctic Research Series, 56.

TJALSMA, R. C. and LOHMANN, G. P., 1983. *Paleocene-Eocene bathyal and abyssal benthic foraminifera from the Atlantic Ocean*, 1-90. Micropaleontology Special Publication 4.

VAIL, P. R., MITCHUM, JR. R. M. and THOMPSON, S., 1977. Seismic stratigraphy and global changes in sea level. *American Association of Petroleum Geologists Memoirs,* 26: 83-9.

Manuscript received September 10, 2006
Manuscript accepted April 3, 2007

The Oligocene and Miocene record of the diatom resting spore genus *Liradiscus* Greville in the Norwegian Sea

Itsuki Suto

Department of Earth and Planetary Sciences, Graduate School of Environmental Studies, Nagoya University, Furo-cho, Chikusa-ku, Nagoya 464-8602, Japan

e-mail: sutoitsu@geobio.eps.nagoya-u.ac.jp

ABSTRACT: Occurrences of fossil marine diatom resting spore genus *Liradiscus* Greville are described from the middle Eocene to middle Miocene samples of Deep Sea Drilling Project Leg 38 Site 338 in the Norwegian Sea. The genus *Liradiscus* is characterized by a thick frustule sculptured by numerous veins. In this paper, five new taxa (*L. cucurbitus*, *L. castaneus*, *L. castaneus* var. *reticulatus*, *L. caepus* and *L. nimbus*) are described, and their stratigraphical ranges are presented. These species are short-ranging and may be potentially useful biostratigraphic markers to improve resolution of diatom biostratigraphy of the Norwegian Sea. *Liradiscus castaneus* var. *castaneus* may be evolved from var. *reticulatus* in the middle part of the Zone NPD 2A (18.4-20.3 Ma). The geologic ranges of *L. reticulatus* and *L. petasus* in the Norwegian Sea (*L. reticulatus*: early Miocene, *L. petasus*: late early Oligocene to middle early Miocene) are differentiated from those in the North Pacific (*L. reticulatus*: middle late Miocene, *L. petasus*:early late Miocene), suggesting possible the regional environmental differences.

INTRODUCTION

Chaetoceros is a planktonic centric diatom genus forming clonial chains. One third of *Chaetoceros* species are known to form resting spores (Stockwell and Hargraves 1984), which are thick-walled and morphologically distinct from vegetative cells (Garrison 1984). Because of their thick silicification, spores are preserved as fossils in sediments, and a large number of fossil resting spore morpho-genera of *Chaetoceros*-like taxa have been reported and described, indicating *Dicladia*, *Syndendrium*, *Xanthiopyxis*, *Liradiscus* and *Monocladia* (e.g. Ehrenberg 1844, 1854; Greville 1865a; Suto 2003a, b, 2004e). However, the taxonomy and biostratigraphic studies treating fossil resting spores have been very limited (e.g. Gersonde 1980; Akiba 1986; Lee 1993; Suto 2003a, b, 2004a-e, 2005a, b), because their respective vegetative cells are rarely preserved with resting spores.

Of these genera, *Liradiscus*, which was erected by Greville in 1865 (Greville 1865a), is characterized by a thick frustule sculptured by veins with a single ring of puncta on the hypovalve (Suto 2004a). Since *Chaetoceros* plays a significant role in marine primary production (Garrison 1984; Hasle and Syvertsen 1996), it is important to build a firmer taxonomic basis of *Liradiscus* for understanding past environmental change. Suto (2004a) has already described eleven *Liradiscus* species in the North Pacific. However, further taxonomic studies are needed to complete the taxonomy of this genus, because detailed examination has been limited to the Neogene of the North Pacific. In this paper, taxonomy and biostratigraphy of the genus *Liradiscus* including five new species are described in the Norwegian Sea using Eocene, Oligocene and Miocene samples from the Deep Sea Drilling Project Leg 38 Site 338.

MATERIALS AND METHODS

In this study, eighty samples of a nearly complete section of Tertiary sediments of DSDP Leg 38 Site 338 (67°47.11'N, 05°23.26'E; water depth 400.8m) are examined (text-fig. 1). These samples contain well-preserved diatoms of middle Eocene, Oligocene and early to middle Miocene in age. The diatom biostratigraphy of this site was reported in detail by Schrader and Fenner (1976), Dzinoridze et al. (1978) and Fenner (1985) and the zonation in the Miocene was revised by detail LM diatom observation in this study. North Pacific samples from DSDP Site 436 and 438, and the Newport Beach Section have been described in Suto (2004a). Most samples investigated in this study include well-preserved and abundant diatom and resting spore assemblages. The preparation and counting methods of resting spores followed Suto (2004a).

RESULTS

This paper describes five new taxa, *L. cucurbitus*, *L. castaneus* var. *castaneus* and, *L. castaneus* var. *reticulatus*, *L. caepus* and *L. nimbus* (text-figs. 2, 3). The results of counting of *Liradiscus* species encountered during a count of 100 resting spore valves in LM and their stratigraphical distributions are shown in table 1 and text-figure 4, respectively. General morphological terms are after Anonymous (1975) and Ross et al. (1979). The morphogeneric name of *Liradiscus* is used for the fossil resting spores according to Articles 3.3 and 3.4 of the International Code of Botanical Nomenclature (Greuter et al. 2000). This study follows the diatom zonation of Akiba (1986) and Yanagisawa and Akiba (1998) for the Miocene, Pliocene and Pleistocene, and that of Scherer and Koç (1996) addition to Schrader and Fenner (1976) for the Eocene and Oligocene.

TAXONOMY

Liradiscus cucurbitus Suto **n. sp.**

Text-figures 2B, 2C; plate 1, figs. 1a-10

Liradiscus ovalis Greville *sensu* FENNER 1978, p. 524, pl. 34, figs. 24, 25.

Description: Frustule isovalvate, circular in valve view, apical axis 11.3-25.0μm, pervalvar axis of epivalve 10.0-11.3μm. In girdle view, both valves hyaline, strongly vaulted, mantle dis-

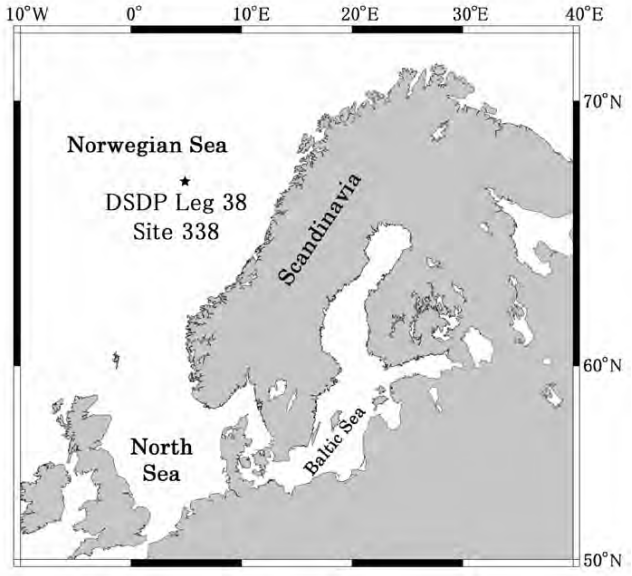

TEXT-FIGURE 1
Location map of DSDP Leg 38 Site 338 in the Norwegian Sea.

tinct, covered with large flexuose weak net-like veins on the central part of both valves, continuing towards the margin as radiating net-like veins. Flexuose net-like veins on both valves with elongated spines. The spines at the bifurcations of the net-like veins nearly perpendicular to the valve surface. Both valves with distinct mantle. Mantle of epivalve hyaline. Mantle of hypovalve hyaline with a single ring of puncta at its base.

Holotype: Slide MPC-02593 (Micropaleontology Collection, National Science Museum, Tokyo, England Finder Q32-1S; illustrated in Plate 1, figs. 7a, b).

Type locality: DSDP Site 338-17-4, 79-80cm, Norwegian Sea.

Comparison: This species is distinguished from other species by radiating and weak net-like veins with elongated spines on circular valve. This species has a close resemblance to *L. barbadensis* Greville, but the flexouse net-like veins on valve face bears some elongated spines. This species differs from *L. minitus* Greville, *L. akibae* Suto, *L. castaneus* var. *castaneus* Suto and *L. castaneus* var. *reticulatus* Suto by the flexouse net-like veins.

Stratigraphic occurrence: At DSDP Site 338, the rare but continuous occurrences of this species are recognized from the earliest Miocene Zone NPD 1 to the middle Miocene Zone NPD 4B (text-fig. 4).

Remarks: L. ovalis in Fenner (1978) is identical to *L. cucurbitus* by its flexuose net-like veins on both valves with elongated spines.

Etymology: The Latin *cucurbitus* means "pumpkin".

Liradiscus castaneus Suto **n. sp.**
Text-figure 2H-J; Plate 2, figs. 1a-3c, 7a, b, 14a, b

Description: Frustule heterovalvate, circular in valve view, apical axis 8.6-13.2 µm. In girdle view, epivalve strongly vaulted. Epivalve face covered by net-like veins over the whole valve face and with small spines. The spines at the bifurcations of the net-like veins nearly perpendicular to the valve surface. Mantle of epivalve low, hyaline with net-like veins, with small spines. Hypovalve hyaline, slightly convex in central area. Hypovalve face covered by net-like veins in marginal zone. The central area of hypovalve hyaline or with simple veins (see Plate 2, figs. 7a, b). Mantle of hypovalve low, with a single ring of puncta at its base.

Holotype: Slide MPC-02591 (Micropaleontology Collection, National Science Museum, Tokyo, England Finder O32-2E; illustrated in Plate 2, figs. 2a, b).

Type locality: DSDP Site 436-9-2, 148-150cm, northwestern Pacific Ocean.

Comparison: This species is characterized by the epivalve strongly vaulted with net-like veins and the hypovalve with net-like veins on the marginal area. The epivalve of the typical variety is the same as that of *L. castaneus* var. *reticulatus*, but hypovalve of this variety differs by the central hyaline area. The epivalve of this species is very similar to that of *L. akibae*, but is differentiated by its low mantle of epivalve without palisade spines (see text-fig. 2E). Comparison with *L. cucurbitus* has been made in the section for the taxon.

Stratigraphic occurrence: At DSDP Site 338, epivalves of the typical variety of *L. castaneus* and var. *reticulatus* occur rarely and continuously from the middle early Oligocene to the middle Miocene (text-fig. 4). On the other hand, the hypovalve of *L. castaneus* var. *castaneus* occurs rarely from the late early Miocene Zone NPD 2A through the late middle Miocene Zone NPD 5B. At DSDP Site 436, one sporadic occurrence of the taxon is recognized in the early Piocene Subzone NPD 7Bb (text-fig. 4). The hypovalve of var. *castaneus* occurs from the Subzone NPD 7Bb through the middle Pleistocene Zone NPD 11 at DSDP Site 436. In the Newport Beach Section, the sporadic occurrences of the hypovalve of this variety are recognized in the upper Miocene (text-fig. 4).

Remarks: The typical variety of *L. castaneus* may be evolved from var. *reticulatus*, because the first occurrence of this variety almost coincides with the last occurrence of var. *reticulatus*.

Etymology: The Latin *castaneus* means "chestnut".

Liradiscus castaneus var. ***reticulatus*** Suto **n. var.**
Text-figure 2H, I, K; Plate 2, figs. 4a-6b, 10a-13b, 16a-18b, 20

Description: Frustule heterovalvate, circular in valve view, apical axis 8.6-12.3µm. The characteristics of epivalve of this variety are the same as that of var. *castaneus*. Hypovalve hyaline, slightly convex in central area, entirely covered by net-like veins. The central area of hypovalve with net-like veins. Mantle of hypovalve low, with a single ring of puncta at its base.

Holotype: Slide MPC-02592 (Micropaleontology Collection, National Science Museum, Tokyo, England Finder L27-1S; illustrated in Plate 2, figs. 5a, b).

Type locality: DSDP Site 338-17-3, 110-111cm, Norwegian Sea.

Comparison: Its separation from *L. cucurbitus* and *L. castaneus* var. *castaneus* is given under those taxa.

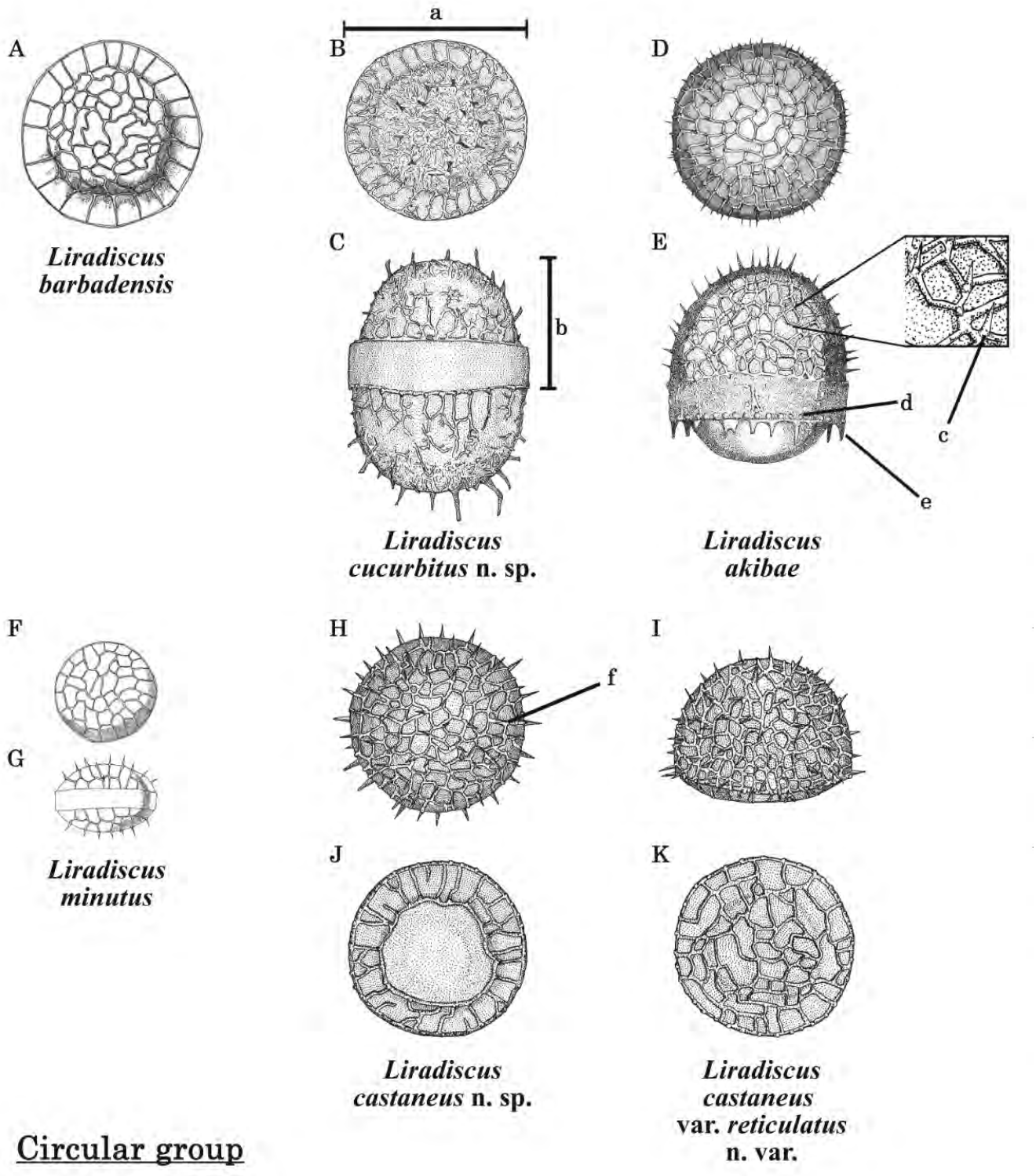

TEXT-FIGURE 2
Sketches of various circular species of *Liradiscus*; *Liradiscus barbadensis* (**A:** illustrated after Greville 1865a), *L. cucurbitus* (**B:** valve view; **C:** girdle view), *L. akibae* (**D:** valve view; **E:** girdle view), *L. minutus* (**F:** valve view; **G:** girdle view; illustrated after Greville 1865b), *L. castaneus* (**H:** epivalve in valve view; **I:** frustule in girdle view; **J:** hypovalve of *L. castaneus* var. *castaneus* in valve view; **K:** hypovalve of *L. castaneus* var. *reticulatus* in valve view). Key to structures: **a:** apical axis, **b:** pervalvar axis, **c:** short spine on the crossing of veins, **d:** a ring of puncta, **e:** palisade spines, **f:** net-like veins. All sketches were made using LM except species as mentioned above.

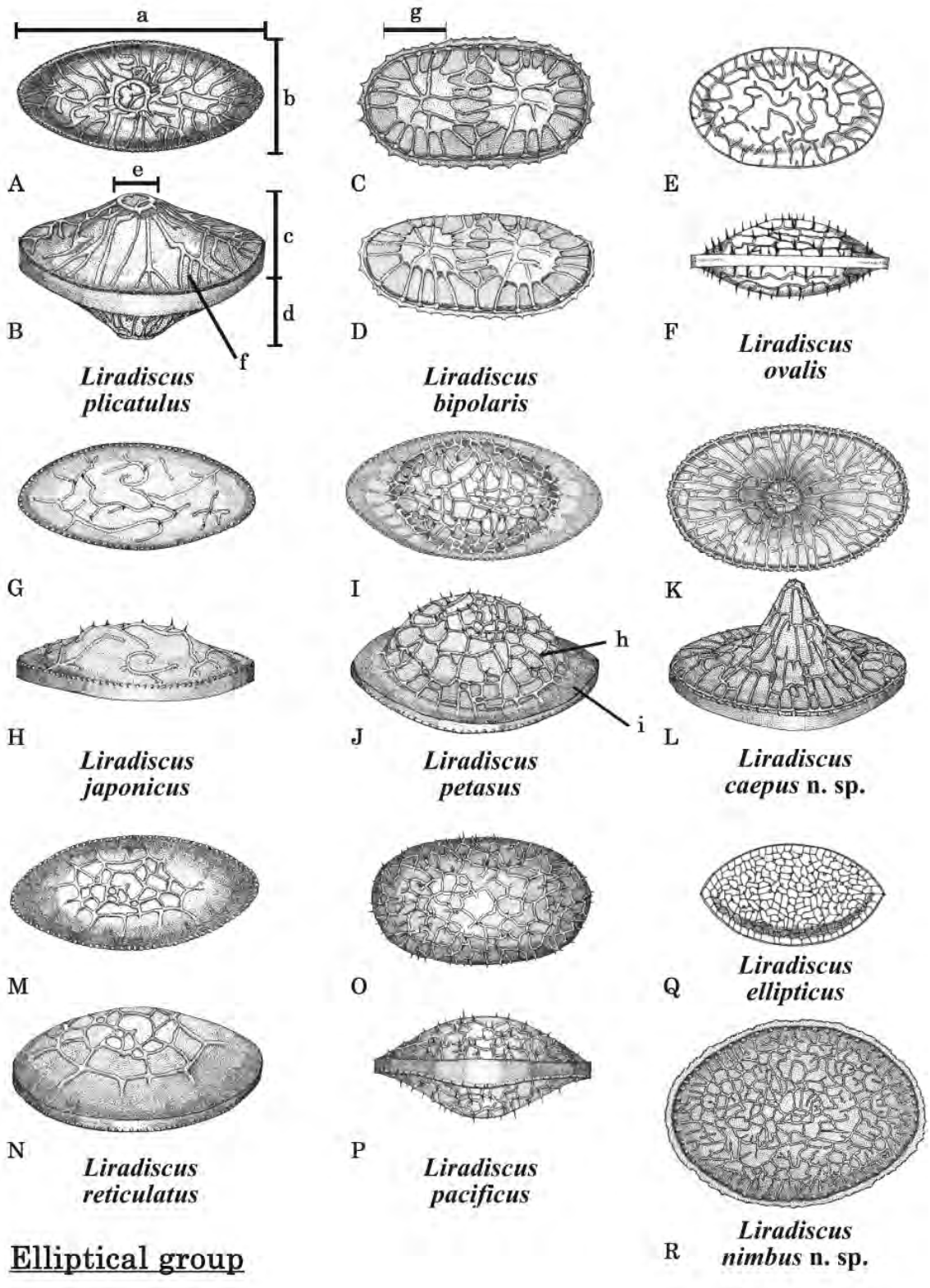

TEXT-FIGURE 3
Sketches of various elliptical species of *Liradiscus*; *Liradiscus plicatulus* (**A:** valve view; **B:** oblique view), *L. bipolaris* (**C**: valve view; **D:** oblique view), *L. ovalis* (**E:** valve view; **F:** girdle view; illustrated after Greville 1865c), *L. japonicus* (**G:** valve view; **H:** oblique view), *L. petasus* (**I:** valve view; **J:** oblique view), *L. caepus* (**K:** valve view; **L:** oblique view), *L. reticulatus* (**M:** valve view; **N:** oblique view), *L. pacificus* (**O:** valve view; **P:** girdle view), *L. ellipticus* (**Q:** valve view, illustrated after Greville 1865c), *L. nimbus* (**R:** valve view). Key to structures; **a:** apical axis, **b:** transapical axis, **c:** epivalve, **d:** hypovalve, **e:** circular veins, **f:** branched veins, **g:** low and gentle elevation, **h:** net-like veins, **i:** marginal zone. All sketches were made using by LM except species as mentioned above.

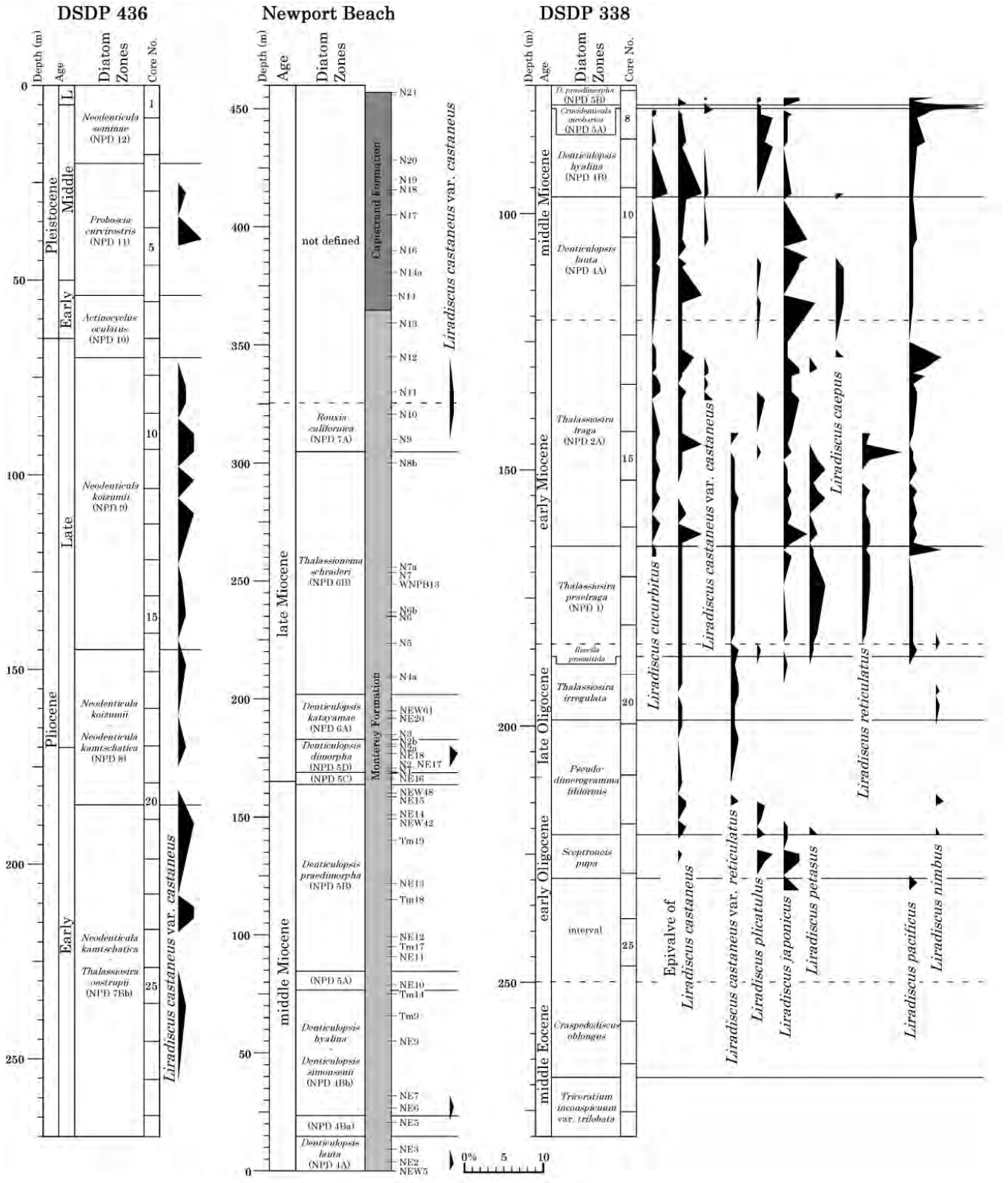

TEXT-FIGURE 4
Stratigraphic occurrences of species in the genus *Liradiscus* at DSDP Sites 338 and 436, and in the Newport Beach Section. Diatom zones and NPD codes in the Miocene, Pliocene and Pleistocene are revised after Yanagisawa and Akiba (1998), and diatom zones in the Oligocene and Eocene after Schrader and Fenner (1976).

Stratigraphic occurrence: Occurrences of epivalves of *L. castaneus* var. *castaneus* and var. *reticulatus* have been discussed above. The hypovalve of this variety occurs from the late early Oligocene *Pseudodimerogramma filiformis* Zone to the late early Miocene Zone NPD 2A at DSDP Site 338 (text-fig. 4).

Remarks: This taxon possibly evolved to *L. castaneus* var. *castaneus.*

Etymology: The Latin *reticulatus* means "net".

Liradiscus caepus Suto **n. sp.**
Text-figure 3K, L; Plate 3, figs. 1a-5

Description: Valve elliptical in valve view, apical axis 12.2-33.2µm, transapical axis 8.6-10.5µm. Hypovalve hyaline, strongly elevated near the center of the valve in girdle view, with distinct mantle, covered with radiating net-like veins originating from the top of the elevation. Mantle of hypovalve low, hyaline, with a single ring of puncta at its base. Frustule not observed, epivalve unknown.

Holotype: Slide MPC-02590 (Micropaleontology Collection, National Science Museum, Tokyo, England Finder K34-1W; illustrated in Plate 3, figs. 4a, b).

Type locality: DSDP Site 338-12-2, 40-41cm, Norwegian Sea.

Comparison: This species is distinguished from other *Liradiscus* species by the strongly elevated valve covered with radiating net-like veins originating from the top of the elevation. This species is similar to *L. plicatulus* Hajós in possessing an elevation of valve, but is distinguished from the latter by lacking circular veins on the elevation.

Stratigraphic occurrence: This species is recognized only in the Norwegian Sea in the interval from the latest early Miocene Zone NPD 2A through the early middle Miocene Zone NPD 4B (text-fig. 4).

Etymology: The Latin *caepus* means "onion".

Liradiscus nimbus Suto **n. sp.**
Text-fig. 3R; Plate 3, figs. 6a-9b

Liradiscus ovalis Greville *sensu* SHIRSHOV 1977, pl. 33, fig. 8. – NIKOLAEV et al. 2001, p. 25, pl. 38, figs. 1-7.

Description: Valve oval in valve view, apical axis 11.3-20.9µm, transapical axis 10-16.9µm. Hypovalve hyaline, convex in girdle view, mantle distinct, covered with net-like veins. Mantle of hypovalve low, with a single ring of puncta at its base. Frustule not observed, epivalve unknown.

Holotype: Slide MPC-02594 (Micropaleontology Collection, the National Science Museum, Tokyo, England Finder S33-4N; illustrated in Plate 3, Figs. 8a, b).

Type locality: DSDP Site 338-19-3, 20-21cm, Norwegian Sea.

Comparison: This species is distinguished from other species by having a flat valve with net-like veins without spines. Its separation from other *Liradiscus* species covered with net-like veins is given in under those taxa. This species is separated from *L. ellipticus* by the oval valve shape.

Stratigraphic occurrence: At DSDP Site 338, rare and sporadic occurrences of this species are recognized from a late early Oligocene thorough the latest late Oligocene interval (text-fig. 4).

Remarks: Liradiscus ovalis Greville *sensu* Shirshov (1977) collected from oceanic bottom sediments, and that of Nikolaev et al. (2001) reported from the late Cretaceous Moreno Formation in California are identified as *L. nimbus* because their specimens are completely covered with net-like veins without spines.

Etymology: The Latin *nimbus* means "cloud".

Liradiscus plicatulus Hajós
Text-figure 3A, B

Liradiscus plicatulus HAJÓS 1968, p. 114, pl. 28, fig. 10. – SUTO 2004a, p. 66, pl. 2, figs. 1a-20b.

Stratigraphic occurrence: The rare and sporadic occurrences of this species are recognized from an early Oligocene to middle Miocene interval at DSDP Site 338 (text-fig. 4).

Liradiscus japonicus Suto
Text-figure 3G, H

Liradiscus japonicus SUTO 2004a, p. 69, pl. 3, figs. 1a-10

Stratigraphic occurrence: At DSDP Site 338, this species is recognized from early Oligocene to middle Miocene (text-fig. 4).

Liradiscus petasus Suto
Text-figure 3I, J; Plate 3, figs. 10a-13b

Liradiscus petasus SUTO 2004a, p. 70, pl. 2, figs. 26a-35.

Stratigraphic occurrence: At DSDP Site 338, the occurrences of this species are recognized in the interval from the late early Oligocene to middle early Miocene (text-fig. 4). The age of occurrences in the Norwegian Sea differs from that of in the North Pacific Ocean (early late Miocene, see Suto 2004a).

Liradiscus reticulatus Suto
Text-figure 3M, N; Plate 3, Figs. 14a-16b)

Liradiscus reticulatus SUTO 2004a, p. 70, pl. 2, figs. 21a-25

Stratigraphic occurrence: At DSDP Site 338, this species occurs continuously in the early Miocene Zone NPD 1 thorough Zone NPD 2A (text-fig. 4). The age of occurrences in the Norwegian Sea is different from that of in the North Pacific Ocean (middle late Miocene, see Suto 2004a).

Liradiscus pacificus Suto
Text-figures 3O, 3P

Liradiscus pacificus SUTO 2004a, p. 70, pl. 3, figs. 11a-15.

Stratigraphic occurrence: In the Norwegian Sea, this species occurs continuously from a latest Oligocene to middle Miocene interval (text-fig. 4).

DISCUSSION

The genus *Liradiscus* is composed of sixteen species (text-figs. 2, 3; table 2). These species are divided into two groups by their valve outline; circular and elliptical groups.

The circular group is composed of six species; *L. barbadensis*, *L. minutus*, *L. akibae*, *L. cucurbitus*, *L. castaneus* var. *castaneus*, *L. castaneus* var. *reticulatus* (text-fig. 2). *Liraduscus barbadensis*, *L. minutus* and *L. akibae* were not encountered in this study.

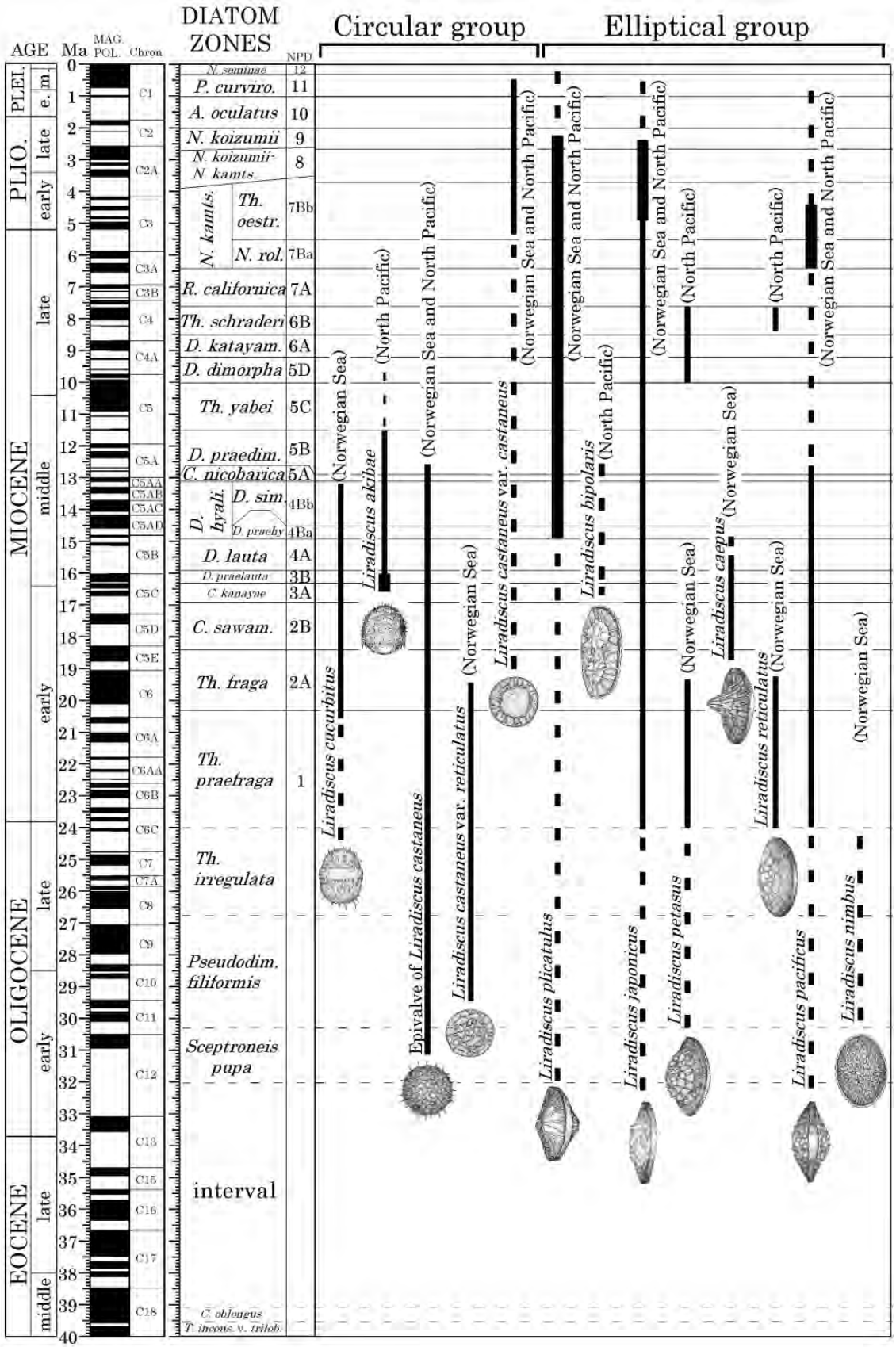

TEXT-FIGURE 5
Stratigraphic ranges of *Liradiscus* species at DSDP Sites 338, 436 and 438, and in the Newport Beach Section. Diatom zones and NPD codes are after Yanagisawa and Akiba (1998) for the Pleistocene, Pliocene and Miocene, and those after Schrader and Fenner (1976) for the Oligocene and Eocene.

TABLE 1
Occurrences of *Liradiscus* species in DSDP Site 338. Numbers indicate individuals encountered during 100 counts of resting spore valves; + indicates epivalves encountered after the count; blank indicates absence of any taxa. Diatom zones and NPD codes in the Miocene are after Yanagisawa and Akiba (1998), and those in the Oligocene and Eocene after Schrader and Fenner (1976).

							Circular group					Elliptical group							
	Diatom zones	NPD	Core-Section, Interval (cm) Leg 38 Site 338	Depth (m)	Preservation	Abundance	*L. cuervitus* sp. nov.	*L. castaneus* (Epivalve)	*L. castaneus* var. *castaneus* var. nov.	*L. castaneus* var. *reticulatus* var. nov.	*L. plicatulus* Hajós	*L. japonicus* Suto	*L. petavus* Suto	*L. caepus* sp. nov.	*L. reticulatus* Suto	*L. pacificus* Suto	*L. nimbus* sp. nov.	Total number of resting spore valves counted
middle Miocene	*Denticulopsis praedimorpha*	5B	8-1, 140-141	77.40	G	A			+		+	2				3		100
			8-2, 48-49	77.98	G	A		+			+	2				+		100
			8-2, 99-100	78.49	G	A		1				1				2		100
	C. nicobarica	5A	8-3, 10-11	79.10	G	A			+		+					9		100
	Denticulopsis hyalina	4B	8-3, 80-81	79.80	G	A	+		1		+					3		100
			8-4, 10-11	80.60	G	A	+	+			+	1				2		100
			8-4, 80-81	81.30	G	A		+			2	+				1		100
			9-1, 50-51	86.00	G	A	+	1			1	+				2		100
			9-1, 148-149	86.98	G	A		+			2					1		100
			10-1, 106-107	96.06	G	A	2	3	+			1		1		+		100
	Denticulopsis lauta	4A	10-2, 80-81	97.30	G	A		1								+		100
			11-1, 50-51	105.00	G	A	1	+	+			3				1		100
			11-2, 50-51	106.50	G	C	1	1						+		+		100
			11-3, 98-99	108.48	G	A	1					3				+		100
			11-4, 70-71	109.70	G	A	+	1			+	2		+		+		100
			11-4, 148-149	110.48	G	A	1	+			+	2		1		+		100
			12-2, 40-41	115.90	G	A	+	3				+		1		+		100
			12-3, 38-39	117.38	G	A	+	+			+	4		1		+		100
early Miocene	*Thalassiosira fraga*	2A	13-1, 148-149	124.98	G	A		+				+						100
			13-2, 148-149	126.48	G	A	+	+				+				2		100
			13-3, 148-149	127.98	G	A	+	2				+		1		4		100
			13-5, 70-71	130.20	G	A	+	1	+			2	1			2		100
			13-6, 10-11	131.10	G	A		+	+			2				+		100
			13-6, 70-71	131.70	G	A	+	+				1				2		100
			14-1, 20-21	133.20	G	A	1		+			1				+		100
			14-2, 20-21	134.70	G	A	1	1				1				1		100
			14-3, 20-21	136.20	G	A		+	1		1	2				1		100
			15-1, 30-31	142.80	G	A	1	+		1		1			1	+		100
			15-2, 100-101	145.00	G	A	+	3				+			1			100
			15-3, 100-101	146.50	G	A	1	1			1	1	1		5	1		100
			15-4, 100-101	148.00	G	A	+	+		+			1		1	+		100
			15-5, 138-139	149.88	G	A	1	+		+		+	2			1		100
			16-1, 10-11	152.55	G	A	+			+		+	+					100
			16-2, 10-11	154.05	G	A	+			+		1	1		1	1		100
			16-3, 10-11	155.55	G	A	1			1		+	2		+	+		100
			16-5, 10-11	158.55	G	A		1		+		1			+	1		100
			16-6, 50-51	160.45	G	A	1			+		+	+		1	+		100
			17-1, 100-101	162.50	G	A	+	3		+		3	1		1	1		100
			17-2, 119-120	164.19	G	A		+		+		1			1	+		100
	Thalassiosira praefraga	1	17-3, 110-111	165.60	G	A	+	+		+			+		+	4		100
			17-4, 79-80	166.79	G	A	+	+		+		1	+		1			100
			18-1, 148-149	172.48	G	A		+		+			2		1	+		100
			19-1, 130-131	181.80	G	A		+		+		1	1		+	+		100
			19 3, 20 21	183.70	G	A		+					+			+	+	100
late Oligocene	*R. praenitida*		19-4, 10-11	185.10	G	A		+		1	+		+			1		100
	Thalassiosira irregulata		19-5, 148-149	187.98	G	A		+		+		+						100
			20-2, 30-31	191.80	G	A		+		1								100
			20-3, 20-21	193.20	G	C				1							+	100
			20-3, 90-91	193.90	G	C				1								100
			20-4, 148-149	195.98	G	A		+		+							+	100
early Oligocene	*Pseudodimerogramma filiformis*		21-1, 32-33	199.82	G	A		+		+								100
			21-2, 148-149	202.48	G	A				1								100
			22-2, 10-11	211.00	G	R		+										100
			22-3, 80-81	213.20	G	C												100
			22-4, 79-80	214.69	G	R		1		1							1	100
			22-5, 10-11	215.50	G	C		1			1							100
			22-6, 148-149	218.38	G	C					+							100
			23-1, 80-81	219.60	G	C		1				+						100
			23-2, 80-81	221.10	G	A		+			1	+	1				+	100
	Sceptroneis pupa		23-3, 10-11	221.90	G	C						+						100
			23-4, 80-81	224.10	G	C												100
			23-5, 10-11	224.90	G	C		+			2	2						100
			23-6, 10-11	226.40	G	A					1	2						100
			24-1, 100-101	229.00	G	R												100
	inteval		24-2, 100-101	230.50	G	C						1				1		100
			24-3, 100-101	232.00	G	R						2						100
			barren until:															
middle Eocene	*Craspedodiscus oblongus*		26-2, 110-111	249.60	G	R												30
			26-3, 80-81	250.80	G	R												30
			26-4, 80-81	252.30	G	R												100
			26-5, 80-81	253.80	G	R												30
			27-1, 58-59	257.08	G	R												30
			27-2, 50-51	258.50	G	R												30
			27-3, 40-41	259.90	G	R												30
			27-4, 30-31	261.30	G	R												30
			27-5, 19-20	262.69	barren													
			28-1, 120-121	267.20	G	R												30
	Triceratium inconspicuum var. *trilobata*		28-2, 148-149	268.98	G	R												30
			29-1, 130-131	276.80	G	R												30
			29-2, 120-121	278.20	G	R												30
			29-3, 148-149	279.98	G	R												10

TABLE 2
List of *Liradiscus* species in the Norwegian Sea and North Pacific described in Suto (2004a) and in this study, and their characteristics, type localities and known geological ranges. "+" and "-" means presence and absence of spines on their valve faces, respectively.

		Species	Year	Type of vein	Spines	Valve face	Length of apical axis	Type locality	Known geological age
Genus *Liradiscus*	Circular group	*Liradiscus barbadensis* Greville	1865a	net-like	-	wide net-like veins passing towards the margin into radiating lines	50-175 µm	Bissex Hill Formation, Cambridge Estate, Barbados	upper early Miocene
		L. minutus Greville	1865b	net-like	+	both valves covered by net-like veins with short spines over the whole valve surface	12-25 µm	Bissex Hill Formation, Cambridge Estate, Barbados	upper early Miocene
		L. akibae Suto	2004	net-like	+	epivalve covered by net-like veins with short spines over the whole valve surface. Hypovalve hyaline.	9-35 µm	DSDP Site 438A-71-3, 7-11cm, northwestern Pacific	early ~ middle Miocene (North Pacific)
		L. cucurvitus sp. nov.	this study	branched	+	both valves covered by large flexuose weak net-like veins with elongated spines on the central part of valves, continuing towards the margin as radiating net-like veins.	11.3-25 µm	DSDP Site 338-17-4, 79-80 cm, Norwegian Sea	early ~ middle Miocene (Norwegian Sea)
		L. castaneus sp. nov.	this study	net-like	+	epivalve covered by net-like veins with short spines over the whole valve surface. Hypovalve hyaline in central area, and covered by net-like veins in marginal zone.	8.6-13.2 µm	DSDP Site 436-9-2, 148-150 cm, northwestern Pacific	early Miocene ~ Pleistocene (Norwegian Sea and North Pacific)
		L. castaneus var. *reticulatus* var. nov.	this study	net-like	+	epivalve covered by net-like veins with short spines over the whole valve surface. Hypovalve covered by net-like veins over the whole valve surface	8.6-12.3 µm	DSDP Site 338-17-3, 110-111 cm, Norwegian Sea	early Oligocene ~ early Miocene (Norwegian Sea)
	Elliptical group	*L. ovalis* Greville	1865a	branched	+	both valves covered by branched veins with short spines over the whole valve surfaces	25-62 µm	Bissex Hill Formation, Cambridge Estate, Barbados	late Cretaceous ~ middle Miocene
		L. ellipticus Greville	1865c	net-like	-	epivalve covered by very small net-like veins over the whole valve surface. Central part of the valve slightly convex. Valve ends subacute	27-41 µm	Bissex Hill Formation, Cambridge Estate, Barbados	upper early Miocene
		L. bipolaris Lohman	1948	branched	-	epivalve possesses linear anastomosing markings radiating from two elevations	38-56 µm	Calvert Formation, Ohio Oil Co. Larry G. Hammond No. 1 Well, Maryland	early Oligocene ~ middle Miocene (North Pacific)
		L. plicatulus Hajós	1968	circular veins with branched	-	both valves possess one or two circular veins near the center of the valve with branched veins originating from the circular veins	5.5-19.5 µm	Szurdokpüspöki diatomite quarry, Hungary	early Oligocene ~ Recent ? (Norwegian Sea and North Pacific)
		L. japonicus Suto	2004	branched	+	hypovalve covered by branched veins with spines on the central part of the valve	7.5-16 µm	DSDP Site 438A-25-5, 16-20cm, northwestern Pacific	early Oligocene ~ Recent ? (Norwegian Sea and North Pacific)
		L. petasus Suto	2004	net-like	+	hypovalve covered by net-like veins with short spines at the bifurcations of the net-like veins. Central part of the valve strongly convex with short spines at branching points of veins	7.5-13,5 µm	DSDP Site 438A-44-3, 10-15cm, northwestern Pacific	early Oligocene ~ early Miocene (Norwegian Sea) early middle Miocene (North Pacific)
		L. pacificus Suto	2004	net-like	+	both valves covered by net-like veins over the whole valve surface with short spines at the bifurcations of the net-like veins. Central part of the valve slightly convex	15-25 µm	DSDP Site 438A-66-2, 82-84cm, northwestern Pacific	early Oligocene ~ Recent ? (Norwegian Sea and North Pacific)
		L. reticulatus Suto	2004	net-like	-	hypovalve covered by net-like veins. Central part of the valve slightly convex	8.5-18 µm	DSDP Site 438A-44-3, 10-14, northwestern Pacific	early Miocene (Norwegian Sea) middle late Miocene (North Pacific)
		L. caepus sp. nov.	this study	net-like	-	hypovalve covered by net-like veins over the whole valve surface. Central part of the valve strongly elevated.	12.2-33.2 µm	DSDP Site 338-12-2, 40-41 cm, Norwegian Sea	early ~ middle Miocene (Norwegian Sea)
		L. nimbus sp. nov.	this study	net-like	-	hypovalve covered by net-like veins over the whole valve surface. Central part of the valve slightly convex	11.3-20.9 µm	DSDP Site 338-19-3, 20-21 cm, Norwegian Sea	early Oligocene ~ earliest Miocene (Norwegian Sea)

The elliptical group consists of ten species; *L. ovalis*, *L. ellipticus*, *L. bipolaris*, *L. plicatulus*, *L. japonicus*, *L. petasus*, *L. pacificus*, *L. reticulatus*, *L. caepus* and *L. nimbus* (text-fig. 3). *Liradiscus ovalis*, *L. ellipticus* and *L. bipolaris* were not found in this study.

The occurrences of *L. petasus* and *L. reticulatus* are differentiated from those of other species. In the North Pacific, *L. petasus* occurs in a short interval from the early late Miocene Zone NPD 5D through the middle late Miocene Zone NPD 6B and *L. reticulatus* has a very short range in the middle late Miocene Zone NPD 6B (Suto 2004a). On the other hand, their occurrences in the Norwegian Sea are from the late early Oligocene to the middle early Miocene and from the early Miocene Zone NPD 1 to the Zone NPD 2A, respectively (text-figs. 4, 5). Suto (2004a) mentioned that these species might constitute a phylogenetically related group because they are very similar each other, however, the differences in age ranges of these species between the North Pacific and Norwegian Sea may suggest that they are allopatric and constitute distinct species, or they may be due to the regional environmental differences. It is necessary to investigate these species in other regions in order to claify these differences in age ranges indicate that these species are same or different ones.

Liradiscus is characterized by a thick frustule sculptured by veins with a single ring of puncta on the hypovalve and similar to the fossil *Chaetoceros* resting spore morpho-genera *Vallodiscus* Suto and *Truncatulus* Suto, because all of them possess several types of veins on the valve surfaces. *Vallodiscus* is clearly distinguished from this genus by possessing a single ring of veins along the epivalve margin and a hypovalve covered with circular depressions of several sizes with gentle elevations (Suto 2005a). *Truncatulus* is separated easily from *Liradiscus* by the circular, elliptical or polygonal flat plate on the truncated elevation of oval to elliptical epivalves and/or hypovalves (Suto 2006). *Vallodiscus* and *Truncatulus* may be in a close phylogenetic relationship between them because all of them possess ring of puncta on their hypovalve mantles. They must be fossil resting spores produced from vegetative cells of *Chaetoceros*, but the evolutional relationships are not unclear because their vegetative valves do not preserved as fossils.

ACKNOWLEDGMENTS

I am especially grateful to Yukio Yanagisawa (Geological Survey of Japan, AIST), who encouraged me to study resting spores and carefully reviewed the manuscript. I wish to thank Fumio Akiba (Diatom Minilab Akiba Ltd.) for invaluable discussions and his careful review of the manuscript. I also thank Dr. John A. Barron (U. S. Geological Survey) for kind reviews of the manuscript. I am very thankful to Yoshihiro Tanimura (National Science Museum, Tokyo), who kindly curated the holotype specimens described in this paper. I wish also to thank Kenshiro Ogasawara (University of Tsukuba) and my colleagues for their helpful advice and encouragement. This research used samples provided by the Ocean Drilling Program (ODP). ODP is sponsored by the U.S. National Science Founda-

tion (NSF) and participating countries under management of Joint Oceanographic Institution (JOI), Inc.

REFERENCES

AKIBA, F., 1986. Middle Miocene to Quaternary diatom biostratigraphy in the Nankai Trough and Japan Trench, and modified Lower Miocene through Quaternary diatom zones for middle-to-high latitudes of the North Pacific. In: Kagami, H., Karig, D. E., Coulbourn, W. T., et al., Eds., *Initial Reports of the Deep Sea Drilling Project Volume 87*, 393-481. Washington, DC: US Government Printing Office.

ANONYMOUS, 1975. Proposals for a standardization of diatom terminology and diagnoses. *Nova Hedwigia,* Beiheft, 53: 323-354.

DZINORIDZE, R. N., JOUSE, A. P., KOROLEVA-GOLIKOVA, G. S., KOZLOVA, G. E., NAGAEVA, G. S., PETRUSHEVSKAYA, M. G. and STRELNIKOVA, N. I., 1978. Diatom and radiolarian Cenozoic stratigraphy, Norwegian Basat DSDP Leg 38. In: Supko, P.R., Perch-Nielsen, K., et al., Eds., *Initial Reports of the Deep Sea Drilling Project*, *Volume 38*, 289-385. Washington, DC: US Government Printing Office.

EHRENBERG, C. G., 1844. Über zwei neue Lager von Gebirgsmassen aus Infusorien als Meeresabsatz in Nord-Amerika und eine Vergleichung derselben mit den organischen Kreidegebilden in Europa und Afrika. *Deutsche Akademie Wissenschaften zu Berlin, Berichte*, 1844: 253-275.

EHRENBERG, C. G., 1854. *Mikrogeologie*. *Das Erden und felsen schaffende Wirken des unsichtbar kleinen selbständigen Lebens auf der Erde*. Leipzig: Leopold Voss*,* 374 pp, 40 plates.

FENNER, J., 1978. Cenozoic diatom biostratigraphy of the equatorial and Southern Atlantic Ocean. In: Supko, P.R., Perch-Nielsen, K. et al., Eds., *Initial Reports of the Deep Sea Drilling Project*, *Volume 39*, 491-623, supplement. Washington, DC: US Government Printing Office.

FENNER, J., 1985. Late Cretaceous to Oligocene planktic diatoms. In: Bolli, H. M., Saunders, J. B., and Perch-Nielsen, K., Eds., *Plankton Stratigraphy*, 713-762. Cambridge: Cambridge University Press.

GARRISON, D. L., 1984. Planktonic diatoms. In: Steidinger, K. A., Ed., *Marine plankton life cycles strategies,* 1-17. Boca Raton: CRC Press Inc.

GERSONDE, R., 1980. "Paläoökologische und biostratigraphische Auswertung von Diatomeenassoziationen aus dem Messinium des Caltanissettabeckens (Sizilien) und einiger Vergleichs-profile in So-Spanien, NW-Algerien und auf Kreta."Dissertation, Christian-Albrechts-Universität, Kiel, 393 pp.

GREVILLE, R. K., 1865a. Descriptions of new and rare diatoms, Series XIV. *Transactions of the Microscopical Society of London, New Series*, 13: 1-10.

———, 1865b. Descriptions of new and rare diatoms, Series XVI. *Transactions of the Microscopical Society of London, New Series,* 13: 43-75.

———, 1865c. Descriptions of new and rare diatoms, Series XVII. *Transactions of the Microscopical Society of London, New Series,* 13: 97-105.

GREUTER, W., MCNEILL, J., BARRIE, R., BURDET, H. M., DEMOULIN, V., FILGUEIRAS, T. S., NICOLSON, D. H., SILVA, P. C., SKOG, J. E., TREHANE, P., TURLAND, N. J. and HAWKSWORTH, D. L., 2000. International Code of Botanical Nomenclature (Saint Louis Code) adopted by the Sixteenth International Botanical Congress, St. Louis, Missouri. *Regnum Vegetabile,* 138: 1-474.

HAJÓS, M., 1968. Die Diatomeen der Miozänen Ablagerungen des Matravorlandes. *Geologica Hungarica,* 37: 1-401.

HASLE, G. R. and SYVERTSEN, E. E., 1996. Marine diatoms. In: Tomas, C. R., Ed., *Identifying marine diatoms and dinoflagellates*, 5-385. San Diego: Academic Press.

PLATE 1

Liradiscus cucurbitus Suto n. sp.

1a-b Valve view of epivalve, DSDP Site 338-8-3, 80-81cm. LM, scale bar = 10µm.

2a-b Valve view of hypovalve, DSDP Site 338-10-2, 80-81cm. LM, scale bar = 10µm.

3a-b Valve view of hypovalve, DSDP Site 338-11-1, 50-51cm. LM, scale bar = 10µm.

4a-b Girdle view of epivalve, DSDP Site 338-15-2, 100-101cm. LM, scale bar = 10µm.

5a-b Girdle view of epivalve, DSDP Site 338-16-1, 10-11cm. LM, scale bar = 10µm.

6a-b Valve view of epivalve, DSDP Site 338-15-3, 100-101cm. LM, scale bar = 10µm.

7a-b Holotype, Girdle view of frustule, DSDP Site 338-17-4, 79-80cm. LM, scale bar = 10µm.

8a-b Oblique girdle view of frustule, DSDP Site 338-16-3, 10-11cm. LM, scale bar = 10µm.

9a-b Valve view of epivalve, DSDP Site 338-17-4, 79-80cm. LM, scale bar = 10µm.

10 Valve view of epivalve, DSDP Site 338-11-4, 148-149cm. SEM, scale bar = 5µm.

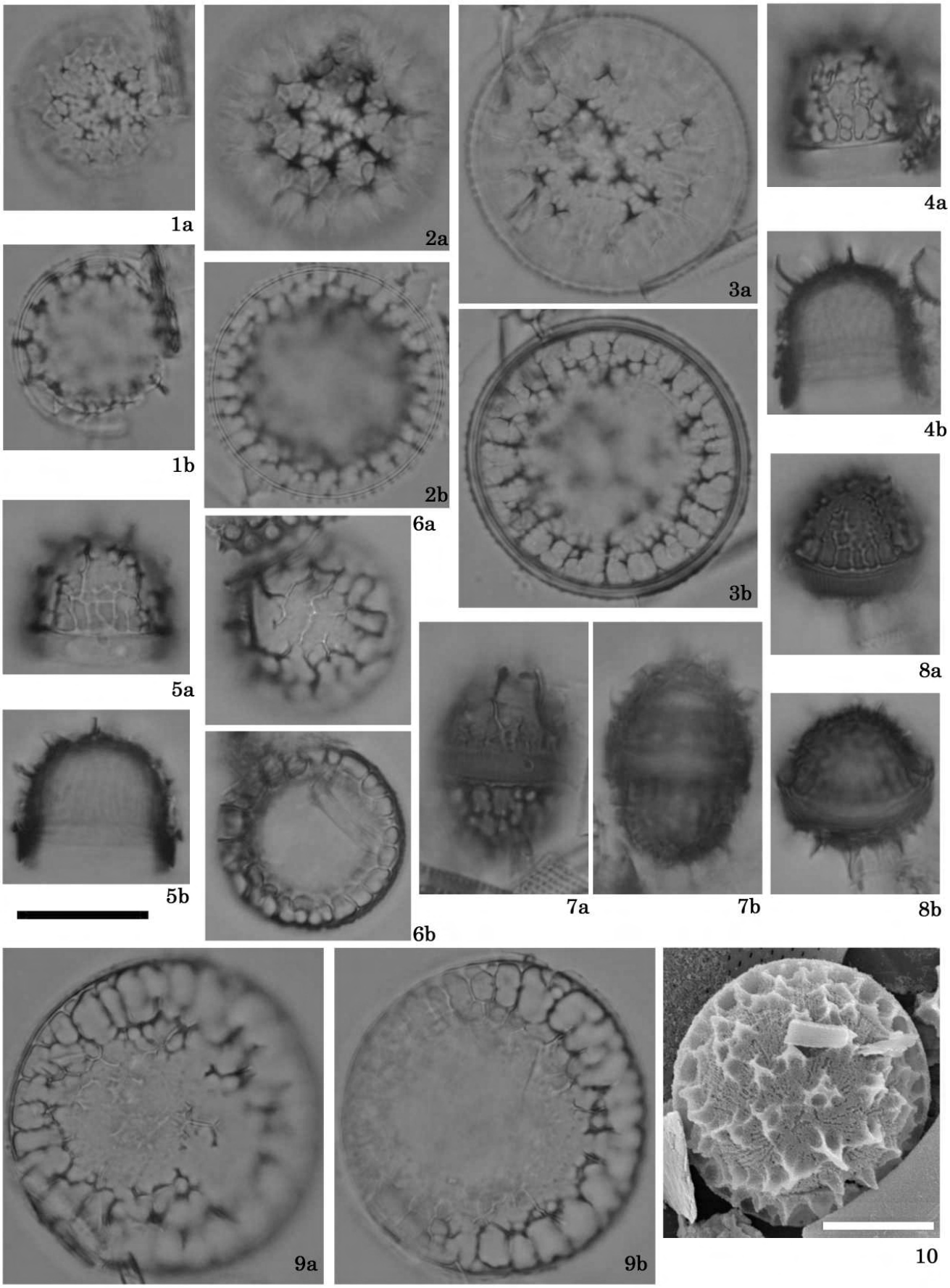
1a
2a
3a
4a
1b
2b
3b
4b
6a
5a
8a
5b
7a
7b
8b
6b
9a
9b
10

LEE, Y. G., 1993. The marine diatom genus *Chaetoceros* Ehrenberg flora and some resting spores of the Neogene Yeonil Group in the Pohang Basin, Korea. *Journal of the Paleontological Society of Korea,* 9: 24-52.

NIKOLAEV, V. A., KOCIOLEK, J. P., FOURTANIER, E., BARRON, J. A. and HARWOOD, D. M., 2001. Late Cretaceous diatoms (Bacillariophyceae) from the Marca Shale Member of the Moreno Formation, California. *Occasional papers of the California Academy of Sciences*, 152: 1-119.

ROSS, R., COX, E. J., KARAYEVA, N. I., MANN, D. G., PADDOCK, T. B. B., SIMONSEN, R. and SIMS, P. A., 1979. An amended terminology for the siliceous components of the diatom cell. *Nova Hedwigia, Beiheft,* 64: 513-533.

SCHERER, R. P. and KOÇ, N., 1996. Late Paleogene diatom biostratigraphy and paleoenvironments of the northern Norwegian-Greenland Sea. In: Thiede, J., Myhre, A. M. et al., Eds., *Proceedings of the Ocean Drilling Program, Scientific Results*, *Volume 151,* 75-99. College Station, TX: Ocean Drilling Program.

SCHRADER, H. J. and FENNER, J., 1976. Norwegian Sea Cenozoic diatom biostratigraphy and taxonomy. In: Talwani, M., Udintsev, G. et al., Eds., *Initial Reports of the Deep Sea Drilling Project, volume 38*, 921-1099. Washington, DC: US Government Printing Office.

SHIRSHOV, P. P., 1977. *Atlas of microorganisms in bottom sediments of the oceans.* Moscow: Publishing House NAUKA, 32.

STOCKWELL, D. A. and HARGRAVES, P. E., 1984. Morphological variability within resting spores of the marine diatom genus *Chaetoceros* Ehrenberg. In: Richard, M., Ed., *Proceedings of the 8th Diatom Symposyum on Living and Fossil Diatoms*, 81-95. Koenigstein: S. Koeltz.

SUTO, I., 2003a. Taxonomy of the marine diatom resting spore genera *Dicladia* Ehrenberg, *Monocladia* gen. nov. and *Syndendrium*

PLATE 2

Liradiscus castaneus Suto n. sp.

1a-b *L. castaneus*, Valve view of hypovalve, DSDP Site 436-5-2, 148-150cm. LM, scale bar = 10μm.

2a-b Holotype of *L. castaneus*, Valve view of hypovalve, DSDP Site 436-9-2, 148-150cm. LM, scale bar = 10μm.

3a-c *L. castaneus*, Valve view of frustule, DSDP Site 338-8-3, 80-81cm. LM, scale bar = 10μm.

4a-b *L. castaneus* var. *reticulatus*, Valve view of frustule, DSDP Site 338-11-2, 50-51cm. LM, scale bar = 10μm.

5a-b Holotype of *L. castaneus* var. *reticulatus*, Valve view of hypovalve, DSDP Site 338-17-3, 110-111cm. LM, scale bar = 10μm.

6a-b *L. castaneus* var. *reticulatus*, Valve view of hypovalve, DSDP Site 338-15-3, 100-101cm. LM, scale bar = 10μm.

7a-b *L. castaneus* var. *castaneus*, Valve view of hypovalve, DSDP Site 338-13-5, 70-71cm. LM, scale bar = 10μm.

8a-b Girdle view of frustule, DSDP Site 338-8-4, 10-11cm. LM, scale bar = 10μm.

9a-b Girdle view of frustule, DSDP Site 436-5-2, 148-150cm. LM, scale bar = 10μm.

10a-b *L. castaneus* var. *reticulatus*, Valve view of hypovalve, DSDP Site 338-19-4, 10-11cm. LM, scale bar = 10μm.

11a-b *L. castaneus* var. *reticulatus*, Valve view of hypovalve, DSDP Site 338-16-2, 10-11cm. LM, scale bar = 10μm.

12a-c *L. castaneus* var. *reticulatus*, Valve view of frustule, DSDP Site 338-17-1, 100-101cm. LM, scale bar = 10μm.

13a-b *L. castaneus* var. *reticulatus*, Valve view of frustule, DSDP Site 338-14-1, 20-21cm. LM, scale bar = 10μm.

14a-b *L. castaneus*, Valve view of frustule, DSDP Site 436-5-2, 148-150cm. LM, scale bar = 10μm.

15a-b Oblique valve view of epivalve, DSDP Site 338-19-4, 10-11cm. LM, scale bar = 10μm.

16a-b *L. castaneus* var. *reticulatus*, Valve view of hypovalve, DSDP Site 338-15-3, 100-101cm. LM, scale bar = 10μm.

17a-b *L. castaneus* var. *reticulatus*, Valve view of hypovalve, DSDP Site 338-15-1, 30-31cm. LM, scale bar = 10μm.

18a-b *L. castaneus* var. *reticulatus*, Valve view of hypovalve, DSDP Site 338-21-1, 32-33cm. LM, scale bar = 10μm.

19 Valve view of epivalve, DSDP Site 338, 8-1, 140-141cm. SEM, scale bar = 5μm.

20 *L. castaneus* var. *reticulatus*, Valve view of hypovalve, DSDP Site 338-10-1, 106-107cm. SEM, scale bar = 5μm.

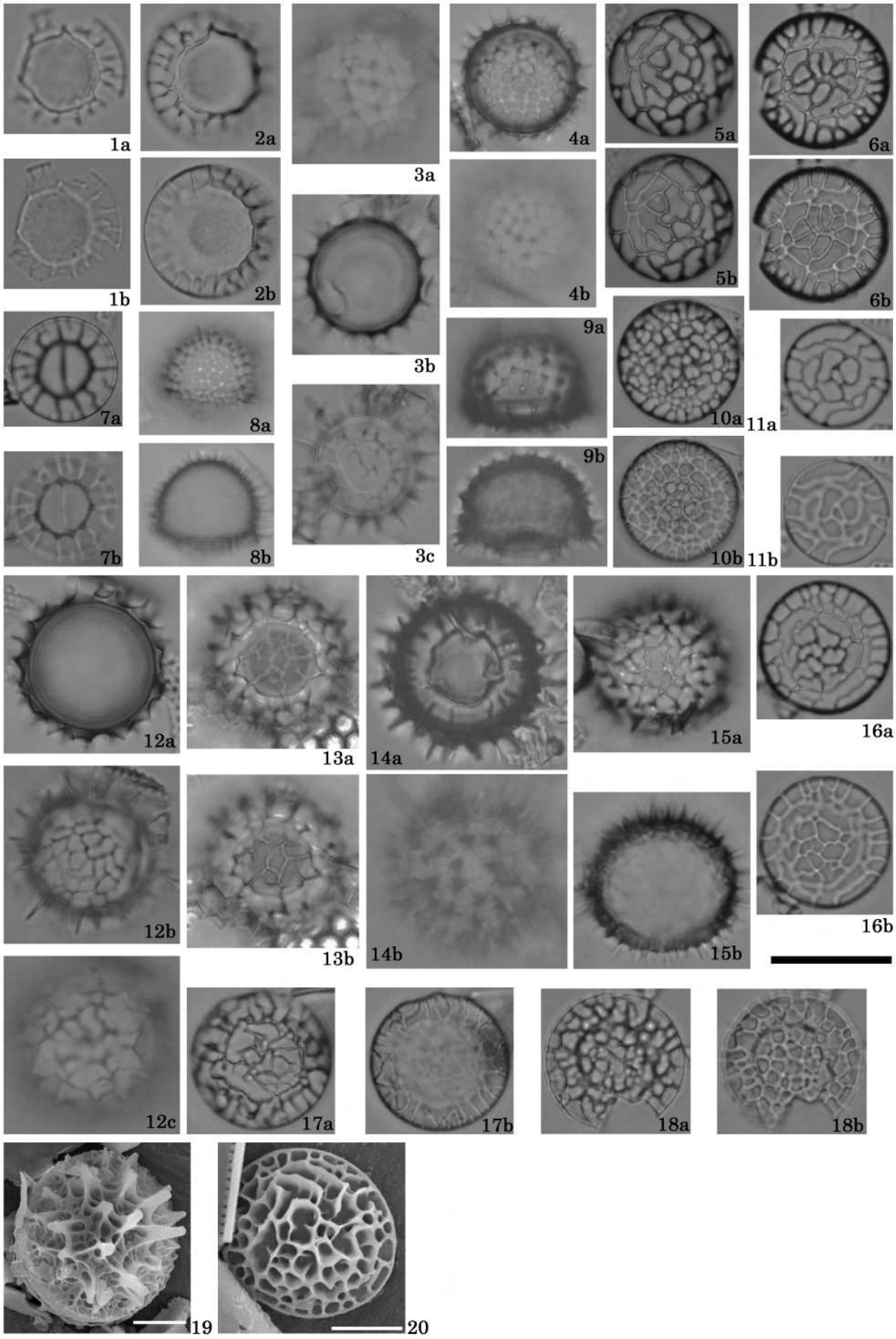
1a
2a
3a
4a
5a
6a
1b
2b
3b
4b
5b
6b
7a
8a
9a
10a
11a
7b
8b
3c
9b
10b
11b
12a
13a
14a
15a
16a
12b
13b
14b
15b
16b
12c
17a
17b
18a
18b
19
20

Ehrenberg and their stratigraphic significance in Miocene strata. *Diatom Reseach,* 18: 331-356.

———, 2003b. *Periptera tetracornusa* sp. nov., a new middle Miocene diatom resting spore species from the North Pacific. *Diatom*, 19: 1-7.

———, 2004a. Taxonomy of the diatom resting spore genus *Liradiscus* Greville and its stratigraphic significance. *Micropaleontology*, 50: 59-79.

———, 2004b. *Dispinodiscus* gen. nov., a new diatom resting spore genus from the North Pacific and Norwegian Sea. *Diatom*, 20: 79-94.

———, 2004c. *Coronodiscus* gen. nov., a new diatom resting spore genus from the North Pacific and Norwegian Sea. *Diatom*, 20: 95-104.

———, 2004d. Fossil marine diatom resting spore morpho-genus *Gemellodiscus* gen. nov. in the North Pacific and Norwegian Sea. *Paleontological Research*, 8: 255-282.

———, 2004e. Fossil marine diatom resting spore morpho-genus *Xanthiopyxis* Ehrenberg in the North Pacific and Norwegian Sea. *Paleontological Research,* 8: 283-310.

———, 2005a. *Vallodiscus* gen. nov., a new fossil resting spore morpho-genus related to the marine diatom genus *Chaetoceros* (Bacillariophyceae). *Phycological Research,* 53: 11-29.

———, 2005b. Observations on the fossil resting spore morpho-genus *Peripteropsis* gen. nov. of marine diatom genus *Chaetoceros* (Bacillariophyceae) in the Norwegian Sea. *Phycologia*. 44: 294-304.

———, 2006. *Truncatulus* gen. nov., a new fossil resting spore morpho-genus related to the marine diatom genus *Chaetoceros* (Bacillariophyceae). *Phycologia*, 45: 585-601.

YANAGISAWA, Y. and AKIBA, F., 1998. Refined Neogene diatom biostratigraphy for the northwest Pacific around Japan, with an introduction of code numbers for selected diatom biohorizons. *Journal of the Geological Society of Japan,* 104: 395-414.

Manuscript received November 27, 2006
Manuscript accepted March 14, 2007

PLATE 3

1a-5 – *Liradiscus caepus* Suto n. sp.

1a-b Valve view of hypovalve. DSDP Site 338-10-1, 106-107cm. LM, scale bar = 10µm.

2a-b Girdle view of hypovalve. DSDP Site 338-11-4, 148-149cm. LM, scale bar = 10µm.

3a-b Valve view of hypovalve. DSDP Site 338-11-4, 70-71cm. LM, scale bar = 10µm.

4a-b Holotype, Oblique valve view of hypovalve. DSDP Site 338-12-2, 40-41cm. LM, scale bar = 10µm.

5 Valve view of hypovalve. DSDP Site 338-11-4, 148-149cm. SEM, scale bar = 5µm.

6a-9b – *Liradiscus nimbus* Suto n. sp.

6a-b Valve view of hypovalve, DSDP Site 338-20-3, 20-21cm. LM, scale bar = 10µm.

7a-b Valve view of hypovalve, DSDP Site 338-20-4, 148-149cm. LM, scale bar = 10µm.

8a-b Holotype, Valve view of hypovalve, DSDP Site 338-19-3, 20-21cm. LM, scale bar = 10µm.

9a-b Valve view of hypovalve, DSDP Site 338-22-4, 79-80cm. LM, scale bar = 10µm.

10a-13b – *Liradiscus petasus* Suto.

10a-b Valve view of hypovalve, DSDP Site 338-19-3, 20-21cm. LM, scale bar = 10µm.

11a-b Valve view of hypovalve, DSDP Site 338-19-4, 10-11cm. LM, scale bar = 10µm.

12a-b Valve view of hypovalve, DSDP Site 338-15-3, 100-101cm. LM, scale bar = 10µm.

13a-b Valve view of hypovalve, DSDP Site 338-15-3, 100-101cm. LM, scale bar = 10µm.

14a-16b – *Liradiscus reticulatus* Suto.

14a-b Valve view of hypovalve. DSDP Site 338-15-4, 100-101cm. LM, scale bar = 10µm.

15a-b Valve view of hypovalve. DSDP Site 338-15-3, 100-101cm. LM, scale bar = 10µm.

16a-b Valve view of hypovalve. DSDP Site 338-18-1, 148-149cm. LM, scale bar = 10µm.

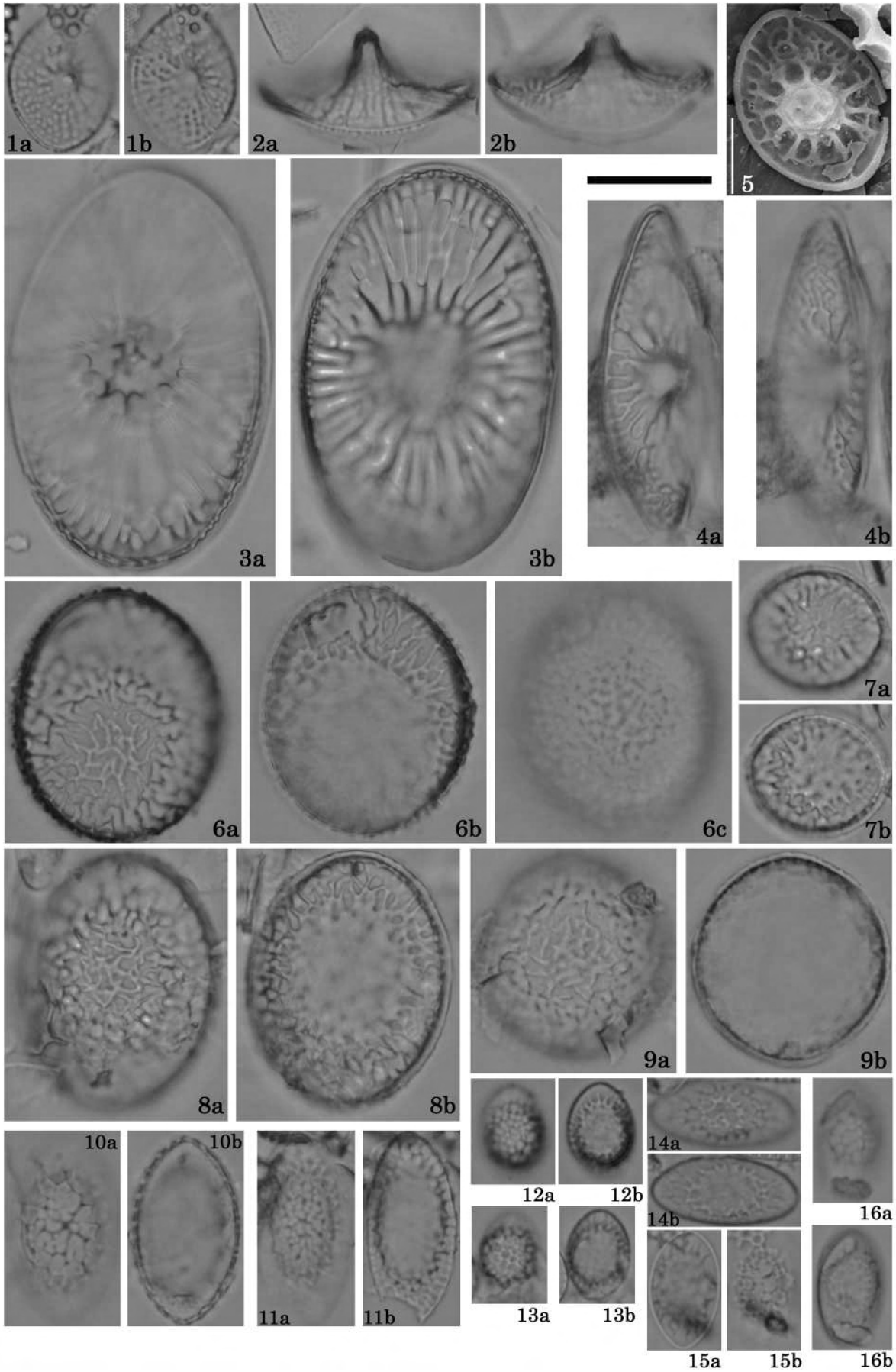
1a
1b
2a
2b
5
3a
3b
4a
4b
6a
6b
6c
7a
7b
8a
8b
9a
9b
10a
10b
11a
11b
12a
12b
13a
13b
14a
14b
15a
15b
16a
16b